Aerosol, Cloud, Ecosystems (ACE) Final Report

ACE Science Study Team
Arlindo da Silva, Hal Maring, Felix Seidel

Michael Behrenfeld, Richard Ferrare, and Gerald Mace

with contributions from
Robert Swap, Brian Cairns, David Diner, Lisa Callahan, Chris Hostetler, Ralph Kahn, Kirk Knobelspiesse, Roj Marchand, J. Vanderlei Martins, David Starr, Matthew McGill, Derek J. Posselt, Simone Tanelli, Nicholas Meskhidze, John E. Yorks, Gerard van Harten, and Feng Xu

October, 2019

ACE Key Personnel and Affiliations

Sub-Teams	Name	Affiliation	Sub-Teams	Name	Affiliation
Management					
HQ	Maring, Hal	NASA HQ	**Clouds**		
	Felix Seidel	NASA HQ	Theory	Jensen, Eric	NASA ARC
	Bontempi, Paula	NASA HQ	Modeler	Stephens, Graeme	NASA JPL
	Turner, Woody	NASA HQ		Feingold, Graham	NOAA/ESRL
	Neeck, Steve	NASA HQ		Wu, Dong	NASA GSFC
Science Lead	da Silva, Arlindo	NASA GSFC		Marchand, Roger	Univ Wash
	Starr, David	NASA GSFC		Fridlind, Ann	NASA GISS
	Wu, Dong	NASA GSFC		Jackson, Gail	NASA GSFC (now HQ)
Coordinator	Vane, Deb	NASA JPL		Hou, Arthur	NASA GSFC
ESTO	Famiglietti, Joseph	NASA GSFC (ret.)	Retrievals	Ackerman, Steve	Univ Wisc
Ocean Biogeochemistry				Feng Xu	NASA JPL
Theory/	Behrenfeld, Mike	Oregon State		Platnick, Steve	NASA GSFC
Modeler	Boss, Emmanuel	Univ Maine		Mace, Jay	Univ UT
	Follows, Mick	MIT		Haddad, Ziad	NASA JPL
	Siegel, Dave	UCSB	Radar	Im, Eastwood	NASA JPL
Retrievals	Ahmad, Zia	NASA GSFC		Heymsfield, Gerry	NASA GSFC
	Wang, Menghua	NOAA/NESDIS		Racette, Paul	NASA GSFC
	Gordon, Howard	Univ Miami		Durden, Steve	NASA JPL
	Arnone, Bob	NRL		Tanelli, Simone	NASA JPL
	Frouin, Robert	Scripps			
OES	Smith, Jay	NASA GSFC	**Aerosols**		
	Waluschka, Gene	NASA GSFC	Theory/	Ferrare, Rich	NASA LaRC
	Wilson, Mark	NASA GSFC	Modeler	Colarco, Pete	NASA GSFC
	Kotecki, Carl	NASA GSFC		Toon, Brian	Univ CO
	Meister, Gerhard	NASA GSFC		Reid, Jeff	NRL
	Holmes, Alan	NASA GSFC	Retrievals	Remer, Lorraine	NASA GSFC
	Brown, Steve	NASA GSFC		Mishchenko, Michael	NASA GISS
Cal/Val	Hooker, Stan	NASA GSFC		Kahn, Ralph	NASA GSFC
	Maritorena, Stephane	UCSB		Hu, Yong	NASA GSFC
	Nelson, Norm	UCSB	Polarimeter/	Diner, David	NASA JPL
	Stramski, Dariuz	Scripps	Imager	Martins, Vanderlei	UMBC
	Halsey, Kimberly	Oregon State		Cairns, Brian	NASA GISS
Radiation			Lidar	Yorks, John	NASA GSFC
	Loeb, Norm	NASA LaRC		Hostetler, Chris	NASA LaRC
	Kato, Sejii	NASA LaRC		McGill, Matt	NASA GSFC
	Pilewskie, Peter	Univ CO		Welton, Judd	NASA GSFC
Mission Design				Winker, David	NASA LaRC
	Callahan, Lisa	NASA GSFC		Hair, John	NASA LaRC
	Ellis, Armin	NASA JPL	Cal/Val	Starr, David	NASA GSFC
Global Modeler				Redemann, Jens	NASA ARC
	Ghan, Steve	PNNL		Knobelspiesse, Kirk	NASA GSFC
Aerosol/Ocean Science					
	Saltzman, Eric	UC Irvine			
	Mahowald, Natalie	Cornell Univ			
	Gasso, Santiago	NASA GSFC			
	Meskhidze, Nicholas	NC State			
	Gao, Yuan	Rutgers Univ			

List of main contributors to the ACE Science Study effort since 2009.

Table of Contents

Executive Summary **4**
Introduction 4
Scientific Merit and Continued Relevance of the Mission 7
The Goals of ACE 9
Expected Benefits of ACE 10
Contribution to long-term Earth Observational Record 12
Synergies with Existing and Planned Observational Systems 12
Technical Readiness and Key Risks and Risk Reductions 12

1 Introduction **15**

2 Mission Science Objectives and Measurement Requirements **18**
2.1 Aerosols 18
2.2 Clouds 21
2.3 Summary 31
2.3 Ocean Biology and Biogeochemistry 34
2.4 Aerosol-Ocean 38
Summary and Recommendations 43

3 Assessment and Instrument Concept Development **45**
3.1 Radar 45
3.2 Polarimeters 54
3.3 Lidar 64
3.4 Ocean Color Sensor 76
3.5 Ocean Color Validation Sensors 77

4 Measurement Algorithms **79**
4.1 Aerosol 79
4.2 Clouds 89
4.3 Ocean 96
4.4 Aerosol-Ocean 107

5 Field Campaigns **109**
5.1 Aerosol Related Campaigns 109
5.2 Cloud Related Campaigns 122
5.3 Ocean Related Field Campaigns 133

6 Funding History: FY16-FY18 Update **139**
6.1 Support for Field Campaigns 139
6.2 ACE Funding by Institutions 139
6.3 ACE Grants 140
6.4 Justification for No-cost Extension of Grants 141

7 ACE and the 2017 Decadal Survey **142**
7.1 Aerosols Observable 143
7.2 Aerosol-Ocean Ecosystems Synergisms 145
7.3 Other Cross-cutting aspects 145

8 Programmatic Assessment and Recommendations **147**

Executive Summary

Introduction

From its first images of the *Blue Marble* on through to its Mission to Planet Earth (MTPE) and Earth Observing System (EOS), NASA has forever changed human understanding of the interconnectedness and complexity of the Earth's physical and biological systems. With the mandate to advance the intellectual foundation provided by MTPE and EOS, the National Research Council conducted its first Decadal Survey in 2007 to provide a vision regarding the imperatives for earth systems science. With its opening statement of the Executive Summary, "*Understanding the complex, changing planet on which we live, how it supports life, and how human activities affect its ability to do so in the future is one of the greatest intellectual challenges facing humanity,"* the Decadal Survey Panel imparted its vision for NASA, NOAA and the USGS, a vision sharply focused on increasing interdisciplinary science of biogeophysical processes related to the functioning of the coupled human-natural earth system. As the report progressed, a more specific, intellectual challenge for the Earth Sciences emerged: *how do aerosol-cloud-ecosystems and their interactions modify the physical and biogeochemical processes of the earth system?*

The earth systems science community interested in physical attributes of the radiation budget has converged around the broad area of Aerosol-Cloud Interactions and their impacts on global radiation, hydrological and biogeochemical systems. The opening line of the 2013 IPCC's Chapter 7 Executive Summary states that "clouds and aerosols continue to contribute the largest uncertainty to estimates and interpretations of the Earth's changing energy budget" (p. 573). The authors further assert that "…*until sub-grid scale parameterizations of clouds and aerosol–cloud interactions are able to address these issues, model estimates of aerosol–cloud interactions and their radiative effects will carry large uncertainties*." (p. 574). These unanswered questions from both the decadal survey and the most recent IPCC point to the continued need for a satellite mission to produce the necessary observations to support process studies required to understand how a changing climate affects the role of aerosols and clouds in the transfer and balance of the earth's radiation, and how interactions between aerosols and clouds modify clouds temporally, spatially and physically from their formation through their transition into precipitation systems and beyond.

In parallel to these important climate system uncertainties, the earth systems science community interested in consequences of climate change on the biosphere has converged around the broad areas of trophic energy transfer, ecosystem feedbacks, and biosphere-atmosphere interactions. Uncertainties in our understanding of biospheric responses to climate change are even greater than uncertainties in climate predictions due to aerosol-cloud interactions and, critically, it is these biospheric responses that most directly impact human welfare. Ocean ecosystems present a particularly challenging problem because they respond

quickly (order days) to climate fluctuations. The observable response (e.g., change in standing stock) underrepresents its significance to carbon cycling, and much of the plankton biomass of the global ocean exists below the detection depth of heritage ocean color sensors. Currently, consensus has not yet been reached on, for example, the sign (i.e., increase or decrease) of change in global plankton productivity in response to a warming surface ocean. Addressing these issues requires global satellite observations from multiple sensor technologies and in conjunction with improved characterizations of atmospheric properties (i.e., accurate ocean retrievals require accurate atmospheric corrections).

In response to these diverse and interdisciplinary questions, the NRC Decadal Survey proposed the Aerosol-Cloud-Ecosystem (ACE) mission as a Tier 2 Decadal Survey mission focusing on Aerosol, Cloud systems, ocean Ecosystems, and the interactions among them so as to reduce the uncertainty in climate forcing due to aerosol-cloud interactions and assessments of consequences for ocean ecosystem CO_2 uptake (NRC Decadal Survey (2007), pg. 4-4). As one of its fifteen recommended satellite missions put forward by the Decadal Survey, the ACE mission brings together aerosol, cloud, ocean ecosystem and other earth system scientists in a multiple-sensor, multiple-platform, low earth orbit, sun-synchronous satellite mission that combines active and passive sensors to observe the Earth at microwave, infrared, visible and ultraviolet wavelengths.

ACE has built upon experience gained from the current generation of Earth observing satellites e.g. the NASA Terra, Aqua, TRMM, CloudSat, CALIPSO, SeaWIFS and GPM platforms. In doing so, the ACE mission has made significant progress regarding mission requirements and instrument technical readiness during its pre-formulation phase by using the mission resources and leveraging opportunities well. Should ACE become a fully-fledged free-flyer mission, it will extend and complement similar observations produced by the afternoon constellation (A-Train) and the planned ESA EarthCARE (Cloud, Aerosol and Radiation Explorer) mission.

The fundamental science questions that ACE intends to address have not changed over the course of pre-formulation activities, neither has our fundamental approach to addressing those questions. The mission continues to focus on understanding physical processes that require synergistic, vertically-resolved, active and passive remote sensing measurements for those processes to be diagnosed observationally. ACE has and continues to leverage the advances in technical development and readiness of both instrument concepts (with ESTO support) and their related algorithm development (with ACE Decal Survey Study support). Accordingly, ACE has initiated a series of polarimeter and radar field definition experiments over the past 3 years. The Polarimeter Definition Experiment (PODEX) took place in January-February 2013, while the first Radar Definition Experiment (RADEX-14) was executed in May-June 2014, with the second RADEX-15 conducted in November-December, 2015. For ocean ecosystem science, ACE pre-formulation has leveraged separately-funded field campaigns (Azores 2012, SABOR, NAAMES). ACE leadership

has also initiated monthly teleconferences for the Lidar and Polarimetry working groups.

Perhaps the clearest demonstration of the scientific relevance of ACE lies with the sizeable scientific demand from the community for the participation of ACE science team in a series of high profile field campaigns (see *Table E.1*). ACE science and instrument teams have been entrepreneurial and successful in their leveraging the scientific demand by the larger community for the use of their ACE instrument simulators. Major support for the participation of ACE scientists and instrument teams in a series of high profile field campaigns during the past eight years has come from a variety of sources from within NASA, and external partners such as the DoE, the NSF, as well as European sources, e.g. the U.K. Atlantic Meridional Transect (AMT) Program.

Field Campaign Name	Funding Organization
SEAC4RS - Studies of Emissions and Atmospheric Composition, Clouds and Climate Coupling by Regional Surveys	NASA RSP
SABOR - Ship-Aircraft Bio-Optical Research	NASA OBB
DISCOVER-AQ - Deriving Information on Surface Conditions from Column and Vertically Resolved Observations Relevant to Air Quality	NASA EVS
NAAMES - North Atlantic Aerosols and Marine Ecosystems Study	NASA EVS-2
ORACLES - ObseRvations of Aerosols above CLouds and their intEractionS	NASA EVS-2
2012 Azores Campaign	NASA AITT, CALIPSO
OLYMPEX - the GPM Olympic Mountain Experiment	NASA OBB, ACE, CALIPSO
TCAP - Two-Column Aerosol Project	DoE, NASA GPM, ACE, RSP
CHARMS - Combined HSRL and Raman Measurement Study	DoE

Table E.1. List of major field campaigns that have utilized ACE-related instrument concepts and related science questions in their observational framework. Responsible funding organizations are also listed.

Several ACE related concepts, such as the, the Cloud Aerosol Transport Systems (CATS) lidar and the Hyper-Angular Rainbow Polarimeter (HARP) have even drawn

the attention and support of ISS and ESTO funding sources enabling their deployment on the ISS (CATS in January 2015; HARP schedule for a 2016 launch).

This report details how the ACE mission has, in its pre-formulation phase, worked towards its goal of extending key measurements made by the aforementioned sensors through its incorporation of several new airborne sensors, both passive and active, specifically, a multi-angle polarimetric imager, a high-spectral-resolution lidar and a multiple frequency Doppler cloud radar. The additional measurements provided by these new sensors will enable determination of properties associated with many cloud, aerosol and ocean-ecosystems interactions that either cannot be determined from current satellites or can only be determined with large uncertainties to advance state of the art earth system models. Examples of these properties include vertical distributions of cloud, precipitation water content and particle size, as well as aerosol number concentration and single scattering albedo. Accurate determination of microphysical properties such as these is critical to conducting process studies to further our understanding of cloud-aerosol interactions that drive much of the uncertainty in our understanding of climate change. Details related to this approach have evolved over the past eight years with advances in understanding, modeling capabilities, and technology and are presented in detail in Sections 3, 4 and 5 of this report.

Science Traceability Matrices for the ACE mission are presented in more detail in Section 2 and broadly cover five equally-important thematic areas:

1) Aerosol Sources, Processes, Transports and Sinks (SPTS)

2) Direct Aerosol Radiative Forcing (DARF)

3) Aerosol-Cloud Interactions (ACI);

4) Clouds (Morphology; Microphysics and Aerosols; Energetics); and

5) Oceans (Standing Stocks, Composition and Productivity (SSCP); Biogeochemical Cycle Dynamics; Material Exchange between Atmosphere/Oceans; ACI impacts on Ocean Biogeochemisty; Impacts of Physical Processes on Ocean Biogeochemistry and Ocean Biogeochemistry on Physical Processes; Distribution of Harmful Algal Blooms and Eutrophication Events (HAB and EE, respectively).

Scientific Merit and Continued Relevance of the Mission

Calls for this type of science reach beyond the 2007 Decadal Survey and the IPCC and can be found across a range of white papers, proceedings, and the scientific literature. A grand challenge for Earth System science in the coming decades is moving beyond simple resource-based views of climate interactions toward mechanistic interpretations of observed change that address the complexity of natural communities and resolve key feedbacks such that this new understanding informs and advances coupled earth system models.

For example, the World Climate Research Program has emphasized the necessity of addressing a grand challenge associated with observing and modeling clouds, circulations and climate sensitivity and of working across their numerous time and space scales (http://www.wcrp-climate.org/gc-clouds; Bony et al. (2015)). Examples of the types of outstanding scientific questions produced as part of the 2014 NSF-supported synthesis of the EarthCube End-User Workshop series, the "Engaging the Atmospheric Cloud / Aerosol / Composition Community" workshop[1] include the following:

1) What are the exact roles of the clouds in the cloud systems and in the entire earth system?

2) How do clouds affect the cloud feedback on climate sensitivity?

3) What is the role of clouds on biosphere or ecosystems and vice versa?

4) What is the spatial, temporal, size distribution and composition distribution of aerosol particles in the atmosphere and the aerosol particle emissions globally?

5) What are the exact roles of aerosols in the cloud and climate?

6) What is the impact of aerosol on severe marine storms?

7) What are the changes to Cloud Condensation Nuclei (CCN) with changes in aerosol loading?

From the standpoint of the global earth system modeling community, substantial progress on the aforementioned science questions necessitates at a minimum an observing system capable of providing coincident aerosol, cloud and precipitation.

Further examples of key emergent questions regarding ocean ecosystem change are:

1) How exactly do changes in upper ocean physical properties (e.g., temperature, stratification, storm frequency, surface mixing) impact plankton ecosystems and carbon biogeochemistry?

2) How do aerosols and clouds influence ocean ecosystems and, in turn, what roles to ocean ecosystems play in aerosols and climate? How do key material exchanges processes change from the land-ocean interface to the open ocean?

1 Retrieved from http://earthcube.org/sites/default/files/doc-repository/CombinedSummaries_12Dec2014.pdf, p. 70

3) What are the implications of global ocean ecosystem change on goods and services for humanity? How can improved understanding inform improved management of ocean resources?

The Goals of ACE

In order to address a number of the aforementioned grand challenges, ACE set out to assist in reducing uncertainties related to Effective Radiative Forcing (ERF) and Biospheric Impacts of Climate by answering fundamental science questions associated with aerosols, clouds, and ocean ecosystems. ACE intended to accomplish this by making improved and more comprehensive measurements through the use of innovative and advanced remote sensing technologies. Aerosols measured by ACE include those of both man-made and natural origins, the latter of which is contributed significantly by ocean ecosystems.

For aerosols, ACE seeks to distinguish aerosol types and associated optical properties and size. For cloud systems and processes, the mission as conceived will provide unique information that will allow for diagnosis of microphysical processes that cause clouds, perhaps as modified by anthropogenic aerosol, to produce precipitation within turbulent vertical updrafts. This connection to process will be achieved via multiple independent observational constraints on microphysical properties within the vertical column.

Planktonic ecosystems of the Earth's surface ocean are a crucial link in the global carbon cycle. These ecosystems are hypothesized to impact the cloud, precipitation and climate processes through their productivity and their emission of trace gases that are subsequently converted to aerosols (e.g. Meskhidze and Nenes, 2006; Krüger and Graßl, 2011). Likewise, the wet and dry deposition of biogeochemically important species to the ocean surface are hypothesized to impact the productivity of these globally important ecosystems (e.g. Duce, 1986; Jickells et al., 2005; and Meskhidze et al., 2005). ACE measurements will allow the first-ever depth-resolved characterization of ocean ecosystems, including the standing stocks of phytoplankton and total particulate populations, ecosystem composition, and photosynthetic carbon fixation. ACE measurements will further permit global assessments of ecosystem health (through diagnostics of stress), improved separation of optically-active in-water constituents, and the first detailed characterization of plankton annual and interannual changes in high-latitude polar regions, where impacts of climate change have been particularly severe. With these advanced observations, coupled to the atmospheric measurements of ACE, a far improved understanding will be gained on climate impacts on ocean ecology and the goods and services they provide, as well as feedbacks between ocean ecosystems and aerosols, clouds, and climate.

The specific goals of ACE were:

1. Provide a data stream of Near-Real Time (NRT) observations of highly resolved temporal and spatial distributions of coincident aerosols, clouds and precipitating systems to the global earth observing modeling community;
2. Improved understanding of Earth system interactions specifically among aerosols, cloud-precipitation systems, and ocean ecosystems;
3. Quantification of the direct radiative effect of aerosols at the surface as well as at the top of the atmosphere;
4. Assessment of the indirect effects of aerosols through modification of hydrometeor profiles in cloud-precipitation systems and cloud radiative properties;
5. Assessment of changes in cloud properties in response to a changing climate;
6. Providing the first 3-dimensional reconstruction of global plankton ecosystems to improve understanding on how these ecosystems respond to the 3-dimensional physical and chemical forcings that govern them.
7. Provide a data stream of coincident atmosphere and ocean retrievals to reduce uncertainties in all retrieved geophysical products, better distinguish key ocean ecosystems components, and identify critical ocean-atmosphere forcings and feedbacks.
8. Observation and distinguishability of those ocean ecosystem components that actively take up and/or store carbon dioxide;
9. Measurement and quantification of the linkages between atmospheric aerosols and underlying ocean ecosystems.

Achievement of these goals will result in enhanced capabilities to observe and predict changes in the Earth's atmosphere, biosphere, hydrological cycle and energy balance in response to climate forcings.

Expected Benefits of ACE

Scientific

1. Reduced uncertainty in aerosol-cloud-precipitation and radiative interactions and thereby quantification of the net role of aerosols in climate.
2. Improved knowledge of cloud processes, especially advancing knowledge of the partition of liquid and ice-phase.
3. Accurate measurements characterizing the net radiative effects of multi-layer cloud decks, especially low clouds in the tropics and mid-latitudes that will

help climate modelers make more precise and accurate predictions of climate.

4. Measurement of the ocean ecosystem changes resulting from aerosol-cloud-precipitation system interactions.

5. Improved air quality forecasting by determining the height and speciation of aerosols being transported long distances.

6. Leveraged and extended observations from existing space-based assets currently deployed by NASA and our international partners.

7. Improved understanding of the impacts on ocean ecosystems, including the ocean biological carbon pump, by atmospheric aerosols and clouds, as well as by climate change at large.

Programmatic

1. Establish and incentivize the next generation of earth system sciences through their involvement with the mission from undergraduate/graduate students on through to professionals.

2. Harness and leverage the expertise resident at three major NASA centers - Goddard Space Flight Center, Langley Research Center and the Jet Propulsion Laboratory.

Societal Relevance

1. Improved accuracy of climate prediction, including the prediction of climate change impact on temperature, precipitation and water availability resulting in the possible reduction of human, economic and marine biodiversity loss around the world.

2. Improvement of and extension of air quality monitoring and forecasting on a global scale.

3. Improved predictions of potential climate change implications on the marine ecosystem playing a vital role in human welfare.

4. Improved understanding of the functioning of the remote regions of the world's oceans.

5. Advancement of earth system science as a means to achieving these goals, while not just being an end in itself.

6. Development of a NRT coupled observation-modeling architecture for earth system science.

Contribution to long-term Earth Observational Record

While contributing to the long-term climate effort is a laudable goal, ACE leadership is mindful that programmatic resource constraints could reduce the ability of the mission to provide an additional observational continuity over and above what is possible from the operational missions of the S-NPP/JPSS and GOES programs. However, ACE will contribute by extending the observational records of unique A-Train assets (CALIPSO, CloudSat, PARASOL), SeaWIFS. PACE, as well as EarthCARE and CATS.

Synergies with Existing and Planned Observational Systems

The ACE mission has potential synergy with the following activities:

Solar reflectance imagery/polarimetry – Mission for Climate and Atmospheric Pollution (MCAP): polarimeter, CSA APOCC (Atmospheric Processes Of Climate and its Change) as well as the 3MI polarimeter on the Eumetsat 2nd generation polar system (EPS-SG), JPSS missions, GEOS-R missions, MAIA, and ACCP.

Precipitation – SnowSat (35/94-GHz Doppler cloud radar): CSA APOCC; AMSR2/GCOM-W2, -W3: JAXA; GPM; ACCP

Atmospheric Composition – GEO: TEMPO, GEO-CAPE, GEMS, SENTINEL-4; LEO: 3MI (Meteosat), ACCP

Ocean Ecosystems - PACE

Other – EarthCare, JPSS S-NPP.

Technical Readiness and Key Risks and Risk Reductions

Technical Readiness

The ACE team has made demonstrable progress in the evolution and deployment of new sensor technology, the acquisition, assimilation and analysis of the resulting data as the concepts embraced by ACE continue to move from technology development, to sub-orbital and even to the ISS on their way to a complete mission. This progress has been the result of ACE leadership investing heavily over the past eight fiscal years in two general areas: science and risk reduction. The development of sensors, related algorithms and opportunities to test the larger ACE science mission concept in the field have occurred through involvement of ESTO and its related R&D programs, in a designated ACE-led field campaign, or by leveraging payload deployment opportunities related to funded EVS and R&A field campaigns.

Specifically, the technical readiness level and evolution of sensor technology has been advanced with respect to the development of three polarimeter concepts, two radar concepts and two lidar concepts. Regarding the polarimeters, the AirMSPI instrument TRL is currently 5 with an anticipated increase to 6 by early 2016. The

RSP APS instrument TRL currently stands at 8 or 9 whereas the PACS instrument stands at a TRL of 6. Advances in the ACERAD concept have seen its TRL rise to 5 and is anticipated to increase to 6 by the end of 2017. The TRL of the LaRC HSRL, currently stands between 4 and 5 and has flown successfully on ER-2 test flights in May 2015. This airborne HSRL is also scheduled to be deployed on the ER-2 for the ORACLES EV-S mission in August, 2016. Additionally, the recently launched CATS lidar is now operational onboard the ISS.

Technical Risks

Starting in FY13, ACE has increasingly prioritized investments in risk reduction, specifically via algorithm development and the data acquisition and analyses to support that activity. Furthermore, ACE leadership now supports a robust multi-sensor algorithm development activity in the cloud science area. This is regarded as a critical area to reduce technical risk and rapidly advance prior mission formulation, similar to on-going investments in aerosol algorithm development by the polarimeter teams.

ACE Leadership has also convened working groups where participants from a variety of instrument concept teams are brought together regularly (on a monthly to bi-monthly basis) to discuss, in a transparent forum, advances and challenges of their concept as it relates to the larger ACE mission. This has been successful with the Polarimeter and Radar working groups, and most recently, with the creation of a Lidar working group. The open competition of the instrument technology relative to ACE mission objectives ensures the development and enhanced TRL of multiple instrument designs thereby ensuring enhanced optionality for ACE mission leadership regarding instruments and their deployment.

Assessment and Recommendation

First and foremost, the scientific vision still stands and is as much in demand now as it was in 2007. The ACE mission as first conceived puts forth a bold and ambitious vision regarding the observation and study of Aerosol-Cloud-Ecosystem processes, especially its vision for seeking to combine the best of a surveying and a process-oriented mission. Over the past eight years, ACE Science Team Leadership has acted upon the recommendations the last Decadal Survey and the directive of NASA ESD leadership and made significant progress during the pre-formulation stage of the mission.

Furthermore, the ACE Study Team was actively providing input into the National Academies of Sciences, Engineering and Medicine's Space Studies Board's 2017 Decadal Survey for Earth Science and Applications from Space process. ACE leadership and Science Team members are part of the larger dialogue that will define NASA Earth Science moving forward and open to advancing in the most parsimonious fashion possible. A number of white papers have been contributed by the ACE Study to recent Request for Information by the 2017-2027 Decadal Survey panel where ACE science questions and measurements concept play a central role.

In light of the aforementioned scientific relevance, continued progress and success in the maturation of instrument technology and algorithm development, ACE leadership has the following recommendations:

1) Continue to evolve/mature the TRLs of polarimeter, radar and lidar concepts
2) Continue to evolve/mature associated algorithms
3) Continue to work closely with PACE Mission leadership to exploit points of intersection and leverage PACE and ACE concepts to enhance scientific return on investment.
4) Develop or extend an existing an airborne campaign to jointly fly ACE-related lidar and polarimeter concepts onboard the NASA ER-2 suborbital platforms to test and refine combined active-passive aerosol and cloud retrieval algorithms.
5) Progress the ACE Mission from pre-formulation to formulation phase in an adaptive fashion in harmony with the recommendations of 2017 DS.

1 Introduction

One of the most pressing contemporary Earth System Science questions is, incontrovertibly, how will life on Earth respond to climate change over the coming century? Global satellite measurements already provide among the greatest insights into this question by observing how today's ocean and terrestrial ecosystems respond to natural, and to some extent anthropogenic forms of climate variation. However, new and innovative measurement approaches are required to advance our understanding of the living Earth System. Current limitations are particularly acute for studies of ocean biology, for direct aerosol climate forcing, for cloud-aerosol interactions, and for precipitation-producing processes. For example, NASA's ocean color missions fail to observe high-latitude ecosystems over much of the annual cycle, yet these climate-critical ecosystems are experiencing the greatest rate of climate-driven change. Furthermore, heritage ocean color sensors only detect the plankton properties in a thin layer of the ocean's surface, leaving major uncertainties in our understanding of ocean productivity, biomass distributions, and interactions between biological stocks and rates, and related physical forcings that will be strongly altered by a changing climate.

Within this grand Earth System Science Challenge of understanding how the biosphere will respond to climate change are two primary sub-questions: (1) How will these responses of the biosphere feedback on atmospheric factors controlling climate? and (2) To what extent and where will changes in climate forcing impact the physical environment in which the biosphere exists? With respect to this latter sub-question, one particular uncertainty supersedes all others: aerosol-cloud interactions and the impact of clouds and aerosols on global radiation, hydrological, and biogeochemical systems. Indeed, the Executive Summary of Chapter 7 in the 2013 IPCC's states that "*clouds and aerosols continue to contribute the largest uncertainty to estimates and interpretations of the Earth's changing energy budget*" (p. 573). The underlying issues are further clarified by noting that "…*until sub-grid scale parameterizations of clouds and aerosol–cloud interactions are able to address these issues, model estimates of aerosol–cloud interactions and their radiative effects will carry large uncertainties*." (p. 574). It is also widely recognized that the treatment of meteorological influences on clouds and aerosols is an equally important subject that needs to be concurrently addressed.

These outstanding issues from the most recent IPCC assessment point to a series of unanswered questions regarding the roles of aerosol, clouds, and precipitation in Earth's changing climate system. These questions highlight the continued need for global observations allowing process studies addressing how the transfer and balance of energy in a changing climate are influenced by aerosols, clouds, and precipitation, and how the interactions between aerosols and clouds from their formation through their transition into precipitation systems influence the response of the Earth system to a rapidly changing atmosphere and ocean composition. Thus, to fully understand the threat that climate change poses to life on Earth in a quantitative manner, it is essential to relate observed changes in the contemporary

biosphere to the magnitude of future change, which in turn requires process-level understanding of biological feedbacks on climate along with the details of aerosol-cloud and other interactions of the physical climate system.

In response to a similar set of questions posed by the Earth Science community, and recognizing the scientific and observational overlaps in ocean ecosystem and atmospheric sciences, the 2007 the NRC Decadal Survey recommended the Aerosol-Cloud-Ecosystem (ACE) mission. At the time, ACE was recommended as a Tier 2, pre-formulation mission focusing on observational requirements to advance understanding of ocean ecosystems, aerosols, and clouds and their interactions and feedbacks. (NRC Decadal Survey, 2007, pg. 4-4). As one of its fifteen recommended satellite missions, ACE represents the primary global mission to advance understanding of the climate-biosphere system. It brings together ecosystem, aerosol, cloud, and other Earth system scientists in a multiple-sensor, multiple-platform, low sun-synchronous satellite mission. The recommendation stresses that to achieve mission objectives active (primarily lidars and radars) and passive sensors need to be combined to observe the Earth at microwave, infrared, visible and ultraviolet wavelengths.

The fundamental science questions that ACE addresses, and the fundamental approach to addressing those questions, have only come into sharper focus over the course of the pre-formulation activities. The mission concept continues to target collecting synergistic active and passive measurements that will aid understanding of ocean biological stocks, rates, and changes from pole-to-pole and from the surface to deep communities, along with the physical processes associated with the Earth's water and energy cycles. ACE activities involve participation from a broad segment of the Earth Science community, in particular from the ocean ecology and biogeochemistry, aerosol, cloud, precipitation, and radiation disciplines.

Since the ACE mission recommendation by the 2007 Decadal Survey Report, pre-formulation activities have made major advances toward refining its observational and science requirements. These developments have resulted in several reports. Most recently, the ocean science community has produced a very detailed description of requirements for the ACE advanced ocean color sensor as part of the Pre-ACE (PACE) Science Definition Team activities; the PACE Science Definition Team Report is available from http://decadal.gsfc.nasa.gov/pace-resources.html . In addition, guidance on numerous ACE-relevant objectives were provided in a recent NASA SMD community meeting (May, 2014, NASA Ames Research Center); recommendations from this workshop were published in a report entitled "*Outstanding Questions in Atmospheric Composition, Chemistry, Dynamics, and Radiation for the Coming Decade*", available from https://espo.nasa.gov/home/content/NASA_SMD_Workshop. The radiation, aerosols, clouds, and convections sections of that report highlight questions and possible observational courses of action that pertain to the roles of aerosols, clouds, precipitation in the climate system. The novel observational approaches attend to

significant shortcomings in our present observational systems for tackling the grand challenges in Earth science for the next decade.

In compliance with guidance received from the Associate Director of Flight Programs in the Earth Science Division of the Science Mission Directorate by each 2007 Decadal Survey Mission Team, the ACE Science Team has produced the present document that summarizes the results of the past eight years (2011-2018) of pre-formulation work accomplished by the ACE mission team. The paper details the efforts, accomplishments and plans of the ACE mission team for the following aspects: Instrument concept development and assessment; measurement algorithms; field campaigns; mission architecture; and mission funding history. Further, the ACE mission team provided an overall assessment as well as its own recommendations regarding the future of the ACE mission.

This Report is structured in the following main sections:

1. Introduction
2. Mission Science Objectives and Measurement Requirements in the format of Science Traceability Matrices
3. Assessment and Instrument Concept Development for the radar, polarimeter, lidar and ocean color instrument concepts
4. Measurement Algorithms for aerosols, clouds and oceans
5. Field Campaigns for aerosol, cloud and ocean related campaigns
6. Funding History updte for the period FY16 through FY18
7. ACE and the 2017 Decadl Survey
8. Programmatic Assessment and Recommendations

These sections are followed by sections containing references and list of acronyms.

2 Mission Science Objectives and Measurement Requirements

2.1 Aerosols

Global measurements of the horizontal and vertical distributions of aerosols, and their optical, microphysical, and chemical properties are required to quantify the impacts of aerosols on human health, global and regional climate, clouds and precipitation, and ocean ecosystems. Although spaceborne instruments on the Aqua, Aura and Terra satellites have significantly improved our global understanding of aerosols, critical measurements are either absent or have unacceptably large uncertainties. Therefore, the ACE aerosol Science Traceability Matrix (STM) has been designed to address objectives that are significantly beyond the capabilities of current satellite sensors.

Following the release of the NAS report, work began during 2007 and 2008 on the development of a white paper and STM to capture the specific aerosol-related science questions, aerosol and cloud parameters required, and measurement and mission requirements. A meeting of NASA aerosol scientists was held at GSFC in February 2009 to accelerate development of the aerosol STM, including requirements for two core aerosol-related instruments: polarimeter and lidar. Following this meeting, further discussion and revisions of the STM were facilitated by regular telecons. A revised version of the STM was presented for comment at a meeting held in Santa Fe, NM in August 2009. Based on comments received at this meeting, the STM was revised further. Most notably, increasing the emphasis on the cloud-aerosol interactions (CAI).

The aerosol STM addresses three major science themes: 1) sources, processes, transport and sinks (SPTS); 2) direct radiative aerosol forcing (DARF); and 3) cloud-aerosol interactions (CAI). The first theme addresses the global aerosol budget, long-range transport, and air quality. Comparisons among current global aerosol chemical transport models reveal large diversity in the modeled distribution and attribution of aerosol species, which indicates significant uncertainties in model chemical evolution, microphysics, transport, and deposition, as well as source strength and location. As models become more advanced and simulate aerosol mass, number, and size for multiple aerosol types and modes, aerosol characterization requires additional measurements beyond total column aerosol optical depth (AOD). Consequently, the ACE approach is to provide measurements to permit improved estimates of aerosol source strength and location, vertical distribution, and distributions of aerosol optical properties, mass, number, and composition. The required parameters include vertically resolved microphysical properties to translate retrieved AOD and aerosol type to mass, number concentration, and size distribution and to partition the transported aerosol into different aerosol components.

Table 2.1 ACE Aerosol Science Traceability Matrix

Themes	Focused Science Questions	Geophysical Parameters	Measurement Requirements	Mission Requirements
Sources, Processes, Transport, Sinks (SPTS)	Q1. What are key sources, sinks, and transport paths of airborne sulfate, organic, BC, sea salt, and mineral dust aerosol? Q2. What is the impact of specific significant aerosol events such as volcanic eruptions, wild fires, dust outbreaks, urban/industrial pollution, etc. on local, regional, and global aerosol burden?	Column: Q1 Q2 Q3 Q4 • $\tau_a(\lambda)$ • $\tau_{a,abs}(\lambda)$ • $m_a(\lambda)$ • $r_{eff\,a}(\lambda)$ • $v_{eff\,a}(\lambda)$ • Morphology Vertically Resolved: Q1 Q2 Q3 Q4 • $\tau_{a,abs}(\lambda)$ • $m_a(\lambda)$ • $r_{eff\,a}(\lambda)$ • $v_{eff\,a}(\lambda)$ • Morphology Cloud Top: Q3 Q4 • τ_c • $r_{eff,c}$ • $v_{eff,c}$ • Thermodynamic phase	High Spectral Resolution Lidar (HSRL) • Backscatter (355, 532, 1064 nm) • Extinction (355, 532 nm) • Depolarization (two wavelengths of 355, 532, 1064 nm) Imaging Polarimeter • Minimum 6 to 8 wavelengths spanning either UV or 410 nm to either 1630 nm or 2250 nm • Multiangle TBD, range ±50° • Polarization accuracy 0.5% • Combination polarized and nonpolarized channels • Resolution: 250 m in at least one channel	Integrated satellite, modeling, and data assimilation approach is required to meet science objectives. Expand high-resolution global and regional modeling capabilities to assimilate cloud and aerosol microphysical parameters such as number concentration and optical properties. Required ancillary data: • Land surface albedo map • Ground network $\tau_a(\lambda)$, shortwave and longwave F_d and F_{net} • Ground and airborne: column and vertically resolved $\tau_a(\lambda)$, $\tau_{a,abs}(\lambda)$, $m_a(\lambda)$ (2 modes), morphology, $P_{a,pol}(\theta)$ • Space measurements: Top of atmosphere shortwave and longwave F_u, collocated T(z), q(z), V(z), fire strength, frequency, location
Direct Aerosol Radiative Forcing (DARF)	Q3. What is the direct aerosol radiative forcing (DARF) at the top-of-atmosphere, within atmosphere, and at the surface? Q4. What is the aerosol radiative heating of the atmosphere due to absorbing aerosols, and how will this heating affect cloud development and precipitation processes?			
Cloud-Aerosol Interactions (CAI)	Q5. How do aerosols affect cloud micro and macro physical properties and the subsequent radiative balance at the top, within, and bottom of the atmosphere? Q6. How does the aerosol influence on clouds and precipitation via nucleation depend on cloud updraft velocity and cloud type? Q7. How much does solar absorption by anthropogenic aerosol affect cloud radiative forcing and precipitation? Q8. What are the key mechanisms by which clouds process aerosols and influence the vertical profile of aerosol physical and optical properties?	Vertically Resolved: Q5 Q6 Q7 Q8 P1. N_a P2. $\tau_{a,abs}(\lambda)$ P3. $r_{eff,a}$ P4. N_c P5. LWC P6. Precip Cloud Top: Q5 Q6 Q7 Q8 P7. Cloud top height P8. Cloud albedo P9. LWP P10. τ_c P11. $r_{eff,c}$ P12. Cloud radiative effect Cloud Base: Q5 Q6 Q7 Q8 P13. Cloud base height P14. Updraft velocity	**Threshhold (i.e. minimum)** **HSRL:** P1 P2 P3 P10 **Imaging Polarimeter:** P1 P2 P3 **W band Radar:** P4 P5 P7 P13 P14 **Narrow swath High-Resolution VIS-MWIR Imager:** P9, P11 *Baseline* (additions to threshold): W + Ka Band Doppler radar P6 P14	

The second theme addressed by the STM is the direct radiative aerosol forcing (DARF). Here ACE aims to provide firm, observationally-based estimates of DARF and its uncertainties with the ultimate goal of better constraining future climate predictions of DARF. ACE goes beyond addressing top of atmosphere (TOA) radiative forcing by providing global estimates of surface and within atmosphere, vertically resolved radiative forcing; the latter is especially important for representing how atmospheric heating by absorbing aerosols affects on cloud development and precipitation. In order to derive within-atmosphere DARF, a key ACE objective is for the first time to provide layer-resolved measurements of aerosol absorption from space. Here ACE goes well beyond current satellite measurement capabilities and provide a global, comprehensive dataset of three dimensional aerosol properties to constrain aerosol transport model estimates of globally averaged DARF within the atmosphere and at the top and bottom boundaries.

The third theme is to address the interactions between aerosols and clouds. These interactions include the impacts of aerosols on cloud micro- and macrophysical properties, and the degree to which clouds and precipitation impact aerosol concentrations. The ACE satellite measurements described in the STM are intended to provide strong constraints on the sensitivity of cloud radiative forcing and precipitation to aerosol number density, vertical distribution, and optical properties (e.g., absorption). ACE measurements are intended to constrain model representations of cloud microphysical and optical properties and model simulations of Cloud Condensation Nuclei CCN amount and aerosol absorption near clouds by providing observational targets that are comprehensively characterized. Here again, the detailed, vertically resolved measurements of aerosol optical and microphysical properties from ACE go well beyond the current satellite measurements of total column aerosol measurements. The ultimate goal is to assimilate ACE measurements into advanced earth system models representing aerosol and cloud microphysical processes, extending the information content of the measurements to conditions not directly observed by satellites (*e.g.,* under clouds).

In general, the geophysical parameters required for the three major themes are similar. The parameters listed in the STM are needed to characterize the optical and physical characteristics of the aerosol to specified accuracies, with a combination of satellite and suborbital measurements. The required aerosol characteristics include spectral optical thickness, spectral single scattering albedo, spectral phase function, and composition. These parameters are retrieved from the satellite measurements or derived from other parameters (e.g., size distribution, refractive index, nonsphericity) retrieved from the satellite measurements. In the case of direct radiative forcing and aerosol-cloud interaction themes, layer-resolved aerosol optical (scattering, absorption) and microphysical (e.g., effective radius, nonsphericity) properties are also required. The required spatial coverage for these measurements varies with objective. For example, while resolving global monthly mean trends in AOD and detecting decadal scale trends at continental scales can

likely be accomplished using narrow swath measurements, wider swaths will likely be required to reduce the uncertainties at regional and seasonal scales. Further studies regarding sampling should focus on the impact of measurements on aerosol radiative forcing and address aerosol absorption as well as AOD, and consider data assimilation as a tool for extending the usefulness of the data. Aerosol particle number concentration is an additional parameter required to specifically address aerosol-cloud interactions.

The ACE measurement requirements advances the state-of-the art of cloud and aerosol measurements and therefore are technologically ambitious. Even with these ACE measurements, there are important aerosol measurements that cannot be achieved from space. For example, particle water uptake (hygroscopicity), required to account for humidity-dependent particle optical property changes as well as particle activation conditions that initiate cloud formation, cannot be derived from remote-sensing observations. Similarly, *in situ* measurements are required to obtain aerosol Mass Extinction Efficiency (MEE), needed to translate between remote-sensing-derived particle optical properties and aerosol mass, which is the fundamental quantity tracked in aerosol-transport and climate models. And it is not clear how adequately even advanced remote-sensing instruments will constrain particle spectral light absorption properties, a key to simulating atmospheric heating profiles, cloud evolution, especially in polluted or smoky environments, distinguishing anthropogenic from natural particles, and assessing broader aerosol-climate effects. As there are always gaps in measurement spatial and temporal coverage, and variations in data quality, modeling provides the informed interpolation, extrapolation, and prediction required to complete the picture. Therefore, suborbital measurements, including systematic measurements of particle microphysical and chemical properties (e.g., Kahn et al., 2017), and a strong modeling component, are critical to address the ACE aerosol science objectives as well as to validate the ACE satellite measurements. The ACE aerosol STM calls for a combination of satellite and suborbital measurements, combined with a comprehensive data assimilation component, to advance the cloud/aerosol science and enable an advanced climate prediction capability, with reduced uncertainties.

2.2 Clouds

Among other objectives, the ACE measurement suite was designed to better constrain the characterization of cloud and precipitation microphysical properties. Understanding cloud and precipitation microphysical properties is critical to improving the representation of many physical processes in climate models, which are themselves poorly constrained at present. Uncertainties in the coupling between microphysical processes and atmospheric motions are the underlying cause of the large spread in cloud feedbacks and climate change uncertainty in today's climate models (Knutti et al., 2013; Klein et al. 2013; Stevens and Bony, 2013). To meet this objective, the ACE white paper that was completed in 2010 and updated in 2014 identified a diversity of measurements and sensors that, when combined synergistically (Posselt et al 2016; Mace et al., 2016, Mace and Benson., 2016),

would provide independent, vertically resolved, and vertically integrated constraints on near-cloud-aerosols, cloud/precipitation particle-size-distributions (PSDs), and cloud-scale vertical motion.

The ACE cloud science requirements and the imperative for multi-sensor synergy to meet those requirements have not changed since the original white paper was completed in 2010. The ACE team sought to develop a coherent and achievable strategy for accomplishing the science goals of ACE using innovative approaches that provide the required measurement synergy in the most efficient and cost effective means possible. Changes in the measurement requirements since the initial 2010 report were documented in the 2014 update due to advancements in both technology and data processing. These advancements would have allowed us to extract more information from a focused and streamlined set of measurements.

ACE cloud science objectives were directed at understanding microphysical processes that take place in the vertical column that convert aerosol particles to cloud droplets and to snowflakes and rain droplets within turbulent vertical motions in clouds. Understanding these processes continue to be the limiting factor in simulating the water cycle in the atmosphere (Stephens, 2005; Stevens and Bony, 2013). Put another way, the microphysical/dynamical processes that drive the aerosol indirect effects and cloud-precipitation microphysical processes in general, especially those that involve the ice phase, continue to be the major science motivation of ACE clouds; and all science questions continue to be derived from this motivation.

Clouds and associated precipitation have long been known to be integral components of the planetary energy balance, accounting for almost half of Earth's planetary albedo (e.g., Stephens et al. 2012). Changes in the statistics of global cloud properties in response to warming remain the largest uncertainty in accurately projecting the future climate response to anthropogenic forcing (Soden and Held 2006). The feedbacks due to changes in clouds and precipitation remain the single greatest source of spread in general circulation model (GCM) estimates of global climate sensitivity (Klein et al., 2013; Bony and Dufresne 2005; Zelinka et al. 2012, 2013).

The ACE Clouds Science Traceability Matrix

In this section we discuss the current state of modeling and observation of clouds and pose questions that might be addressed by future observing platforms, including both satellite missions and field experiments. Our focus here is on the thermodynamic-dynamic-microphysical-radiative process coupling that controls the occurrence of clouds and their areal coverage when present and thus determines their feedbacks under climate change. However, there is always sufficient aerosol to nucleate liquid-phase clouds, and thus indirect effects only become relevant after the dynamics and thermodynamics initiates cloud formation. This differs markedly

from the situation for cirrus where nucleation itself is poorly understood because the concentration and properties of nucleating aerosols in the upper troposphere is poorly known. Indeed, the documented compensating forcing and feedback errors that allow many GCMs to correctly simulate the 20th Century temperature record (Kiehl 2007; Forster et al. 2013) can be thought of as two sides of the cloud problem – forcing uncertainty due to aerosol indirect effects and feedback uncertainty due to dynamic and thermodynamic processes and their interaction with radiation.

It has become clear that there is a natural break in measurement strategy between shallow clouds that can be strongly influenced by aerosol and deeper cloud systems where "nearby" aerosols can't be observed and where ice microphysics tend to be important. Accordingly, ACE cloud science questions divide naturally into aerosol-cloud, cloud-radiation and cloud-precipitation themes according to the measurements needed to address those questions.

ACE science objectives are focused on microphysical processes that take place in the vertical column, converting aerosol particles to cloud droplets and to snowflakes, ice crystals, and rain droplets within turbulent vertical motions. Understanding these processes continues to be the limiting factor in simulating the water cycle in the atmosphere. The microphysical and dynamical processes that drive the 1st and 2nd aerosol indirect effects and cloud-precipitation microphysical processes continue to be the major science motivation of ACE clouds. Of special interest and importance are questions that involve ice phase processes.

With a natural break in measurement strategy occurring between shallow clouds that can be strongly influenced by aerosol (1st and 2nd indirect effects), and deeper cloud systems where "nearby" aerosols cannot be observed and where ice microphysics tend to be important, ACE science questions were divided along aerosol-cloud and cloud-precipitation themes according to the measurements needed to address them. In the following paragraphs, we discuss issues that cut across both classes of questions and broad priorities, then we consider how measurement needs differ between aerosol-cloud, cloud-precipitation and cirrus clouds. A simplified Science Traceability Matrix is presented following this discussion. Throughout the text, we pay special attention to the evolution in our thinking that has influenced the final revised STM and overall mission strategy.

The ACE Clouds STM is constructed around the realization that the processes that couple atmospheric motions to cloud and precipitation processes are the fundamental issues that underpin uncertainty in climate prediction (Bony and Dufresne, 2005; Dufresne and Bony, 2008; Stevens and Bony, 2013). While the details of these processes vary across cloud genre (i.e. cumulus, stratocumulus, cirrus, altostratus, etc.), a distinct need for furthering our understanding of these processes is quite independent of cloud type and our final STM (Table 2.2) , therefore, utilizes a general framework independent of cloud type but focused on the aerosol-cloud-precipitation nexus.

The revised ACE clouds STM is organized around overarching scientific themes (left-most column). These themes range from how the overall three-dimensional distribution of clouds and precipitation may be changing to what the distributions of cloud and precipitation microphysical properties are. As mentioned, we are particularly interested in the processes that cause populations of cloud droplets and ice crystals to evolve into precipitation – in particular how aerosol and atmospheric motions modulate and feedback on these processes (i.e. Mace and Abernathy, 2016; Mace and Avey, 2016). Ultimately, what we learn from ACE measurements and associated modeling studies will help us to understand better the energetics of the earth's atmosphere or just how clouds and precipitation participate in the poleward transport of energy and how that may be changing as the climate system evolves.

Addressing these themes ultimately comes down to science questions for which rigorous answers can be formulated from ACE measurements. We present 4 broad categories of questions that are drawn from a 2014 community white paper entitled *Outstanding Questions in Atmospheric Composition, Chemistry, Dynamics and Radiation for the Coming Decade*, available from:

https://espo.nasa.gov/home/content/NASA_SMD_Workshop

These questions are focused on the role of clouds and aerosol in understanding climate sensitivity, changes to shortwave and longwave climate forcing, and the processes that control the water cycle and energetics of the climate system. A careful reading of the clouds, radiation, aerosol, and convection sections of the Ames 2014 whitepaper, where these questions are discussed in detail, suggests that answers to them rest on better observations of cloud and precipitation microphysics, cloud-scale vertical motion, and aerosol microphysics.

What geophysical parameters are needed to address the ACE science questions are listed in the STM and referenced back to the science questions and themes. Broadly, these geophysical parameters include cloud and precipitation microphysics, vertical motion, aerosol, and radiative properties that will allow us to derive heating rate profiles as well as top of atmosphere and surface radiative budgets. Using italicized and bold fonts, we suggest the notional trades that would occur if a threshold set of instruments were used instead of a more aggressive baseline set of instruments. The threshold set of measurements will allow us to retrieve geophysical parameters that address many if not most of the science questions while the baseline mission would allow for more accurate geophysical parameter retrievals over a broader range of conditions.

A centerpiece of the ACE instrument suite is a dual frequency Doppler cloud radar that will operate in the Ka and W bands. The ACE radar combines the CloudSat and GPM capabilities and goes well beyond what either of those instruments could accomplish scientifically. This radar will also include passive radiometer capabilities that allow for passive microwave measurements at least along the nadir track that will enable accurate retrievals of cloud and precipitation properties in optically

deep cloud systems such as fronts and shallow convection. Additionally, radar and microwave retrievals of many cloud types benefit greatly by knowing the visible and near infrared reflectances because they constrain cloud droplet properties in the upper portions of many cloud types where the radar and microwave retrievals are challenged by the small droplet sizes. Combined with a High Spectral Resolution Lidar, the visible measurements will provide threshold constraints on the surrounding aerosol. While this set of measurements is here characterized as a threshold or minimum set, we must note that this minimum set goes well beyond the capabilities of the A-Train, GPM, or EarthCare and would allow for significant advances in our understanding of cloud and precipitation processes.

The baseline set of instruments includes various options each of which will incrementally either enhance the accuracy of retrieved geophysical parameters or broaden of the scope of the cloud types we can address. (Table 2 describes what measurements constrain specific aspects of cloud and precipitation microphysics) For instance, adding a third frequency to the ACE radar allows for probing deeper precipitating systems such as heavily raining convection and frontal systems. Adding a polarimeter and an HSRL lidar will enhance some cloud retrievals but will primarily benefit our understanding of the near-cloud aerosol properties that are a critical aspect of many of our science questions. Additional passive constraints provided by higher microwave frequencies or sub-millimeter radiometers would enhance ice-phase precipitation retrievals in deeper convective systems and allow for more accurate characterization of high latitude snowfall.

Table 2.2 ACE Cloud Science Traceability Matrix

Themes	Focused Science Questions	Geophysical Parameters	Measurement Requirements	Mission Requirements
T1. Morphology **Document occurrence, macroscale structure, and decadal scale changes of clouds and precipitation and their interaction with large-scale meteorological and thermodynamic forcing.**	**Q1. Climate Sensitivity** **What is the sensitivity of the climate system to cloud structure and variability? T1 T2 T3 T4** • *What is the role of natural and anthropogenic aerosol in modulating cloud system occurrence and properties? T1* • **What microphysical processes dictate the lifecycle and coverage of clouds under various atmospheric conditions? T1 T2** • *What dictates the processes that cause and modulate precipitation in cloud systems? T3*	GP1. **Hydrometeor Layer Detection** Q1 Q2 Q3 Q4 GP2. *Simultaneously occurring* **Cloud and Precipitation Thermodynamics Phase profile** Q1 Q2 Q3 Q4 GP3. *Simultaneously occurring* **Cloud and precipitation microphysical properties profiles (Water Content, particle sieze, and number concentration)** Q1 Q2 Q3 Q4 GP4. **Precipitation Rate Profile in light** *and heavy (>5 mm/hr)* **precipitation** Q1 Q2 Q3 Q4 GP5. **Profiles of Cloud Optical Depth,** *single scattering albedo, and asymmetry parameter* Q1 Q2 Q3 Q4 GP6. **Surface, TOA Cloud Radiative Effects** Q1 Q2 Q3 Q4 GP7. **Latent Heating Profile in light** *and heavy (>5 mm/hr)* **precipitation** Q1 Q3 Q4 GP8. *Radiative Heating Profile* Q1 Q2 Q3 Q4 GP9. **Cloud-Scale Vertical Motion** Q1 Q4 GP10. *Aerosol/CCN number concentration profile* Q1 Q2 Q3	**M1. M2. Threshold Mission** **TM1. 2-Frequency (W- , Ka-bands), Scanning Doppler Radar (with radiometer channels)** GP1 GP2 GP3 GP4 GP5 GP6 GP7 GP8 GP9 TM2. **High Spectral Resolution Lidar** GP1 GP2 GP3 GP5 GP6 GP8 GP10 TM3. **Narrow Swath Vis Imager (0.6 microns, 1.6 microns, 2.1 microns)** GP2 GP4 GP5 GP6 GP8 GP10 *Baseline Mission* *BM1. 3-Frequency (W- , Ka-, Ku-bands), Scanning Doppler Radar (with radiometer channels)* GP1 GP2 GP3 GP4 GP5 GP6 GP7 GP8 GP9 *(replaces TM1)* *BM2. High Spectral Res. Lidar (HSRL)* GP1 GP2 GP3 GP5 GP6 GP8 GP10 *(replaces TM2)* *BM3. High Resolution Narrow Swath VNIR-SWIR Polarimeter* GP6 GP8 GP10 *(Replaces TM3)* *BM4. Narrow Swath High Freq. (183, 389 GHz) Microwave* GP2 GP3 GP4 GP5 GP6 GP7 GP8	We define the **threshold** ACE Clouds Mission as those elements of this matrix that are in **bold font**. We suggest that boldface science objective and questions in columns 1 and 2 could ultimately be addressed by the measurements listed as the Threshold Mission in the Measurement Requirements Column. Elements of this matrix in *italicized font* are defined as a *Baseline Mission* and designate important science questions that require a more aggressive set of coordinated measurements that are listed in italicized font. The set of baseline and threshold ACE clouds retrieval algorithms will be synergistic such that multiple measurements contribute to the retrieval of a geophysical parameter. For instance while microwave brightness temperatures cannot generally be used to retrieve cloud microphysics, when passive microwave is combined with multi frequency Doppler radar, the microwave brightness temperatures provides an important constraint on the retrieval algorithm.
T2. Microphysics **Document the microphysical properties of liquid, ice, and mixed phase clouds and precipitation with a specific focus on high latitude snow and light liquid precipitation (less than 1 mm/hr) at all latitudes that influences cloud morphology and lifecycle and ultimately radiative balance.**	**Q2. Climate Forcing – Solar (T4)** **How will shortwave cloud forcing change as the climate warms? T1 T2 T3 T4** • **Will the coupling between cloud occurrence and morphology with atmospheric motions and thermodynamic structure result in fundamental changes to the planetary albedo? T1 T2** • *What is the specific role of aerosol in modulating the properties of clouds and the planetary albedo under a changing climate? (T2, T3)*			
T3. Microphysical Processes **Identify the occurrence of microphysical processes that cause changes to profiles of aerosol, clouds, and precipitation properties.** *Concurrently quantify the process rates of important microphysical processes such as autoconversion and accretion in liquid and ice-phase stratiform and convective clouds.*	**Q3. Climate Forcing – Infrared (T4)** **How will longwave cloud forcing change as the climate warms? T1 T2 T3 T4** • **What is the coupling between thermodynamic structure convective processes and the properties of convective anvils in modulating the coverage and properties of tropical anvil cirrus T1 T2 T3** • *What is the role of aerosol in changing the microphysical properties of tropical anvils and modulating their coverage, persistence, and feedbacks to the water cycle in the upper troposphere?* **T1 T2 T3**			
T4. Energetics *Understand the maintenance of and changes to the energetic balance of the atmosphere and earth system due aerosol, clouds, and precipitation.*	**Q4. Water Cycle and Energy Transport (T4)** **What is the role of cloud processes (specifically mixed phase) in snow and rain production in middle and high latitude cloud systems? T1 T2 T3 T4** • **What role does the seasonal cycle of middle latitude cloud radiative forcing play in the poleward transport of heat and how is this radiative forcing partitioned as function of cloud genre? T4** • *To what degree do various microphysical processes when coupled with large-scale dynamics modulate the precipitation production within middle and high latitude frontal systems? T2 T3* • **What is the role of convection versus large-scale dynamics in producing precipitation in the middle and high latitudes? T1 T3**			

Further Discussion and Justification of the ACE Clouds Science Traceability Matrix
Rapid improvements in computing power is allowing global models to approach the cloud resolving scale (Myamoto et al., 2013; Satoh et al., 2008) where convective processes can be resolved and the need for convective parameterizations are diminished (Larson et al., 2012). While it will be some years before global Cloud Resolving Models (CRMs) can be used as true climate models, CRMs are still considered the tool by which traditional coarse resolution climate models can be improved and this improvement will come through statistical representations of cloud microphysics on the GCM grid scale. Therefore, understanding microphysical processes globally is relevant now and will be increasingly important as we move through the 2020's. The ACE questions, therefore, focused on small spatial scales (~ 100's of m) and finely resolved vertical scales (~10's of m) that are typical of CRM or Large Eddy Simulations (LES). In short, high-resolution (~100 to 500 m scale) observations of microphysical processes were considered to be critical. Likewise, since our target theoretical audience is the CRM/LES communities where high-resolution cloud measurements can be assimilated directly, we sought measurements that would cover a swath that is several 10's to 100 km wide along a suborbital track.

In terms of passive microwave measurements, it was thought that most of the ACE cloud requirements could have been provided by including radiometer channels on the radars so that microwave brightness temperature (Tb) at the radar frequencies were collected only along the swath sampled by the radar. If this were the case, stand-alone microwave imagers would not have been required to address ACE-clouds measurement needs. The trade space between the coarse spatial resolution but high accuracy provided by traditional microwave sensors and a footprint that is, by definition, perfectly matched to that of the radar measurements should be carefully examined since not requiring standalone microwave imagers would have significantly reduced the complexity and cost of ACE. It is possible that the radiometer channels on the radar would have been preferable to the more accurate but larger footprints from traditional radiometer measurements - especially in broken cloud fields. Higher frequency microwave (i.e. beyond the highest frequency of the ACE radar - 94 GHz) and sub-millimeter radiometer measurements would be a major benefit to many of the science questions but were not considered as part of the baseline mission. Such high frequency and sub-millimeter measurements could be provided by international partners or otherwise launched independently of ACE and managed as part of a satellite formation or constellation. The A-Train is an excellent example of such a constellation that coalesced opportunistically over time.

As mentioned earlier, our goal was to formulate an ACE mission that addressed the science needs of the Aerosol-Cloud-Precipitation-Ocean Ecosystem communities in the coming decade but that was also achievable in terms of cost and complexity. One approach that could have been considered was to seek natural divisions in the science applications that could, for instance, have allowed for exploitation of natural synergies among measurements. Another approach to an implementation of ACE

was to exploit opportunities for collaboration and synergy. The PACE mission, for instance, afforded one such opportunity. Using PACE as a foundation, an HSRL and Doppler cloud radar flying in formation with PACE would allow ACE to address most, if not all, of the science questions originally posed in the 2010 white papers in addition to addressing emerging science such as ocean-lidar. Exploiting this synergy would require some compromise among the various disciplines but the end result would be a constellation that is truly an advance over the A-Train that would push NASA Earth observational science into the 2020's and beyond.

Aerosol-Cloud Questions

Consensus emerged within the broader community (e.g., IPCC 2013, Chapter 7) that 1) differences in climate sensitivity among models are due to differences in their simulation of shallow marine boundary layer clouds and 2) the primary mechanisms by which aerosol impacts climate is via the process level perturbations within these shallow convective clouds. The aerosol indirect effects are known by various nomenclature. The first (Twomey, 1974) and second (Albrecht et al, 1989) aerosol indirect effects are conceptually simple but very difficult to document observationally. This is because the processes that result in the indirect effects are microphysical in nature taking place at the scales where aerosol evolves into cloud drops and cloud drops into precipitation. These processes typically occur within optically thick hydrometeor columns in often broken cloud fields, and vary rapidly with height over depth scales of a few hundred meters. As such, these effects are largely beyond the reach of traditional passive remote sensing. All studies claiming observational evidence of these effects have necessarily diagnosed them by how the effects are hypothesized to change the broader cloud field.

The indirect effects of aerosol on clouds are expected to be particularly large in boundary layer clouds such as shallow stratocumulus and cumulus that are ubiquitous across the global oceans from the tropics to the high middle latitudes of both hemispheres (Rosenfeld et al., 2014). Uncertainties in the feedbacks of these clouds as they interact with aerosol and changing circulation under climate change are the primary contributors to uncertainty in predictions of the climate response to doubled CO2 (Soden and Vechi, 2011). Progress in the last eight years in this area has been realized primarily through modeling work and analysis of data from the A-Train. The paper by Stevens and Feingold (2009) and references therein demonstrate, using both modeling and A-Train measurements, the importance of dynamical feedbacks (buffering) that exist between aerosol, shallow clouds, and precipitation that modulate the 1st and 2nd aerosol indirect effects in a cloud field. For example, LES studies have shown that clouds that are perturbed by higher aerosol concentrations, become deeper, precipitate more intensely, and result in stronger downdrafts with higher wind at the surface (Mace and Abernathy, 2016; Koren et al., 2014; Xue et al., 2008).

The lessons to be learned are that a cloud field observed in nature at a particular instant has a history that includes repeated processing of aerosol through cloud

elements within large-scale dynamical environments. A field of cumulus or stratocumulus observed by orbiting satellites is a snapshot of a changing system that is responding at the instant of measurement to a perturbed and buffered environment that has been and is undergoing modification by the cloud processes and large-scale motions.

This complexity is a strong argument for global satellite measurements since it will take time to build statistical portraits of cloud fields in various states of evolution especially over remote regions of the global oceans (Mace and Avey, 2016). While field program case studies are useful and necessary, they are not sufficient in terms of either duration or number of cases needed to provide robust statistics. Such limitation is evidenced by the diverse range of contradictory findings that has emerged from recent field experiments seeking to quantify aerosol indirect effects. A satellite-based measurement strategy, therefore, must include data relevant to the changing system that can be assimilated by models that resolve the motions and processes within cloud elements. For shallow convective and stratiform clouds relevant to this class of questions, dual frequency Doppler radar (Ka and W bands) is desirable. However only single frequency W band Doppler radar would likely be considered required (see the aerosol STM) because the dual frequency information in shallow, weakly precipitating clouds is minimal and Ka-band radar will often not provide the required sensitivity to sample these clouds effectively. In addition, high spatial resolution microwave (perhaps provided by the radar), and visible reflectances in a few bands that contain independent information (Nakajima and King, 1990) are critically important for retrieval of cloud properties here, as is information regarding the regional aerosol background that require some combination of lidar (ideally HSRL) and polarimetric visible reflectances as discussed in the aerosol section. Knowledge of the chemical composition and CCN distribution that HSRL and polarimetry could provide (i.e. ultimately composition of the aerosol that act as cloud condensation nuclei) is likely necessary to fully address the 1st and 2nd aerosol indirect effects in shallow cumulus and stratocumulus.

Cloud-Precipitation Questions

The Cloud-Precipitation questions tend to focus on deeper clouds (e.g. frontal layer clouds, moderately deep to deep convection) where ice phase processes that result in precipitation are important to the evolution of the cloud system. Even the most advanced CRMs contain many processes that require observational constraints. For instance, changes in droplet breakup parameterizations, ice crystal collection and riming efficiencies (among others) and their dependence on vertical motion can cause drastic (many hundreds of percent) differences in surface rain/snow accumulations and result in feedbacks on the dynamical environment via latent heat release that totally change the predicted evolution of the cloud field (Van Den Heever et al., 2011). These sensitivities extend across the synoptic spectrum from tropical convective clouds to stratiform rain, to frontal systems and stratiform clouds in the middle and high latitudes (e.g. Adams-Selin et al., 2013; Igel et al., 2013; Saleeby and van den Heever, 2013).

Multi frequency Doppler radar with collocated microwave Tb are fundamental to the measurement strategy needed to address cloud-precipitation centric science questions (Mace and Benson, 2016; Posselt and Mace, 2014). While our earlier thinking focused on dual frequency Ka/W band Doppler radar, the addition of Ku band greatly extends the reach of our science focus into cloud systems that are much deeper and more heavily precipitating. We now include Ku band as an option in the baseline STM. Similarly, higher frequency microwave measurements (> 89 GHz) will provide important constraints on the ice microphysics. However, the quantitative benefit of such measurements when combined with multi- frequency radar has not yet been demonstrated. We therefore, list high frequency microwave and sub-millimeter measurements as part of a threshold mission that could be provided by international partners or other sources. For most of the cloud-precipitation objectives of ACE Clouds, lidar measurements are not as relevant because a lidar attenuates in the first few optical depths of clouds that are very optically thick. Furthermore, these cloud systems tend to be much larger in scale (extending to 1000's of km) making it impossible to constrain the local aerosol environments in which they develop with lidar or polarimeter measurements. Alternative means such as data assimilation will therefore be needed to provide aerosol information in such systems should it be desirable to examine the second-order effects induced by aerosols on these more energetic systems.

Cirrus

We address cirrus as a separate category. Cirrus tend to be optically thin, horizontally extensive, and the role of aerosol is uncertain but likely second order. Cirrus with optical depths less than two drive the radiative heating in the tropics (Berry and Mace, 2014) and it is widely accepted that tropical cirrus impose a positive feedback on a warming climate because tropical cirrus will detrain from deep convection at a constant temperature while the surface warms (Zelinka and Hartmann, 2012). While all models tend to generate this positive feedback, the reason for this agreement is not clear and it is not known if this result is fortuitous or if the global magnitude of this feedback is physically reasonable. Improved understanding of deep convective processes that result in detrainment of ice to the tropical upper troposphere will likely improve our understanding of the role of tropical cirrus in climate change.

Lidar-radar synergy is maximized in thin cirrus near optical depth one (Berry and Mace, 2014) so that both radar and lidar are needed to describe them. However, the specific role of HSRL measurements in addressing cirrus processes remains to be determined. The key science questions here are what controls the amount of ice detrained from deep convection and what processes cause anvils to evolve into self maintaining cirrus layers. Most cirrus questions could be addressed with either the baseline or threshold measurement strategies listed above. For instance, single or dual frequency Doppler radar at W and Ka bands combined with lidar that is considered critical to the aerosol-cloud questions would provide significant and

unique information regarding thin cirrus while thicker cirrus beyond optical depth 10 or so would be informed by the clouds-precipitation measurement objectives.

2.3 Summary

The set of important questions that underpin the uncertainty in climate change projections due to aerosols, clouds and precipitation, and the fundamental approach of the ACE Cloud Working Group to addressing those questions matured significantly in the final years of the ACE program.

We recognize that aerosol-cloud-precipitation processes remain one of the principal underlying causes for uncertainties in climate predictions. To make further progress, these processes require synergistic, vertically resolved, active lidar and radar combined with passive microwave and solar reflectance measurements. The goal for those measurements is to provide better constrains on atmospheric, hydrological, and related processes to ultimately improve future generations of climate models. Unfortunately, no single measurement can thoroughly address process-oriented questions. Those processes are complex and spatially heterogeneous and relate to multiple related processes. As an example, some processes depend on cloud and aerosol microphysical properties, as well as their interactions with the thermodynamic environment across a range of scales. The A-Train satellite constellation has demonstrated that the combination of multiple disparate measurements provides significant measurement synergies and help to advance our understanding well beyond the original scope of any of the single missions.

Instrument	Measurement	Cloud Microphysical Constraint	Additional Information and Comments
Backscatter Lidar High Spectral Resolution Lidar (HSRL)	Extinction, Single Scatter Albedo	• Attenuated Backscatter profiles in thin clouds • Aerosol properties in vertical profiles • Aerosol Composition	• Produces direct evaluation of optically thin cloud and aerosol extinction and aerosol single scattering properties • Provides information on cloud-top-height and more generally insight into vertical structure of thin cloud and aerosol.
Multi Frequency Doppler Radar W/Ka Bands With Ku band	Radar Reflectivity	• Vertically resolved 6th moment of cloud drop size distribution for particles less than 0.1 of the radar wavelength • Differential response to large hydrometeors • Ku provides additional information on heavy precipitation	• Differential frequency radar reflectivity and Doppler velocity for larger particles (> ~0.3 mm) can be used to identify the presence of such particles and help characterize the microphysics of this part of the distribution. • Differential attenuation with respect to 94 GHz is likely to prove useful in identification of cloud and precipitation type (phase) and retrieval of precipitation water content. • Dual-wavelength ratios at Ka-W and Ku-W bands can further discriminate ice species: snow, graupel, and hail

			improving ice water content retrieval accuracy
	Doppler Velocity	• Vertically resolved 2nd/3rd moment of drop size distribution (reflectivity weighted) • Differential response in presence of large hydrometeors.	• Doppler velocity is a measure of total velocity of the cloud particles. In convective cores, the velocity is dominated by cloud vertical motion. In other conditions, the velocity can be separated into contributions from particle fall velocity and air motion (Dynamics). • Cloud liquid water drops generally fall too slowly to be measured via this technique but it is very useful for identification, and characterization of ice clouds, snow, drizzle, and rain. • Ku Band desired to characterize heavy precipitation
	Differential Attenuation, Path Integrated and Vertical Profile	• Profile of Condensed Water • Total column liquid water path.	• One can use surface reflectance to estimate total attenuation in the radar in the column, when the radar is not totally attenuated. The attenuation is determined largely by the amount of liquid water (cloud and precipitation) in the column.
	Radiometer Channels	• Passive microwave Tb	• Constrains integrated liquid water and ice scattering.
Narrow Swath Vis-IR Imager High-Resolution VIS-SWIR Polarimeter	UV, Visible and shortwave infrared radiances at multiple view angles. Polarized reflectances at some visible wavelengths.	• Cloud phase near "cloud top" (in region of cloud where bulk of visible light is reflected) • Radiative-effective ice cloud-habit (constrains possible/likely cloud habit mixtures) near "cloud top". • 2nd moment of drop size distribution near cloud top) • Effective radius near cloud top.	• Multi-view-angle imagery can be used with stereo-imaging technique to derive cloud top height. This approach is insensitive to calibration and does not rely on any assumptions regarding atmospheric temperature lapse rate. The approach works well except for exceptionally diffuse high clouds, representing a failure rate of only a few percent. 50 m resolution images can be used to determine cloud-top-height with precision of about 50 m assuming view angles at +/- 45 degrees from nadir. • Important for defining aerosol type in broken cloud fields • Reflectances constrain column optical depth and effective radius.

Passive Low and High Frequency Microwave Radiometer Channels at: 10.65, 18.7, 23.8, 36.5, 89, 166.5, 183±3, 183±9 GHz	Brightness temperature	• Column liquid water path • Column water vapor path • Surface precipitation rate in wide swath • Ice cloud and ice precipitation • Important wide swath • Significant constraints for nadir viewing	• Column constraint • Will provide wide-swath / cloud system context to narrow-swath observations and in particular information on precipitation. • With radiometer channels on radar, these instruments are considered to be not required.
Passive Sub-mm Radiometer Channels at high frequency: 325.15, 448.00, 642.90, 874.40 GHz	Brightness temperature	• Column ice and particle size constraint for ice clouds; • Proportional to the 3rd moment of particle size distribution	• Column constraint • Will provide wide-swath / cloud system context to narrow-swath observations. • These measurements are not required. Could be provided by partnership.

Table 2.3. Potential ACE Instruments and Measurements and their contribution to Level 1 Geophysical Parameters. The instruments that we consider required are denoted in bold font. Italicized font indicates goals or non-required instruments for ACE Clouds.

2.3 Ocean Biology and Biogeochemistry

The Ocean Ecosystem STM synthesizes the end-to-end requirements associated with addressing 6 groups of overarching *Focused Questions*:

1. What are the standing stocks, composition, & productivity of ocean ecosystems? How and why are they changing? [OBB1]
2. How and why are ocean biogeochemical cycles changing? How do they influence the Earth system? [OBB2]
3. What are the material exchanges between land & ocean? How do they influence coastal ecosystems, biogeochemistry & habitats? How are they changing? [OBB1,2,3]
4. How do aerosols & clouds influence ocean ecosystems & biogeochemical cycles? How do ocean biological & photochemical processes affect the atmosphere and Earth system? [OBB2]
5. How do physical ocean processes affect ocean ecosystems & biogeochemistry? How do ocean biological processes influence ocean physics? [OBB1,2]
6. What is the distribution of algal blooms and their relation to harmful algal and eutrophication events? How are these events changing? [OBB1,4]

Each of these science questions traces directly to one or more of the four broader science objectives of NASA's Ocean Biology and Biogeochemistry (OBB) program, as defined in the document, *Earth's Living Ocean: A Strategic Vision for the NASA Ocean Biological and Biogeochemistry Program*, and indicated above by the bracketed OBBx designations.

To answer the *Focused Questions*, the ACE Ocean Ecosystem team defined a multi-tiered approach involving remote sensing observations, supporting field and laboratory measurements, and ocean biogeochemical-ecosystem modeling, with 9 groups of specific objectives:

1. Quantify phytoplankton biomass, pigments, optical properties, key groups, and productivity using bio-optical models and chlorophyll fluorescence
2. Measure particulate and dissolved carbon pools, their characteristics and optical properties
3. Quantify ocean photobiochemical and photobiological processes
4. Estimate particle abundance, size distributions (PSD), and characteristics
5. Assimilate ACE observations in ocean biogeochemical model fields of key properties (air-sea CO_2 fluxes, export, pH, etc.)

6. Compare ACE observations with ground-based and model data of biological properties, land-ocean exchange in the coastal zone, physical properties (e.g., winds, SST, SSH, etc), and circulation (ML dynamics, horizontal divergence, etc)

7. Combine ACE ocean & atmosphere observations with models to evaluate (1) air-sea exchange of particulates, dissolved materials, and gases and (2) impacts on aerosol & cloud properties

8. Assess ocean radiant heating and feedbacks

9. Conduct field sea-truth measurements and modeling to validate retrievals from the pelagic to near-shore environments

These specific objectives were then traced to the measurement/instrument requirements for the relevant ACE satellite sensors, supporting field and laboratory activities, and modeling. Also identified were specific ACE platform requirements and ancillary supporting global data products from other missions, models, and field studies (see right columns in Ocean STM below).

The three primary instruments on the ACE platform(s) relevant to the mission's ocean ecosystem science objectives are the advanced ocean radiometer, lidar, and polarimeter. In addition to the ACE science team meetings, the ACE Ocean Ecosystem team conducted roughly weekly teleconferences to define the specific measurement and instrument requirements, with outcomes from these deliberations recorded in a series of documents and publications. The team assumed a 'grass roots' approach, beginning with the production of individual Product Assessment Reports for each ocean geophysical property targeted by the ACE instruments. These reports provided detailed descriptions of the derived parameters, their field measurement methodologies, product error analyses, and accuracy assessments.

The ACE Ocean Ecosystem team next constructed a summary table of targeted ocean-relevant properties. These properties include (1) spectral remote sensing reflectance, (2) inherent optical properties (total absorption, phytoplankton absorption, detrital absorption, colored dissolved organic material absorption, backscatter coefficient, beam attenuation), (3) diffuse attenuation coefficient for downwelling plane irradiance at 490 nm, (4) 24-hr flux and instantaneous incident photosynthetically available radiation, (5) surface ocean euphotic layer depth, (6) particulate inorganic carbon concentration, (7) particulate organic carbon concentration, (8) dissolved organic carbon concentration, (9) suspended particulate matter concentration, (10) particle size characteristics, (11) total chlorophyll-a concentration, (12) phytoplankton carbon concentration, (13) normalized fluorescence line-height, (14) fluorescence quantum yield, (15) net primary production, (16) phytoplankton chlorophyll:carbon ratios and growth rate, and (17) phytoplankton functional/taxonomic groups. For each of these 14

properties, the summary table *defined the baseline and threshold value ranges for ACE retrievals*, along with documenting the basis for these range estimates (Cetinic et al 2018).

In addition to the above activities, the ACE Ocean Ecosystem team conducted model simulation studies to identify measurement requirements for the ACE ocean radiometer near-infrared (NIR) and short-wave infrared (SWIR) bands and, using a state-of-the-art spectral inversion algorithm, to define spectral signal-to-noise requirements. Results from all of these activities were synthesized in an ACE Ocean Ecosystem white paper, summarized as the Ocean Ecosystem STM (copied below), and recently published in Cetinic et al (2018).

The ACE Ocean Ecosystem white paper and STM provided the needed framework for conducting a very thorough evaluation of instrument requirements for an advanced ocean radiometer, which was published in 2011 (Meister, et al. 2011). The timing of this publication was ideal, as it appeared in parallel with early deliberations of the Pre-Aerosol Cloud Ecosystem (PACE) Science Definition Team (SDT). Multiple members of the ACE Ocean Ecosystem team were also members of the PACE SDT and the Meister et al (2011) document served as a key reference in defining baseline and threshold requirements for the PACE instrument/mission. The final, 274 page PACE SDT recommendation document provides the most thorough recommendation guidelines for an advanced ocean radiometer suitable for the PACE and the ACE missions.

With respect to lidar and polarimeter measurements for ACE ocean science objectives, significant advances have been realized. In 2013, the first global assessment of ocean plankton stocks using the CALIOP lidar was published (Behrenfeld et al. 2013). Subsequently, CALIOP ocean retrievals were used to study annual cycles of phytoplankton biomass in the polar regions, where traditional satellite ocean color measurements are extremely challenging and for some months impossible (Behrenfeld et al. 2013). Following these and other studies, a recent review of ocean remote sensing with satellite lidar was published and provides a detailed evaluation of measurement requirements for an ACE lidar (Hostetler et al. 2018). With respect to polarimetry measurements, Remer et al (2015) provided a detailed summary of measurement requirements and science advantages.

In summary, the ACE Ocean Ecosystem team conducted end-to-end evaluations of mission measurement requirements necessary to address the 6 groups of overarching *Focused Science Questions*. These evaluations began with an basic assessment of state-of-the-art accuracies and uncertainties in field measurements of targeted key ecosystem properties and then step-wise extended to a very detailed evaluation of satellite instrument requirements and requirements for supporting field, laboratory, and modeling work. Benefitting from the parallel assessments of the PACE SDT, the Ocean Ecosystem team concluded that overall understanding of observational requirements for the Ecosystem aspects of the ACE mission is highly mature.

Ocean Ecosystems STM

Goddard Space Flight Center

Category	Focused Questions*	Approach	Maps to Science Question	Measurement Requirements	Instrument Requirements	Platform Requir'ts	Other Needs
Ocean Biology	1 What are the standing stocks, composition, & productivity of ocean ecosystems? How and why are they changing? [OBB1] 2 How and why are ocean biogeochemical cycles changing? How do they influence the Earth system? [OBB2] 3 What are the material exchanges between land & ocean? How do they influence coastal ecosystems, biogeochemistry & habitats? How are they changing? [OBB1,2,3] 4 How do aerosols & clouds influence ocean ecosystems & biogeochemical cycles? How do ocean biological & photochemical processes affect the atmosphere and Earth system? [OBB2] 5 How do physical ocean processes affect ocean ecosystems & biogeochemistry? How do ocean biological processes influence ocean physics? [OBB1,2] 6 What is the distribution of algal blooms and their relation to harmful algal and eutrophication events? How are these events changing? [OBB1,4]	Quantify phytoplankton biomass, pigments, optical properties, key groups (functional/HABS), and productivity using bio-optical models & chlorophyll fluorescence	1 2 6	**Ocean Radiometer** Water-leaving radiances in near-ultraviolet, visible, & near-infrared for separation of absorbing & scattering constituents and calculation of chlorophyll fluorescence Total radiances in UV, NIR, and SWIR for atmospheric corrections Cloud radiances for assessing instrument stray light	• 5 nm resolution 350 to 755 nm ▷ 1000 – 1500 SNR for 15 nm aggregate bands UV & visible and 10 nm fluorescence bands (665, 678, 710, 748 nm centers) ▷ 10 to 40 nm width atmospheric correction bands at 748, 765, 820, 865, 1245, 1640, 2135 nm • 0.1% radiometric temporal stability (1 month demonstrated prelaunch) • 58.3° cross track scanning • Sensor tilt (±20°) for glint avoidance • Polarization insensitive (<1.0%) • 1 km spatial resolution @ nadir • No saturation in UV to NIR bands • 5 year minimum design lifetime	Orbit permitting 2-day global coverage of ocean radiometer measurements Sun-synchronous orbit with crossing time between 10:30 a.m. & 1:30 p.m. Storage and download of full spectral and spatial data Monthly lunar calibration at 7° phase angle through Earth observing port	Global data sets from missions, models, or field observations: *Measurement Requirements* (1) Ozone (2) Total water vapor (3) Surface wind velocity (4) Surface barometric pressure (5) NO_2 concentration (6) Vicarious calibration & validation** (7) Full prelaunch characterization (2% accuracy radiometric) *Science Requirements* (1) SST (2) SSH (3) PAR (4) UV (5) MLD (6) CO_2 (7) pH (8) Ocean circulation (9) Aerosol deposition (10) run-off loading in coastal zone
		Measure particulate and dissolved carbon pools, their characteristics and optical properties	2 3				
		Quantify ocean photobiochemical & photobiological processes	2 4				
		Estimate particle abundance, size distribution (PSD), & characteristics	1 3 2				
		Assimilate ACE observations in ocean biogeochemical model fields of key properties (cf., air-sea CO_2 fluxes, export, pH, etc.)	2	**Lidar** Vertically resolved aerosol heights, optical thickness, & composition Direct separation of subsurface scattering & absorption, depth resolved to ~3 optical depths	• 0.5 km aerosol vertical resolution • 2 m sub-surface resolution • < 0.3% polarization misalignment • 0.0001 $km^{-1}sr^{-1}$ aerosol backscatter sensitivity at 532 nm after averaging • < 4 ns e-folding transient response • Brillouin scattering capability; Receiver FOVs: 0-60 m; 0-120 m.		
		Compare ACE observations with ground-based and model data of biological properties, land-ocean exchange in the coastal zone, physical properties (e.g., winds, SST, SSH, etc), and circulation (ML dynamics, horizontal divergence, etc)	3 4 5 6	**Polarimeter** Broad spatial coverage aerosol heights and single scatter albedo for atmospheric correction. Subsurface polarized return for typing oceanic particles	• Observation angles: 60° to 140° • Angle resolution: 5° • Degree of polarization: 1%		
		Combine ACE ocean & atmosphere observations with models to evaluate (1) air-sea exchange of particulates, dissolved materials, and gases and (2) impacts on aerosol & cloud properties	4	**Supporting Field & Laboratory Measurements** • Primary production (NPP) measurement & round-robin algorithm testing • Inherent optical properties (IOPs) instrument & protocols development, laboratory & field (coastal and open ocean) measurement comparisons • Measure key phytoplankton groups across ocean biomes (coast/open ocean) • Expanded global data sets of NPP, CDOM, DOM, pCO2, PSDs, IOPs, fluorescence, vertical organic particle fluxes, bio-available Fe concentrations			
		Assess ocean radiant heating and feedbacks	5				
		Conduct field sea-truth measurements and modeling to validate retrievals from the pelagic to near-shore environments	1 4 2 5 3 6	**Ocean Biogeochemistry-Ecosystem Modeling** • Expand model capabilities to assimilate variables such as NPP, IOPs, and phytoplankton species/functional group concentrations. • Improve model process parameterizations, e.g., particle fluxes			

* ACE focused questions are traceable to the four overarching science questions of NASA's Ocean Biology and Biogeochemistry Program [OBB1 to OBB4] as defined in the document: *Earth's Living Ocean: A Strategic Vision for the NASA Ocean Biological and Biogeochemistry Program* (under NRC review)

** See ACE Ocean Ecosystem white paper for specific vicarious calibration & validation requirements

2.4 Aerosol-Ocean

Projections of future climate remain an important scientific goal for much of the Earth science community. A large fraction of the uncertainty in predicting 21st-century climate change lies in the uncertainties associated with anthropogenic aerosol forcing and feedbacks that result from land-atmosphere-ocean interactions and interactions between natural and anthropogenic emissions (IPCC, 2013). As aerosol effects on climate are estimated from the differences between model simulations with present-day and with preindustrial aerosol and precursor emissions, accurate representation of marine aerosols is critical for assessment of anthropogenic aerosol effects in Earth System Science models (Ramanathan, 2001; Andreae, 2007; Hoose et al., 2009; Ghan et al., 2013; Carslaw et al., 2013). Changes in marine ecosystems in response to a wide range of stress factors caused by human activities can further incite complex feedbacks between ocean and atmosphere. Reduction in sea ice cover and changes in physical (temperature, salinity, circulation), chemical (nutrient availability, pH) and biological (bacterial and phytoplankton abundance) properties of seawater can strongly influence production rate and physicochemical properties of marine aerosols. These changes in seawater properties can, in turn, affect the sources, sinks, and properties of marine aerosol, influence concentrations of cloud condensation nuclei (CCN) and ice nucleating particles (INP) in the atmosphere. Today there is a great need for comprehensive observational data on marine aerosols that can be used for improvement/evaluations of climate models (Meskhidze et al., 2013). The collection of such data requires multiscale measurements (from in-situ to remote sensing) through a coordinated and multidisciplinary response, with involvement and expertise from a broad range of scientific communities (including atmospheric sciences, physical and biological oceanography).

Aerosol-Ocean Questions

Current Earth System Science models exhibit a large diversity in their representations of marine aerosol sources and sinks, as well as the processes by which these aerosols impact cloud water and ice formation. This diversity is due in part to the lack of measurements to constrain the models. Measurements of marine aerosols are challenging because of their vast spatiotemporal variability and low concentration. Key questions remain unanswered regarding the impacts of marine aerosols on clouds and climate, limiting our ability to quantitatively predict how the future climate will respond to continued and increasing greenhouse-gas and fine-particle emissions.

1. How much do major classes of marine particles contribute to the CCN and INP number of the marine boundary layer in different regions and seasons?

2. How do environmental parameters (surface wind speed (U_{10}), atmospheric stability), ocean physicochemical properties (sea surface temperature (SST), salinity, whitecap fraction, Chlorophyll a (Chl a), dissolved and particulate organic carbon concentration, surface film coverage), biological indicators (organism type

and abundance, physiological stress), and sea ice extent modify the CCN and INP number over the ocean?

3. How do changes in ocean-derived CCN and INP abundances affect cloud microphysical properties and phase?

4. What are the feedbacks between oceanic emissions, marine aerosols and clouds, aerosol deposition, and ocean ecosystems? How is humankind changing these feedbacks?

These questions can be addressed by the development of improved remote sensing products in combination with recent advances in modeling, remote surface monitoring and in situ field and laboratory measurements.

Space-based Observations are Essential for Addressing Aerosol-Ocean Challenges and Questions

Satellites are, and will likely remain, the dominant means for improved characterization of marine aerosols and aerosol-cloud-climate interactions in a changing climate because they provide global, long-term information on the spatiotemporal variability of many properties affecting marine aerosol production (i.e., surface wind speed, wave parameters, surface Chlorophyll a (Chl-a), dissolved and particulate organic carbon concentration, whitecap fraction, SST, and salinity) and removal (i.e., wet and dry deposition). There is a number of past, existing and planned remote sensing instruments supported through U.S. and international programs that can be used for characterization of marine aerosols, as well as ground-based systems including the MAN, a ship-borne data acquisition initiative (Smirnov et al., 2011) complementing island-based AERONET (Holben et al., 1998) measurements, and satellites such as MODIS, MISR, AATSR, PARASOL, MERIS, SeaWiFS, CALIPSO, GPM, SAGE-III/ISS, CATS, and PACE. However, none of these sensors can achieve coincident (in time and space) retrievals of vertically-resolved aerosol information, ocean sub-surface properties, and ocean biological parameters, i.e., parameters essential for quantitative characterization of marine aerosol-cloud-climate interactions. Moreover, current satellite sensors either do not provide the data or provide at signal-to-noise ratio that is not high enough for retrieval of many ocean ecosystem processes and aerosol speciation and loadings over the oceans. Existing satellites also provide limited data in the Arctic and Southern Ocean regions characterized by high cloudiness and low solar zenith angles. Therefore, only the combination of instrumentation planned for future ACE mission can provide the data on global ocean ecology, biogeochemistry, aerosols and clouds with the accuracy needed to significantly advance our understanding of the coupled ocean-aerosol-cloud system.

Additional investments are needed to link space-based observations with other observations. The supporting satellite measurements are needed to assess environmental conditions affecting marine aerosols including SST, U10, ice cover, humidity and temperature profiles and precipitation rates. In particular, measurements of drizzle and precipitation rates coincident with lidar and

polarimeter observations are required to better constrain aerosol sinks over the oceans. In addition to the ocean's physical state, the chemical composition of the ocean and the sea surface can influence sea spray production, so direct measurements are needed of surface film coverage (e.g., via synthetic aperture radar) and biogeochemical variables that have causal links to sea spray production. Improvements in sensor technology can advance the field past using proxies like [Chl-a] to derive marine chemical state and its impact on aerosol composition.

The detailed mechanisms and the radiative impact of marine aerosols in the Earth's climate system are best understood through the combination of satellite remote sensing, in situ observations, and modeling. For example, controlled lab work can provide detailed insight for exploring the relevant parameter space with greater clarity and specificity. Such lab experiments can be used as a tool to illuminate causal relationships that lead to better field observations. Dedicated field measurements can range from in-water physical, chemical, biological, and optical properties, to number size distribution, chemical characterization, hygroscopicity and CCN and INP properties of aerosols and precursor trace gas concentration measurements. In addition, field campaigns will contribute valuable data for calibration and validation of satellite sensors, as well as provide required data to answer the key challenges and questions raised in this document.

The ACE Aerosol-Ocean Science Traceability Matrix

The Aerosol-Ocean STM provides a roadmap from science questions to sensor and mission requirements (i.e., from wishful thinking to concrete measurements) for exploring the complex interplay between aerosols, clouds, and global ocean ecosystems. The Aerosol-Ocean STM is summarized in 5 groups of overarching Focused Questions:

1. What is the flux of aerosols to the ocean and their temporal and spatial distribution?
2. What are the physical and chemical characteristics, sources, and strengths of aerosols deposited into the oceans?
3. How are the physical and chemical characteristics of deposited aerosols transformed in the atmosphere? How do ocean ecosystems respond to aerosol deposition?
4. What is the spatial and temporal distribution of aerosols and gases emitted from the ocean and how are these fluxes regulated by ocean ecosystems?
5. What are the feedbacks among ocean emissions of aerosols and gases, microphysical and radiative properties of the overlying aerosols and clouds, aerosol deposition, ocean ecosystems and the Earth's climate, and how is humankind changing these feedbacks?

To answer the Focused Questions, the ACE Aerosol-Ocean team defined a coordinated approach through combination of in situ data, satellite remote sensing and models, with 8 groups of Specific Objectives:

1. Identify microphysical and optical properties of aerosols, partition natural and anthropogenic sources, and characterize spectral complex index of refraction and particle size distribution
2. Characterize dust aerosols, their column mass, iron content and other trace elements, and their regional-to-global scale transport and flux from events to the annual cycle
3. Conduct appropriate field observations to validate satellite retrievals of aerosols and ocean ecosystem features

4 Use ACE space and field observations to constrain models to evaluate (1) aerosol chemical transformations and long-range transport, (2) air-to-sea and sea-to-air exchange and (3) impacts on ocean biology

5. Characterize aerosol chemical composition and transformation during transport (including influences of vertically distributed NO_2, SO_2, formaldehyde, glyoxal, IO, BrO) and partition gas-derived and mechanically-derived contributions to total aerosol column
6. Monitor global phytoplankton biomass, pigments, taxonomic groups, productivity, Chl:C, and fluorescence; measure and distinguish ocean particle pools and colored dissolved organic material; quantify aerosol-relevant surface ocean photobiological and photobiochemical processes
7. Relate changes in ocean biology/emissions to aerosol deposition patterns and events
8. Demonstrate influences of ocean taxonomy, physiological stress, and photochemistry on cloud/aerosol properties, including organic aerosol transfer

These Specific Objectives were then traced to the Measurement Requirements for the relevant ACE satellite sensors, supporting field and laboratory activities, and modeling. Also identified were specific ACE platform requirements to provide the increased number of parameters and improved signal resolution necessary for advancing our understanding of these important processes and to improve future projections of climate.

The primary instruments on the ACE platform(s) relevant to the mission's Aerosol-Ocean science objectives are the Spectrometer, Polarimeter, High Spectral Resolution Lidar, and Dual frequency Doppler radar. In addition to the ACE science team meetings, the ACE Aerosol-Ocean team conducted weekly teleconferences to define the specific measurement and instrument requirements, with outcomes from these deliberations recorded in a white paper.

The ACE Aerosol-Ocean team identified both aerosol and ocean-relevant properties. For aerosol properties these include aerosol type (dust, smoke, etc.), optical thickness, complex index of refraction, and height and size distributions with a 2-day global coverage to resolve the temporal evolution of plumes. Although oceanic aerosol sources appear to produce aerosol and gas concentrations in the near noise

level of existing satellite platforms, estimates of natural biogenic concentrations over the ocean were deemed to be essential. For ocean ecosystem properties, key properties include phytoplankton functional type and pigment absorption spectra, colored dissolved organic matter (CDOM) absorption, total and phytoplankton carbon concentration, ocean particle size distribution, phytoplankton and CDOM fluorescence, phytoplankton growth rates and rates of net primary production. Many of these determinations can be made by sampling the top of the atmosphere radiance spectra and polarized radiance spectra for selected UV, visible and SWIR bands. Active (lidar) measurements of aerosol properties along the orbit track are thought to be needed to refine height distribution and composition and to provide independent measurements of ocean particle scattering and its vertical distribution within the water column. Many supporting satellite measurements are needed to assess environmental conditions affecting aerosols and organic hydrosols including sea surface temperature, wind speed and direction, chlorophyll concentration, ice cover, humidity and temperature profiles and precipitation rates. In particular, measurements of drizzle detection and precipitation rates coincident with the ACE lidar and polarimeter observations were identified as required parameters. It was envisioned that many of the other supporting global products would come from operational satellite assets such as NPOESS or Decadal Survey missions.

The ACE Aerosol-Ocean team also proposed that simultaneous determinations of tropospheric concentrations of several trace gas species might be important for linking ocean – aerosol processes. These species include but are not limited to formaldehyde (CH_2O), glyoxal ($C_2H_2O_2$), IO, BrO, NO_2, and SO_2. These determinations could come from future satellite systems such as the GeoCAPE mission, which is planned to have a geostationary orbit.

In addition to the above activities, the ACE Aerosol-Ocean team recognized field observations to be an integral part of the ACE mission from the pre-launch period onward. In situ measurements are essential for calibrating and validating satellite sensors and product retrievals. They also provide observations that are not possible from satellite instruments yet nevertheless critical for achieving science objectives. Suggested field measurements would range from solar radiation observations to in-water chemical, biological, and optical properties and to chemical characterization of aerosols. Two types of field campaigns are envisioned: sustained time-series observations from fixed locations (e.g. the BATS and HOT oceanographic time-series sites, and the AERONET sunphotometer network) and mobile sites (Marine Aerosol Network), and intensive field campaigns to address particular science questions. Both types of field campaigns are seen as contributing valuable data for calibration and validation, as well as data required to answer the focused questions raised in the Science Traceability Matrix. Some possible topics of field campaign studies that address questions of the Aerosol-Ocean STM include:

- North Atlantic Aerosols and Marine Ecosystems Study – A study focusing on comparing/contrasting the atmospheric imprint of coccolithophore and/or

Phaeocystis blooms, and examining the hypothesis that the North Atlantic bloom is a major source of fine particle organic aerosols

- Southern Ocean and DMS – A Southern Ocean (SO) study would be on the dimethylsulfide - cloud connection. Given that oceanic gases are probably the dominant CCN precursors over the SO, this study could be of great climatic significance

- North Pacific Asian Outflow Impact – An examination of the impact of Asian dust and pollutant outflow on oceanic productivity, trace gas emissions, and aerosol/cloud properties.

Summary and Recommendations

In summary, the ACE Aerosol-Ocean team has conducted a comprehensive evaluation of mission measurement requirements necessary for narrowing the gap in the current understanding of anthropogenic and natural contributions to a changing climate. Improving climate predictions will require development of new space-based, field, laboratory instruments, and modeling capabilities. By expanding available satellite-borne sensors to encompass aerosol forcing of ocean biological systems and cloud processes, it will be possible to capture potentially important feedbacks with implications on atmospheric radiative effects and climate. Models, in addition to representing current climate, will be able to better capture the changes that have occurred over the past century and predict the climate changes that would result from different future emission strategies. Achieving such confidence critically depends upon more realistic simulations of the aerosol-ocean ecosystems-cloud system with forcings and feedbacks operating on multiple spatiotemporal scales.

Aerosol-Ocean STM

Goddard Space Flight Center

Category	Focused Questions	Approach	Maps to Science Question	Measurement Requirements	Instrument Requirements	Platform Requir' ts	Other Needs
Aerosol -Ocean Inter-action	1 What is the flux of aerosols to the ocean and their temporal and spatial distribution 2 What are the physical and chemical characteristics, sources, and strengths of aerosols deposited into the oceans? 3 How are the physical and chemical characteristics of deposited aerosols transformed in the atmosphere? 4 How do ocean ecosystems respond to aerosol deposition? 5 What is the spatial and temporal distribution of aerosols and gases emitted from the ocean and how are these fluxes regulated by ocean ecosystems? 6 What are the feedbacks among ocean emissions of aerosols and gases, microphysical and radiative properties of the overlying aerosols and clouds, aerosol deposition, ocean ecosystems and the Earth's climate, and how is humankind changing these feedbacks?	1) Identify microphysical and optical properties of aerosols, partition natural and anthropogenic sources, and characterize spectral complex index of refraction and particle size distribution	2 3 6	**Satellite** • Radiances & polarization at selected UV, visible and SWIR bands for aerosol types (dust, smoke, etc.), complex index of refraction, effective height, optical thickness, and size distribution with 2-day global coverage to resolve temporal evolution of plumes • Active (lidar) measurements of aerosol properties along orbit track to refine height distribution and composition • Drizzle detection and precipitation rates coincident with lidar & polarimeter data • Global phytoplankton pigment absorption, dissolved organics absorption, total & phytoplankton carbon concentration, ocean particle size distribution, phytoplankton fluorescence, Chl:C, and growth rate • Particle scattering & vertical distribution through active (lidar) subsurface returns	**Spectrometer** • requirements as stated in ocean STM **Polarimeter** • requirements as stated in aerosol STM **Lidar** • requirements as in ocean STM **Duel frequency Doppler radar** • requirements as stated in cloud STM	Orbit permitting 2-day global coverage for passive radiometer & polarimeter measurements Sun-synchronous orbit with crossing time between 10:30 a.m. & 1:30 p.m. Storage and download of full spectral and spatial data Monthly lunar calibration at 7° phase angle through Earth observing port Additional platform requirements for polarimeter, lidar and radar as detailed in Ocean, Aerosol, and Cloud STMs	**Supporting Global data** • Humidity profiles • Precipitation • Formaldehyde • Glyoxal • IO • BrO • NO_2 • SO_2 **Other Data** •Ground-based aerosol observational network
		2) Characterize dust aerosols, their column mass, iron content and other trace elements, and their regional-to-global scale transport and flux from events to the annual cycle	1 2				
		3) Conduct appropriate field observations to validate satellite retrievals of aerosols and ocean ecosystem features	1 5				
		4) Use ACE space and field observations to constrain models to evaluate (1) aerosol chemical transformations and long range transport, (2) air-to-sea and sea-to-air exchange and (3) impacts on ocean biology	2 5 6				
		5) Characterize aerosol chemical composition and transformation during transport (including influences of vertically distributed NO_2, SO_2, formaldehyde, glyoxal, IO, BrO) and partition gas-derived and mechanically-derived contributions to total aerosol column	2 3 5	**Supporting Field & Laboratory Measurements** • Dust chemical properties/solubility/ chemical transformation • Aerosol optical properties, heights, chemical composition, and partitioning of gas-derived and mechanically-derived contributions to total column load • DMS flux and dissolved concentration and precursors • Atmospheric boundary layer trace gases, NO_2 / SO_2 height distribution • Diffuse irradiance and in-water optics • Surface layer plankton species, phytoplankton carbon, fluorescence • observational network representative of global range in properties • process/mechanism oriented field and laboratory studies • sustain time series field measurements of key properties over active lifetime of mission			
		6) Monitor global phytoplankton biomass, pigments, taxonomic groups, productivity, Chl:C, and fluorescence; measure and distinguish ocean particle pools and colored dissolved organic material; quantify aerosol-relevant surface ocean photobiological and photobiochemical processes	4 5 6				
		7) Relate changes in ocean biology/emissions to aerosol deposition patterns and events	3 5 4	**Modeling** • Conduct model tracer studies to determine sources, composition, and chemical attributes of aerosols • Model height distribution of NO_2 & SO_2 and dust chemistry • Use satellite data to constrain model aerosol source strengths • Model air-sea exchange rates and temporal variability, including sources of aerosols to atmosphere • Run coupled ocean biogeochemistry model to assess impacts and compare to observed response of ocean ecosystems			
		8) Demonstrate influences of ocean taxonomy, physiological stress, and photochemistry on cloud/aerosol properties, including organic aerosol transfer	1 2 3				

3 Assessment and Instrument Concept Development

This section describes the technological accomplishments toward the ACE mission, including aircraft instrument development and utilization, origin of support and TRL status. For each type of instrument (radar, polarimeter, lidar, and ocean color sensor) we summarize the roadmap adopted, accomplishments thus far and on-going efforts.

3.1 Radar

Significant radar advancements relevant to ACE have been achieved in the 2007-2018 period. They were mostly funded through ESTO's IIP, AITT, ACT and InVEST programs, with important contributions also by JPL and GSFC internal research and development funding, the SBIR program, and several airborne field campaign activities funded by ACE, GPM, the Earth Venture program or other NASA programs. Overall, the ACE mission concept provided the necessary focus for technological advances specifically targeting the observation of clouds, convection and precipitation. ACE enabled the full vision expressed by the science community in the ESDS 2007: instrument capabilities expressed as strong desirements in the early ACE workshops (i.e., 2007-2009) that were assessed as either impossible or not affordable at that time, are now feasible. Without ACE's strategic focus, it is hard to envision how many of these advances would have taken place in the same time period.

Radar developments for ACE followed the four main directions presented in the November 2010 report as detailed below.

Extension of CloudSat-class technology to meet the ACE threshold requirements

Completion of the ACERAD concept (PI: S. Durden, JPL) technology maturation through the IIP'08 funding (see Figure 3.1). This design provides both Ka-band and W-band dual-polarized Doppler observations at nadir, with additional Ka-band measurements over a limited swath (*i.e.*, ~30 km). The key technology developments identified to enable this concept were the Dragonian antenna design (to allow Ka-band scanning; scaled version shown in near-field test chamber), the Dual-Frequency Dual-Polarization Quasi-Optical transmission line, the Ka-/W-band frequency selective surface, and the signal generation and processing strategy. The TRL of each of these was raised through prototype implementation and testing in relevant environment so that the ACERAD overall TRL has been raised to 5 (with many subsystems at higher TRL due to heritage from CloudSat's CPR and airborne cloud and precipitation radars and IIP-funded environmental testing of the frequency selective surface for separating and combining Ka- and W-bands). No further technology maturation is deemed necessary before instrument selection since the remaining steps are only related to scaling and engineering. The level of maturity of ACERAD at this time is higher than the level of maturity of CloudSat CPR at the end of CloudSat's Phase A. This instrument concept meets the minimum requirements set in 2010 by the ACE Science Working Group. The primary

limitations of this technology are in the marginal potential for further miniaturization (because the space-qualified High-Voltage Power Supply units for the Extended Interaction Klystron high power amplifiers are already presenting significant challenges in being as small as they are; and because of the simple waveforms adopted which impose large antenna sizes). In a broad analogy to the TRMM/PR and GPM/DPR precipitation radars produced by JAXA/NICT in the first decade of this millennium, these are mature, proven and reliable radar technologies, which however require significant allocations in Size, Weight and Power and are therefore difficult to scale-up without significantly impacting other mission costs.

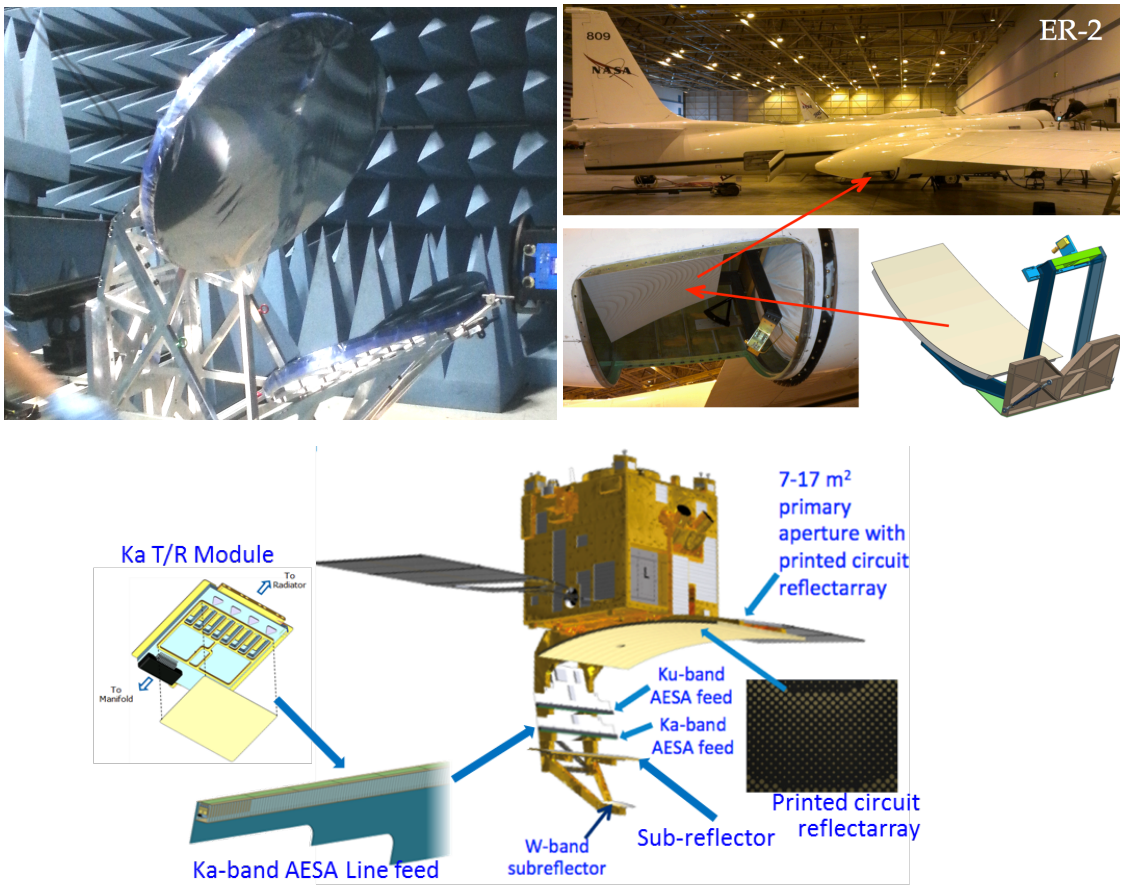

Figure 3.1: Top Left: ACERAD IIP'08 (PI Durden), subscale Dragonian antenna prototype in test chamber; Top Right: WiSCR IIP'10 (PI Racette) sub-scale antenna flight demonstration through IPHEX mission in May, 2014 (see also Figure 3.2) and Middle: WiSCR instrument concept and key technologies.

Maturation of new technologies necessary to meet the ACE goals.

In order to enable instrument performance closer to the scientific needs expressed during the definition of ACE, two additional instrument concepts were defined: WiSCR and 3CPR. Both include use of active electronically scanning linear arrays (AESLA) illuminating a singly-curved parabolic reflector (SCPR) to increase the radar cross-track scanning capabilities while not incurring in the additional challenges and often prohibitive costs associated with large 2-D active arrays. Both

concepts adopt advanced signal generation and processing schemes to achieve the desired radar sensitivities, resolutions and Doppler accuracies. The technological development of WiSCR concept initiated under GSFC internal funding and performed jointly with Northrop Grumman, received critical funding through IIP'10 (PI: Paul Racette) and IIP'13 (PI: Lihua Li) and hinges upon AESLA for Ka-band and innovative W-/Ka-band reflectarray main reflector to enable use of CloudSat heritage technology at W-band. The reflectarray technology enables co-located beams for all frequency bands with capability to support either fixed nadir or scanning W-band beams. The antenna WiSCR concept provides wide swath imaging at Ka-band. Under the IIP'10, the reflectarray antenna achieved a TRL 5 through airborne demonstration of a subscale antenna. The IIP'13 focused on advancing the TRL of the Ka-band radar AESA line feed and T/R module development. The T/R module developed for space is almost at TRL 5 by 2018. The technological development of 3CPR concept, initiated under JPL internal funding and SBIR received critical funding through ACT'11 (PI: A. Fung) and IIP'13 (PI: Greg Sadowy) and it is performed jointly with Raytheon and Nuvotronics as key partners. It hinges upon mature Ku- and Ka-band line feed array technologies and and matures an innovative W-band active feed array technology to enable scanning at all frequencies. The key to this technology lies in an interleaved pattern of transmit and receive radiative surfaces that allow to avoid use of any T/R switches, and on the modular development in units of 16 MMIC T and R elements in one so called Scanning Array Tile (SAT) which facilitates design and implementation of Active Line Feed Arrays (ALAF) of arbitrary length by mating them alongside in the scanning plane. This instrument concept is at TRL 4 having demonstrated the key functionality, including active scanning, of the W-band SAT in a laboratory environment. It is expected to achieve TRL6 by the end of 2018 through Thermal/Vacuum testing of a scaled W-band array. The roadmap beyond that point includes demonstration of integration of Ku- and Ka-band ALAF with W-band ALAF in the airborne airMASTR prototype (described later in this section) and risk reduction study for larger sizes, up to 3m x 5m, cylindrical parabolic reflector antennas.

Development of alternative instrument concepts and architectures to achieve subsets of the same ACE goals with radically new and more affordable solutions.

One first concept for a possible partial tech demo of selected subsystems of all of the three instrument concepts discussed above was jointly developed by JPL and GSFC in 2013 in response to a request by NASA HQ. This instrument concept was defined for deployment on the ISS, and adopts COTS parts and Type-II standards. It focuses on the demonstration in orbit of some of the Ka- and W-band components, and of a variety of digital processing schemes adopted in the ACE radar concepts. This concept was not implemented, but it served as reference point for three instrument concepts developed independently at JPL and GSFC for submission to the Earth Venture Mission and Instrument programs. In general, these efforts were driven by the need to achieve some of the most challenging scientific goals set by the ACE SWG with architectures that require less resources than the large antenna versions of 3CPR and WiSCR. The development of the respective proposals has enabled focusing

on several key technologies to explore implementation of low-cost cloud and precipitation radars; however, given the constraints and priorities of the EV program ultimately none of these has moved beyond concept formulation.

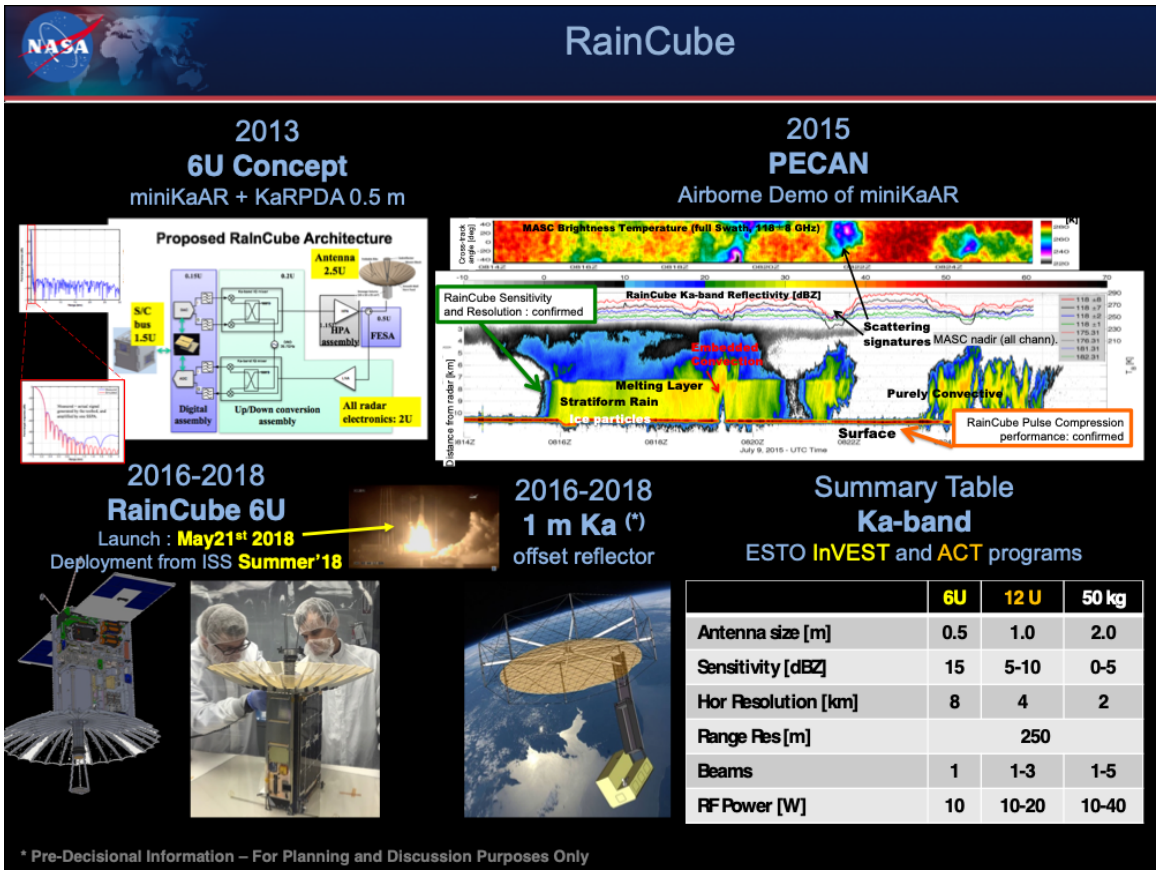

Figure 3.2a: The RainCube progression from concept development and laboratory demonstration to the subsystems, to airbone demonstration of the measurement, to instrument implementation and integration in a 6U cubesat (Tyvak), to launch under InVEST. Ongoing efforts under SBIR aim at bringing a ultra-lightweight deployable 1-m antenna at TRL 6 by 2019 (scalable up to to 2 m).

During the same portion of the last decade, a new disruptive measurement concept was developed to address the scientific need to observe storm dynamics and energetics (see e.g., ACE targeted Geophysical Parameters GP1, GP7 and GP9 in the Science Traceability Matrix): the concept is to enable global observation of the temporal evolution of the vertical structure of storms at a time-scale that is relevant to the process of interest (that is, minutes), rather than, or in conjunction with, instantaneous snaphots of radar reflectivity (that is, snapshots of the structure in the classical fashion of TRMM, CloudSat and GPM) and Doppler velocity (for instantaneous shapshots of the storm dynamics). This concept envisions a number of small platforms in Low Earth Orbit with downward looking radars, complementing a similar constellation of small microwave radiometers in a fashion similar to GPM. These small platforms can be arranged in trains along one orbital plane (to capture the short time scale evolution) and/or on different orbital planes (to improve the sampling of the diurnal cycle within a sufficiently small temporal

window, such as a month). This concept fills a gap left open by ground based radar networks (limited in global coverage since they mostly over land, and over developed countries), and Geostationary Earth Orbit radar concepts (which demand extremely large antennas and are limited in their zonal coverage). Implementation of this concept had to be set aside until last decade, because of the significant cost of implementation and access to space for a single cloud or precipitation radar instrument. Four key factors enabled this concept in the early 2010's : a) maturation of technologies that allow to miniaturize the radar antenna and the electronic subsystems, b) arrival of the small-satellite and low-cost launch options, c) definition of a new simplified radar architecture and waveform generation scheme that reduce the number of parts by two orders of magnitude with respect to predecessor spaceborne cloud and precipitation radars and, d) the occurrence of the ACE workshops and definition of its Science Traceability Matrix that provided clear scientific objectives to motivate engineers to even look into what appeared initially to be a daunting challenge. Initial studies on expected performance of aggressive solutions in the arena of high-purity signal processing were directly supported by ACE (Beauchamp et al. 2017). The result of this challenge, to date, is that the RainCube technology demonstration (6-U cubesat with a Ka-band nadir pointing precipitation profiling radar implemented under the InVEST program, see Figure 3.2a) was deployed from the International Space Station in July 2018 and at the end of August 2018 it achieved its primary objective by demonstrating successfully profiling of thunderstorms over the Sierra Madre Oriental in Mexico. RainCube entered in extended mission and is continuing to acquire data. RainCube demonstrated a few items directly relevant to ACE: a) the ultra-compact back end architecture (which includes the digital system and the up-/down-conversion units, performing real time ultra-low range sidelobe pulse compression, with direct modulation and demodulation between baseband and Ka-band) which could be inherited by any future cloud and precipitation radars, hence reducing the size, weight and power of the digital subsystem and up/down conversion assemblies), b) the specific waveform and filtering for pulse compression (designed keeping in mind the ACE radar requirement of confining the ground clutter to only 500 m above the surface), and c) one first version of an ultra-compact lightweight deployable 0.5 m Ka-band antenna for radar applications (a technology currently under further development under ESTO and SBIR funding to achieve larger apertures which would be directly applicable to the ACE requirements). The TRL of these elements is 6 at the time of writing (having gone through full hardware qualification for flight and airborne flight demonstration of the signal and processing scheme during the PECAN'15 field experiment) and is expected to become 9 before the end of Summer 2018.

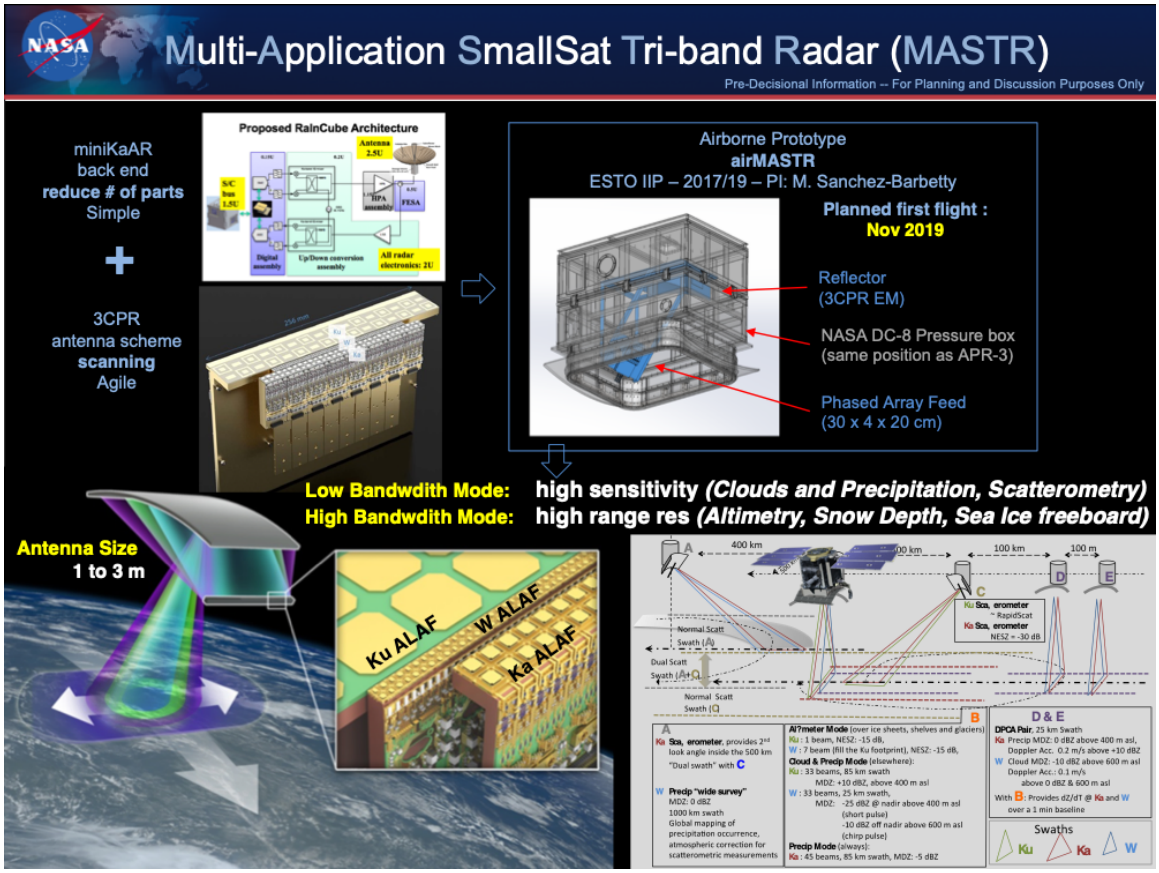

Figure 3.2b: Multi-Application Small-satellite Tri-band Radar (MASTR and airMASTR) instrument concept. It enables measurements of cloud properties and precipitation, sea ice and snowpack thickness, as well as ocean surface winds if used on a spinning scanning platform.

Portion of the technology developed for RainCube (that is, the back-end architecture) has already been reused towards the specific needs of ACE (or CCP) by being integrated in a selected IIP'17 project: the Multi-Application Small-satellite Tri-band Radar (MASTR, PI: Mauricio Sanchez-Barbetty, see Figure 3.2b). In essence, this instrument concept unifies the 3CPR front end technologies described earlier (i.e., Ku-, Ka- and W-band Active Line Array Feeds and singly curved parabolic reflector) with the RainCube signal architecture to deliver an instrument that can address both the cloud and precipitation measurements as well as innovative altimetric measurements focusing on sea ice freeboard and the thickness of the snowpack above it, snowpack over ground, or, if installed in a spinning scanning platform, scatterometric measurements for ocean surface winds. Because of the miniaturized nature of each subsystem, and the modular scalability of the ALAF, this instrument can be scaled to antenna sizes ranging from 0.3 m to 3 m, making it suitable for a variety of accommodations according to specific instrument performance and SWAP allocations (ranging from 6U cubesats, to buses capable to accommodate instruments of a few 100 kg mass and requiring in the order of 1000W), and including any or all of the 3 bands. The airborne prototype (airMASTR) is scheduled for completion under this IIP in 2019 and first test flights are planned

for November 2019. This will demonstrate the measurement capability of the full instrument and elevating the instrument TRL to 5. The key subsystems are also planned to be tested in a relevant environment under separate efforts in 2018-2019 (i.e., thermal-vacuum testing for the ALAF under the 3CPR IIP, and Low Earth Orbit environment for the RainCube back end itself). Once these tasks are completed, no further technological development is necessary to move to engineering and full-scale instrument implementation. The only additional technological developments that are currently planned or envisioned are to further improve the current MASTR performance or further reduce mission cost. These include solid state technology with improved power efficiency to reduce power consumption, and ultra-lightweight deployable singly reflector suitable for W-band operation to reduce mass and volume at-launch. Specific tailoring of future engineering efforts depends entirely on the guidelines and requirements that will be produced by the ACCP studies.

Use Airborne campaigns to demonstrate some of the innovative solutions, develop algorithms, and refine science requirements vs goals.

In order to enable the acquisition of observational datasets specifically tailored to advance ACE science definition as well as algorithm development, NASA's airborne cloud and precipitation radar capabilities have been augmented as follows. For the high-altitude platforms (ER-2 and GH) the existing GSFC radars (PI: G. Heymsfield) have been upgraded and re-engineered to enable simultaneous observations at the ACE frequencies (i.e., Ka- and W-band) plus other supporting frequencies (i.e., X- and Ku-band) to provide a complete view of cloud and precipitation systems. Most notably, the CRS (W-band nadir Doppler), HIWRAP (Ku- and Ka-band nadir Doppler) and EXRAD (X-band scanning Doppler) have flown in the RADEX-14/IPHEx experiment to provide the first-ever 4-frequency airborne radar dataset of clouds and precipitation (see one example in Figure 3.3a and 3.3.b). For the mid-altitude platforms (DC-8 and P-3) the existing JPL radars APR-2 (Ku- and Ka-band) and ACR (W-band), PI: S. Durden, S. Tanelli and S. Dinardo, were reengineered under the AITT'14 program to radiate through a single antenna to enable collocated scanning acquisition at Ku-, Ka- and W-band for the view below the aircraft, and fixed zenith acquisition at Ka- and W-band. In this architecture the pre-existing hardware of the two instruments was interfaced and the control software in ACR modified so that APR-3 could operate as master and ACR as slave in order to enable both independent and master-slave operation. The resulting APR-3 3-frequency Doppler scanning polarimetric cloud and precipitation radar system was scheduled to be completed by April 2016 under the AITT program. While APR-2 (Ku-and Ka-band) was baselined to participate onboard the NASA DC-8 in the OLYMPEX GV experiment in November/December 2015, when ACE identified augmentation of that experiment to achieve the goals of RADEX-15, a new priority was set to accelerate completion of APR-3 to enable acquisition of also W-band measurements in that particular experiment. This accelerated schedule was met thanks to ACE support, and APR-2 successfully acquired the first ever triple frequency scanning radar dataset of clouds and precipitation. The RADEX/OLYMPEX combined radar

datasets from the ER-2 and DC-8 platforms, jointly with the significant amount of in situ (airborne and ground based) and ground based remote sensing data have been already recognized by the scientific community as an unparalleled trove of of information on cold-season and orographic precipitating events, with several papers already published and more than a dozen groups actively working on them at present (e.g., Chase et al. 2018, Houze at al. 2017, Heymsfield et al. 2017).

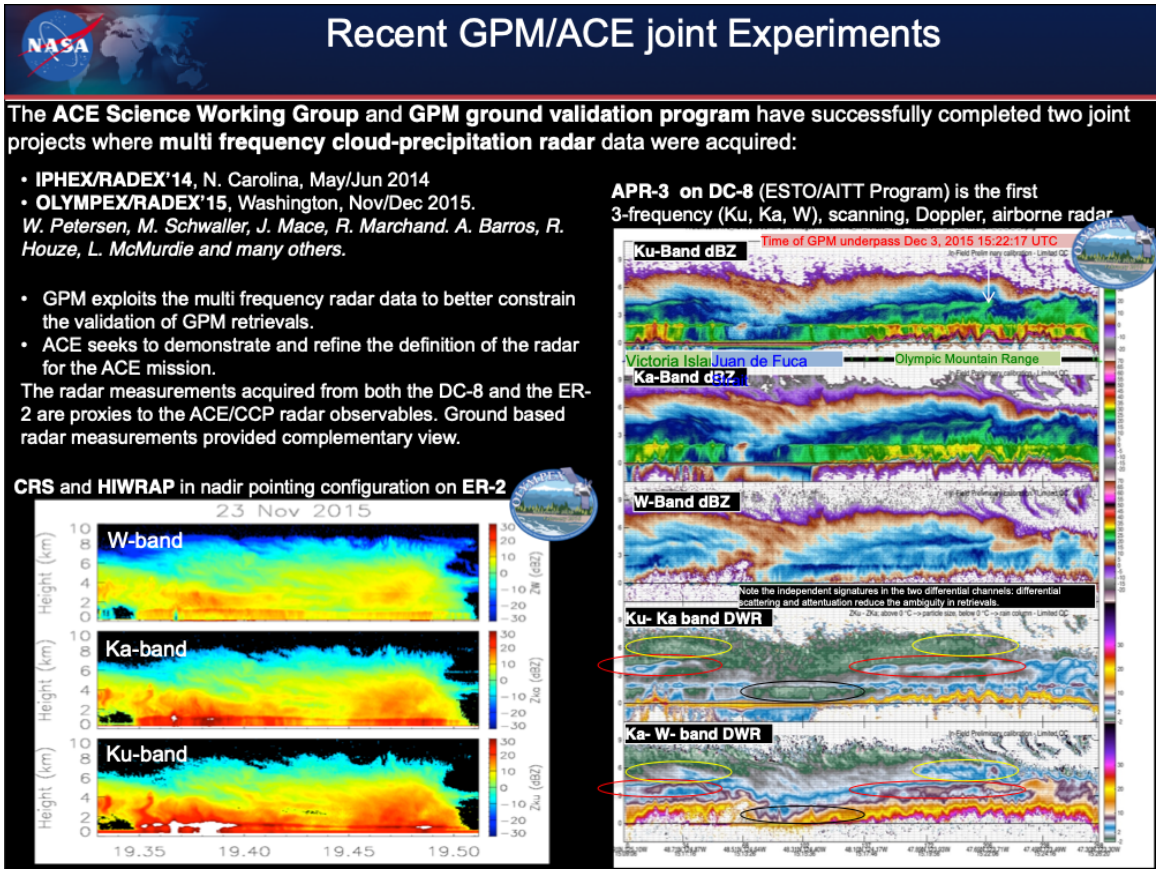

Figure 3.3a: ACE augmented two GPM Validation field experiments (IPHEX'14 and OLYMPEX'15) specifically to acquire remote sensing datasets focused primarily on multi-frequency radar. These were to be used to demonstrate the capabilities and limitations, and to support algorithm development for multi-frequency radar observations of clouds and precipitation. The two ACE contributions were named RADEX'14 and RADEX'15, respectively, and brought to the field X-, Ku-, Ka- and W-band Doppler radar on the NASA ER-2 (in RADEX'14) and on both the NASA DC-8 and ER-2 (in RADEX'15), which delivered the most comprehensive dataset of airborne multi-frequency radar data on cloud and precipitation to date.

Another airborne dataset of interest for ACE was acquired during the Studies of Emissions and Atmospheric Composition, Clouds and Climate Coupling by Regional Surveys SEAC4RS field experiment (Aug/Sept 2013) by the APR-2 instrument (see Figure 3.3c). That datasets focuses on cumulus congestus observations over land, and deep convective storms over the Gulf of Mexico. It included only the APR-2 Ku-/Ka-band radar, primarily because there was no possibility to accommodate an additional W-band radar such as ACR (this being a key factor motivating the creation of APR-3) and therefore could address only the precipitation aspects of the

aerosol-cloud interaction (see e.g., Heath et al. 2017).
A natural upgrade and extension of this research is planned for the CAMP²Ex field deployment (currently planned for the summer of 2019) where APR-3 is selected to operate from the NASA P-3.
Further airborne radar datasets acquired in the last decade that are advancing the science of ACE are those acquired in the context of the ORACLES Earth Venture Suborbital mission (PI: J. Redemann).

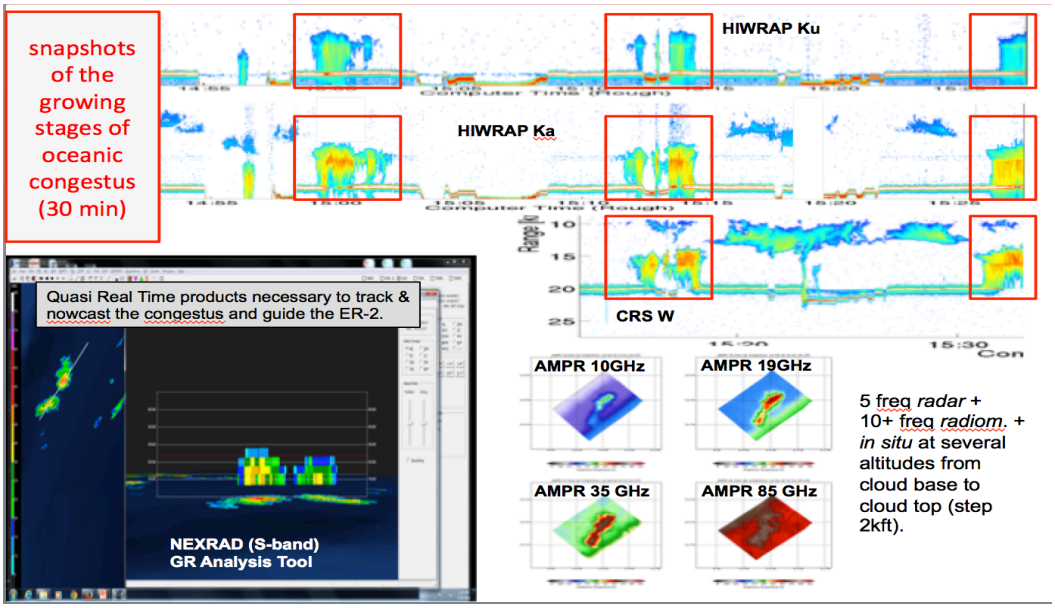

Figure 3.3b: Example of data collected in one of the ACE-specific flights during IPHEX/RADEX (NC, May-June 2014): May 28, Oceanic Cumulus Congestus. Top: 3 of the radar channels from the ER-2; lower left: view from NEXRAD coastal weather radar; lower right: 4 of the radiometric channels from ER-2. (N.B. all ER-2 data are preliminary uncalibrated quicklooks). UND citation performed several penetrations of the cloud imaged here at various altitudes to capture the evolving microphysics.

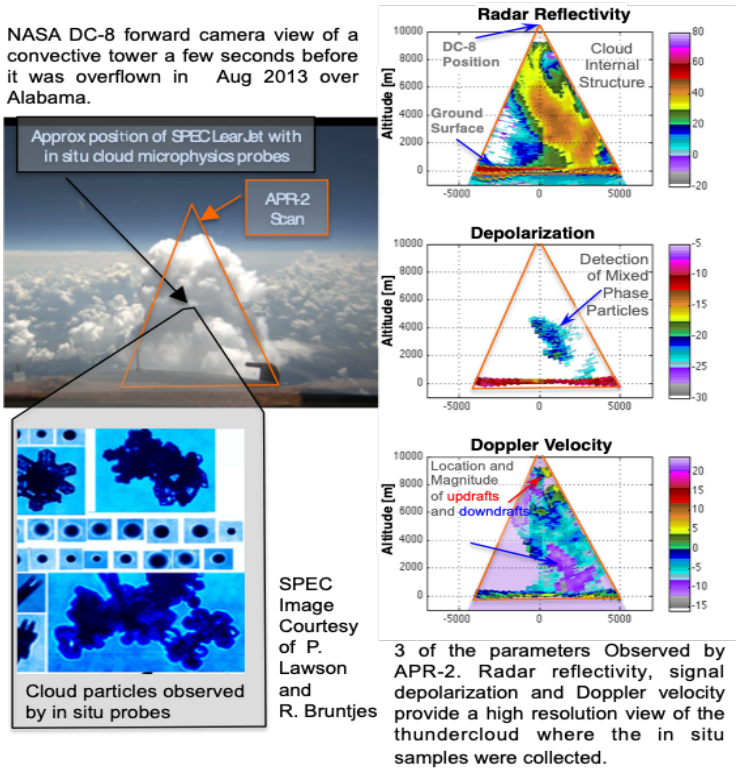

Figure 3.3c: Example of data collected in one of the Convection-focused flights during SEAC4RS (TX, Aug-Sept 2013): Aug 23, Cumulus Congestus over Alabama. Top left: DC-8 forward camera view of the cloud of interest, Lower left: example of in situ particle probe imagery for the upper portion of the congestus cloud; right: APR-2 scans of the convective cloud (3 of the 6 calibrated L1 products shown here). Similar datasets are expected from RADEX-15/OLYMPEX with the addition of the W-band channel.

3.2 Polarimeters

AirMSPI/MSPI

The most significant Multiangle SpectroPolarimetric Imager (MSPI)/Airborne MSPI (AirMSPI) advancements relevant to ACE have been achieved under ESTO's Instrument Incubator Program (IIP) and the Airborne Instrument Technology Transition (AITT) program. Specifically, IIP-04, IIP-07, and IIP-10 support from ESTO has been used to advance the technology readiness level (TRL) of the key MSPI subsystems, and AITT has supported airborne flight testing.

The key to accurate polarimetry in the MSPI measurement approach is rapid rotation of the plane of linear polarization (without the use of moving parts) coupled with synchronous demodulation of the resulting signals. Utilization of polarization modulation as a highly sensitive measurement methodology has been pioneered by the solar and stellar astronomy communities (e.g., Povel et al., 1990; Tinbergen, 1996), and the MSPI technology development effort has adapted this approach to meet ACE science requirements. There are two critical technology components to this scheme: (1) a retardance modulator to rapidly rotate the plane of polarization, comprised of a pair of photoelastic modulators (PEMs) and achromatic, athermalized quarter-waveplates (QWPs), and (2) a specialized focal plane consisting of stripe filters with patterned wiregrid polarizers to provide spectral and polarization selection for the detector line arrays, and detector readout integrated circuits that sample the modulated signals with high speed and low noise

(Diner et al., 2007, 2010). Because the PEMs are made of fused silica, they efficiently transmit light from the ultraviolet (UV) through the visible/near-infrared (VNIR) and shortwave infrared (SWIR). A reflective telescope design enables optical imaging throughout this spectral range and minimizes instrumental polarization.

Support under IIP-04 led to the construction of a ground-based camera, GroundMSPI, which demonstrated the basic measurement concept. GroundMSPI has been used to explore the polarimetric and angular reflectance properties of terrestrial surfaces to help constrain the lower boundary condition for aerosol retrievals (Diner et al., 2012). Under AITT, a second camera was assembled and integrated into the NASA ER-2 high-altitude aircraft, using the housing and electronics rack originally built for AirMISR. The resulting instrument, named AirMSPI (Diner et al., 2013a), has been flying on the ER-2 since 2010, and participated in several field campaigns, including PODEX (2013) (Diner et al., 2013b; Van Harten et al., 2018; Knobelspiesse et al., 2019), SEAC4RS (2013) (Van Harten et al., 2018), pre-HyspIRI (2014), pre-PACE (2014), CalWater-2 (2015), RADEX/OLYMPEX (2015), SPEX-PR (2016), ImPACT-PM (2016) (Kalashnikova et al., 2018), ORACLES (2016) (Xu et al., 2018), and ACEPOL (2017). AirMSPI Level 1 data products have been delivered to the NASA Langley Atmospheric Science Data Center for public distribution, along with supporting User Guide, Quality Statement, and Data Product Specification documents, see https://eosweb.larc.nasa.gov/project/airmspi/airmspi_table.

The second-generation AirMSPI-2 instrument, developed under IIP-07 and IIP-10, extends the measurements into the SWIR and adds band center and wing channels for the O2 A-band. The suite of currently operational MSPI instruments is shown in Figure 3.4. The AirMSPI-2 instrument, currently undergoing improvements to the vacuum system with AITT support, is shown in Figure 3.5.

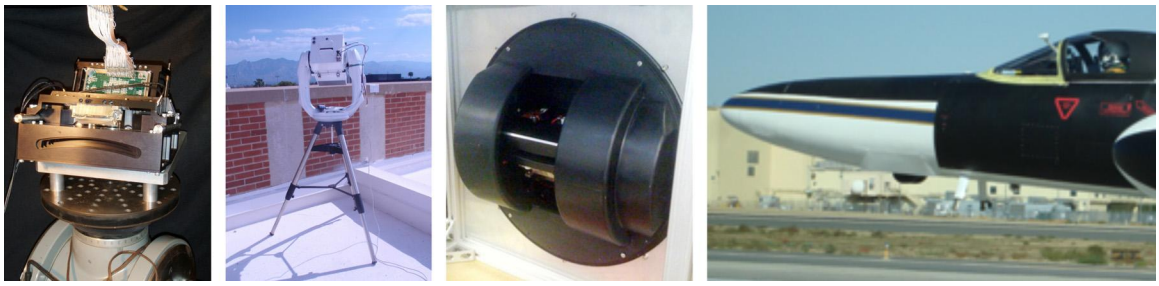

Figure 3.4: LabMSPI, GroundMSPI Camera GroundMSPI on Tripod AirMSPI Camera & Housing AirMSPI mounted in the nose of the NASA ER-2.

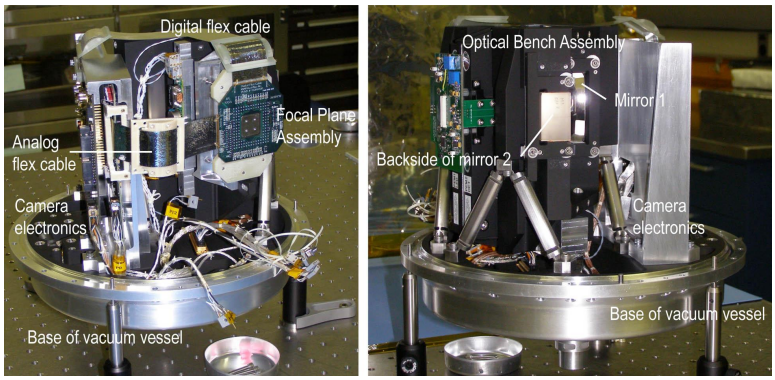

Figure 3.5: Two views of the JPL AirMSPI-2 instrument. AirMSPI-2 was integrated, calibrated, and tested in flight on the ER-2 in 2015. AirMSPI-2 is currently undergoing improvements to the vacuum system at JPL.

There are three main steps involved in maintaining polarimetric accuracy of the MSPI instruments. The first step is a laboratory calibration to account for optical polarization aberrations within the camera. An example of this is mirror diattenuation (different reflectance for p- and s-polarization). These aberrations lead to crosstalk between the intensity and linear Stokes parameters I, Q, and U. The necessary calibration coefficients are determined by constructing a Polarization State Generator (PSG), a laboratory instrument capable of generating accurately calibrated linear polarization in any orientation. In IIP-10, an earlier version of the PSG (Mahler and Chipman, 2011) was upgraded to achieve an uncertainty in the degree of linear polarization (DOLP) output of < 2 x 10-4, i.e., more than an order of magnitude better than the ACE requirement. This high accuracy is necessary in order to accurately assess the capabilities of the MSPI imaging polarimeter. Fully polarized (DOLP = 1.0), partially polarized (DOLP = 0.01, 0.05, 0.10, 0.20), or unpolarized (DOLP = 0.0) light generated by the upgraded PSG was viewed by AirMSPI to generate a set of polarimetric calibration coefficients that compensate for instrumental polarization aberrations (Diner et al., 2010; Van Harten et al., 2018). As shown in Figure 3.6, systematic errors in DOLP determined from AirMSPI are ~0.001, implying that random measurement noise (primarily due to photon shot noise) dominates the total DOLP uncertainty. AirMSPI signal-to-noise ratios are sufficiently high to enable meeting the ACE requirement on DOLP error (i.e., within ±0.005) on a 20 m x20 m spatial scale.

The second step involves in-flight maintenance of the PEM operating parameters. This is accomplished using an optical probe built into the AirMSPI and AirMSPI-2 cameras. A beam of light from an LED is polarized and sent through the dual PEMs at a location not used for imaging, and the modulations are sensed with a high-speed photodiode. Analysis of the signals allows determination of the retardances of the two PEMs and the PEM oscillation phase. These are controlled to the desired values (the same values as used for laboratory calibration) using a feedback control loop. The optical probe is in conjunction with the third step, which is periodic in-flight verification of PEM retardances and phase by viewing an on-board polarization validator, consisting of a set of LEDs that illuminate a diffuse panel and polarizers in different orientations. By viewing the validator with the AirMSPI camera during flight, the modulation functions used to analyze polarization data can be determined

and verified to be governed by the proper values of the PEM operating parameters. Deviations from the desired values can be corrected in ground data processing.

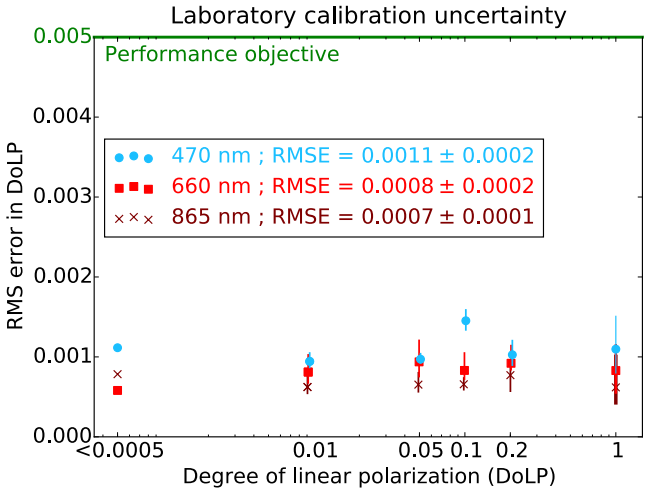

Figure 3.6: Laboratory polarization calibration of AirMSPI using the PSG keeps systematic errors in DOLP well below the ACE requirement.

A custom dual-PEM retardance modulator package was engineered and built to withstand launch loads, and was vibrated in all three axes at 15 g RMS. PEM functionality was retested to verify that there had been no damage to the bond line holding the PEM head to the piezoelectric transducer. PEM retardance stability was tested in the laboratory at a number of fixed set point temperatures from -30°C to +50°C. In space, the PEMs will be thermally stabilized. In addition, a dual PEM operated in the lab nearly continuously for more than 8 years. The achromatic QWPs are compound retarders comprised of three materials (quartz, sapphire, and MgF2) that are often used in space applications. IIP-07 work extended the performance of the QWP into the SWIR. A similar compound QWP for OCO-3 demonstrated survivability of the bonds through thermal cycling in vacuum between -20°C and 35°C. Vibration testing of the OCO-3 article showed no vibration-induced structural defects.

The MSPI spectropolarimetric filters are butcher block assemblies of patterned wiregrid polarization analyzers and miniaturized stripe filters. Structural replicates of the MSPI filters were run through thermal stress tests in vacuum, consisting of 123 thermal cycles between 220K and 313K and 108 additional cycles between 180K and 313K. The tested filters survived thermal cycling and met bondline integrity requirements with substantial margin. The other element of the focal plane is the sensor chip assembly (SCA), consisting of the readout integrated circuit (ROIC) and hybridized HgCdTe detector for the SWIR. A separate ROIC on the same chip provides UV/VNIR sensing using embedded Si-CMOS photodiodes. The ROICs enable sampling of the PEM modulation patterns at the required readout speeds (~25 Mpix/sec), leading to photon shot-noise limited sensing over a wide dynamic range. Single Event Latchup (SEL) testing using heavy ion bombardment indicates a latchup probability of once per 5000 years. Latchup was also determined to be

nondestructive, meaning that in the unlikely event of occurrence, a reset restores normal operation. Total ionizing dose exposure of the ROIC was also completed, using the JPL cobalt-60 source in 5 krad steps up to 25 krad. All tested parts remained fully functional, and dark current remained within specifications at doses corresponding to low Earth orbit. Finally, characterization of the hybridized ROIC/detectors at operating temperature and following thermal cycling was performed. An SCA underwent 100 thermal cycles between room temperature and 235K, and was subjected to an additional 30 cycles between room temperature and 180K. The part remained functional following these environmental stresses.

The above environmental stresses represent "relevant environment" qualification testing of all key MSPI technologies, including the retardance modulator and specialized focal plane. As a consequence, each of these subassemblies is currently at TRL 5. In addition, the MSPI onboard processing algorithm that converts the sampled modulation signals to linear Stokes polarization parameters was tested aboard the CubeSat On-board processing Validation Experiment-2 (COVE-2), providing the first spaceborne application of a new radiation-hardened Virtex-5QV field programmable gate array (FPGA). COVE-2 was launched in December 2013. Telemetry demonstrated successful processing, bringing the maturity of this key component to TRL 7 (Pingree, 2014).

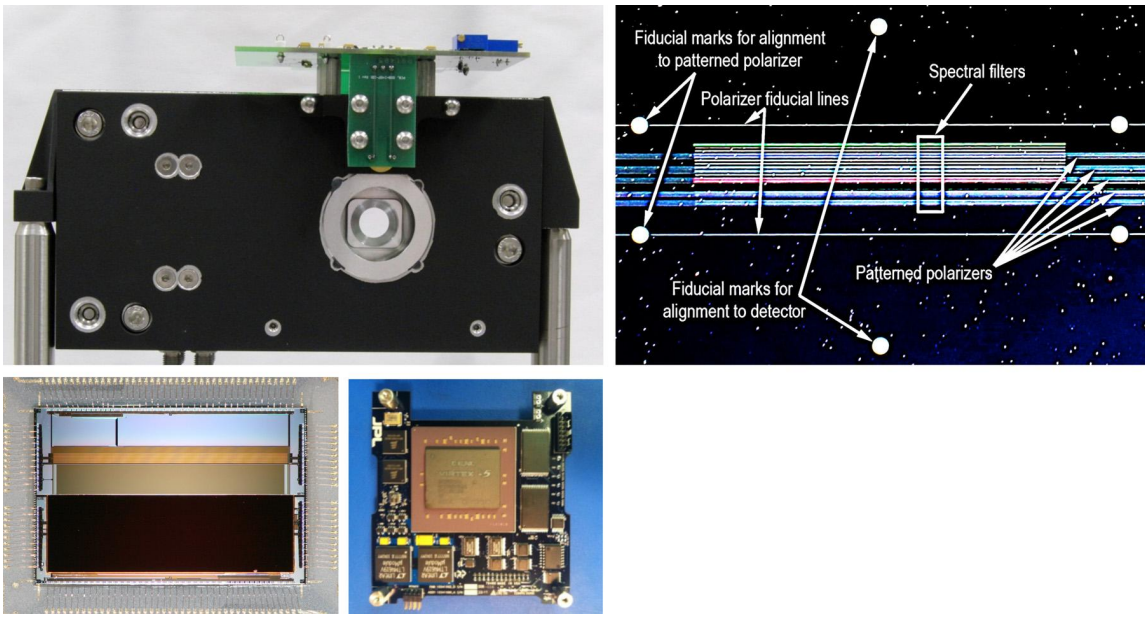

Figure 3.7: Top left: retardance modulator. Top right: filter assembly. Bottom left: ROICs and detectors. Bottom right: COVE payload with Virtex-5QV FPGA.

Key technology components of the MSPI system are shown in Figure 3.7. At upper left is the dual-PEM retardance modulator (including QWPs) in a space-qualified package. The green assembly at top is the optical probe. At upper right is a front- and back-lit photograph of the AirMSPI-2 spectropolarimetric filter showing the

stripe spectral filters and patterned polarizers. Lower left shows the UV/VNIR/SWIR detectors and ROICs built for AirMSPI-2. Lower right shows the JPL COVE payload featuring the Xilinx Virtex-5QV FPGA.

The AirMSPI-2 instrument has been integrated; system characterization has been performed; and the instrument has been flight tested on the NASA ER-2 in October 2015. These flights demonstrated the functionality of the end-to-end UV/VNIR/SWIR camera system, raising the TRL to 6.

Regarding the Level 0 to Level 1 processing approach for MSPI (Jovanovic et al., 2012), a generalized photogrammetry software library developed for the Terra Multi-angle Imaging SpectroRadiometer (MISR; Jovanovic et al., 2002) serves as the basis for this. Critical functionality includes collinearity, which makes use of the camera/orbit geometric model to establish the view vectors for each line and pixel in the focal plane. It is expanded to include simultaneous bundle adjustment, which employs ground control points and a digital elevation model to solve for static and/or dynamic changes in certain parameters describing the instrument pointing geometry. This functionality, along with pixel-by-pixel application of radiometric and polarimetric calibration coefficients, is used to convert raw instrument (Level 0) data to calibrated, georectified, and co-registered radiance and polarization imagery at Level 1, and has been prototyped for ACE using AirMSPI. In addition to MISR-like Level 0 to Level 1 processing that generates ellipsoid-projected imagery, georectified imagery map-projected to the surface terrain is used as input to aerosol retrievals (Figure 3.8a). A similar approach is envisioned for MSPI, and has been prototyped using AirMSPI data.

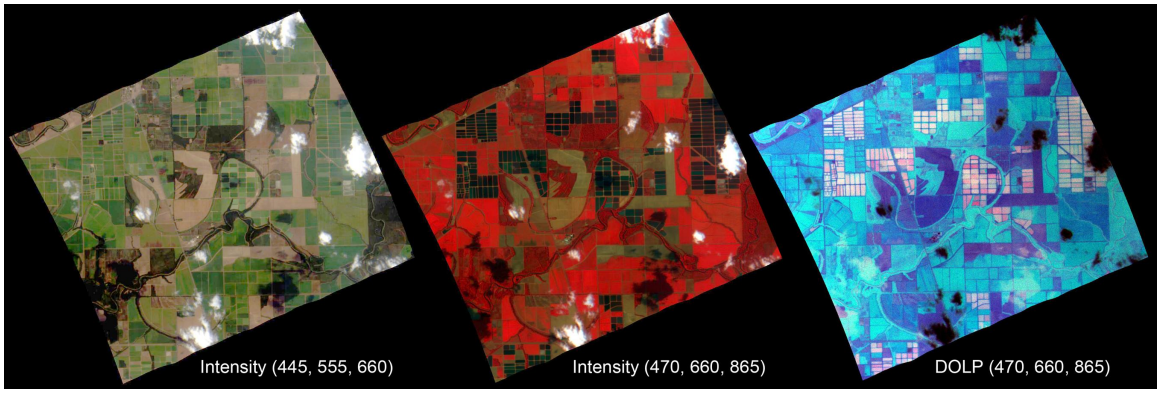

Figure 3.8a: Example AirMSPI imagery over Leland, MS, acquired on 9 September 2013 during SEAC4RS. Left: Intensity imagery at 445, 555, and 660 nm. Middle: False color intensity imagery at 470, 660, and 865 nm. Right: DOLP image at 470, 660, and 865 nm. Georectification provides subpixel registration of the different instrument channels as well as registration of images acquired at different angles of view.

RSP

The Research Scanning Polarimeter (RSP) is a functional prototype of the Aerosol Polarimetry Sensor that flew on the NASA Glory mission, which failed to reach orbit. The measurement concept used in this sensor has a long heritage starting with the Imaging PhotoPolarimeter on Pioneer 10 and 11 then the Cloud PhotoPolarimeter on Pioneer Venus and more recently the PhotoPolarimeter Radiometer on Galileo. The development of the RSP has been achieved with support from the NASA Radiation Science Program, ESTO's AITT program, the Glory mission and contributions from SpecTIR LLC, the company that built the RSP.

The major difference between RSP and preceding planetary instruments is the implementation of a rotating pair of mirrors in front of the telescopes that provide scene definition and spectral and polarimetric analysis. This allows the field of view of the instrument to be scanned while introducing negligibly small amounts of instrumental polarization into the observed scene. The scanning system also allows well characterized scenes of both low (using a pseudo-depolarizer) and high (using polarizers) polarization to be observed on every scan providing continuous polarimetric calibration and guaranteed polarimetric accuracy over the entire range of possible polarization states, in addition to continuous radiometric calibration/stability monitoring. This ensures that measurements of the degree of linear polarization are made with an absolute uncertainty of less than 0.2% absolute accuracy when the degree of polarization is less than 20% and less than 0.5% when the degree of polarization is greater than 20%.

The polarization compensated scan mirror assembly scans the fields of view of six bore-sighted, refractive telescopes, with an instantaneous field of view of 14 mrad, to obtain scene data over a range of +/-60° from the normal with respect to the instrument baseplate. The refractive telescopes are paired, with each pair making measurements in three spectral bands. One telescope in each pair makes simultaneous measurements of the linear polarization components of the intensity in orthogonal planes at 0° and 90° to the meridional plane of the instrument, while the other telescope simultaneously measures equivalent intensities in orthogonal planes at 45° and 135°. This approach ensures that the polarization signal is not contaminated by scene intensity variations during the course of the polarization measurements, which could create false polarization. These measurements in each instantaneous field of view in a scan provide the simultaneous determination of the intensity, and the degree and azimuth of linear polarization in all nine spectral bands.

The instrument has nine spectral channels that are divided into two groups based on the type of detector used: visible/near infrared (VNIR) bands at 410 (30), 470 (20), 550 (20), 670 (20), 865 (20) and 960 (20) nm and shortwave infrared (SWIR) bands at 1590 (60), 1880 (90), and 2260 (120) nm. The parenthetic figures are the full width at half maximum (FWHM) bandwidths of the spectral bands. These spectral bands sample the spectrum of reflected solar radiation over most of the

radiatively significant range, with measurements under typical clear sky conditions ranging from significant Rayleigh scattering (410nm) to single scattering by aerosol (2260nm) within a single measurement set.

The desired polarization-insensitive scanning function of the RSP is achieved by the use of a two-mirror system with the mirrors oriented such that any polarization introduced at the first reflection is compensated for by the second reflection. Bore-sighted refractive telescopes define the 14mrad field of view of the RSP. Dichroic beam splitters are used for spectral selection, interference filters define the spectral band-passes and Wollaston prisms spatially separate the orthogonal polarizations onto the pairs of detectors. The detectors for the VNIR wavelengths are pairs of UV-enhanced silicon photodiodes. The detectors for the SWIR wavelengths are pairs of HgCdTe photodiodes with a 2500 nm cutoff that are cooled to 163K to optimize performance. The average data rate of 110kbps provides readout of the 36 signal channels together with instrument status data at a scan rate of 71.3 rpm and is similar to the data rate from APS. A scan rate of ~ 70 rpm is compatible with getting contiguous (nadir view to nadir view) coverage with aircraft ranging from a Cessna 210 to the NASA ER-2. It is also compatible with the velocity and altitude of a typical low earth orbit for the 8 mrad IFOV of an instrument such as APS.

The RSP instrument was designed to meet the scientific requirements for high quality polarimetric data, by having high accuracy, simultaneous collection of all polarization components and spectral bands within an instantaneous field of view, the ability to observe a scene from multiple angles and a broad spectral range. The RSP instrument meets the polarimetric accuracy requirements (less than absolute 0.2% error) and has been used to obtain more than a thousand hours of multi-angle, multi-spectral data since 2000. Instrument performance has been flawless and it has been operated on a wide range of aircraft most recently the NASA Langley Research Center B200 since 2008 and the NASA ER-2 since 2012. All radiance and polarization data are publicly available and is generally calibrated and made public within 2-3 days of acquisition. Funding for flights of the RSP came from the Glory and CALIPSO missions and the Research and Analysis programs, primarily the Radiation Science Program through support of RSP deployment for SEAC4RS and the Ocean Biology and Biogeochemistry program through support of the RSP deployment for SABOR and on HySPIRI airborne preparatory program flights.

The RSP group participated in the Earth Systematic Mission Directorate program office's Systems Engineering Working Group (SEWG) assessment of Technology Readiness Level (TRL) for an Aerosol Polarimetry Sensor (APS) rebuild. The assessment was that the sensor had a TRL of 7 and while there are always disagreements about the exact TRL of a complete system and the definition of TRL occasionally changes it is clear that the APS is a mature design with substantial design heritage. In particular the APS successfully completed both sensor level and observatory level EMI/EMC, vibration, thermal/vacuum and shock testing with a total of more than 1200 operational hours in thermal/vacuum testing. The successful performance during sensor level testing is documented in the Raytheon

Requirements Verification Matrix and supporting documentation, together with the Consent to Ship Review package. The successful performance during observatory level testing is documented in the observatory Pre-Ship Review package and supporting Orbital Science Corporation requirements verification documentation.

The only likely change to the APS design for the ACE mission would be if a clean view to deep space were not to be available for cooling. In that case two Thermo Electric Coolers, a cold plate, redundant ethane heat pipes, and a radiator can be used to maintain the SWIR detectors at a temperature of 183K ± 2K. A similar thermal system was flown on Swift and more recently on the Landsat Data Continuity Mission (LDCM) Thermal Infrared Sensor (TIRS), providing design heritage. A model of this proven design was assembled and successfully tested under GSFC Internal Research and Development (IRAD) funding to demonstrate feasibility. In addition to providing proof-of-concept for this specific application, the prototype provided realistic mass and power estimates and will allow for the sizing of the SWIR Heat Rejection Radiator early in ACE mission development.

The Level 0 to Level 1 processing of RSP data follows the same flow in terms of required calibration coefficients and their on-board calibration sources, as presented in the Glory APS L1B Algorithm Theoretical Basis Document (http://glory.giss.nasa.gov). These coefficients are used to generate the calibrated Stokes parameters I, Q and U and the code developed for the Glory project is used for geolocation and geo-rectification. In addition, the L1B data product includes index arrays that can be used to remap the RSP data to any altitude, simplifying the implementation of cloud retrievals. A L1C product is also provided for which this remapping to cloud top, or to the surface in cloud-free cases, is already applied.

PACS/HARP

The Passive Aerosol and Cloud Suite (PACS) is a modular concept with multiple passive imagers side by side ranging from UV to TIR wavelengths. As part of this concept, the HARP (Hyper-Angular Rainbow Polarimeter) is a compact and robust imaging polarimeter with no operational moving parts (except for internal calibrators). HARP is designed for three wavelength ranges covering from 350 to 2250nm: HARP UV, HARP VNIR, and HARP SWIR.

A HARP VNIR polarimeter module was built for space applications under the HARP Cubesat project funded under the NASA ESTO InVest program. HARP is currently slated to be the first hyper-angular polarization imager flying in space (Martins et al. 2018; Dubovik et al. 2018).

In the HARP design, each telescope has a telecentric back end and a Philips prism that splits the signal into three identical images over three independent detector arrays controlled by a single FPGA electronics. HARP's FPGA has been fully developed to perform all data acquisition and required processing in order to eliminate the need for an onboard instrument computer, substantially reducing cost, mass, power consumption and risk. Wavelengths and angles are defined (and

software selectable) by a striped filter mounted on the surface of the detector. For each viewing angle and wavelength, the HARP polarimeter provides 3 intensity images acquired through polarizers aligned at 0, 45 and 90º relative to each other. These 3 images are related to the Stokes vector of the incoming light by a 3X3 characteristic matrix that fully represents all the elements of the optical system (Fernandez-Borda et al., 2009). The simultaneous measurements of the 3 polarization orientations assures the high accuracy of the measurements. This approach has been demonstrated and validated in the UMBC lab and on three aircraft campaigns (PODEX, LMOS and ACEPOL) confirming a polarization accuracy better than 0.5%. This measurement accuracy has been validated with a polarization generator that can modulate the degree of linear polarization of the light generated by an unpolarized integrating sphere in the range of 0 to 60%.

Design studies and TRL assessments were completed for the HARP UV and SWIR modules but no hardware assembly these modules has been funded to completion. The HARP VNIR module has been fully developed in the three configurations shown in Figure 3.8b. In all three cases, HARP VNIR has a 94° cross track swath and 113° along track coverage in viewing angle, four wavelengths (440, 550, 670 and 870nm), 60 along track viewing angles at 670nm, and 20 along track viewing angles for the other three wavelengths. The detector arrays have 2048 pixels cross track which can be binned onboard for reducing the data rate requirements as needed.

AirHARP

An airborne version of the HARP VNIR system has been fully assembled and tested on the NASA Langley UC12 aircraft during the LMOS (Lake Michigan Ozone Study) campaign in June 2017, and on the NASA ER2 aircraft during the ACEPOL campaign in October-November 2017.

HARP CubeSat

HARP CubeSat was developed with funding from the NASA ESTO InVEST program and carries a full version of the HARP VNIR telescope, which was specially miniaturized for this application. Limitations on the CubeSat form factor, mass, thermal system, and data rates pose a major challenge for an instrument like HARP but, nevertheless, HARP CubeSat will provide important demonstration of this technology from space. Due to the data rate limitations, only a few regions can be targeted by HARP CubeSat in a daily basis. HARP CubeSat is currently scheduled for launch in the Spring 2019 in the ISS orbit.

HARP2 for PACE

A contributed version of HARP is under construction to join the PACE mission and supplement the measurements by the main payload, the Ocean Color Instrument (OCI). HARP2 is a copy of the HARP VNIR polarimeter fully adapted to work in a large spacecraft, with the capability to provide global coverage in 2 days, better signal to noise ratios, and multiple features to support onboard calibration including an internal flat field calibrator.

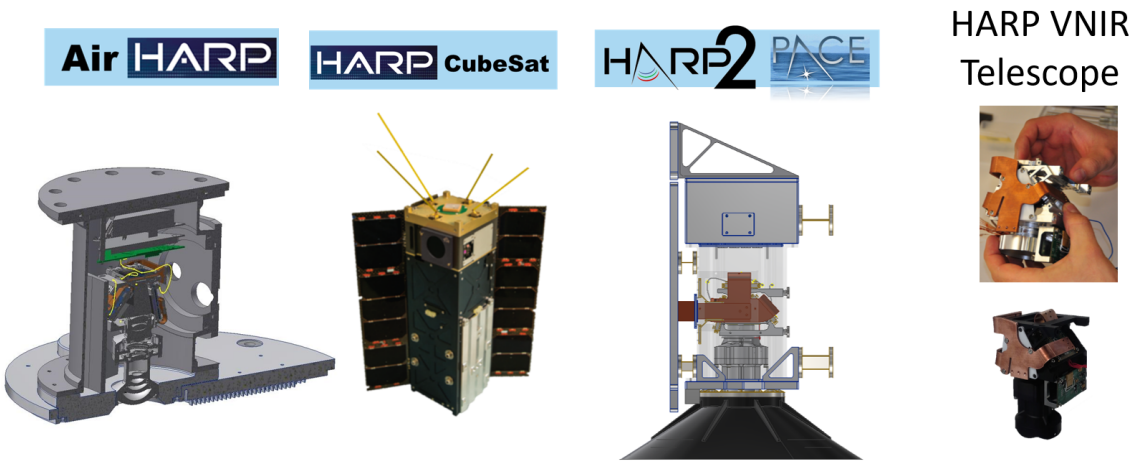

Figure 3.8b: Three current configurations for the HARP VNIR polarimeter including the AirHARP instrument that has flown in the Langley UC12 and the NASA ER2 aircrafts, the HARP Cubesat scheduled for launching in the Spring 2019, and the HARP-2 instrument under construction as an add on to the PACE mission. The figure also shows a photograph of the core of the HARP VNIR telescope illustrating the small size of the telescope assembly.

3.3 Lidar

Lidar vertical profile measurements of backscatter, depolarization, and extinction, in day and night conditions, provide the science community with the aerosol properties that are necessary to complement passive aerosol retrievals and examine aerosol impacts on climate and air quality. Current/past space-based lidars such as Cloud-Aerosol Lidar with Orthogonal Polarization (CALIOP) on the Cloud-Aerosol Lidar and Infrared Pathfinder Satellite Observations (CALIPSO) satellite and Cloud-Aerosol Transport System (CATS) on the International Space Station (ISS) have been providing essential measurements of aerosol vertical distribution (Winker et al., 2009; McGill et al., 2015). However, in the foreseeable future the availability of this critical data is endangered due to limited laser lifetime. To continue and advance CALIPSO and CATS measurements of aerosol vertical distribution, a lidar that can detect optically thin layers with high accuracy and global coverage is required.

There are several types of cloud-aerosol lidars, such as simple elastic backscatter lidars and High Spectral Resolution Lidars (HSRLs), that can provide the desired geophysical parameters. Early in the ACE program, two lidar instrument concepts were developed for use in ACE mission design studies. One was a multi-beam backscatter lidar that provided some information in the cross-track direction via a pushbroom-like sampling strategy. The other was a single-beam multi-wavelength High Spectral Resolution Lidar (HSRL) that provided only a nadir curtain of lidar measurements but with higher SNR and information content in that curtain. Both concepts were analyzed in the initial GSFC Integrated Mission Design Lab (IMDL) mission studies.

In February 2009, the Aerosol Working Group met at GSFC to refine lidar requirements. Agreement was reached that ACE aerosol requirements called for implementation of single-beam multi-wavelength high spectral resolution lidar (HSRL) providing the so-called "3β + 2α + 2δ" suite of profiles: 3 aerosol backscatter wavelengths, 2 aerosol extinction wavelengths, and 2 polarization-sensitive wavelengths. Cloud and ocean requirements were also met by this concept, and therefore it was used in subsequent mission design studies (GSFC IMDL and JPL Team-X studies).

Over the course of the ACE pre-formulation effort, significant advances have been made in technology readiness, retrieval development, scientific demonstration, and validation. Many of the advances funded by ACE are based on the NASA LaRC HSRL-2 airborne prototype instrument that implements the full 3β + 2α + 2δ ACE lidar concept and which has been flown on eight major field missions starting in 2012. Although mostly funded through other sources, exciting technology and algorithm advances for some of the ACE capabilities have also been achieved with the CALIOP, CATS, and the Airborne Cloud-Aerosol Transport System (ACATS) instruments.

HSRL

Requirements on the ACE lidar stem from all ACE STMs (aerosols, clouds, ocean, and aerosol-ocean STMs). The discussion of the HSRL technique and advances made under ACE is separated below into sections focused on atmosphere (aerosols and clouds) and ocean requirements.

HSRL for meeting atmospheric requirements

The wavelengths required for the 3β + 2α + 2δ measurements are UV, mid-visible, and near-IR, which can be achieved with mature laser technology (Nd:YAG, or Nd:YVO4), using the fundamental (~1064 nm), doubled (~532 nm), and tripled (~355 nm) wavelengths of a single pulsed laser transmitter. Unambiguous aerosol extinction measurements required at the 355 and 532 nm wavelengths necessitate use of the HSRL technique. This combination of three backscatter and two extinction wavelengths is the only published method for retrieving the required vertically resolved aerosol optical properties (scattering and absorption) and microphysical properties (size, index of refraction, concentration) using only lidar measurements (Müller et al., 2001, 2002, 2014; Veselovskii et al., 2002; Wandinger et al., 2002; Sawamura et al. 2017) called for in the ACE STM. The requirement for depolarization measurements at two wavelengths was imposed to provide enhanced skill for aerosol typing (Burton et al., 2012, 2013, 2014) beyond that using only backscatter and extinction measurements. It remains to be determined which two of the three wavelengths are required for depolarization, but heritage measurements with airborne systems have been made with the 532 and 1064 nm wavelengths. Studies are underway to determine whether a simpler lidar combined with a polarimeter can satisfy the aerosol requirements (e.g., Liu et al., 2017). Lidar measurements required for the cloud objectives include cloud top height and profiles of cloud phase, backscatter, and extinction in tenuous clouds. These

requirements could be met with fewer channels (e.g., a 532 nm HSRL with polarization sensitivity).

Airborne prototypes have demonstrated the required ACE lidar technologies and measurements. The LaRC HSRL-2 instrument is a full-up prototype for achieving the ACE 3β + 2α + 2δ atmospheric measurements. It implements the HSRL technique at 355 and 532 nm and the standard backscatter technique at 1064 nm and is polarization sensitive at all 3 wavelengths. The development of HSRL-2 originated with ESTO Instrument Incubator Program (IIP) funding in 2004 and continued through an Airborne Instrument Technology Transition (AITT) award in 2007, LaRC internal funding, and current funding to extend the capability to ocean profiling under an IIP award. The receiver employs an iodine vapor filter to implement the HSRL technique at 532 nm (Piironen and Eloranta, 1994) and a field-widened, off-axis Michelson interferometer at 355 nm (Seaman et al. 2015). Funding for advancement of the interferometer implementing the HSRL technique at 355 nm has been provided via an ESTO QRS award, ACE pre-formulation funding, Directed Technology and Research (formerly GOLD) labor support, and LaRC internal funding. HSRL-2 builds on a long history of technology and science demonstration of the two-wavelength HSRL-1 instrument (Hair et al., 2008), the development of which was initiated in 2000 and which has flown on 25 airborne field missions starting in 2006. The ACE-prototype HSRL-2 instrument has been deployed on eight major airborne field missions starting in 2012. Operational software code produces full lidar "curtains" of ACE-like aerosol optical and microphysical properties within a few hours after each flight (Müller et al., 2014). Several of the eight HSRL-2 field missions involved additional participating aircraft making in situ aerosol measurements coincident with the HSRL-2 measurements. Aerosol measurements made on the participating aircraft, along with coincident AERONET observations, have been used to assess the multi-wavelength lidar aerosol retrievals and the development of new algorithm approaches (e.g., Sawamura et al. 2017). Since 2015, HSRL-2 is capable of autonomous operation and two major science deployments have been conducted from the ER-2 high-altitude aircraft (see Figure 3.9).

In addition, the LaRC Ultra-Violet Differential Absorption Lidar (UV DIAL) instrument, a flagship instrument flown since the 1980s on over 30 chemistry focused field missions, was was upgraded under an AITT award to include HSRL capability at 532 nm in both the nadir and zenith directions. It has flown on three field missions in that configuration and aerosol data products are operationally produced within a few hours after each flight using software modules from the HSRL-1 and -2 processing code. Cirrus cloud retrievals of backscatter, extinction, and depolarization have also been demonstrated with the UV DIAL/HSRL data set. Also, ongoing is the High Altitude Lidar Observatory (HALO) program, an ESTO funded IIP based on the HSRL-2 instrument architecture to advance TRL for DIAL technologies for water vapor and methane while simultaneously providing HSRL capability at 532 nm. The HALO instrument deployed on two successful series of test flights so far in 2018.

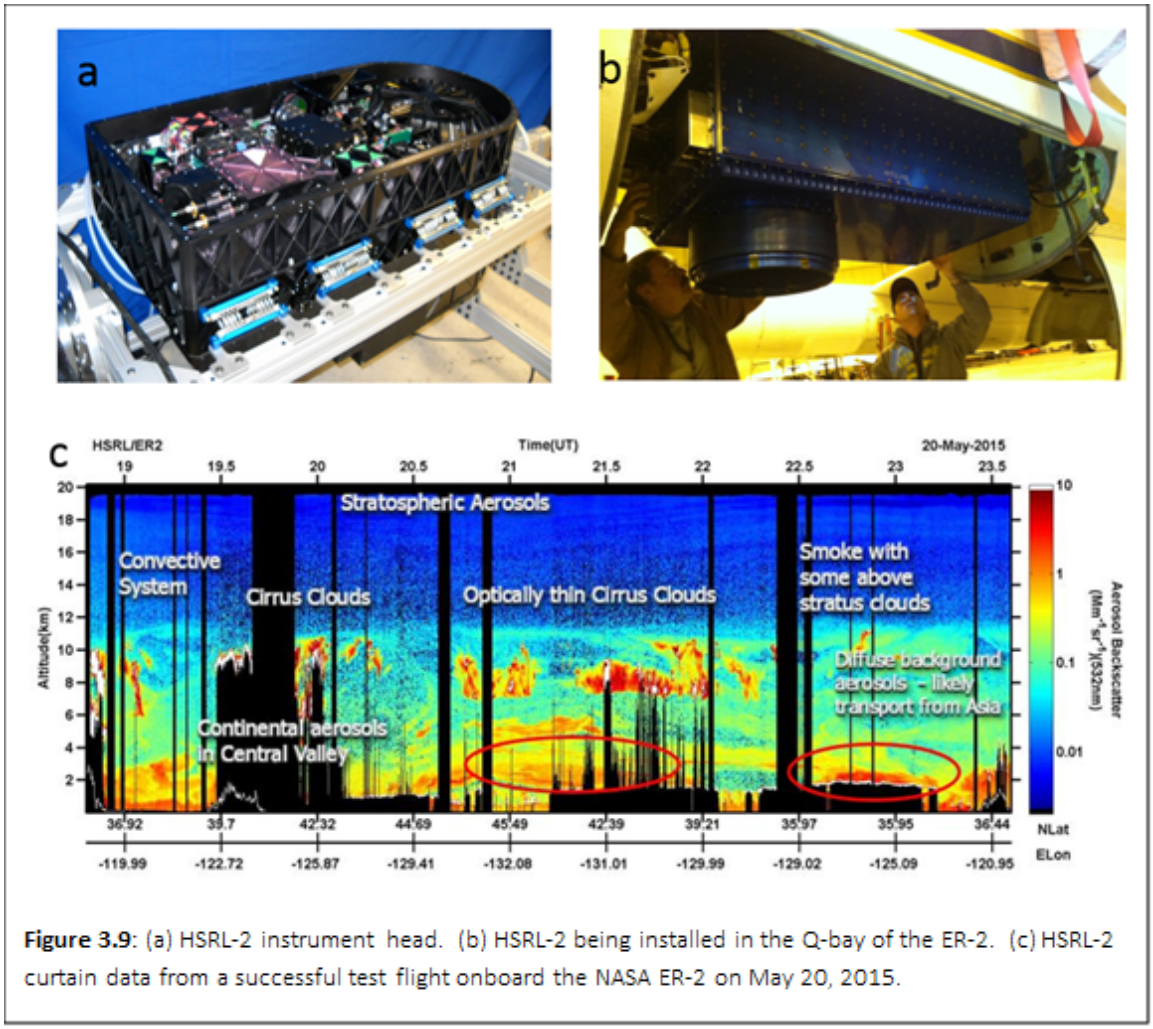

Figure 3.9: (a) HSRL-2 instrument head. (b) HSRL-2 being installed in the Q-bay of the ER-2. (c) HSRL-2 curtain data from a successful test flight onboard the NASA ER-2 on May 20, 2015.

A TRL assessment of the 3β + 2α + 2δ ACE lidar concept was conducted in 2013. This lidar concept was based significantly on CALIOP heritage. The TRL assessment focused on elements requiring technology development only and excluded elements that could be developed via straightforward engineering (e.g., commonly deployed electronic subsystems, thermal subsystems, structures, etc.) or based on CALIOP designs. Considering only atmospheric measurements, the readiness level was assessed at TRL-5. The subsystems limiting the TRL at that time were the laser transmitter and the interferometric optical filter used as an HSRL receiver. Significant technology development efforts have been made in both areas since 2013.

The laser transmitter consists of a seed laser subsystem and a pulsed laser. The baseline for the seed laser is the TRL-6 Tesat laser that is employed on two European Space Agency missions, the ALADIN lidar on ADM-Aeolus (launched in 2018) and the ATLID lidar on EarthCARE (launch in 2021). The development of a US source for the seed laser has being fostered under a series of SBIR awards to AdvR, Inc., that have incrementally advanced the TRL of various component technologies.

The AdvR seed laser subsystem consists of a compact, highly-efficient direct-diode laser, a planar lightwave circuit that integrates frequency doubling and phase modulation in a single fiber-coupled component, a compact iodine cell that provides an absolute frequency reference, and compact low-noise current and temperature controllers in a feedback loop that locks the diode seed laser wavelength. The direct-diode laser source at the heart of the seed laser system uses a distributed-feedback architecture and is undergoing independent space qualification at a component level. A direct diode source requires less than half the electrical power of the competing Tesat solid-state laser (8 W vs 20 W), provides sufficient short- and long-term stability for HSRL, and provides a stabilized optical output power of 10 mW, sufficient to seed a Nd:YAG laser without the need for additional amplification. The AdvR seed laser subsystem should reach TRL 6 by FY19 (funding dependent). Moreover, this technology approach is being further advanced by related developments under the HALO program. The performance of the seed laser developed under HALO, as well as size, weight and power all meet requirements for a future space-based implementation. Radiation studies on the hardware developed under HALO will be carried out starting in FY19.

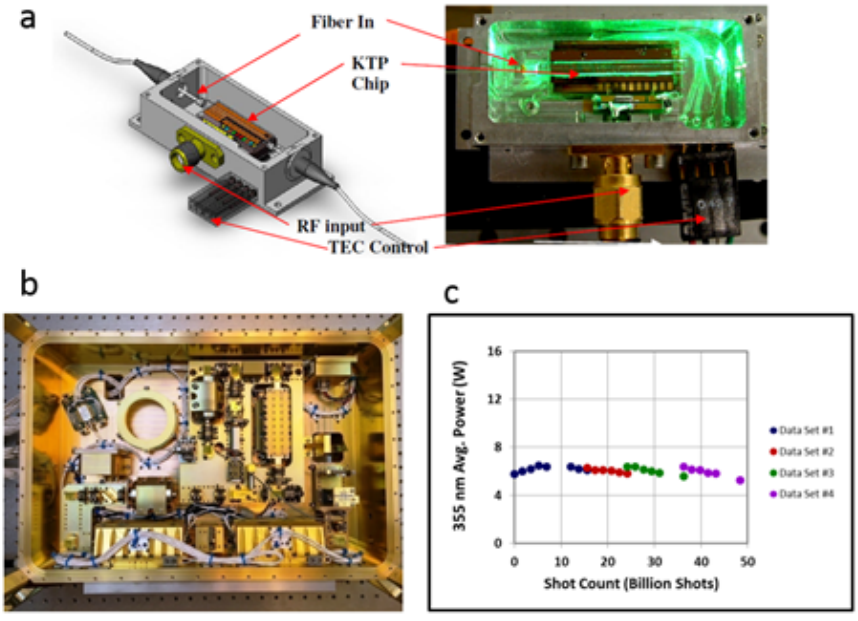

Figure 3.10: (a) Planar lightwave circuit that frequency doubles and phase modulates CW light from the seed laser. (b) HEUVD laser head. (c) 355 nm output power measured in accelerated life tests (50 billion shots would be equivalent to 16 years on orbit for ACE assuming a 100 Hz rep rate.

The pulsed laser is being advanced through the ESTO funded High Energy UV Demonstration Project (HEUVD) with Fibertek, Inc. Under this program, Fibertek has built an Engineering Development Unit (EDU) with architecture suitable for both the ACE and direct detection 3-D Winds Decadal Survey missions. This EDU design was based on lessons learned from the CALIPSO, CATS, and ICESat-2 space

laser development programs and incorporates design principles that insure it will meet environmental testing requirements and long-term operation in space.

A major concern for the pulsed laser is the lifetime of the laser in the UV wavelengths. An assessment of this risk by Fibertek concluded that the high-risk component was the third harmonic generator crystal, specifically the coating on the exit face of that crystal, which is an area of high UV fluence and on which small amounts of contamination can lead to damage. An ACE-funded program conducted over several years led to the development of contamination control procedures and identification of suitable coating vendors. Using a 20 kHz laser source, accelerated life tests in FY15 on crystals with these new coatings and prepared under the new contamination control procedures have demonstrated significant improvements in lifetimes: results showed negligible output power degradation at 50 billion laser shots (Figure 3.10), which would be equivalent to 16 years of on-orbit operations of the ACE lidar assuming a 100 Hz pulse rate. These results are extremely encouraging but alone are not conclusive. This is due to the fact that damage mechanisms are associated with defects in the coatings, and the small beam diameter of the irradiation source used in these tests resulted in sampling a small area that may have been serendipitously free of defects. To address this, life tests at ACE-like beam sizes have been conducted with the HEUVD laser itself to better evaluate the higher energy UV lifetime. A 1.5 billion shot test was successfully completed with no damage to the tripling crystal coatings at the 355-nm energies consistent with ACE requirements (50 mJ/pulse). A final test at twice the ACE energies (100 mJ/pulse) is underway and has achieved over 1 billion shots with no damage to the LBO and downstream optics as of the time of this writing. UV laser lifetime issues have been addressed by ESA for the lidars on ADM-Aeolus (launch in 2018) and EarthCARE (launch in 2019) and information from those programs as well as future on-orbit data will provide additional information on UV laser lifetime.

The only remaining step required to advance the readiness level of the HEUVD laser head to TRL 6 is environment testing. ESTO is currently considering whether to fund the required environmental tests in the final months of FY18.

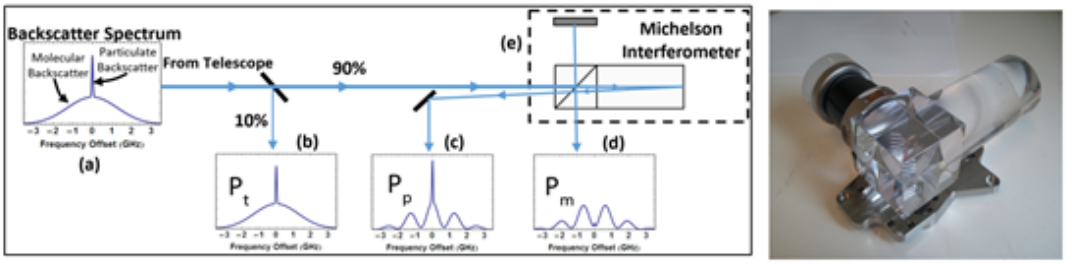

Figure 3.11: Off-axis Michelson interferometric receiver concept and photograph of the space-like quasi-monolithic interferometer tested in the lab and recently installed in HSRL-2 for operational testing.

To elevate the TRL of the HSRL interferometric receiver, an advanced interferometer was developed for space application (Figure 3.11). This interferometer is based on a quasi-monolithic design which has flown on three airborne HSRL-2 field missions is more stable in frequency and more mechanically robust than the piezoelectrically controlled version currently flown on earlier HSRL-2 missions. A spaceflight interferometer EDU has been developed, the design of which is based on an extensive structural-thermal-optical-performance (STOP) modeling effort focused on maximizing mechanical robustness, minimizing wavefront error (insuring optimal optical performance as an HSRL optical filter), and enabling reliable thermal tuning of the optical passband to the laser frequency (insuring robust on-orbit operation and control). Laboratory testing showed excellent optical performance as an HSRL optical filter, and vibration testing in FY18 elevated the readiness level to TRL-6. This unit was built for the 355-nm wavelength, and minor modifications to the design are being implemented in a 532-nm unit, which will be delivered and tested in fall of 2018. Based on similarity, the HSRL interferometric receiver is at TRL 6, regardless of wavelength. Operational algorithms for calibration and production of Level-2 aerosol extinction and backscatter products from the interferometric HSRL data have been demonstrated on airborne field missions since 2014.

Table 3.1.: TRL summary assuming CALIOP (TRL-9) as a basis and examining only major technology deltas from the CALIOP design and excluding subsystems falling into the category of straightforward engineering.

Subsystem	Baseline	Current TRL	Effort remaining to achieve TRL-6
Seed Laser	Tesat	6	None: identical lasers launching on ADM Aeolus in 2018 and EarthCARE in 2019
Pulsed Laser	HEUVD	5	Vibration and TVAC testing; may occur in 2018
HSRL interferometer	Quasi-monolithic Michelson	6	None: 355 nm unit passed environmental testing; 532 nm unit based on similar design
Overall	CALIOP and HSRL-2	5	HEUVD environmental testing

Advancing the TRL comprehensively by developing a space-like version of the entire ACE lidar remains impractical due to cost. Eliminating from TRL demonstration those elements which can developed via straightforward engineering and focusing instead on those elements which require technology development remains the most practical approach for an instrument like the lidar. Following this approach, the TRL of the ACE lidar remains at 5 with the prospect of increasing to TRL-6 within less than a year. The high TRL is based on spaceborne and airborne lidar demonstrations and technology development done under ACE and other NASA funding. For instance, the deployment of CALIOP on CALIPSO and CATS on ISS demonstrated some of the

capabilities required from the ACE lidar and showed that long-term operation in space is feasible (CALIOP has been operating for 12 years on orbit). Full-up airborne prototypes featuring all of the capabilities required for the ACE lidar have been developed and their measurements validated on numerous airborne field missions. The TRL summary in Table 3.1 is based on those technologies which represent deltas from the CALIOP design and excludes elements which can be accomplished via straightforward engineering. The limiting step to TRL 6 is funding the environmental testing of the HEUVD laser head.

The algorithms for processing ACE multiwavelength HSRL data are considered highly mature. They will be based on algorithms developed and employed for CALIOP and the airborne HSRL data for over a decade. The Level-1 algorithms for producing attenuated backscatter and volume depolarization will follow those developed for CALIOP (Winker et al. 2009). The algorithms for retrieving Level-2 aerosol/cloud backscatter and extinction, particulate depolarization, and aerosol type will follow those developed for the airborne HSRL program (Hair et al. 2008; Burton et al. 2012, 2013, 2018); however, to produce a data record consistent with the 12-year CALIOP record for purposes of trend studies, CALIOP-like Level-2 products will also be produced using algorithms developed for CALIOP (Winker et al. 2009). The more advanced algorithms for producing the Level-2 aerosol microphysical products (effective radius, concentration, refractive index, and single scatter albedo) were largely funded under ACE and have been demonstrated operationally using airborne HSRL-2 field data since 2012 as described in section 4. Extensive validation studies have been conducted that show the lidar retrievals of concentrations and effective radii compare well with corresponding values derived from airborne in situ measurements (Müller et al., 2014; Sawamura et al., 2017).

The GSFC Airborne Cloud-Aerosol Transport System (ACATS) has HSRL, standard backscatter, and Doppler wind capabilities at 532 nm (Yorks et al., 2014). The ACATS telescope rotates to four different look angles and is set at an off-nadir view angle of 45 degrees. After undergoing modifications to improve performance of the telescope, ACATS was tested on the ER-2 aircraft during August 2015. Performance was satisfactory, and additional future flights are planned. ACATS employs an interferometric HSRL technique that is different than the NASA LaRC HSRL technique. CATS was designed to implement an interferometric receiver at 532 nm using a multi-channel detector technique similar to ACATS, but issues with the laser stability prohibited science quality data. The hardware for this subsystem is at TRL 6 but data products produced from this ACATS approach require further assessment.

HSRL for meeting ocean requirements

The ocean objectives call for ocean-profiling HSRL measurements necessary to retrieve diffuse attenuation and particulate backscatter coefficients. Ocean objectives would be satisfied with measurements at 532 nm, but measurements at both 355 and 532 nm would be preferred, as together they allow the separation of

pigment absorption from absorption by colored dissolved organic matter (Hostetler et al. 2018). Huge advances in ocean profiling technology development, measurement demonstration, algorithm development, and measurement validation were made under ACE, Airborne Instrument Technology Transition (AITT), ESTO IIP, Ocean Biology and Biogeochemistry (OBB), and Earth Venture Suborbital programs over the course of the ACE pre-formulation period.

The airborne HSRL-1 instrument was first upgraded to enable ocean profiling capability at 532 nm in 2012 under an AITT award. Since then, it has flown five ocean-focused field missions on which the required ACE ocean measurements were demonstrated. These deployments include a deployment to the Azores in 2012 (Behrenfeld et al., 2013), the OBB-sponsored Ship-Aircraft Bio-Optical Research (SABOR) mission (Hair et al. 2016; Schulien et al. 2017) conducted in 2014, and three deployments for the North Atlantic Aerosols and Marine Ecosystems (NAAMES) Earth Venture Suborbital mission in 2015, 2016, and 2017.

The ACE HSRL design concept for the atmospheric requirements requires very little modification to meet the ocean requirements (Hostetler et al. 2018). The only modification involves the detectors and detection electronics to meet the required 2-m vertical resolution and reduce potential susceptibility to artifacts caused by strong specular reflection of the laser pulse from the ocean surface. The latter issue is the technology driver, as the specular reflection creates a strong signal pulse that can create artifacts in the subsurface profile, which in turn could limit the depth to which the ocean measurements can be accurately made. The airborne HSRL-1 instrument is typically operated in an off-nadir configuration to avoid receiving these specular reflections, and, while perfectly acceptable for airborne measurements, operating significantly off-nadir is suboptimal for the space application. To address this issue, considerable effort to design and develop detection subsystems immune to these artifacts has been conducted since 2014. One method using microchannel plate photo-multiplier tubes (MCP-PMTs) and an analog detection scheme is being implemented in HSRL-2 as part of the 2014 IIP project and will be field tested in 2019. Another method using multi-anode MCP-PMTs and a photon-counting detection scheme is being developed under a 2018 ESTO Advanced Component Technology award. Lab testing of early prototype hardware indicates that this approach is extremely effective and preferred over the analog detection scheme.

The TRL for ocean profiling is identical to that for the atmospheric measurements with the possible exception of the modifications required for the detection subsystem. The TRL for that subsystem is somewhat fluid, depending on the required fidelity and depth of the measurement. CALIOP data from CALIPSO have been used in numerous studies (e.g., Behrenfeld et al. 2013 and 2017) to demonstrate the scientific value of near-surface ocean measurements made by spaceborne lidar. PMT detectors similar to those used on CALIOP or ICESat-2 could be coupled to mature detection electronics designs to profile to 1-2 optical depths. This approach falls into the category of straightforward engineering rather than

technology development. Higher fidelity measurements to 3 optical depths are likely to require the more advanced photon-counting MCP-PMT approach being developed under the ACT project. This approach should reach TRL-6 by 2021. Notably, photon-counting MCP-PMT will also provide advances in the accuracy and precision of atmospheric measurements. It will improve the precision of signals from weaker targets (e.g., tenuous aerosols and molecular calibration targets in the stratosphere) and enable the ability to measure the profile of extinction in the tops of optically thick water clouds, which, when combined with cloud droplet size distributions retrieved from the polarimeter cloudbow data, will provide a scientifically important benefit for cloud science by enabling accurate estimates cloud droplet number concentration.

Algorithms for producing the ACE ocean products, diffuse attenuation and particulate backscatter backscatter coefficients (Hostetler et al. 2018), are similar to those developed for HSRL aerosol retrievals of extinction and backscatter. These algorithms are mature and have been validated against in situ measurements made from ships and satellite ocean color retrievals (Hair et al. 2016; Schulien et al. 2017).

Elastic Backscatter Lidar

While a simple elastic backscatter lidar cannot provide higher-order data products (i.e., cloud/aerosol microphysical properties), it does provide most required observables (i.e., layer top/base height, backscatter, depolarization). Over the course of the ACE pre-formulation effort, there were two elastic backscatter lidars operating from space that were not directly funded through ACE but are relevant to the ACE lidar concept. The CALIOP lidar, managed by NASA LaRC, was launched in April 2006. For over a decade, CALIOP has provided vertical profiles of cloud and aerosol properties essential to studies of the Earth's climate system, as demonstrated by over 2000 publications. The NASA GSFC CATS is an elastic backscatter lidar that operated for 33 months on-orbit (12 Feb. 2015 to 29 Oct. 2017) from the ISS, firing over 200 billion laser pulses. The CATS instrument was designed to demonstrate new in-space technologies for future Earth Science missions while also providing properties of clouds and aerosols. The CATS instrument provided spaceborne demonstration of a high repetition rate photon-counting approach to elastic backscatter lidar (Yorks et al., 2016). CATS operated the first 6 weeks in a mode that provided dual wavelength backscatter and depolarization measurements (532 and 1064 nm) using 2 beams. After the first laser failed, the last 31 months of operation were limited to single wavelength backscatter and depolarization measurements using one beam.

Several advances in elastic backscatter lidar algorithm and technology development were achieved in parallel with the ACE pre-formulation effort (mostly funded by sources other than ACE). CALIPSO processing algorithms based on the $2\beta+1\delta$ design advanced from Version 1 to Version 4, producing robust data products (Figure 3.12). CATS algorithms leveraged the heritage of the CALIPSO algorithms and implemented lessons learned to create algorithms for the multi-beam $2\beta+2\delta$ design

(Mode 7.1) and single beam 1β+1δ operations (Mode 7.2). Thus, elastic backscatter lidar algorithms are very mature for several different combinations of measurement capabilities (single or multiple backscatter and depolarization wavelengths). The elastic backscatter lidar subsystem components are all very reliable, with most reaching TRL 9 over the last decade. CALIOP has operated for over eleven years, well past its three-year proposed lifetime. The CALIOP laser, telescope, analog detectors, and other subsystem components are all TRL 9. CATS was designed to operate for 6 months but provided science quality data for 33 months. Many of the CATS subsystem components, especially the photon-counting detectors, are also TRL 9. Additionally, ESTO has funded the technology readiness advancement of a compact high-rep-rate laser capable of fitting a SmallSat architecture.

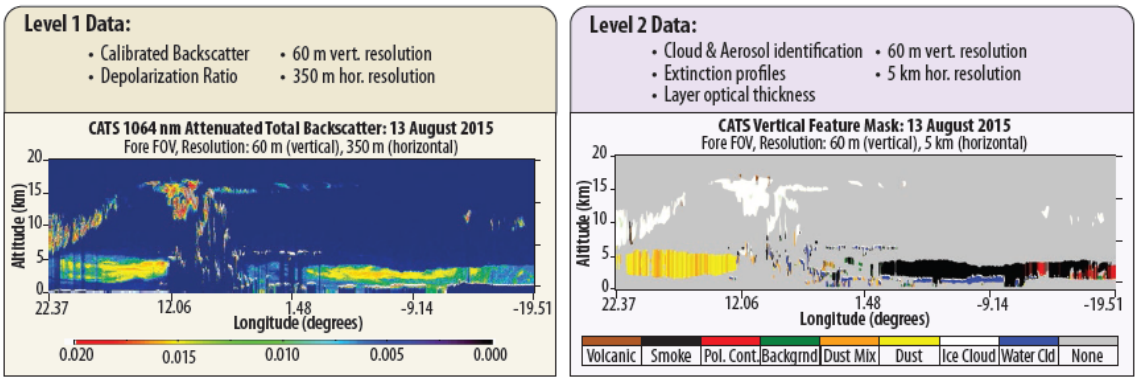

Figure 3.12. CATS data products including many of the observables the scientific community desires, such as backscatter coefficient, depolarization ratio, layer boundaries, and estimates of aerosol type, cloud phase, optical depth, and extinction.

CATS has provided valuable insight to inform a path forward (science goals, instrument design, implementation strategy) that optimizes science return versus cost. Examples are:

- *Diurnal Cycle*: Given the orbit of the ISS, a three-day repeat cycle that passes over the same locations but at different local times, CATS has shown that sensors in sun-synchronous orbits (passing over the same location at the same local time every overpass) are only capturing a "snapshot" of the cloud diurnal cycle (Noel et al., 2018). Future missions should consider an orbit and/or multiple SmallSat implementation that can complement GOES/ABI and capture the diurnal variability of clouds and aerosols.

- *Single Wavelength*: Many of the popular lidar data products (layer heights, backscatter, depolarization, cloud phase, aerosol type) can be accurately produced using a single wavelength (1β+1δ) lidar like CATS Mode 7.2 (Yorks et al., 2016; Emmanouil et al., 2017; McGill et al., 2018). A multiple SmallSat implementation of a 1β+1δ lidar would provide these data products with higher temporal/spatial coverage.

- *Near-Real Time (NRT) Data*: Simple NRT (data latency of <6 hours) CATS data products (backscatter profile, layer heights, etc.) demonstrate improvements in aerosol and volcanic plume transport forecasts (Hughes et al., 2017). A future mission's ability to produce NRT data is critical for air quality and aerosol forecast models, but models are still evolving to incorporate simple lidar products.

- *1064 nm Signal*: The CATS 1064 nm signal is robust and calibrated directly by normalizing to the Rayleigh profile. It also provides spectacular detail (due to high rep rate-photon, counting technique) and has proven critical to accurate detection of above cloud aerosols (ACA; Rajapakshe et al., 2017). A future space-based lidar needs to have similar or better signal strength at 1064 nm for accurate ACA detection and 1064 nm optical properties.

These results from CATS suggest an elastic backscatter lidar is a viable potential path forward, as a low-cost alternative to the 3β + 2α + 2δ HSRL, for a future space-based lidar mission, even as a single wavelength (1β+1δ) instrument implemented as multiple SmallSats. Information on CATS and access to the CATS data can be found at http://cats.gsfc.nasa.gov.

Lidar Summary and Recommendations

The progress made in advancing the ACE lidar concepts has put NASA in an excellent position for a near-term implementation of the Aerosols mission recommended in the 2017 Decadal Survey. An elastic backscatter lidar can leverage the heritage from CATS and CALIPSO to minimize risk and offer affordability. Such a lidar is a reliable (TRL 9) and cost-effective instrument that can be adapted to different orbit altitudes and several types of spaceborne architecture, such as a free-flyer mission like ACE or as part of a SmallSat constellation concept. The ACE pre-formulation effort focused primarily on significant advances towards an HSRL that meets the 3β + 2α + 2δ measurement requirements for higher-order cloud/aerosol microphysical properties. The cost and schedule for advancing HSRL subsystem components to TRL 6 is achievable for a near term mission (e.g., KDPA in 2020 or after).

We recommend that efforts in the near-term focus on the following activities:

- Advancing the TRL of key lidar subsystems, including the laser transmitter and detection electronics

- Advancing and validating retrieval algorithms, especially combined retrievals using lidar+polarimeter data and lidar+radar data.

- Improving simulation capabilities for conducting sensitivity studies, retrieval studies, and OSSEs using various lidar and spacecraft configurations.

- Refining lidar instrument designs, development schedules, partnering approaches, and cost estimates.

3.4 Ocean Color Sensor

Technology assessment and instrument concept development for an advanced ocean color sensor capable of satisfying all measurement requirements for the ACE radiometer began well before release of the 2007 Decadal Survey Report. This history has been documented in detail in McClain et al. (2012) and is briefly summarized here.

During 2000-2001, a study was conducted to assess satellite, field, and modeling requirements for a NASA carbon program (McClain et al., 2002, Gervin et al., 2002). One of the resultant recommendations was for an advanced ocean biology satellite sensor that expanded upon heritage sensor measurements by including UV bands for more accurate retrieval of colored dissolved organic matter (CDOM). This recommendation was merged with parallel work being conducted on an ocean lidar system for measuring phytoplankton biomass, yielding a new mission concept call the Physiology Lidar Multispectral Mission (PhyLM). The PhyLM mission was focused on improving the characterization of ocean carbon stocks and flows through both a refined separation of optically active in-water constituents and improved atmospheric corrections. At this point, the advanced ocean color sensor was envisioned as having only 3 UV bands, 11 visible bands, two NIR bands, and two SWIR bands. Importantly, the concept garnered enough interest to be granted funding in 2003 from NASA Goddard to conduct two Instrument Design Laboratory (IDL) studies, largely focused on the ocean radiometer. Thus, technology and instrument development work, ultimately in support of ACE, began more than 15 years ago.

Following the IDL studies, an external science team was assembled for PhyLM to define the science objectives and develop an initial Science Traceability Matrix (STM). The ACE Ocean Ecosystem STM (see Section 2 above) bears many similarities to this early draft. Continued developments to the PhyLM concept yielded, by 2005, an expanded mission including a polarimeter and lidar for characterizing aerosols and improving atmospheric corrections and an ocean radiometer with 5 nm resolution retrievals from the near UV into the NIR. At this point, the concept was called the Ocean Carbon, Ecosystem, and Near-Shore (OCEaNS) mission and it was submitted as a white paper for consideration during the NRC Decadal Survey study.

In 2006, NASA HQ requested formulation studies for several mission concepts in preparation for the Decadal Survey results, one of which was called the Global Ocean Carbon, Ecosystems, and Coastal Processes (GOCECP) mission. This formulation study provided funding for a third IDL assessment, yielding further design changes and refinements for an advanced ocean radiometer. The Decadal Survey results were released in late 2007 and included the interdisciplinary Aerosol, Cloud, and Ecosystems (ACE) mission, equivalent to the OCEaNS mission concept submitted in 2006, but with the addition of a cloud radar.

In June 2008, the ACE science team was formed and began the development of mission STMs for each of the science disciplines (see Section 2 above). Deliberations

by the ACE science team resulted in seven additional required specific bands on the ocean radiometer (plus 5 nm hyperspectral UV to NIR resolution), bringing the minimum number of 'aggregate' bands to 26 and including three bands in the SWIR. In the spring of 2009, as part of an ACE Mission Design Laboratory study of the baseline ACE mission, a fourth IDL study was conducted.

In 2010, President Obama released the NASA Plan for Earth Observations (NPEO 2010), announcing the PACE mission with an ocean radiometer as the primary instrument and dedicated to making advanced ocean measurements in preparation for the ACE mission. Soon thereafter, the PACE Science Definition Team (SDT) was formed and, as part of the SDT activities, a fifth IDL study was conducted, largely focused on assessing costs for an advanced radiometer.

In parallel with these mission concept developments, work was also undertaken to build a prototype 'proof-of-concept' advanced ocean color instrument named the Ocean Radiometer for Carbon Assessment (ORCA). Initial development of the ORCA prototype was supported by GSFC Internal Research and Development (IRAD) funds and focused on all optics components from a primary telescope to a 'blue channel' detector array. This work was further supported through an Instrument Incubator Program (IIP) grant and expanded to include a fully functioning prototype with both blue and red channels, along with system level testing at the National Institute of Standards and Technology. Instrument performance goals were significantly guided by an ocean radiometer specifications document developed by the ACE ocean science team (Meister et al., 2011). In 2010, a second IIP grant provides support for the design, fabrication, testing, and integration of flight-like focal planes and electronics in the ORCA prototype. All of these activities significantly advanced the technological readiness of an ocean radiometer meeting ACE and PACE requirements.

3.5 Ocean Color Validation Sensors

Optical Sensors for Planetary Radiance Energy (OSPREy)

ACE ocean color science objectives include geophysical property retrievals in the coastal ocean and contemporaneous observations of the ocean and atmosphere. The OSPREy project has been focused on developing and deploying a new suite of radiometers to support the increasing demands of NASA's ocean color research (Figure 3.13), with an emphasis on the data quality challenges associated with vicarious calibration and algorithm validation. OSPREy instruments are thermally regulated, ruggedized, and designed to operate autonomously (Hooker et al. 2012). An OSPREy system makes observations of the sea surface plus celestial targets (Sun, sky, and Moon) across the UV–SWIR domain (305–1,670 nm) to derive an unprecedented number of near-simultaneous atmospheric and oceanic parameters. OSPREy can also be used for land, snow, and ice targets, but has not been deployed for those observations. The radiance and irradiance sensors have highly accurate microradiometers (19 and 18, respectively), which can be used to continuously

calibrate the temperature-stabilized spectrograph. This type of measurement approach is referred to as hybridspectral, because it uses two types of detector technologies to improve the quality of the collected data. The spectrographs provide high resolution UV-NIR data, and the microradiometers extend the spectral domain to the SWIR. ACE pre-formulation funding for OSPREy development allowed for the addition of a 9-position filter wheel for three-axis polarimetry and improved dark correction for the spectrograph, plus novel performance characterization measurements using diverse celestial targets. The latter included the following during 2012: the Perigee (or Super) Moon on 6 May; the solar eclipse on 20 May; the Venus transit on 5 June; and the Blue (full) Moon on 31 August. Celestial observations provide autonomous above-water systems unique monitoring sources (as is done with the spaceborne sensor) with respect to in-water methods. OSPREy has a TRL of 9.

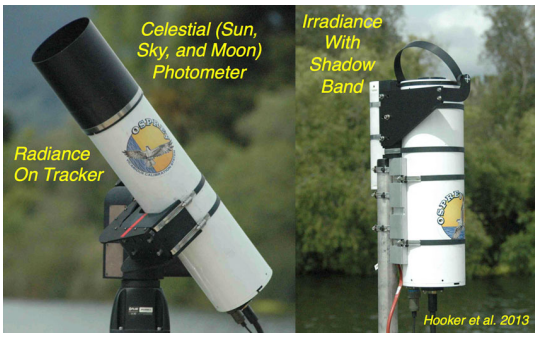

Figure 3.13: An OSPREy radiance &irradiance dyad deployed at a lake in 2013.

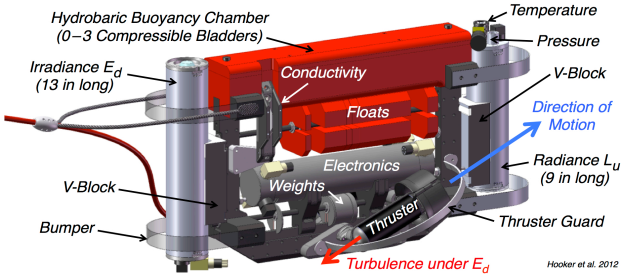

Figure 3.14: C-PrOPS thrusters (one on back) with conductivity probe mounted on a C-OPS instrument. The ydrobaric buoyancy permits descent rates as small as 5 cm/s with stable, ±5°, vertical tilts.

Compact-Optical Profiling System (C-OPS)

To ensure a state-of-the-art in-water validation data set for OSPREy data products of the sea surface, the Compact-Optical Profiling System (C-OPS) instrument (Morrow et al. 2010) was fitted with two digital thrusters as part of the Compact-Propulsion Option for Profiling Systems (C-PrOPS) accessory (Hooker 2014), which also added a conductivity probe. The programmable thrusters allow the C-OPS, which is built with the same microradiometers as OPSREy, to be maneuvered horizontally before a near-simultaneous profile of the water mass is made in close proximity to the OSPREy instrument system. The C-PrOPS prototype (Figure 3.14) was field commissioned with ACE support and significantly improved the data quality for in-water validation exercises by reducing the amount of time needed to acquire the optical data, because no vessel maneuvering is needed to position the profiler and the thrusters can be used to bring the profiler rapidly to the surface in between optical casts. In addition, the small thrusters orient the profiler vertically and produce negligible turbulence that is directed below the upward pointing irradiance sensor, so water column optical properties (now spanning 312–875 nm) are only minimally influenced by the motion of the profiler. The C-OPS instrument has a TRL of 9.

4 Measurement Algorithms

This section presents an overview of the Level 2 (L2) algorithms being developed for the ACE instruments. Level 0 (L0) and Level 1 (L1) algorithms are generally instrument specific and represent the steps needed to transform voltages captured by an instrument to geo-located, calibrated set of geophysically meaningful parameters. They are therefore described in Section 3 under Technology Assessment and Instrument Concept Development separately for each instrument.

While there is an expectation that L1 or L2 ACE measurements will be assimilated into comprehensive earth system models capable of representing cloud and aerosol microphysics, the details of such models and L4 algorithms are not described here.

4.1 Aerosol

The ACE requirements on retrieving the size distribution, complex refractive index and non-sphericity of aerosols mean that a retrieval approach is required that makes full use of the information content of the measurements.

The basis of L2 aerosol retrieval algorithms for both passive polarimetric observations and multi-spectral high spectral resolution lidar is necessarily the inversion of the observations to retrieve a microphysical model (size and complex refractive index) and amount (number concentration, surface area concentration, volume concentration) of aerosol that is consistent with the observations, with some form of regularization to suppress unphysical, or unlikely solutions. The regularization generally has the effect of forcing the retrieved aerosol properties (e.g. size distribution, spectral refractive index) to be smooth (Dubovik et al. 2011) or impose constraints on retrieved values (Hasekamp et al. 2011). The passive polarimetric observations depend non-linearly on the required aerosol properties and the inversion is therefore iterative in nature and the application of these schemes to the type of global data that is expected from a future ACE mission will be challenging, but currently both standard parallelization techniques (Wu et al., 2015), implementations using Graphics Processing Units (GPUs) and analytical simplifications of radiative transfer (Chaikovskaya et al., 2014) and neural networks (Di Noia et al. 2017) are being applied successfully to processing of global polarimetric data from POLDER.

While different groups will adapt specific implementations of optimal estimation techniques to the measurement set provided by their sensor, there are two aspects of aerosol remote sensing from passive polarimetric observations that are general to any approach. The first is an adequate model of the underlying surface and the second is a fast and accurate radiative transfer model for the atmosphere that ideally provides analytic determination of functional derivatives of the radiation field with respect to the aerosol parameters being retrieved, commonly known as Jacobians. We note that a recent review paper (Dubovik et al. 2019) provides an overview of available polarimetric observations, their history and expected developments, and the state at the time of writing of resulting aerosol products.

Surface Characterization

Surface models can be divided between water and land surfaces, with the primary water surface of interest being the ocean. For remote sensing of aerosol over the ocean the specular reflection of light from the surface is well represented by the model of Cox and Munk (1954). We note that while this model always provides a reasonable representation of the sunlight scattered off the ocean surface, if it is estimated from multi-angle observations as part of an aerosol retrieval, the wind speed and direction retrieved will not necessarily correspond to the actual wind speed and direction (Su et al. 2002, Chowdhary et al. 2005). In addition to surface scattering there is also a contribution from light scattered under water that is not negligible in the visible part of the spectrum. The brightness and spectrum of this light depends on the biomass content of the ocean, such that variations in the color of the ocean can be observed even from space. Rayleigh scattering by pure sea water, and Rayleigh-Gans type scattering by plankton, causes this light to be polarized with a distinctive angular distribution. Chowdhary et al. (2012) review a hydrosol model and discuss its sensitivity to variations in colored dissolved organic matter (CDOM) and the scattering function of marine particulates. They show that the impact of variations in CDOM on the polarized reflectance is comparable to or less than the standard error of this reflectance whereas their effects on total reflectance may be substantial (i.e. up to > 30%). This emphasizes the value of multiple polarization measurements through the visible part of the spectrum when performing aerosol remote sensing over the ocean. The model for ocean body scattering developed by the RSP group has recently been incorporated into the Generalized Retrieval of Aerosol and Surface Properties (GRASP) algorithm (Dubovik et al. 2011) in collaboration with the University of Lille. In General land surface models are somewhat ad hoc with the parameters that control the total bidirectional reflectance factor of the surface being unrelated to those controlling the polarized reflectance of the surface (Cairns et al. 2009a). The RSP group has worked with the groups at SRON and the University of Lille to develop a more advanced physically based surface model where the total and polarized reflectance are controlled by the same parameters, which describe the underlying physical scattering processes, that generate the reflection of light at a surface (Litvinov et al. 2012). The observations obtained prior to PODEX during a test flight of the RSP on the NASA ER-2 and some earlier data from the Carbonaceous Aerosols and Radiative Effects Study (CARES) (Zaveri et al. 2012) have been used to establish the polarization properties of snow (Ottaviani et al. 2012, 2015). The small magnitude of the polarized reflectance of snow and its weak spectral variation over 400 to 2300 nm hold the promise of robust aerosols retrievals over snow from sensors that have a sufficient spectral range of polarized observations.

RSP Aerosol Algorithms

One key aspect of aerosol retrievals over ocean using polarization observations is to have a physically based model of ocean body scattering to provide a lower boundary condition. The ocean body scattering model that RSP aerosol retrieval algorithms use (Chowdhary et al. 2012) has therefore being updated in line with current trends

in ocean color remote sensing (Maritorena et al. 2010) to allow scattering by particulate matter, absorption by colored dissolved organic matter and Chlorophyll concentration to all vary independently.

Aerosol retrievals using RSP observations over land for the PODEX and SEAC4RS field campaigns were evaluated against collocated AERONET measurements (Wu et al. 2015) and found to show good agreement for aerosol optical depth (AOD), size distribution, single scattering albedo (SSA) and refractive index. The critical importance of multi-angle polarization measurements in the near-UV and blue part of the spectrum for passive remote sensing of aerosol layer height was identified and good agreement of the retrieved aerosol layer height from RSP with measurements from the Cloud Physics Lidar (CPL) showing a mean absolute difference of less than 1 km was found (Wu et al. 2016). The Phillips-Tikhonov algorithm used in these retrievals was then coupled with a neural-network that was used to provide an initial guess for the iterative scheme (Di Noia et al. 2017). The resulting algorithm appears capable of accurately retrieving aerosol optical thickness, fine-mode effective radius and aerosol layer height from RSP data. Among the advantages of using a neural network as initial guess for an iterative algorithm are a decrease in processing time and an increase in the number of converging retrievals.

An alternative optimal estimation retrieval framework, the Microphysical Aerosol Properties from Polarimetry (MAPP) algorithm was developed using the GISS vector radiative transfer code (Stamnes et al. 2018). This iterative scheme is particularly focused on simultaneous retrieval of aerosol microphysical properties and ocean color bio-optical parameters using multi-angular total and polarized radiances. aerosol retrievals over ocean. Measurements collected during the 2012 Two-Column Aerosol Project (TCAP) campaign and the 2014 Ship-Aircraft Bio Optical Research (SABOR) campaign were analyzed and good agreement between the RSP retrievals and co-incident lidar measurements made by NASA High Spectral Resolution Lidar 1 and 2 systems was found. The compatibility of the passive (RSP) and active (HSRL) sensors is a key milestone on the path to a combined lidar+polarimeter retrieval using both HSRL and RSP measurements.

MSPI Aerosol Algorithms

Optimization based algorithms have been developed to retrieve aerosol loading and aerosol optical and microphysical properties from AirMSPI observations over three different types of lower boundaries: ocean (Xu et al., 2016), land (Xu et al., 2017), and stratocumulus cloud (Xu et al., 2018). Boundary properties are coupled into aerosol retrievals, which include water-leaving radiance for water, bidirectional surface reflectance factors for land, and cloud droplet size distribution, cloud top height, and cloud optical depth for stratocumulus clouds. Water-vapor abundance is also retrieved from AirMSPI's water vapor band. The retrievals impose various types of constraints on horizontal variations of aerosol microphysical properties following Dubovik et al. (2011), spectral invariance constraints on the angular shape

of surface bidirectional reflectance factor and polarized surface reflectance (Diner et al., 2005, 2012), and relations between under-water optical properties with the water-leaving radiance (Zhai et al., 2010). A hybrid radiative transfer (RT) code that combines the strength of Markov chain (Xu et al., 2012) and adding-doubling (Hansen and Travis, 1974) RT methods has been developed to improve the modeling efficiency (Xu et al., 2017).

In addition to the various algorithms for the retrieval of aerosol properties, an algorithm was developed for the retrieval of liquid water cloud properties, including the droplet size distribution and cloud optical depth (Diner et al., 2013b; Xu et al., 2018). This algorithm utilizes the polarized primary and supernumerary cloudbows in AirMSPI's continuous sweep imagery, based on Bréon and Goloub (1998). AirMSPI Level 2 liquid water cloud products have been delivered to the NASA Langley Atmospheric Science Data Center for public distribution, along with supporting Quality Statement and Data Product Specification documents, see https://eosweb.larc.nasa.gov/project/airmspi/airmspi_table.

The MSPI retrieval algorithms have been tested using GroundMSPI observations, and AirMSPI observations over ocean, land and stratocumulus clouds acquired in multiple field campaigns such as PODEX, SEAC4RS, CalWater, ImPACT-PM, ORACLES, and ACEPOL. Examples are shown in Figures 4.1, 4.2, 4.3a, and 4.3b. Initial results show that spectral optical depths, aerosol microphysical properties, and normalized water-leaving radiance compare favorably to independent reference data derived from AERONET, NASA HSRL-2 (Hair et al., 2008), and RSP (Cairns et al., 1999). To address the sensitivity of the coupled aerosol-surface retrieval to initial guesses, multiple types of constraints have been imposed on retrievals. For image-based remote sensing technologies, data processing efficiency without losing modeling accuracy is a major concern for ACE. Several speed enhancements to the JPL MSPI algorithm are being investigated, including tradeoff of speed and accuracy in the forward radiative transfer module, combination of the optimization algorithm with lookup tables, and use of a Graphical Processing Unit (GPU).

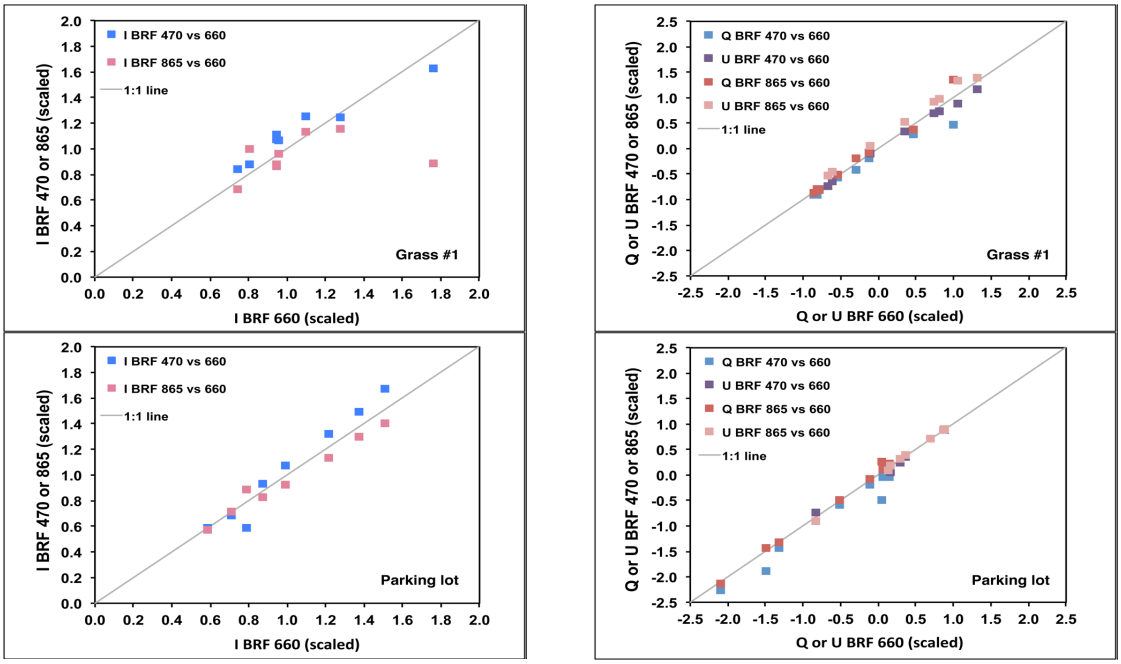

Figure 4.1: Left: GroundMSPI data collected over surface targets as the scattering angle changed due to motion of the Sun across the sky. Scaled bidirectional reflectance factors (BRF) at 470 and 865 relate linearly to the BRF at 865 nm, showing spectral invariance in the angular BRF shape. Right: Relationship between polarized BRF calculated using Q and U at 470 and 865 nm to 660 nm, showing spectral invariance in both the magnitude and angular shape.

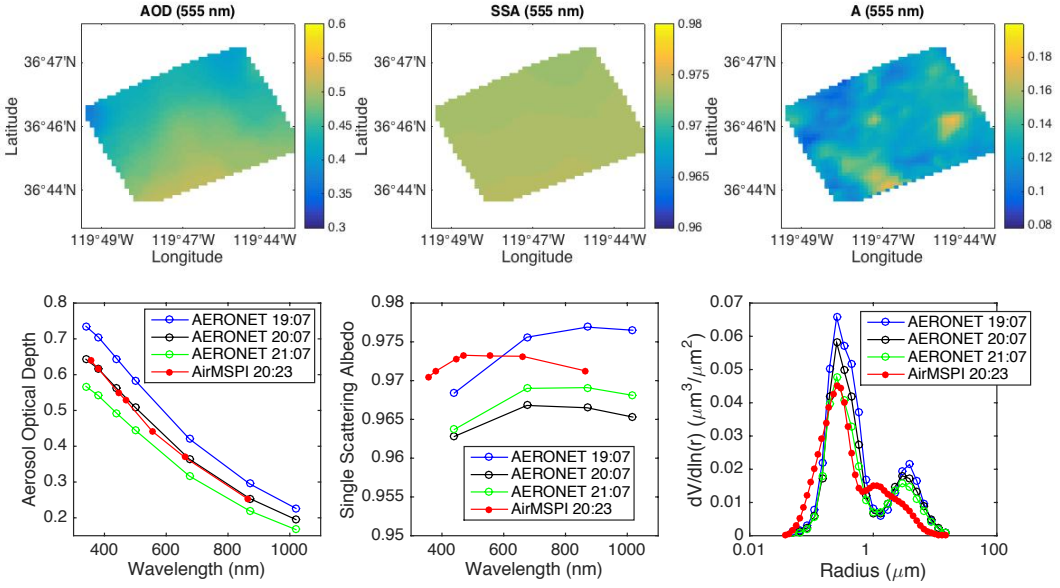

Figure 4.2: Example aerosol aerosol optical depth (AOD), single scattering albedo (SSA), surface albedo (A) retrieval using MSPI over-land retrieval algorithm applied to AirMSPI data over Fresno, CA, 6 January 2012 during an

engineering flight of AirMSPI. Comparisons in the three bottom panels were made to spatiotemporally collocated AERONET reference data. Figures were adapted from Xu et al. (2017).

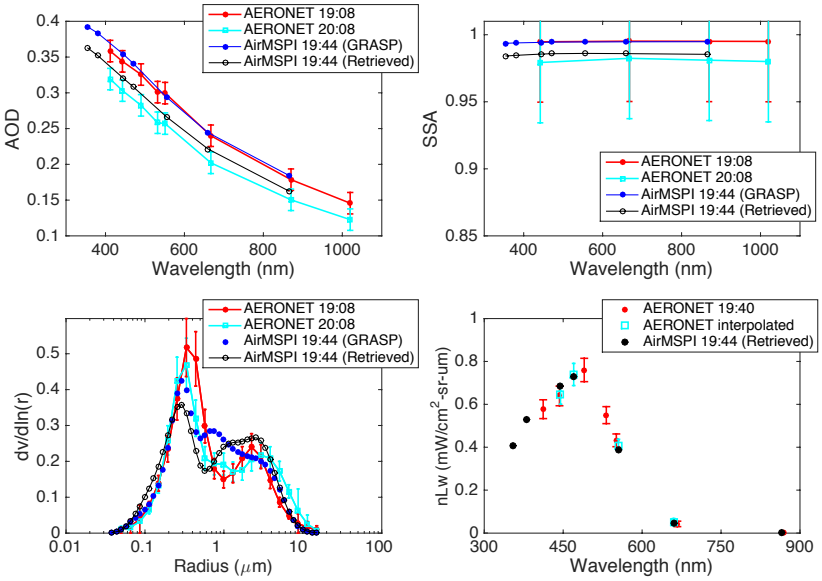

Figure 4.3a: Example aerosol AOD, single scattering albedo (SSA), volume-weighted aerosol size distribution, and normalized water-leaving radiance (nLw) retrieval using the MSPI over-ocean retrieval algorithm applied to AirMSPI data over the USC SeaPRISM AERONET site off the coast of southern CA, 6 February 2013 during PODEX. Figures adapted from Xu *et al.* (2016).

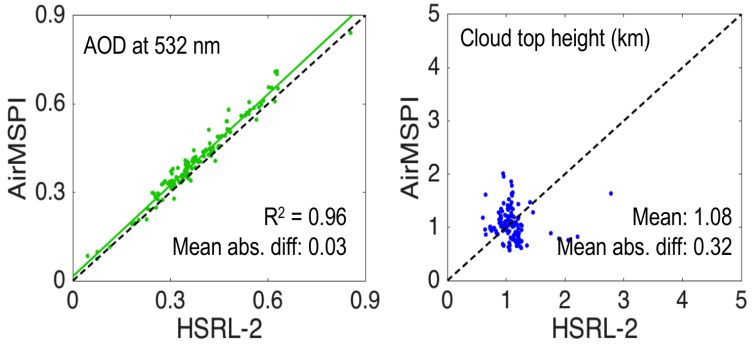

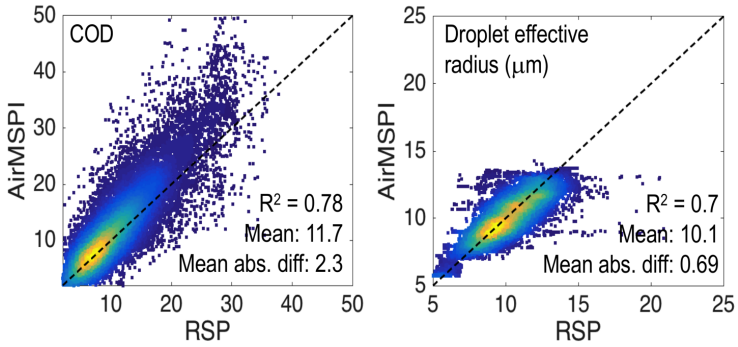

Figure 4.3b: Example above-cloud aerosol optical depth (AOD, upper left), cloud-top height (upper right), cloud optical depth (lower left), and cloud-top droplet effective radius (lower right) retrieved using MSPI aerosol and cloud coupled retrieval algorithm. As the input data, AirMSPI cloud imageries were acquired during ORACLES campaign over South Atlantic Ocean (off the coast of Namibia), which took place in August and September 2016. Retrieval comparison was made to the reference data of above-cloud aerosol optical depth and cloud-top height from NASA HSRL-2 measurements, and to reference data of cloud optical depth and effective radius of cloud-top droplets from NASA RSP measurements. Figures adapted from Xu *et al.* (2018).

PACS/HARP Aerosol Algorithms

The HARP group has worked with Dr. Oleg Dubovik;'s group on a version of the GRASP algorithm that is optimized for HARP retrievals using its unique angular sampling and wavelength combination (Dubovik et al. 2011; Dubovik et al. 2014). The GRASP algorithm has been fully integrated to the UMBC servers and is now operationally available for the fit and retrieval of aerosol microphysical data from the HARP polarimeter.

Figure 4.3c shows an example of inversion of the aerosol microphysical properties using GRASP over HARP data collected in prescribed fires in Arizona during the ACEPOL experiment. In this example GRASP provided a very good fit over this challenging case, allowing for the retrieval of the particle size distribution, total aerosol optical depth, single scattering albedo, particle asymmetry, etc.

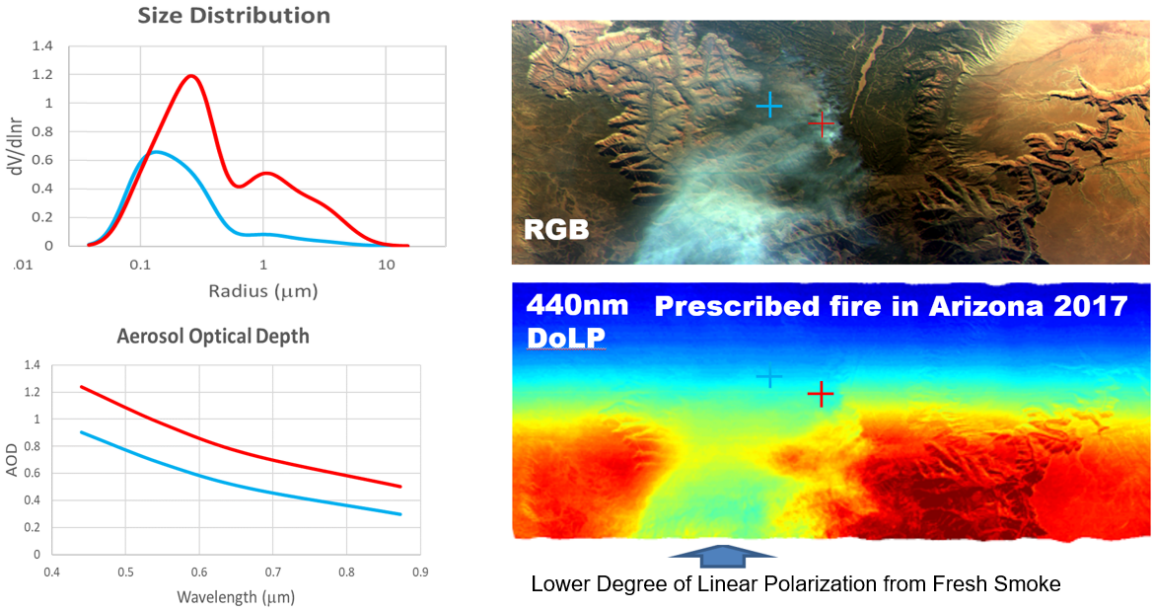

Figure 4.3c: The top figure on the right-hand side shows a single angle RGB image of a prescribed fire collected by AirHARP in Arizona during the ACEPOL flight campaign. The bottom figure shows an image of the degree of linear polarization at 440nm wavelength emphasizing the break of the typical Rayleigh scattering pattern by the mostly non-spherical fresh smoke particles. Both plots on the left-hand side show results of retrievals by the GRASP algorithm over this smoke.

HSRL Aerosol Algorithms

Operational code for lidar retrievals of ACE aerosol products has been developed and used to produce ACE-like Level-2 data products from the eight field missions flown with the LaRC 3β + 2α + 2δ ACE prototype HSRL lidar. These products fall into three categories. First are the basic Level-2 optical products retrieved from the lidar signals (aerosol backscatter, extinction, depolarization). The algorithms for these products, including prerequisite instrument calibrations, are described in Hair et al. (2008), Burton et al. (2014), and Burton et al. (2018).

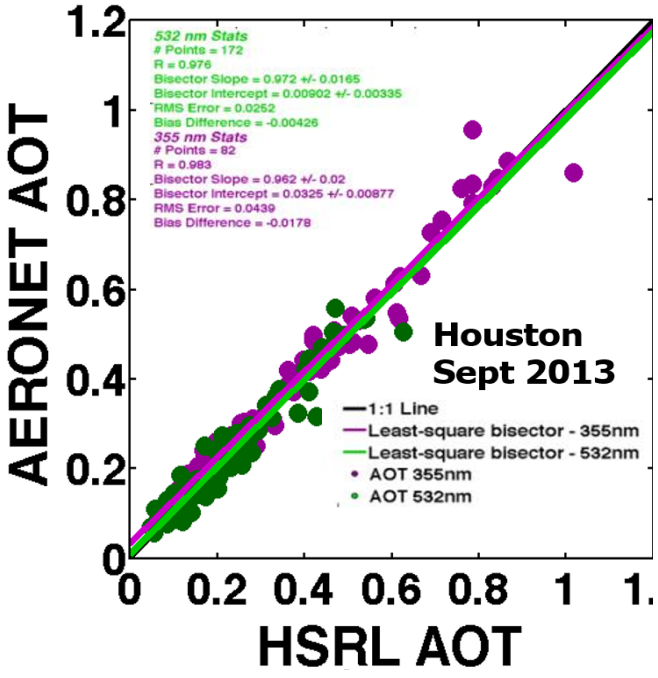

Figure 4.4: Comparison of AOT (355 and 532 nm) from HSRL-2 and DRAGON-AERONET measurements over Houston during

Second is aerosol type, which is a qualitative rather than a

quantitative product. Aerosol type (e.g., marine, smoke, dust, urban pollution, etc.) is inferred from lidar intensive parameters (e.g., parameters like aerosol extinction-to-backscatter ratio, depolarization ratio, and backscatter color ratio, which are independent of aerosol loading and depend only on particle properties). Aerosol typing algorithms and results from airborne field missions are described in Burton et al. (2012, 2013, and 2018). While there is no agreed-upon universal definition of aerosol type as a geophysical variable, interest in aerosol type from HSRL measurements steadily increased over the ACE era, due in large part to the papers produced from the numerous field campaigns flown by the LaRC airborne HSRLs. In fact, the typing methodology has been adopted, with modification, by European lidar groups for the interpretation of their airborne, spaceborne, and ground-based measurements (e.g., Groß et al., 2015, Papagiannopoulos et al., 2018). Significantly, progress has also been made connecting HSRL aerosol types to chemical speciation in chemical transport models (Dawson et al., 2017), suggesting at least one method to use HSRL measurements to assess and improve model predictions.

Third are advanced aerosol optical/microphysical products derived from the basic Level-2 aerosol optical products. These include effective radius, index of refraction, single scatter albedo, absorption, and concentration, and are derived using advanced inversion techniques. The accuracy of these retrieved aerosol products has been extensively assessed using data acquired on numerous airborne field missions from other sensors flying on participating aircraft and retrievals from ground-based AERONET instruments placed along the flight tracks (e.g., Sawamura et al., 2014, 2018; Müller et al., 2014). Figure 4.4 shows a comparison of aerosol optical thickness from the basic HSRL-2 measurements (at both 355 and 532 nm) with coincident AEROCOM measurements acquired during the NASA DISCOVER-AQ mission over Houston. Figure 4.5 shows a comparison of aerosol concentration and effective radius profiles derived from the HSRL-2 $3\beta + 2\alpha$ measurements with coincident airborne in situ measurements acquired from the DOE G-1 aircraft during the DOE Two Column Aerosol Project (TCAP). More extensive comparisons with both airborne in situ data and AERONET retrievals have been conducted using data from three NASA DISCOVER-AQ deployments (two in 2013 and one in 2014) and three ORACLES deployments (2016, 2017, and 2018)(see Figure 4.6). Moreover, Burton et al. (2016) conducted a theoretical study of the information content in $3\beta + 2\alpha$ data to determine the limits of what parameters could and could not be retrieved. This study indicated that retrievals would have the greatest sensitivity to aerosol effective radius and concentration and the least sensitivity to aerosol absorption.

To provide more accurate aerosol optical/microphysical products, a joint lidar+polarimeter aerosol retrieval algorithm was developed with funding from both ACE and the ROSES Remote Sensing Theory element. The algorithm employs and optimal estimate framework to retrieve vertically resolved aerosol properties. This retrieval has been applied to HSRL-2 and RSP data collected from the 2016 ORACLES ER-2 deployment. The joint lidar+polarimeter algorithms shows promise

for improving the accuracy of the lidar-only retrievals and providing vertically resolved products that are otherwise available only from column-wise polarimeter retrievals.

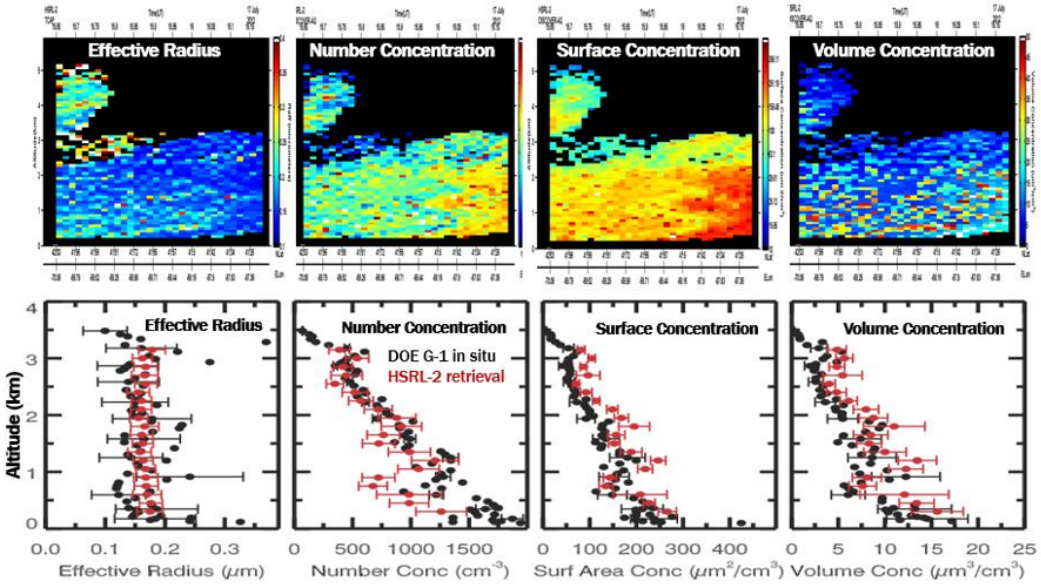

Figure 4.5. (top) Curtains showing HSRL-2 retrievals of microphysical parameters and (bottom) comparisons of microphysical parameters retrieved from the HSRL-2 3b+2a inversion method (red) and from the G-1 in situ measurements (black) on 17 July 2012 (from Müller et al. 2014).

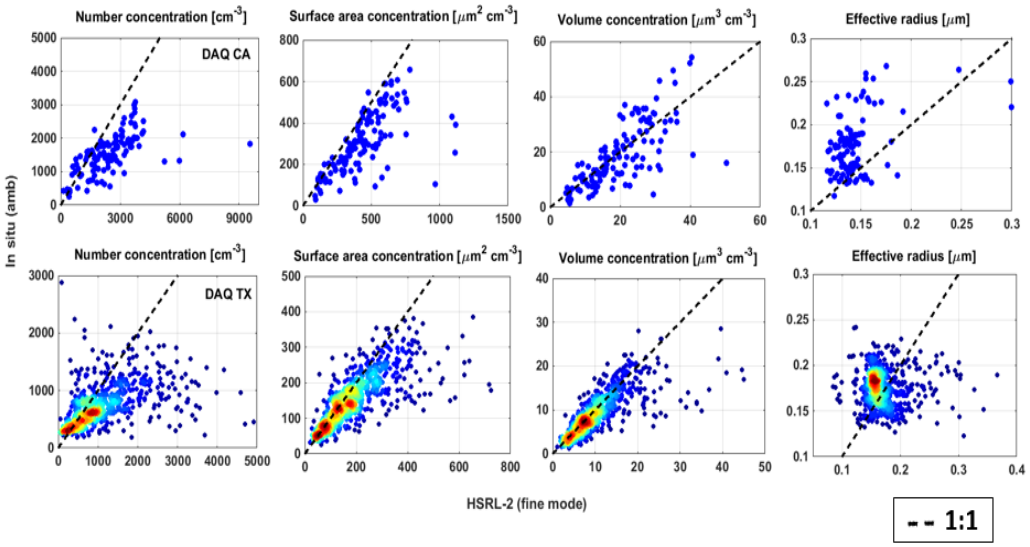

Figure 4.6. Comparison of aerosol microphysical parameters derived from HSRL-2 3ß+2α inversion method and coincident airborne in situ measurements acquired during the NASA DISCOVER-AQ missions over the California central valley (top) and Houston (bottom).

4.2 Clouds

In this subsection we describe the general approach for assessing the impact of the ACE observing system on the retrieval of cloud and precipitation geophysical parameters, and the simplifications necessary for operational implementation of an algorithm suite. This is followed by the description of emerging L2 algorithms being developed for ground based and airborne sensors that will inform the operational ACE clouds processing.

General Approach

In the development of L2 algorithms for ACE Clouds, we have two very specific research objectives that address short and long terms goals. Our most immediate need is to develop tools that allow us to rigorously define the trade space between science objectives and instrument suite complexity, and our more long term goals are to develop L2 algorithms that would be suitable for operational implementation prior to launch of ACE assets.

In our earlier work summarized in the 2010 ACE Report, tools to rigorously define the trade space were not available. While we used a rigorous method to estimate requirements on geophysical parameters, it was impossible to characterize quantitatively how the requirements on geophysical parameters mapped to instrument requirements. This is especially challenging because the L2 algorithms for ACE clouds will rely on synergistic combinations of active and passive measurements that have evolved from the A-Train era (*i.e.,* Mace et al., 2016). While we could theorize what measurements would constrain what aspects of the geophysical quantities of interest appearing in the Science Traceability Matrices of

that earlier report (Section 2), we could not say rigorously what the instrument requirements would be when combined in synergistic algorithms. Advanced statistical tools for L2 algorithm development are now becoming available that will allow us to address this issue rigorously as ACE moves forward (Posselt et al., 2016; Posselt and Mace, 2014).

We take the approach that a set of measurements *(y)* have some level of uncertainty and represent an atmospheric state (*x*) and there exists a set of forward models relating x to y that have assumptions with quantifiable uncertainties. We can then utilize methodologies based in Bayesian statistics:

$$p(x|y) = \frac{p(x)\,p(y|x)}{p(y)}$$

Then, the atmospheric state that we seek to characterize is represented as a posterior probability distribution, *p(x|y),* that results from mapping the measurements through a set of forward models that replicate the uncertain measurements as a function of the uncertain atmospheric state. In the short term, we seek to know the optimal set of measurements that produce an atmospheric state probability that satisfies our requirements on geophysical quantities while in the long term, we seek algorithms that efficiently provide *p(x|y)* with reasonable characterizations of uncertainty.

A hierarchy of techniques exist to accomplish both our near- and longer-term goals. To accomplish our near-term goals, we make computational efficiency a secondary objective and seek an approach that is least constrained by assumptions in mapping the relationships between measurements and the posterior probability distribution of the atmospheric state. What is needed is a way to *generate rigorously the posterior p.d.f.* Markov Chain Monte Carlo (MCMC, Tamminen 2004; Tarantola 2005; Posselt et al., 2008; Posselt and Vukicevic 2010) methods provide such a tool. MCMC algorithms consist of a guided random walk through the probability space. See Posselt and Mace (2014) for an example of MCMC applied to a mixed phase snow cloud using ground-based combinations of radar, microwave radiometer, and surface solar flux and Posselt et al. (2016) for application of this approach to shallow warm cumulus. We envision that such an approach, when combined with actual measurements and model-base observation system simulation experiments (OSSE), will rigorously define the trade space between instrument requirements and geophysical parameter requirements.

Our longer-term goals of developing operational L2 algorithms will utilize more computationally efficient approaches to solving Bayes theorem but at the cost of reduced accuracy in producing the posterior solution probability. Optimal estimation (OE) has emerged as a preferred approach in this regard. To make OE more computationally efficient than MCMC, the PDF's are assumed to be adequately described by Gaussians and the relationships between forward models and measurements are assumed to be described by the first derivative of the

measurement with respect to the atmospheric state – i.e. linearity in the relationship is assumed so that a first order Taylor expansion is sufficient to characterize these relationships. OE algorithms that are now under development (Mace *et al*. 2016, among others) will form the basis of the L2 algorithm suite that will ultimately be implemented on ACE flight data. We will use the more rigorous MCMC results, field data, and OSSE studies to develop and validate the OE results.

RSP Cloud Algorithms

The property of a cloud that is required first, for a multi-angle sensor, is the cloud top height so that views from all angles can be collocated to cloud top. Operationally, cloud top heights retrieved from RSP hyper-stereo intensity observations are used for this. These cloud top heights haven been verified against lidar derived cloud top heights (Sinclair et al 2017). In addition, cloud top pressure is retrieved using short wavelength (410 and 470 nm) polarized reflectances (Van Diedenhoven et. al. 2013). Cloud top height estimates are used to remap the multi-view RSP data such that they are coincident at the cloud top altitude and provide contiguous angular sampling over a view angle range of ±60° from nadir for each spatial sample of a cloud.

For a sensor in low Earth orbit this view angle range would frequently include a scattering angle range from 135° to 165°, which exhibits a sharply defined cloud bow structure for water clouds. The retrieval of droplet size distributions from cloud bow observations was originally implemented by Bréon and Goloub (1998) using a parametric fit in which the size distribution is represented by the effective radius and variance of a gamma size distribution. The accuracy of this type of approach, its range of applicability and robustness against 3-D effects was evaluated more recently (Alexandrov et al. 2012a) using Monte-Carlo simulations of radiative transfer through a modeled (Ackerman et al. 2004) cloud field, and using in situ measurements obtained during the NAAMES campaign (Alexandrov et al. 2018). While parametric fitting provides a simple method for estimating cloud droplet size distributions, it was found that contiguous high (~ 1°) angular resolution observations of the cloud bow can used in a rainbow Fourier transform (RFT) that provides an accurate non-parametric estimate of the shape of the droplet size distribution (Alexandrov et al. 2012b). The RFT is valuable in the analysis of cases such as fogs, or multi-layer water clouds where the assumption that the cloud bow is generated by a single gamma distributed droplet size distribution is incorrect. Application of this approach to warm and supercooled liquid cloud layers was demonstrated using data from the PODEX and SEAC4RS campaigns (Alexandrov et al., 2015, 2016). It should be noted that variations in droplet size distribution may be substantial, even within a quite homogeneous cloud deck, but can be retrieved for each pixel from RSP observations. The high angular resolution of the RSP polarized measurements is crucial for the cloud droplet size retrieval products. Since the RSP makes shortwave infrared (SWIR) radiance measurements at 1590 and 2260 nm, optical depth and effective radius retrievals similar to those

developed for MODIS/VIIRS/SEVIRI etc. are also performed (cf. Nakajima and King 1990). This allows for the comparison and evaluation of the different size retrievals.

RSP observations are also used to provide a unique measurement-based estimate of cloud geometric thickness. This is accomplished using polarimetric measurements in the 960 nm water vapor absorption band to retrieve the amount of both above-cloud and in-cloud water vapor and then relate in-cloud water vapor amount to physical thickness based on the assumption that the in-cloud water vapor mixing ratio is saturated. The cloud geometric thickness, together with the droplet size and optical depth retrievals are then used to estimate the cloud droplet number concentration (Sinclair et al. 2019), without making any assumptions about the adiabatic profile of liquid water content in cloud (cf. Grosvenor et al. 2018).

Presence of the cloud bow structure associated with spherical cloud drops also provides a virtually unambiguous indication of a liquid cloud top phase (Goloub et al. 2000). Operationally, a liquid index (van Diedenhoven et al. 2012a) is calculated that quantifies the strength of the rainbow signal in RSP polarized reflectances at scattering angles around 140°. Generally, a liquid index value below 0.3 indicates no liquid is present in the cloud top, which is then classified as ice. Larger liquid index values indicate liquid or mixed-phase cloud tops.

For RSP measurements over ice clouds, information on ice crystal shape, crystal distortion, scattering asymmetry parameter and effective radius, as well as cloud optical thickness, are operationally retrieved (van Diedenhoven et al. 2012b, 2013, 2016a; van Diedenhoven 2018). Cloud optical thickness and effective radius are retrieved using a combination of visible and nadir shortwave infrared bands (cf. Nakajima and King 1990). Generally, such retrievals need the assumption of an ice optical model. However, the multi-angle polarimetry allows the ice crystal model to be to constrained at an RSP pixel level. In addition to scattering asymmetry parameter, the mean aspect ratio of crystal components and crystal distortion level is retrieved by this method. For this retrieval, single hexagonal prisms are used as proxies for complex ice crystals. This approach has been evaluated with simulated measurements using optical properties of various complex ice habits and their mixtures (van Diedenhoven et al. 2012b; 2016b), as well as using in situ measurements (van Diedenhoven et al. 2013). In general, the asymmetry parameter was found to be retrieved within 5% on a pixel level. After constraining the asymmetry parameter using this approach, the ice effective radius and cloud optical thickness is retrieved from visible and two shortwave bands using an ice model consistent with the retrieved asymmetry parameter. This approach is also applied to a combination of MODIS and POLDER measurements (van Diedenhoven et al. 2014). Furthermore, van Diedenhoven et al. (2016) demonstrated that the considerable difference in probing depths within cloud top associated with the 1590 and 2260 nm bands of RSP yield relevant information about the vertical structure of ice sizes within convective cloud tops.

MSPI Algorithms

Cloud retrievals for MSPI, as with MISR, use imagery map-projected to the WGS84 surface ellipsoid. Algorithms fall into two principal categories: (a) stereophotogrammetric and radiometric retrievals of cloud-top heights and cloud fractions as a function of altitude, making use of feature and area-based pattern image matching and thresholding (both leveraging heritage from MISR), and (b) particle scattering and radiative transfer-based retrievals of cloud microphysical properties, which combine the novel information content of polarimetric data with more conventional approaches based on spectral radiances.

Figure 4.7 shows a retrieval of cloud-top heights using multi-angle stereo pattern matching applied to AirMSPI data from 31 August 2011, using algorithms similar to those employed operationally with MISR. The stereo retrieval makes use of 555 nm images acquired at view angles of nadir and 26.5º forward and backward of nadir. Unlike MISR, however, at aircraft altitudes Earth curvature is insufficient to enable separating stereo parallax from the effects of advection due to wind, hence the heights shown in Figure 4.7 are not corrected for wind. Application of the MISR stereo algorithms to ACE multiangle imagery will enable simultaneous retrieval of cloud-top heights and cloud motion vector winds.

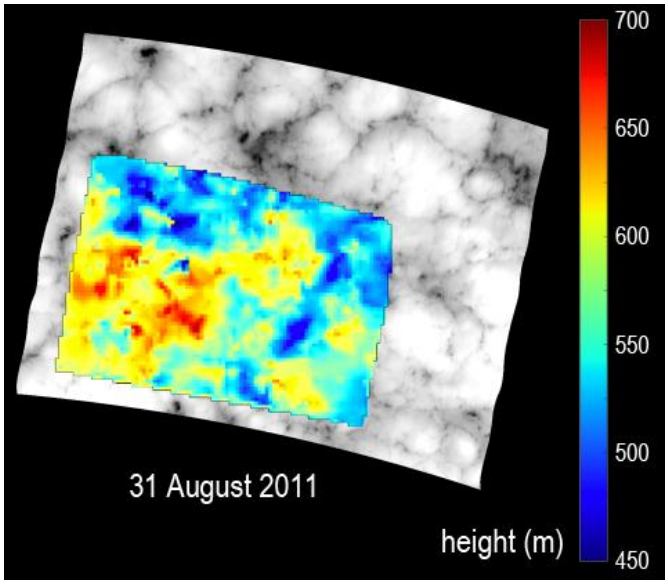

Figure 4.7: Stereoscopic retrieval of cloud-top heights using AirMSPI imagery at 3 view angles. Computational pattern matching is used to identify similar features in the different images and retrieve the cloud-top height field using the spatial disparities, or parallax, between the features in the imagery.

Building upon methodologies described by Bréon and Goloub (1998) and Alexandrov et al. (2012a,b), AirMSPI data have been used to retrieve cloud-top liquid water droplet size distributions for near-homogeneous marine stratocumulus clouds using measurements of the polarization of supernumerary cloud bows (Diner et al., 2013a). Because the polarization signals are dominated by single scattering, they are less susceptible to 3D radiative transfer effects, which are a known source of bias for radiance-based droplet size retrievals (e.g., Liang and Di Girolamo, 2013), hence have the potential for retrieving spatial variability in cloud-top droplet size in

broken cloud scenes. Figure 4.8 shows an example of cloud bow and glory imagery from AirMSPI, acquired on 31 August 2011. At left are intensity and DOLP images acquired by sweeping the instrument's gimbal along-track to image an area approximately 110 km in length x 10 km at nadir. At right are fits to the supernumerary bows in the lower portion of the image (south of the glory) using the single-scattering method of Bréon and Goloub (1998) over the scattering angle range 140º-165º. The parametric gamma distribution was employed, and the best-fitting solution yields an effective droplet radius of 9.13 μm and effective variance of 0.006. The region above 165º is used here as a consistency check. The model correctly predicts the location of the interference fringes associated with the higher-order supernumerary bows and glory, though some deviation in magnitude, particularly at the shorter wavelengths, is observed. This may be due to a departure of the droplet sizes from a purely gamma distribution, spatial variability in the droplet sizes, and/or multiple scattering. Multiple AirMSPI images are being used to examine each of these factors in greater detail.

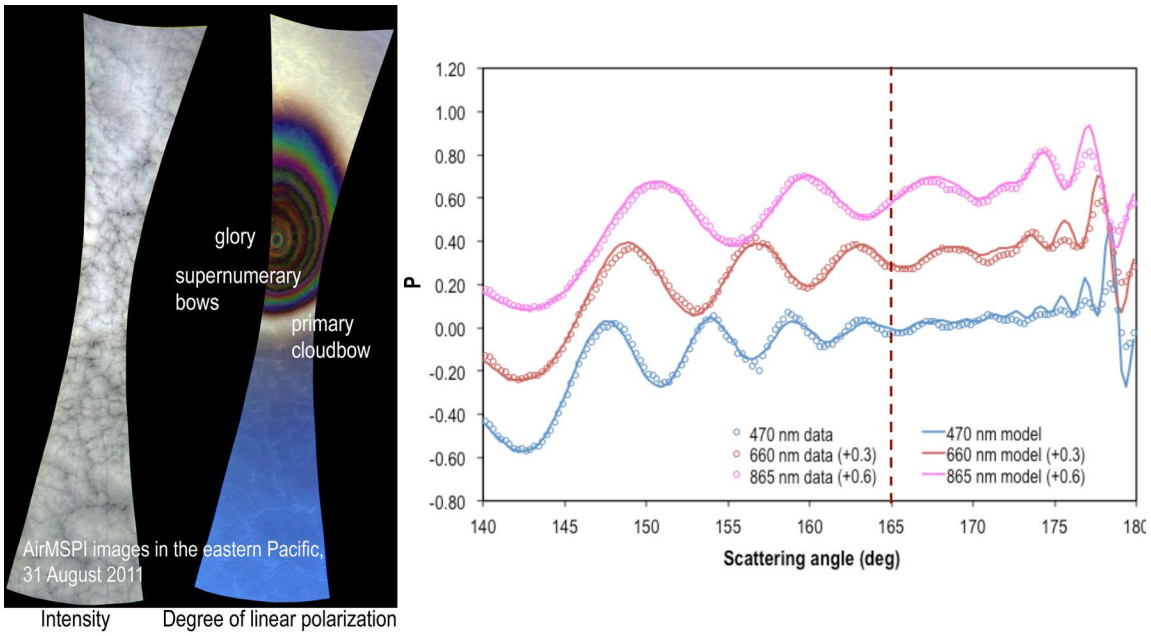

Figure 4.8: Example of cloudbow and glory imagery from AirMSPI. At left are intensity and DOLP images. At right are fits to the supernumerary bows at 3 wavelengths in the lower portion of the image (south of the glory) using the method of Bréon and Goloub (1998). The dashed line indicates scattering angle of 165º.

Armed with knowledge of the droplet size distribution from polarized light, AirMSPI team members are also investigating the use of 1D radiative transfer theory to estimate cloud optical thickness from natural light in the presence of 3D adjacency effects. Specifically, application of a statistical-physics analysis technique (Davis et al., 1997) to AirMSPI cloud imagery enables an objective determination of the radiative smoothing scale, beyond which 3D adjacency effects become negligible.

Invoking 1D radiative transfer theory at this and larger scales minimizes 3D adjacency effects. In the near future, the AirMSPI team plans to (1) extend polarimetry-based microphysical retrievals to heterogeneous clouds, and (2) refine new radiance-based retrievals that exploit 3D radiative transfer effects on multiple scales and yield macrophysical cloud properties, namely, optical depth and geometrical thickness (hence a vertically-averaged cloud droplet number density). Although the later type of retrieval depends critically on the fine-scale imaging achievable with AirMSPI from the ER-2 (10–20 m pixels), an anticipated spin-off will be cloud property retrieval algorithms adapted to ACE-type pixel scales (hundreds of meters) that will be robust in 3D cloud structures. Ultimately, the systematic exploitation of passive multi-spectral/multi-angle/multi-pixel data using accelerated 3D radiative transfer forward models will benefit greatly from observational constraints using data from collocated active sensors (namely, ACE's radar and lidar).

For ice clouds a new remote sensing technique to infer the average asymmetry parameter of ice crystals near cloud top from multi-directional polarization measurements has been developed. The method is based on previous findings that (a) complex aggregates of hexagonal crystals generally have scattering phase matrices resembling those of their components and (b) scattering phase matrices systematically vary with aspect ratios of crystals and their degree of microscale surface roughness (Van Diedenhoven *et al.* 2012). Ice cloud asymmetry parameters are inferred from multi-directional polarized reflectance measurements by searching for the closest fit in a look-up table of simulated polarized reflectances computed for cloud layers that contain individual hexagonal columns and plates with varying aspect ratios and roughness values. The asymmetry parameter of the hexagonal particle that leads to the best fit with the measurements is considered the retrieved value. For clouds with optical thickness less than 5, the cloud optical thickness must be retrieved simultaneously with the asymmetry parameter, while for optically thicker clouds the asymmetry parameter retrieval is independent of cloud optical thickness. Evaluation of the technique using simulated measurements based on the optical properties of a number of complex particles and their mixtures shows that the ice crystal asymmetry parameters are generally retrieved to within 5%, or about 0.04 in absolute terms. The retrieval scheme is largely independent of calibration errors, range and sampling density of scattering angles and random noise in the measurements. The approach can be readily applied to measurements of past, current and future airborne and satellite instruments that measure multi-directional polarized reflectances of ice-topped clouds.

PACS Cloud Retrievals

On the cloud side, we have implemented the CloudPro algorithm that optimizes the usage of the HARP hyperangular measurements for the retrieval of the thermodynamical phase and the droplet size distribution of water clouds. This algorithm is based on a parametric fit and look up tables based on Mie calculations previously used by Breon and Goloub 1998, and Breon and Boucher 2005.

The unique hyperangular imaging capability of the HARP sensor allow for unprecedented coverage of the cloudbow supernumerary arcs with pixel resolution, producing detailed characterization of the effective radius and effective variance of the cloud droplet sizes. These additional measurements provide more detailed characterization of the interaction between aerosols and clouds. Particularly, the HARP design allows for continuous coverage of the cloudbow features covering a wide swath imaged area. Figure 4.9 shows an example of cloudbow retrieval from the LMOS experiment. HARP allows for two approaches in performing retrievals with the cloudbow technique:

1- Cloudblow profile along the cross-track swath

2- Single pixel retrieval with the Hyperangular sampling

The single pixel retrieval with the Hyperangular sampling is a unique characteristic of the HARP system and can provide high resolution cloud microphysical retrievals in patchy and heterogeneous cloud fields. The same HARP hyperangular feature also provides a close monitoring of the microphysical properties of ice crystals linked to the ice surface roughness (Van Diedenhoven et. al. 2012).

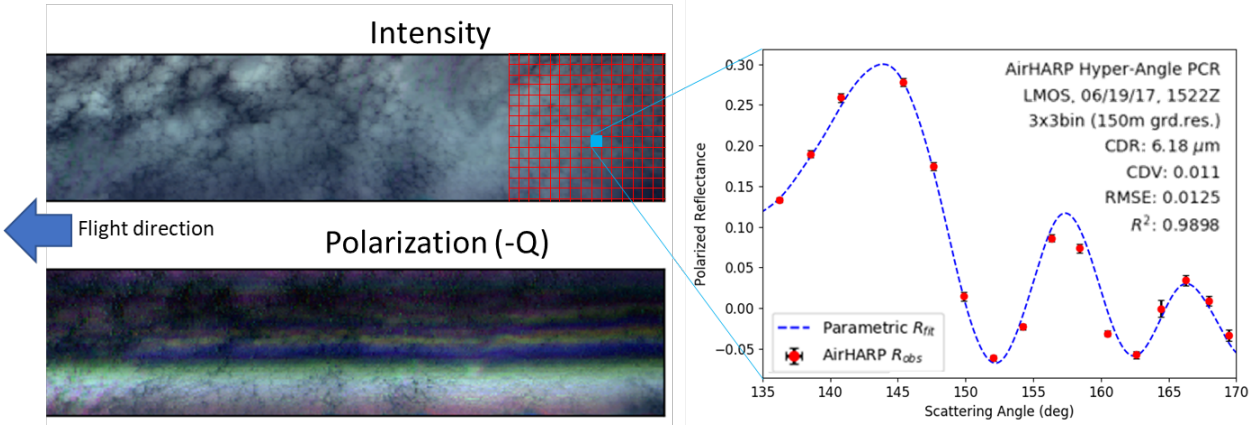

Figure 4.9: Example of cloud microphysical properties retrieved with the unique hyperangular imaging capability of HARP. The top cloud image shows an intensity image of a cloud field collected during the LMOS experiment while the bottom image shows an image of the polarization field (-Q component of the Stokes parameters) emphasizing the structure of the cloudbow. The plot on the right-hand side shows the unique characteristic of HARP which provides a full profile of the cloudbow for each individual pixel throughout the image. In this particular case we show a full cloudbow profile with 150m resolution and its equivalent microphysical retrieval.

4.3 Ocean

As detailed in Section 2, the ACE ocean ecology science objectives require an expansion in the spectral range and resolution of passive ocean color measurements compared to heritage sensors, the development of algorithms for deriving plankton properties from lidar subsurface scattering returns, an evolution in satellite inversion algorithms, and the retrieval of new ocean ecosystem and carbon cycle

properties. ACE pre-formulation studies have focused on key advances in ocean retrievals needed to prepare for mission launch. In particular, algorithm development studies have targeted (1) inversions for inherent optical properties and added value of remote sensing measurement at ultraviolet wavelengths, (2) evaluation of remotes sensing of phytoplankton functional groups, (3) advancement of retrievals for colored dissolved organic matter and attenuation coefficients over the full range of open-ocean to near-shore environments, (4) evaluation of physiological signatures in chlorophyll fluorescence retrievals, (5) expansion of net primary production (NPP) algorithms to accommodate the advanced ocean geophysical parameters retrieved during ACE, (6) advanced understanding of phytoplankton physiology to reduce uncertainties in NPP, (7) assessment of Raman scattering impacts on ocean color inversion algorithms, (8) development of space lidar retrievals of global plankton carbon stocks, (9) demonstration of lidar retrievals of vertical (depth) structure in ocean properties, and (10) improved algorithms for atmospheric corrections. The following subsections briefly describe advances made on these topics in preparation for ACE.

Inversion Algorithms for Inherent Optical Properties

Semi-analytical algorithms (SAAs) provide one mechanism for inverting the color of the water observed by the ACE ocean radiometer into inherent optical properties (IOPs). Few SAAs are currently parameterized appropriately for retrieval from all water masses and all seasons. A community-wide discussion of these limitations was therefore initiated and two workshops conducted to accelerate progress toward consensus on a unified SAA framework. These efforts resulted in the development of generalized IOP (GIOP) model software that could be appropriate for implementation during the ACE mission. The GIOP permits isolation and evaluation of specific modeling assumptions, construction of SAAs, development of regionally tuned SAAs, and execution of ensemble inversion modeling. A preliminary default configuration for GIOP (GIOP-DC) was identified during the workshops, with alternative model parameterizations and features defined for subsequent evaluation. An example global image of phytoplankton absorption based on MODIS Aqua data is show in Figure 4.10 and details on the GIOP algorithm were published in Werdell et al. (2013a).

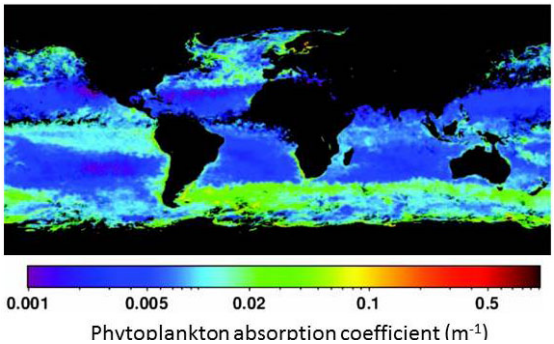

Figure 4.10 Example GIOP global product based on MODIS Aqua data.

Following development of the GIOP algorithm, an additional study was conducted to evaluate the sensitivity of SAAs to the assumed constant spectral values for seawater absorption and backscattering and spectral shape functions for absorption and scattering by phytoplankton, non-algal particles, and colored dissolved organic matter (cDOM). The study revealed that use of temperature- and salinity-dependent seawater spectra significantly elevates SAA-

derived particle backscattering coefficients, reduces non-algal particle and cDOM values, and leaves phytoplankton absorption coefficients unchanged. Detailed results from the study were published in Werdell et al. (2013b).

In parallel with the above inversion algorithm developments, work was also been conducted on improving the Garver-Siegel-Maritorena algorithm, which is one of the leading inversion algorithms applied to heritage ocean color data. This work aimed at improving various components of the model, including phytoplankton absorption, slope of particulate backscattering, absorption by non-algal particles and dissolved matter, the relationship between reflectance and backscattering-to-absorption ratio, reflection and refraction processes at the air-sea interface, and extension of the model into the UV domain measured by ACE. The outcome of this work improved the spectral accuracy of the model, yielding lower retrieval biases.

An important source of uncertainty in the UV is associated with in situ measurements of oceanic optical properties, including the spectral absorption coefficient. A focused study was conducted to quantify uncertainties in the UV spectral region for the commonly-employed filter pad method of measuring the absorption coefficient of marine particles. These measurements require a correction for pathlength amplification resulting from light scattering by glass fiber filters onto which particles are concentrated. This correction can be expressed as the relationship between the reference optical density of a suspension of particles, OD_s, and the corresponding optical density of particles on filters, OD_f (Stramski et al. 2015). Dedicated laboratory experiments utilizing an improved measurement configuration with a sample placed inside an integrating sphere of bench-top spectrophotometer and covering a wide range of seawater environments indicated that the use of previously established corrections for the visible spectral region (Stramski et al. 2015) can be used in the 350–400 nm range with reasonable uncertainties (~13% random error and ~10% bias). The uncertainties increase at shorter UV wavelengths suggesting that further work to develop UV-specific corrections are needed to provide the highest accuracy throughout the UV region.

Phytoplankton Functional Groups

Since the launch of the SeaWiFS satellite, it has become increasing apparent that understanding ocean ecosystem dynamics and carbon cycling requires a more refined separation of phytoplankton types in the surface ocean. Accordingly, the ocean ecosystem science objectives for ACE include the retrieval of primary phytoplankton functional groups. Building from earlier proof-of-concept approaches, a study was therefore conducted to investigate the use of inversion models for identifying key phytoplankton groups. The study was focused on distinguishing two particular phytoplankton types known to dominate surface populations in the northern Arabian Sea. The study identified conditions under which the inversion approach was successful in retrieving specific phytoplankton groups and when the current approach is not successful. In addition, the study indicated that the current state-of-the-art approach already shows promise for

qualitative group separations, but that quantitative assessments require further algorithm development. Detailed results from the study were published in Werdell *et al.* (2014).

Additional studies were also undertaken to evaluate alternative approaches for assessing phytoplankton functional groups. In the work of Chase et al. (2017), diagnostic pigment markers for phytoplankton groups were described as Gaussian distributions and then these Gaussian approximations used to decompose spectral reflectance data into phytoplankton groups. In the study of Cartlett and Siegel (2018), spectral derivative analyses were conducted to identify functional group pigment markers. A key outcome of this study was that it demonstrated the importance of accurate water leaving reflectance data across the full 350 to 700 nm hyperspectral range of the ACE ocean color instrument.

Colored dissolved organic matter and attenuation

In Section 3, a brief summary is provided on progress in instrument development of the C-OPS system. Data from this in situ system has been evaluated in terms of developing improved algorithms for retrievals of in-water spectral diffuse attenuation coefficients (K_d) and cDOM absorption (aCDOM). For example, the left panel in Figure 4.11 illustrates the use of C-OPS data for evaluating subsurface retrievals of K_d from a lidar. The right panel in Figure 4.11 shows particularly encouraging results from an emerging global algorithm for aCDOM retrievals at 440 nm. This result is particularly noteworthy in its robust capabilities over cDOM values spanning three decades of dynamic range, from clear, deep-ocean conditions to turbid, shallow coastal waters (Hooker *et al.* 2013).

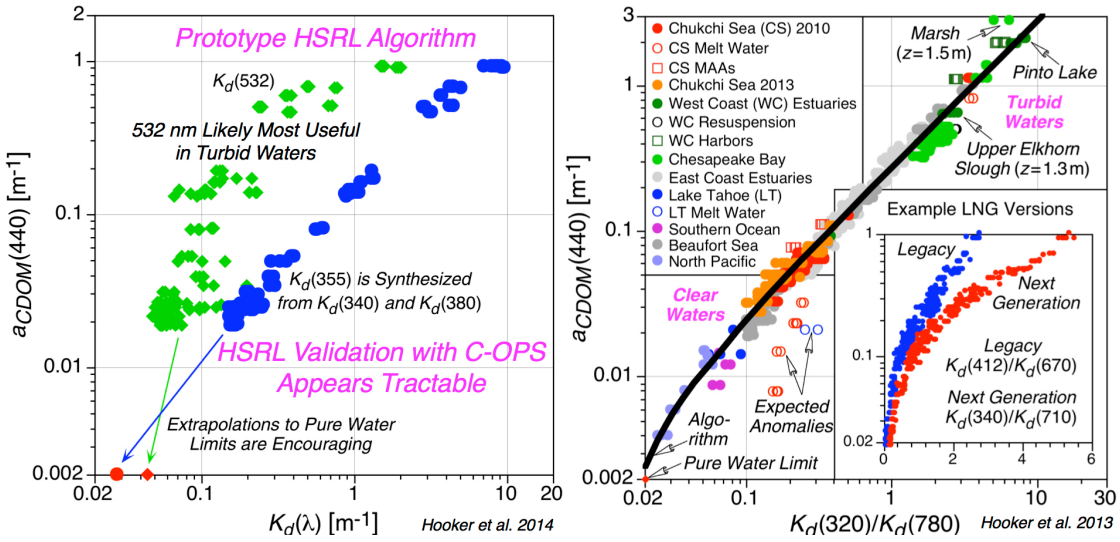

Figure 4.11 A prototype HSRL algorithm and refined aCDOM (440) algorithm based on C-OPS Kd data.

Chlorophyll Fluorescence

Satellite chlorophyll fluorescence (FLH) retrievals have the potential for providing critical information on phytoplankton standing stocks, physiology, and

photosynthesis, but improvements are needed to optimize fluorescence retrieval capabilities for ACE and interpret the underlying physiological signal. Studies were therefore conducted to (1) evaluate sources of error in existing MODIS FLH products based on in situ data and radiative transfer simulations and (2) improve understanding of physiological marks using field data and FLH retrievals from MODIS and the Korean Geostationary Ocean Color Imager (GOCI). During ACE pre-formulation, significant progress was made on the physiological interpretation of FLH data that is essential to ACE ocean ecosystem science objectives. The study of Behrenfeld et al. (2013) provided the first global analysis of MODIS fluorescence data and linked spatial-temporal patterns in fluorescence quantum yields to the presence or absence of iron-limited phytoplankton populations. The subsequent study of Westberry et al. (2013) further developed this link between elevated quantum yields and iron stress by merging MODIS data with field iron enrichment studies. Finally, in the study of O'Malley et al. (2014), chlorophyll fluorescence data from the geostationary GOCI sensor was used to improve descriptions of light-protection mechanisms in phytoplankton, termed non-photochemical quenching (NPQ), and to describe how the extent of NPQ varied over seasons.

Primary Production

One of the key properties of ocean ecosystems with respect to fisheries production and global biogeochemistry is the rate of phytoplankton net primary production (NPP). Approximately 50% of biospheric NPP is currently assigned to the global phytoplankton (Field et al 1998) and this rate shows clear fluctuations with climate variability (Behrenfeld 2001, 2006). These estimates, however, are based upon NPP algorithms applicable to the limited retrieval capabilities of heritage ocean color sensors. For the ACE mission, observational capabilities will be greatly expanded. Accordingly, new NPP algorithms are needed to accommodate the additional retrieved geophysical properties and thus to realize the potential improvements in NPP assessments. To this end, a revised NPP algorithm framework was developed call the Carbon, Absorption, Fluorescence, and Euphotic-resolving (CAFÉ) model (Westberry and Behrenfeld 2014). The CAFÉ model builds around new retrievals of phytoplankton carbon (Behrenfeld et al. 2005, Westberry et al 2008) rather than the traditional approach of estimating NPP from chlorophyll. The model then incorporates additional information on phytoplankton absorption spectra, functional groups, and information on iron stress from fluorescence quantum yield retrievals to improve the description of photosynthetic efficiencies. The CAFÉ approach was further refined by Silsbe et al. (2016) and shown to have improved performance over all other NPP algorithms when compared to field data sets.

Physiology

A fundamental challenge regarding the interpretation of ACE (and heritage OC sensor) ocean ecosystem data is reliably relating observable properties (optical properties) to geophysical properties (e.g., plankton stocks and composition) and biogeochemical processes (e.g., NPP, carbon export) of interest. For assessments of NPP, a key issue is understanding physiological acclimation time-scales and their

species-specific variations. Work was therefore conducted to evaluate how photosynthetic properties change over time in different phytoplankton species. In particular, changes in pigment absorption and biomass accumulation were measured during a simulated major regime shift in light and nutrient availability simulating a deep-mixing event. The collection of photosynthetic properties revealed that trade-offs between energetic investments to non-photochemical quenching, carbon fixation, and growth underlie the extremely rapid response of diatoms to low light/high nitrogen conditions compared to green algae (Figure 4.12). These results suggest that relating phytoplankton changes observed by ACE to changes in NPP and carbon biogeochemistry will require information on both community composition and time scales of change in the physical environment.

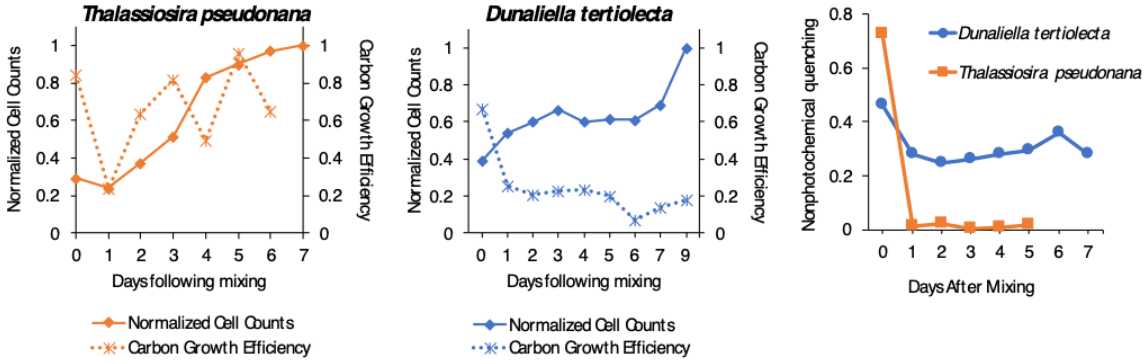

Figure 4.12 Rapid recovery of T. pseudonana growth (left) compared to D. tertiolecta (middle) following a regime shift from high light/low N to low light/high N. NPQ (right) changes show that the diatom dispenses with investments into photoprotection to maintain high growth capacity

Satellite Lidar Retrievals

A unique and powerful aspect of the ACE mission will be its simultaneous measurements of ocean properties with a lidar and ocean radiometer. The ability to retrieve subsurface plankton properties with a space lidar was unproven during initial formulation of the ACE mission concept and was therefore a high-priority target for pre-formulation investigations. A lidar specifically designed for ocean retrievals has never been flown in space. However, the atmospheric CALIOP lidar has been producing global data since 2006 and provided an opportunity for a proof-of-concept evaluation and development of algorithms for the ACE lidar. Through a collaboration of researchers from Oregon State University, LaRC, and Plymouth Marine Lab, the first successful satellite lidar retrievals of phytoplankton carbon stocks and total particular organic carbon was achieved (Figure 4.13), thus demonstrating the feasibility and importance of the advanced lidar capabilities planned for the ACE mission. Detailed results from the study were published in Behrenfeld *et al.* (2013).

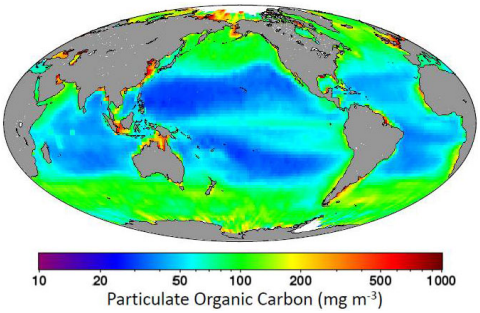

Figure 4.13 CALIOP lidar based global ocean surface particulate carbon *concentration.*

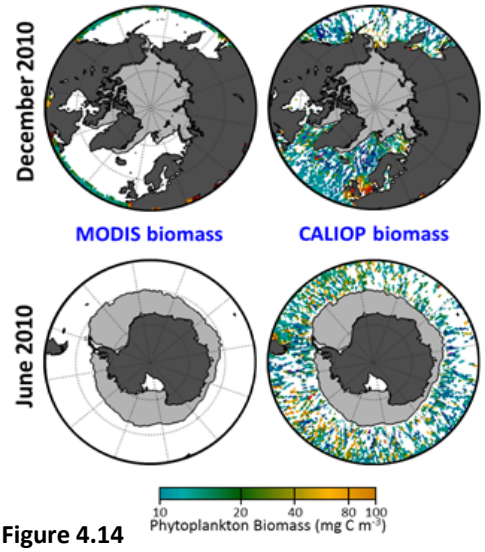

Figure 4.14 Phytoplankton biomass observations from CALIOP (right) and MODIS (left) for latitudes poleward of 45° (white = no data). (Top) northern latitudes (December 2010) and (Bottom) southern latitudes (June 2010; no MODIS data).

With the above noted success, a follow-on study was conducted of plankton bloom dynamics and climate sensitivities for the polar regions. Solar elevations, periods of polar night, and persistent cloud conditions have made ocean color observations of the polar regions historically problematic. Lidar retrievals of plankton properties can be made between clouds and through significant cloud and aerosol loads (Figure 4.14). In addition, the active nature of lidar measurements means that ocean observations can be made throughout the year, including polar night. With these advantages, CALIOP phytoplankton biomass retrievals were used to unravel key aspects of phytoplankton biomass annual cycles and to determine hemispheric differences in ecological versus ice cover change effects on decadal-scale biomass variations (Behrenfeld et al. 2016).

The aforementioned accomplishments represent only a small fraction of the ocean ecology advances that can be realized with a satellite lidar. Notably, CALIOP was not designed for ocean applications and thus has fundamental limitiations restricting further advances. In particular, CALIOP does not have the vertical retrieval resolution to provide critical information plankton depth distributions (Schulien et al. 2017) or the appropriate detection system (e.g., HSRL) for directly separating absorbing and scattering coefficients. Requirements for the ACE lidar identified in the Ocean Ecosystem (and other) STM address the shortcomings of CALIOP for ocean applications. A very detailed review of a future ocean-optimized lidar is provided in Hoestetler et al. (2018), along with a historical account of lidar applications in marine studies.

Airborne HSRL Retrievals

As discussed in Section 3.3, advances in airborne lidar instrumentation during the ACE era have enabled first-ever ocean profiling measurements with the HSRL technique. In addition to providing depth-resolved measurements as called for in the ACE ocean STM, the HSRL technique enables independent measurement of light attenuation and particulate backscatter. The retrieval is similar in nature to that applied in the atmosphere for independent measurement of aerosol extinction and backscatter and is described in Hostetler et al. (2018). HSRL-1 ocean retrievals have been processed and archived from the Ship and Atmosphere Bio-optics Research (SABOR) experiment and three deployments of the North Atlantic Aerosol and Marine Ecosystems (NAAMES) mission. Figure 4.15 shows both ocean and atmosphere retrievals from the May 2016 NAAMES deployment. Initial assessments of the particulate backscatter and diffuse attenuation coefficient from SABOR have been published (Hair et al. 2016 and Schulien et al., 2017) and similar comparisons are ongoing with the NAAMES data. In addition, initial comparisons of the HSRL data products with the current satellite retrievals (MODIS, VIIRS) are ongoing and promising. The airborne HSRL-1 retrievals demonstrate that ocean STM requirements can be met by lidar and Hostetler et al. (2018) describe how this capability can be expanded to a spaceborne ACE HSRL instrument.

Notably, Figure 4.15 illustrates the advantage of coincident HSRL measurements for advancing ocean color algorithms. The atmospheric data show a dense smoke layer from Canadian forest fires that was advected over the Western Atlantic. This strongly absorbing smoke layer would challenge traditional ocean color algorithms, yet the HSRL ocean retrievals are unaffected. Ocean measurements such as these from a spaceborne HSRL would provide a large database for testing and improving OCI atmospheric correction algorithms, which in turn could be applied to the entire OCI data set. Moreover, Stamnes et al. (2018) used the HSRL altitude information on the height of the aerosol layers to improve polarimeter retrievals of both ocean and atmospheric optical parameters (e.g. ocean particulate backscatter, diffuse attenuation coefficient, and aerosol optical thickness). This work set the stage to probe synergies between the ACE HSRL and polarimeter for joint atmosphere-ocean retrievals.

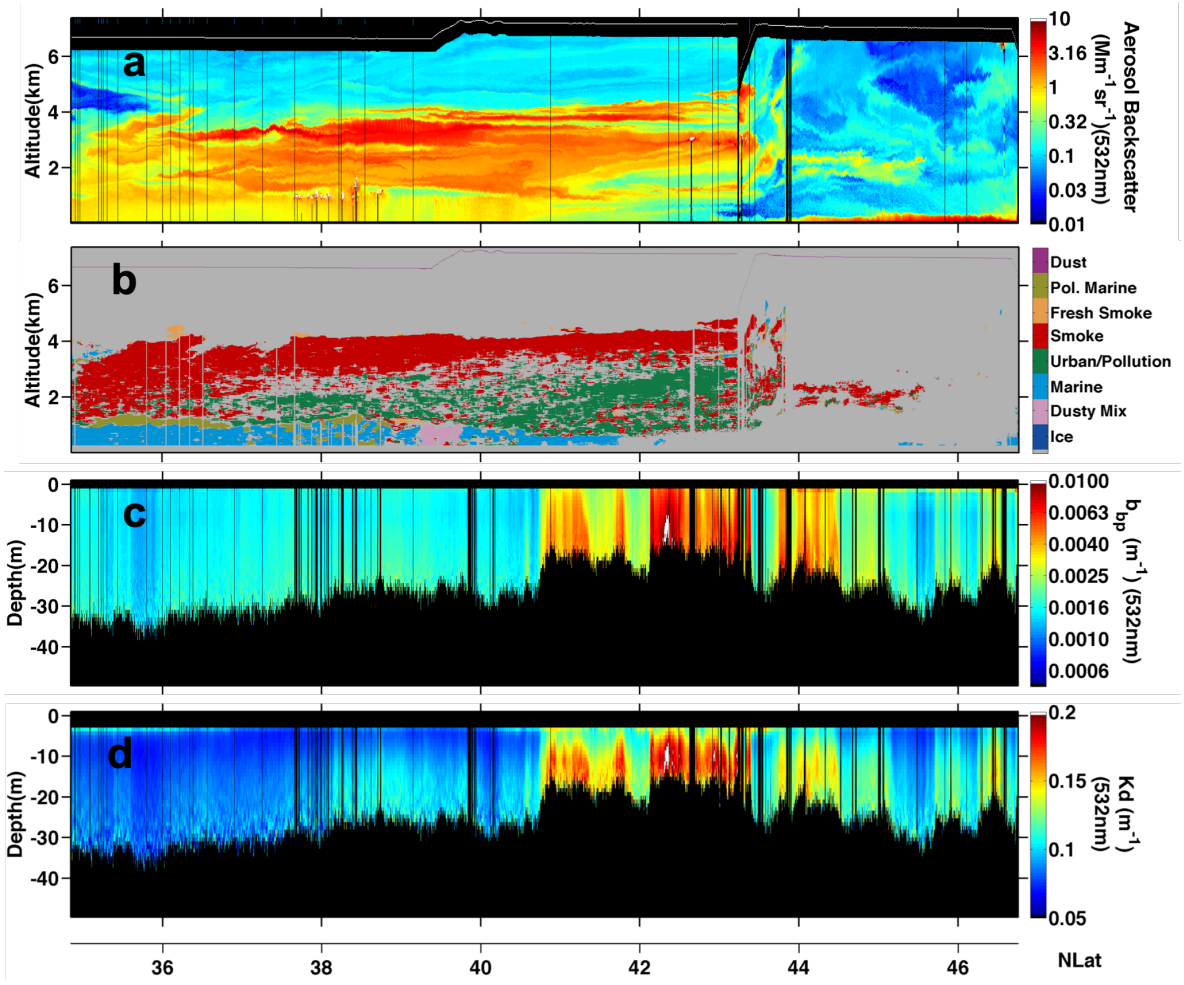

Figure 4.15 Retrieved atmospheric profiles of backscatter and aerosol type simultaneously sampled ocean backscatter (b_{bp}) and attenuation (K_d) along a flight track from off the Virginia coast to just off the Nova Scotia coast during the May 2016 NAAMES transit flight.

Raman Scattering

Raman scattering has the potential to significantly affect ACE retrievals of inherent optical properties (thus, derived geophysical properties) retrieved with semi-analytical inversion algorithms (see above). Studies were therefore conducted to evaluate the magnitude of these potential errors and devised algorithms to correct for Raman effects. These studies demonstrated that errors in particulate backscattering coefficients resulting from Raman contamination can be as large as 30% in clear ocean regions (Lee and Huot 2014). Both analytical and empirical methods were developed to remove the Raman contribution from remote sensing reflectances and then applied to satellite ocean color data from OMI and MODIS (Lee et al. 2010, 2013, Westberry et al. 2013). These studies established important and useful approaches for addressing the Raman scattering issue during analyses of ACE ocean color data. Methods from the Westberry et al. (2013) study were incorporated into the GIOP framework (McKinna et al. 2016).

Atmospheric Correction

Atmospheric correction refers to removing the atmospheric contribution to the top-of-atmosphere (TOA) radiance from the radiance observed by an ocean color sensor. The atmospheric contribution is 85% to 90% over the open ocean (depth > 1000 km) and ~95% and more over coastal regions (e.g. Chesapeake Bay) and mainly consists of Rayleigh scattered photons by air molecules and Mie scattered photons by aerosols. The former varies as λ^{-4} and the latter as λ^{-n} where, n varies from ~0 to 2. The accuracy of the atmospheric correction depends on microphysical and optical properties of aerosols (e.g., particle size distribution, complex index of refraction), which vary spatially and temporally.

As a part of ACE pre-formulation, radiative transfer (RT) studies were conducted to understand absorbing and non-absorbing aerosol effects on satellite ocean color retrievals. Results showed that the atmospheric correction algorithm proposed by Gordon and Wang (1994) typically works very well for open ocean conditions where aerosols are mostly oceanic in nature and non-absorbing. In the presence of absorbing aerosols (e.g., dust, smoke, industrial pollution), errors in retrieved ocean color become very large, often > 20%. Results also showed that knowledge of single scattering albedo (ω_o) and aerosol layer height (h) are extremely important when absorbing aerosols are present. As illustrated in Figure 4.16, an error of 1 km in aerosol layer height changes the TOA radiance at 412 nm by ~ 0.7%, yielding an ~7% change in water-leaving radiance at the ocean surface. This error increases with increasing aerosol optical thickness (τ_{aer}) in the atmosphere. The RT simulations studies were further extended to include absorbing aerosols in the near UV part of the spectrum. Results showed that absorbing aerosols under low aerosol loading conditions (a major concern in atmospheric correction) could be detected with ACE measurements at 340 and 380 nm.

Due to the importance of accurate atmospheric corrections in the presence of absorbing aerosols, additional ACE supported algorithm development studies were conducting based on the Bayesian approach to inverse problems. In this approach, the solution is expressed as a probability distribution that measures the likelihood of encountering specific values of the input variables (spectral marine reflectance) given the observed output variables (spectral top-of-atmosphere reflectance in the visible and near infrared). This allows for computation of both the conditional expectation of the marine reflectance to be computed and the conditional covariance (a measure of uncertainty), the "p-value" (quantifying the likelihood of an observation with respect to the model), and assessment of situations where observations and model output are incompatible (p-value<0.05). Details of the approach and results are reported in Frouin and Pelletier (2014).

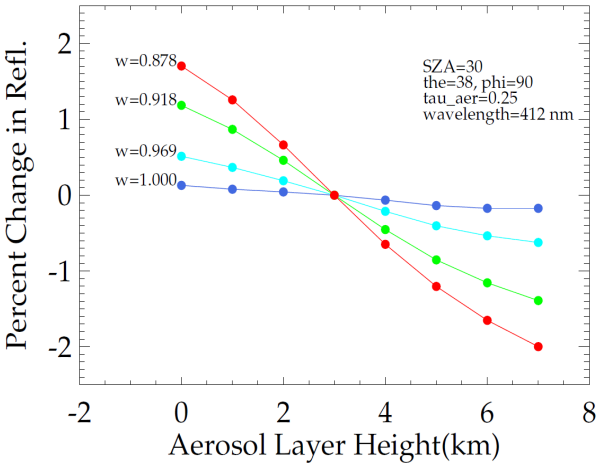

Figure 4.16 Percent change in the top-of-reflectance (TOA) at 412 nm as a function of aerosol layer height. Reflectance values at different heights are normalized with respect to the reflectance values at 3 km with single scattering albedo (ω_o) of 1.0. The simulations are for solar zenith angle of 30°, view zenith angle of 38° and relative azimuth angle of 90°. The aerosol optical thickness defined at 869 nm is 0.25.

The feasibility of using multi-angular measurements of top-of-atmosphere reflectance to estimate aerosol absorption effects on marine reflectance retrievals was also investigated. The method constrains the spectral extrapolation of scattering properties observed in the near infrared by a value of the aerosol absorption effect obtained in the short-wavelength bands. A separate estimation of the aerosol absorption optical thickness and vertical distribution (variables that govern the aerosol absorption effect) is not necessary. First, the top-of-atmosphere reflectance is corrected for molecular and aerosol scattering using spectral bands in the near infrared and/or shortwave infrared, as in the classic atmospheric correction scheme. Second, the residual signal in all viewing directions, $\tilde{\lambda}_{TOA}$', composed of the aerosol absorption effect and the marine signal, normalized by the atmospheric transmittance is related to an absorption predictor, i.e., a function representing the directional effect of an absorbing aerosol, namely the product of molecular reflectance, $\tilde{\lambda}_{mol}$, and air mass, m*. Figure 4.17 illustrates the method for fine and coarse aerosols. Neglecting aerosol transmittance, the marine reflectance (0.02 in this case) is obtained by extrapolating the relation between $\tilde{\lambda}_{TOA}'/T_{mol}$ and $\tilde{\lambda}_{mol}$ m* to zero air mass, where T_{mol} is the molecular transmittance.

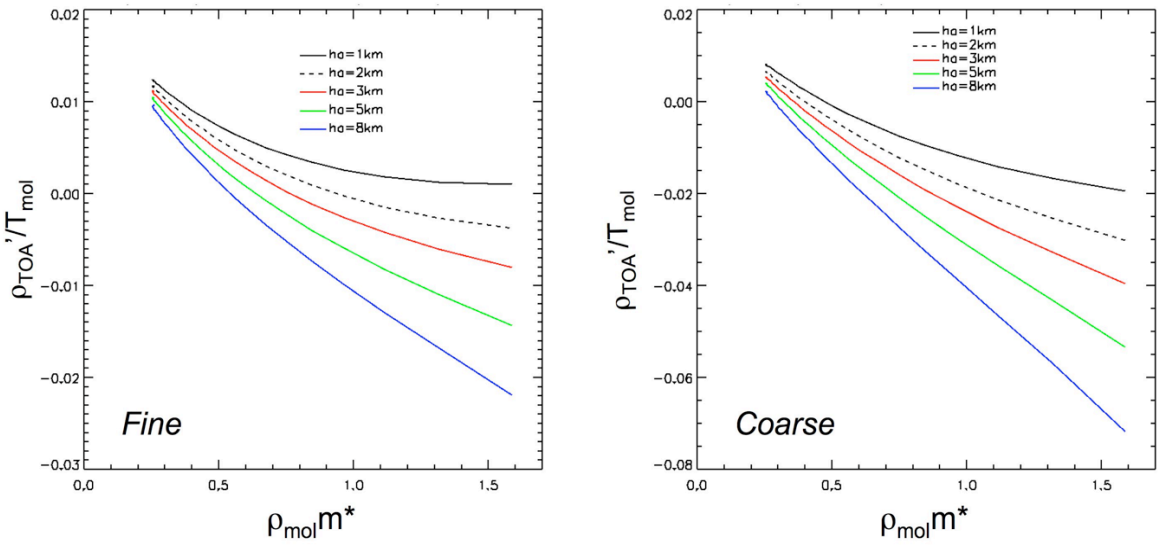

Figure 4.17 Simulated ρ_{TOA}'/T_{mol}, versus ρ_{mol} m* for fine aerosols (left) and coarse aerosols (right). Wavelength is 412 nm and aerosol optical thickness is 0.3. Wind speed is 5 m/s and marine reflectance is 0.02. Solar zenith angle is 30 deg., viewing azimuth angle varies between 0 and 80 deg., and relative azimuth angle is 90 deg. Aerosol scale height varies from 1 to 8 km (8 km correspond to mixed aerosols and molecules). The fine aerosols are defined by r_f = 0.1 µm, σ_f = 0.20, and m_f = 1.40 - 0.010i (single scattering albedo of 0.94), and the coarse aerosols by r_c = 2.0 µm, σ_c = 0.30, and m_c = 1.55 - 0.002i (single scattering albedo of 0.88).

4.4 Aerosol-Ocean

New wind speed-AOD relationship

We have investigated the wind speed dependence of sea spray aerosol optical depth at 532 nm (AOD532) based on five years of satellite retrievals of aerosol optical properties from the Cloud-Aerosol Lidar with Orthogonal Polarization (CALIOP) on board the CALIPSO satellite and the wind speed data from the Advanced Microwave Scanning Radiometer (AMSR-E). The results of our analysis for AOD532 vs. surface wind speed (U10) relationship indicate three distinct regions (Figure 4.18). At

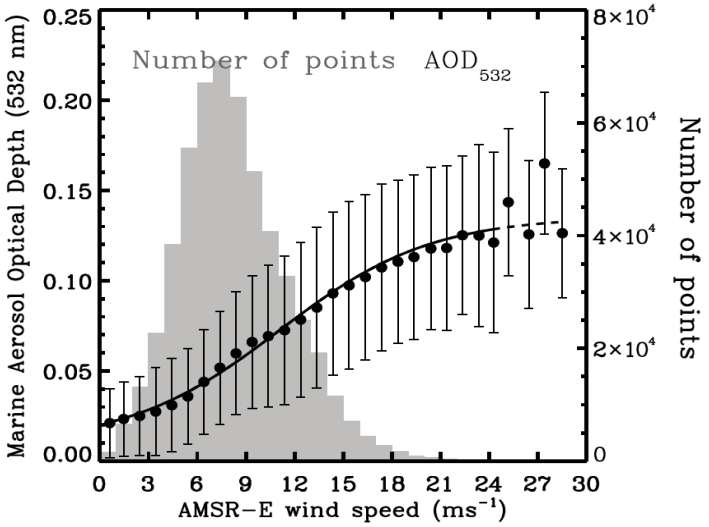

Figure 4.18 The relationship between CALIPSO AOD_{532} and AMSR-E wind speed. Dotted line indicates that the AOD – wind speed relationship for U_{10} >24ms^{-1}. Circles and error bars show mean values and standard deviation of AOD for each 1 ms^{-1} wind speed bin, respectively. Logistic regression relationship between AOD_{532} and wind speed is shown with the solid black line.

low wind speed (U10 ≤ 4 m s-1) sea spray production is minimal and aerosol properties are expected to be dominated by transport. Under such conditions AOD532 is low, weakly dependent on surface wind speed and representative of background marine aerosols. At an intermediate wind speed values (4 < U10 ≤ 12 m s-1) regression analysis revealed a constant slope of 0.0062 s m-1. At high wind speed values (U10 > 12 m s-1) the AOD532-wind speed relationship levels off. Analysis of CALIPSO-retrieved AOD532 and AMSR-E wind speed suggests that at very high wind speed values aerosol effects on optical turbidity of atmosphere appear to level off, asymptotically approaching value of 0.15. These results have been published in (Kiliyanpilakkil & Meskhidze, 2011).

Spaceborne observations of the lidar ratio of marine aerosols.

We have developed a new method to calculate the lidar ratio of sea spray aerosol using two independent sources: the AOD from the Synergized Optical Depth of Aerosols (SODA) algorithm and the integrated attenuated backscatter from CALIOP. With this method, the particulate lidar ratio can be derived for individual CALIOP retrievals in single aerosol layer columns over the ocean. The global mean lidar ratio for sea spray aerosols was found to be 26sr, roughly 30% higher than the current value prescribed by CALIOP standard retrieval algorithm. Data analysis also showed considerable spatiotemporal variability in the calculated lidar ratio over the remote oceans (Figure 4.19). The calculated aerosol lidar ratios are shown to be inversely related to the mean ocean surface wind speed: increase in ocean surface wind speed (U_{10}) from 0 to > 15ms−1 reduces the mean lidar ratios for sea spray particles from 32sr (for 0 <U_{10} < 4ms^{-1}) to 22sr (for U_{10} > 15ms^{-1}). Such changes in the lidar ratio are expected to have a corresponding effect on the sea spray AOD. The outcomes of this study are relevant for future improvements of the SODA and CALIOP operational product and could lead to more accurate retrievals of sea spray AOD. These results have been published in Dawson et al. (2015).

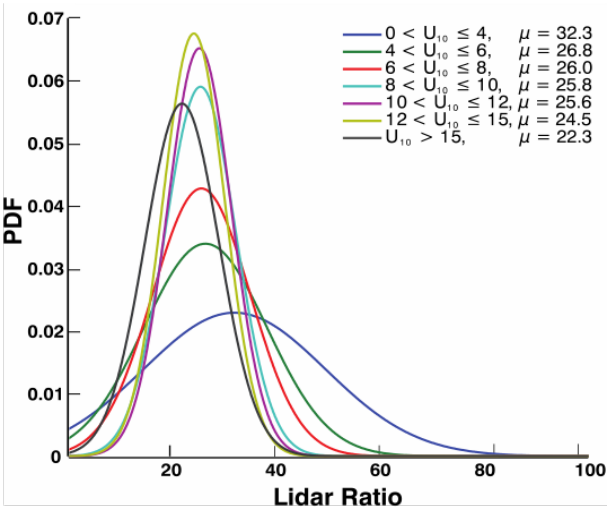

Figure 4.19 Probability density function of clean marine aerosol lidar ratio for selected AMSR-E wind speed regimes. The μ parameter shows the mean of each distribution.

5 Field Campaigns

There were 50 ACE relevant field campaigns performed in the 2007-17 period:

20 deployed a lidar
4 deployed a multi-angle polarimeter
26 deployed both together

18 used high altitude aircraft, such as the ER-2 or Global Hawk
4 were coordinated with shipborne observations

33 were conducted in the Continental United States (CONUS)
12 were primarily over the ocean
2 were at ligh latitudes in North America (Alaska and Canada)
6 were in tropical regions of Africa, Central America or the Caribbean

ACE leveraged the advances in technical development and readiness of both instrument concepts and their related algorithms development made possible with ESTO support. Accordingly, ACE has initiated a series of field experiments with the purpose of better defining the measurement capabilities of the ACE airborne instrument simulators, as well as advance the corresponding L1 and L2 algorithms. These deployments include the Polarimeter Definition Experiment (PODEX) in January-February 2013, the Radar Definition Experiment 2014 (RADEX-14) in May-June 2014, RADEX-15 (November-December, 2015) and Aerosol Characterization from Polarimeter and Lidar (ACEPOL, October-November, 2017).

ACE science and instrument teams have also been leveraging the scientific demand by the larger community for the use of their ACE instrument simulators in their campaigns. NASA, DoE, NSF as well as European partners have provided support for ACE scientists and instrument teams to participate in a series of high profile field campaigns. Among these campaigns are 1) Studies of Emissions and Atmospheric Composition, Clouds and Climate Coupling by Regional Surveys (SEAC^{4}RS), 2) Ship-Aircraft Bio-Optical Research (SABOR), 3) Deriving Information on Surface Conditions from Column and Vertically Resolved Observations Relevant to Air Quality (DISCOVER-AQ), 4) North Atlantic Aerosols and Marine Ecosystems Study (NAAMES), 5) ObseRvations of Aerosols above CLouds and their intEractionS (ORACLES), 6) the 2012 Azores Campaign, 7) the GPM Olympic Mountain Experiment (OLYMPEX, coordinated with RADEX-15), 8) DoE's Two-Column Aerosol Project (TCAP), as well as the European Union Atlantic Meridional Transect (AMT) program.

5.1 Aerosol Related Campaigns

Roughly fifty airborne field campaigns were carried out in the 2007-2017 period that were both relevant to ACE aerosol science and involved participation of multi-angle polarimeters and/or lidars that received support from ACE (see sections 3.2 and 3.3 for a description of these instruments). Of those field campaigns, twenty

were with a lidar alone and four a multi-angle polarimeter only. 26 field campaigns had both. A variety of aircraft were employed, primarily, but not exclusively, from the roster of NASA Airborne Science Program aircraft. 18 of the field campaigns deployed instruments on high altitude aircraft, such as the ER-2 and the Global Hawk, an ideal analog for orbital remote sensing. A majority of field campaigns (33) were performed within CONUS, and a significant fraction (12) were primarily over the ocean. A smaller number were performed in Alaska/Northern Canada, the Caribbean, or sub-Saharan Africa. Four field campaigns had coordinated measurements with instruments deployed on research ships.

The first half of the ACE period (2007-2011) saw the deployment of a single multi-angle polarimeter (RSP), and two lidars (CPL and HSRL-1), and only one field campaign utilizing a high altitude aircraft (TC4). The second half of the ACE period had greater activity. New multi-angle polarimeters were deployed in 2013 (AirMSPI), 2016 (AirSPEX) and 2017 (AirHARP), while the HSRL-2 lidar began operating in 2012. The HSRL-1 was updated in 2013 to provide better observations of in water properties, and was deployed in all four field campaigns that had shipborne observations (SABOR and the three NAAMES deployments). Roughly half of the campaigns employed high altitude aircraft.

				Multi angle polarimeters				Lidars					
Field campaign	Date	Location	Aerosol	AirHARP	AirMSPI	RSP	AirSPEX	CPL	DIAL/HSRL	HSRL-1	HSRL-2	Aircraft	Ship
CATS/CALIPSO val.	1-2007	US east coast	Lidar							yes		B-200	
San Joaquin Valley	2-2007	California	Lidar							yes		B-200	
CHAPS/CLASIC	6-2007	Oklahoma	Lidar					yes		yes		B-200	
TC4	7-2007	Costa Rica	Lidar					yes				ER-2	
Caribbean 1	1-2008	Caribbean	Lidar							yes		B-200	
ARCTAS Spring	4-2008	Alaska	Lidar							yes		B-200	
ARCTAS Summer	6-2008	NW Canada	Pol, Lidar			RSP1				yes		B-200	
Birmingham	9-2008	Alabama	Pol, Lidar			RSP1				yes		B-200	
CALIPSO validation	1-2009	Eastern US	Lidar					yes		yes		B-200	
RACORO	6-2009	Southern Great Plains	Pol, Lidar			RSP1				yes		B-200	
Ocean Subsurface	9-2009	US east coast	Pol, Lidar							yes		B-200, CIRPAS Twin Otter	
CALIPSO validation	4-2010	US east coast	Lidar							yes		B-200	
CALIPSO/Gulf Oil Spill	5-2010	Gulf of Mexico	Pol, Lidar			RSP1				yes		B-200	
CALNEX	5-2010	Calfornia	Pol, Lidar			RSP1				yes		B-200, NOAA P-3	
CARES	6-2010	California	Pol, Lidar			RSP1				yes		B-200	
COCOA	8-2010	Caribbean	Pol, Lidar			RSP1				yes		B-200	
DISCOVER-AQ '11	7-2011	DC-Baltimore	Lidar							yes		P-3, B-200	
EPA	8-2011	SE Virginia	Lidar							yes		B-200	
DEVOTE	10-2011	US east coast	Pol, Lidar			RSP1				yes		B-200, UC-12	
CALIPSO validation	3-2012	Eastern US	Lidar							yes		B-200	
DC3	5-2012	Central US	Lidar						yes			DC-8, G-V	
TCAP	7-2012	Cape Cod	Pol, Lidar			RSP1					yes	B-200	
HS3 '12	9-2012	Atlantic Ocean	Lidar					yes				Global Hawk	
AZORES	10-2012	Azores	Pol, Lidar			RSP1				yes		P-3	
DISCOVER-AQ '13	1-2013	Central California	Lidar								yes	B-200, P-3	
PODEX	1-2013	S. California	Pol, Lidar	PACS (no data)	yes	RSP2		yes				ER-2	
SEAC4RS	8-2013	CONUS, Gulf of Mexico	Pol, Lidar		yes	RSP2		yes	yes			ER-2, DC-8	
HS3 '13	8-2013	Atlantic Ocean	Lidar					yes				Global Hawk	
DISCOVER-AQ '13 fall	9-2013	Houston	Lidar									B-200, P-3	
HyspIRI '13	10-2013	US west coast	Pol		yes	RSP2						ER-2	
Pre-PACE	4-2014	US west coast	Pol		yes							ER-2, Twin Otter	
HyspIRI '14 spring	4-2014	US west coast	Pol			RSP2						ER-2	
CALIPSO validation	6-2014	Eastern US	Lidar							yes		B-200	
Bermuda (Pre-SABOR)	6-2014	Bermuda	Pol, Lidar			RSP1						B-200	
SABOR	7-2014	Atlantic	Pol, Lidar			RSP1				yes		B-200	R/V Endeavor
DISCOVER-AQ '14	7-2014	Denver	Lidar								yes	B-200, P-3	
HS3 '14	8-2014	Atlantic Ocean	Lidar					yes				Global Hawk	
HyspIRI '14 fall	10-2014	US west coast	Pol, Lidar			RSP2						ER-2	
CalWater2	1-2015	California	Pol, Lidar		yes			yes				ER-2	
CCAVE	8-2015	California	Lidar					yes				ER-2	
NAAMES '15	11-2015	NW Atlantic	Pol, Lidar			RSP1				yes		C-130	R/V Atlantis
RADEX/OLYMPEX	11-2015	Washington state	Pol, Lidar		yes			yes				ER-2, UND Citation	
SPEX-PR	2-2016	US west coast	Pol		yes		yes					ER-2	
NAAMES '16	5-2016	NW Atlantic	Pol, Lidar			RSP1				yes		C-130	R/V Atlantis
ImPACT-PM	7-2016	Calfornia central valley	Pol, Lidar		yes		yes					ER-2, Twin Otter	
ORACLES '16	9-2016	SE Atlantic	Pol, Lidar		yes	RSP1, RSP2					yes	ER-2, P-3	
LMOS	5-2017	Lake Michigan	Pol, Lidar	yes								UC-12	
ORACLES '17	8-2017	SE Atlantic	Pol, Lidar			RSP2					yes	P-3	
NAAMES '17	9-2017	NW Atlantic	Pol, Lidar			RSP1				yes		C-130	R/V Atlantis
ACEPOL	11-2017	S. California	Pol, Lidar	yes	yes	RSP2	yes	yes		yes	yes	ER-2	

Table 5.1 2007-2017 field campaigns relevant to aerosols, with involvement by either multi-angle polarimeters or lidars (or both) that received support from ACE. Dates and locations are approximate. Field campaigns highlighted in black received direct funding from ACE, and are described in more detail in

this document. The presence of Lidars or Polarimeters (abbreviated "pol") in each field campaign is described in the 'Aerosol' column, and participation of specific instruments indicate to the right.

Table 5.1 is an overview of Aerosol relevant airborne field campaigns in the ACE period (2007-2017) that included the participation of ACE funded lidars and/or polarimeters. ACE funded missions are highlighted in black. What follows in a brief description of some of the most important missions of relevance to Aerosols. We start with a description of ACE funded campaigns (PODEX, ACEPOL) followed by the same for some of the most important (for aerosol remote sensing) other field campaigns (ARCTAS, SEAC4RS, ORACLES). We conclude with a briefer description of other relevant campaigns. Please see sections 3.2 and 3.3 for a description of polarimeter and lidar instruments, respectively, and section 4.1 for aerosol relevant algorithms from those instruments.

ACE Polarimeter Definition Experiment (PODEX)

The ACE instrument requirements call for a polarimeter to provide retrievals of aerosol optical and microphysical properties. The polarimeter designs currently under development vary widely in their design, spectral and angular coverage, and radiometric calibration/uncertainty requirements. Therefore, the POlarimeter Definition EXperiment (PODEX) mission was funded by ACE and conducted in 2013 to help optimize polarimeter design, assess the polarimeter aerosol and cloud retrievals, and intercompare various methods of retrieving aerosol optical properties (e.g., absorption, phase function, refractive index).

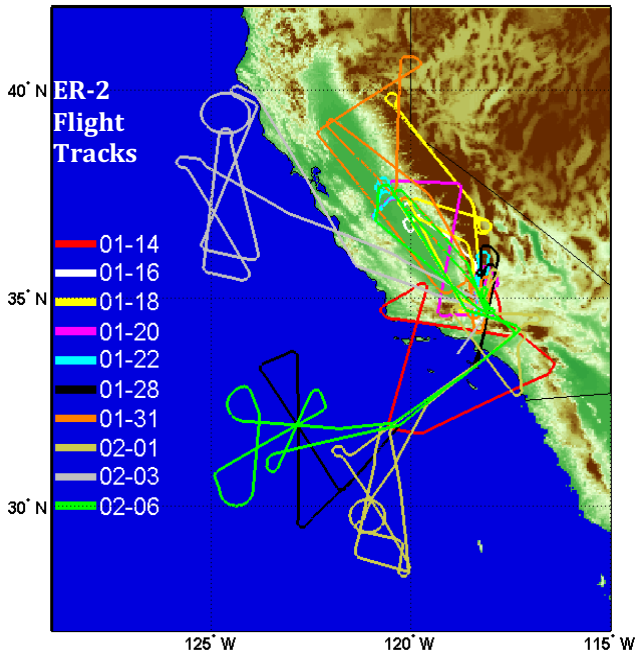

Figure 5.1 ER-2 flight tracks during PODEX.

PODEX was conducted from the Armstrong (formerly Dryden) Flight Research Center (AFRC) facility in Palmdale, California during January and February 2013. Three polarimeters were deployed from the NASA ER-2 (809) aircraft: the Airborne Multiangle SpectroPolarimetric Imager (AirMSPI), the Research Scanning Polarimeter (RSP), and the Passive Aerosol and Cloud Suite (PACS). Additional sensors on the ER-2 included the Autonomous Modular Sensor (AMS) which provided multiwavelength calibrated radiances and cloud products generated using MODIS algorithms, the Cloud Physics Lidar (CPL) which provided real-time and post flight aerosol/cloud backscatter profiles to locate and identify aerosol and cloud

layers, and the Solar Spectral Flux Radiometer (SSFR) which provided spectrally resolved shortwave irradiance measurements. The ER-2 flights conducted during PODEX were coordinated with airborne and ground-based measurements acquired during the third deployment of the DISCOVER-AQ Earth Venture-Suborbital (EV-S1) project. DISCOVER-AQ used the NASA P-3 and NASA LaRC King Air aircraft to study air quality over the California San Joaquin Valley during this period. The NASA P-3 aircraft was equipped with several in situ sensors that measured trace gas concentrations and aerosol optical (scattering, absorption) and microphysical (size, composition) properties. Of particular interest is the Polarized Imaging Nephelometer (the PI-Neph) developed by the PACS group for the detailed measurement of the P11 and P12 elements of the scattering matrix of the aerosol particles, which can be directly compared to the polarimetric retrievals of the PACS, AirMSPI and RSP sensors (Dolgos and Martins, 2014). The King Air deployed the LaRC High Spectral Resolution Lidar-2, which is a prototype of the multiwavelength lidar called for by ACE to provide layer-resolved retrievals of aerosol optical and microphysical retrievals. The Distributed Regional Aerosol Gridded Observation Network (DRAGON) of AERONET sun-sky photometers was also deployed in the southern part of the San Joaquin Valley and provided measurements of aerosol optical depth (AOD) and retrievals of column averaged aerosol optical and microphysical properties.

During PODEX, the ER-2 acquired 49 hours of science data during 10 flights between January 14 and February 6, 2013. The flights were designed so that the polarimeters acquired data over bright (desert, snow) and dark (ocean) scenes, during light and moderate aerosol loading conditions in maritime, rural and urban regions, and over fog, stratus, stratocumulus, and cirrus clouds. Data were also acquired over the calibration targets located at Rosamond Dry Lake, Ivanpah, and Railroad Valley. The flights over the San Joaquin Valley contained several legs above the DRAGON AERONET sensors and were coordinated with the DISCOVER-AQ aircraft so that correlative measurements of aerosol optical and microphysical properties were obtained. DISCOVER-AQ also conducted flights over the ocean to support the PODEX flights. The PODEX flights went well, with the exception of the flight on January 28 when RSP lost operation of the SWIR bands due to operator error. This also prevented the operation of these SWIR bands on subsequent PODEX flights. Post mission repairs and calibration showed that the visible channels were not affected.

Final versions of the PODEX polarimeter datasets have been archived, and are publicly available. AirMSPI Level 1 (L1, at sensor calibrated polarimetric radiances) data are at the LaRC Atmospheric Science Data Center (ASDC):
https://eosweb.larc.nasa.gov/project/airmspi/airmspi_table

See the PODEX AirMSPI data quality statement (Diner et al, 2017) and van Harten et al. (2018) for more details. While Level 2 (L2, geophysical product) data are not available to the public, they have been generated and analyzed in publications such as Xu et al., (2016 and 2017).

PACS data have not been made available due to an unforeseen detector linearity problem, which imposes errors greater than acceptable for L2 product generation. However, this experience informed design changes with the next generation HARP, AirHARP and HARP2 instruments.

Calibrated L1 RSP data are available at the GISS RSP archive:

https://data.giss.nasa.gov/pub/rsp/PODEX

As mentioned previously, no RSP SWIR channel data are available for the January, 28, 2013 flight or subsequent PODEX flights. L2 products are available at this archive for both liquid and ice phase clouds, based on algorithms and analysis described in Alexandrov et al (2012a, 2012b, 2015, and 2016), and van Diedenhoven et al. (2013). RSP PODEX data have also been used to investigate snow properties (Ottaviani et al, 2015), and the MAPP (Microphysical aerosol properties from polarimetry) simultaneous aerosol and ocean retrieval algorithm (Stamnes, et al., 2018) can be applied to PODEX data. Furthermore, a neural network has been used to compute aerosol properties over land (Di Noia et a., (2017)), and methods to derive aerosol layer height have also been determined (Wu et al, 2016).

For the RSP liquid cloud retrievals, note that comparisons of RSP cloud bow and AMS absorbing band droplet size retrievals do not show the type of biases previously reported in comparisons between MODIS and POLDER cloud products (Breon and Doutriaux-Boucher, 2005). In fact, the biases are consistent with the quasi-adiabatic vertical variations in liquid water content observed for the stratocumulus clouds in PODEX and our understanding of the weighting functions associated with 1.6, 2.2 and 3.7 μm spectral bands (Platnick 2000). That is, there is a negligible difference between cloud bow and droplet sizes retrieved using the 3.7 μm absorbing band while the 2.2 μm droplet retrievals, with a weighting function deeper into the cloud, are 1-2 μm smaller (Alexandrov et al. 2015).

Multi-instrument scene comparisons were a primary goal of PODEX, and the justification for the wide variety of scene types observed during the campaign. Comparisons can be performed for both Level 1 and Level 2 data products. L1 comparisons show how well calibrated instrument radiances, reflectances or polarimetric observations agree for a given scene. Factors that can impact the level of agreement include data geolocation, instrument calibration and random errors (noise). An important aspect of these comparisons is to account for expected measurement uncertainty in a statistically appropriate manner. Knobelspiesse et al. (2019) compared L1 data from the AirMSPI and RSP instruments for a variety of scenes. They found the Level of Agreement (Altman and Bland, 1983, Bland and Altman, 1986) to be largely consistent with expectations of measurement uncertainties for the paired instruments. Exceptions were for the 470nm reflectance channel (AirMSPI roughly 6% higher than RSP) and for polarimetric observations of dark oceans, where the contribution of random errors is larger than expected in the uncertainty model. These results represent a significant improvement over the

initial analysis of PODEX data, and are the result of years of refinements to the geolocation, characterization and calibration of both instruments. Knobelspiesse et al. (2019) also reports the uncertainty models for both instruments, and corrections made to geolocation due to wing flex in the ER-2 aircraft. Given these results, one can expect that intercomparisons of the same scenes at L2 would find the same Level of Agreement, provided that the L1-L2 algorithms are successful and that the instruments have similar levels of information content. This particular analysis, however, has yet to be performed.

Aerosol Characterization from Polarimeter and Lidar (ACEPOL)

The ACEPOL field campaign consisted of nine flights between October 19th and November 9th, 2017, with a full complement of multi-angle polarimeter and lidar instruments deployed on the high altitude ER-2 aircraft. Like PODEX, it was based at the Armstrong Flight Research Center in Palmdale, California.

A collaboration between NASA (ACE mission) and the Netherlands Institute for Space Research (SRON), the ACEPOL campaign targeted a wide variety of scene types in order to test and validate observations from the four multi-angle polarimeters onboard the ER-2. Two lidars provided observations of the aerosol vertical profile for context and comparison. ACEPOL also was supported by the CALIPSO mission for validation purposes.

Instruments deployed on the ER-2 aircraft during ACEPOL

Multi-angle Polarimeters

- AirHARP (1st time on the ER-2, 2nd field campaign overall)
- AirMSPI
- RSP
- SPEX (1st full field campaign)

Lidars

- CPL
- HSRL-2

Other coordinated measurements

- Column Aerosol ground observations from AERONET and MPLnet
- Rosamond Dry Lake surface characterization (October 25th)

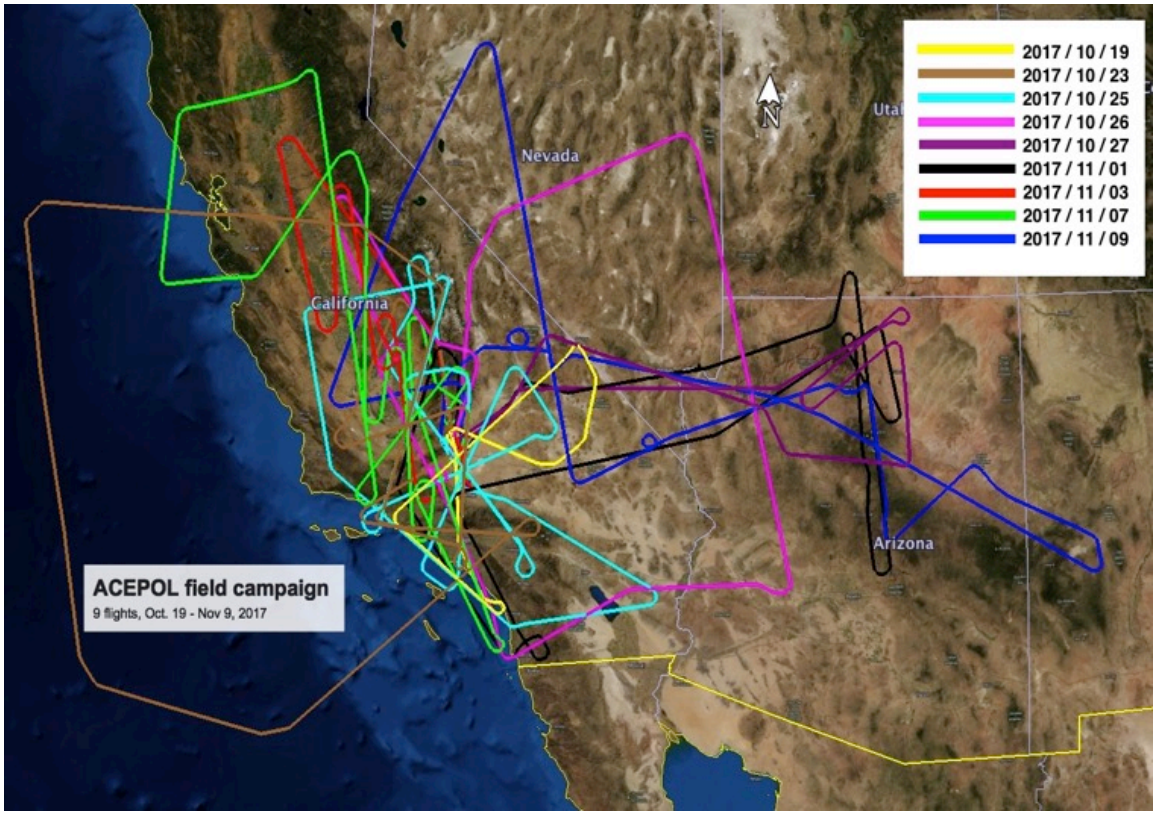

Figure 5.1 Flight tracks for the ACEPOL field campaign.

A variety of target scenes were identified prior to the mission, and most of these were successfully observed with fully functional instruments. This included observations of dark oceans and bright land surfaces with no clouds and minimal aerosol load. A rosette of coordinated flights over Rosamond Dry Lake were performed, while a team from JPL headed by Carol Bruegge characterized the land surface BRDF. Coordinated underflights of CALIPSO and CATS orbital lidars were performed, as well as coincident observations with satellite imagers such as MODIS, MISR and VIIRS. These were done in both cloudy and clear conditions. Overflights of AERONET and MPLnet ground sites were performed in low and moderate aerosol load conditions. Unfortunately, overflights for higher aerosol loads could not occur due to an atypical lack of aerosols in the region. Higher aerosol loads were encountered for flights over controlled burns in Arizona, but these did not have coincident ground observations, so validation data of aerosol retrievals in these areas are limited to the lidar observations.

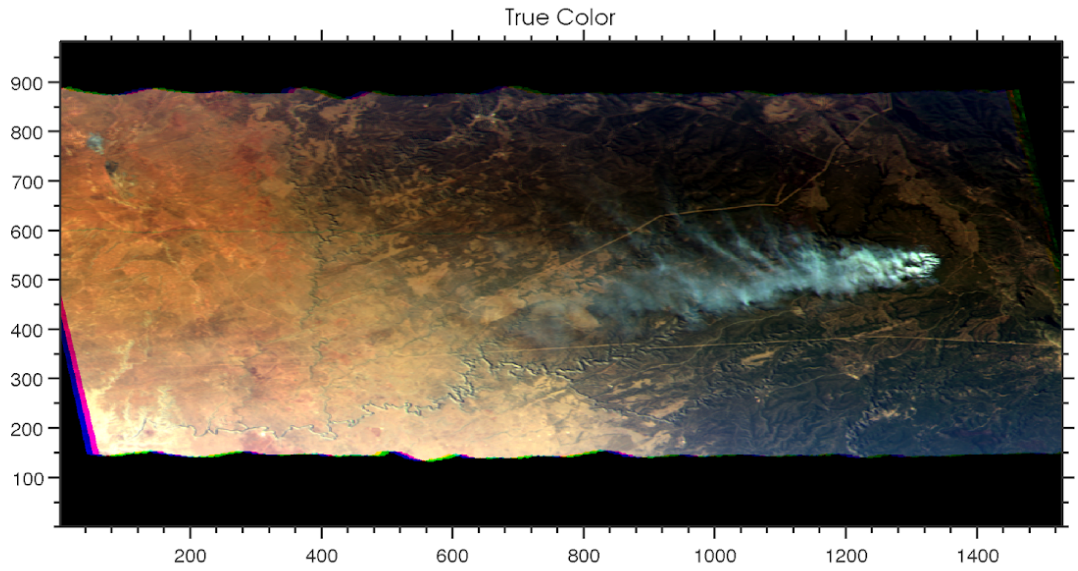

Figure 5.2 HARP True color imagery from November 9th, 2017 of a controlled burn in Arizona. Calibration and geolocation in this scene is preliminary.

One of the most valuable ACEPOL scenes was observed on October 23rd, 2017 for a flight track off Los Angeles in the vicinity of San Clemente and Santa Catalina islands. This flight track was performed in the solar principal plane (the heading was aligned with the solar azimuth angle) in cloud free conditions. This means that the multi-angle polarimeters were able to observe the reflected ocean sun glint at or near the Brewster's Angle, where the reflected light is fully polarized. The multi-angle polarimeter observations can therefore be compared at the maximum potential

Figure 5.3 Carol Bruegge (JPL) and team with the GroundMSPI at Rosamond Dry Lake.

range of polarization values, which are rarely observed in the field. Furthermore, the presence of islands in the flight track can be used to confirm scene geolocation, while the overflight of the USC SeaPRISM AERONET site provides column aerosol and ocean reflectance properties for validation (Zibordi et al, 2009). For these reasons, this scene, among others, is of great interest to the ACEPOL instrument teams as they process, refine, validate and compare their data.

Arctic Research of the Composition of the Troposphere from Aircraft and Satellites (ARCTAS)

The ARCTAS field campaign was conducted in two three-week segments. The first was in Alaska in April of 2008, and the second in June and July of the same year. Three aircraft were deployed for this campaign, of which the Langley B-200 had a payload devoted to remote sensing, containing the HSRL and RSP instruments (RSP was deployed in the summer campaign only). ARCTAS had four science goals: 1) understanding mid-latitude pollution influx, 2) understanding boreal forest fires, 3) characterizing aerosol radiative forcing for these events, and 4) understanding the chemical processes behind these events (Jacob et al, 2010).

The objectives of ARCTAS were broad and involved a large community. From the perspective of aerosol remote sensing with multi-angle polarimeters and lidars, ARCTAS data provided useful insight. Burton et al. (2013) used ARCTAS data (among others) to derive an HSRL classification approach, and validate against CALIPSO results. Knobelspiesse et al (2011) investigated retrievals of aerosol optical properties with combined polarimeter and lidar data. Because of the intensity and age of biomass burning smoke observed in the summer phase of ARCTAS, this is an invaluable dataset for the investigation of the evolution such aerosols in their first hours to days.

Studies of Emissions and Atmospheric Composition, Clouds and Climate Coupling by Regional Surveys (SEAC^{4}RS).

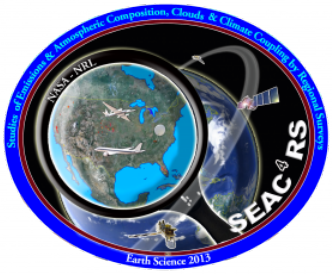

Although PODEX provided a very important initial dataset for evaluating the polarimeter designs and retrieval techniques, it did not provide the full suite of measurement targets that are required to fully evaluate these instruments. Measurements of very high aerosol loadings such as dense forest fire smoke and dust were not obtained because significant forest fires and dust outbreaks did not occur within range of the ER-2 during the PODEX measurement period. There was also no opportunity during PODEX to measure smoke or dense aerosol above clouds, which presents a particularly important and challenging retrieval situation for the polarimeters. There were relatively few measurements of cirrus during PODEX, particularly in cases where there were no underlying clouds.

Fortunately, the SEAC^{4}RS experiment provided another opportunity to obtain these conditions (Toon et al. 2016). Three aircraft were deployed during SEAC^{4}RS: the NASA DC-8 and ER-2 and the SPEC Lear Jet. As in PODEX, AirMSPI and RSP were deployed from the ER-2 and acquired datasets important for evaluating the polarimeter measurements and retrievals. Likewise, CPL and SSFR were also part of the ER-2 payload as in PODEX. However, PACS was not on the ER-2 for SEAC^{4}RS. In place of AMS, the enhanced MODIS Airborne Simulator (eMAS) was deployed on the ER-2 and provided high spatial resolution imagery of aerosol and cloud fields. The DC-8 payload included several in situ instruments for measuring aerosol and optical properties, an airborne HSRL instrument, and the new 4STAR instrument for providing sun and sky measurements from which aerosol optical and microphysical properties are retrieved in a manner similar to AERONET. The SPEC Lear Jet carried in situ sensors for measuring cloud and ice particle size distributions and liquid and ice water content. As in PODEX, a network of AERONET Sun-Sky photometers was deployed over the southeastern US to provide measurements of aerosol optical depth (AOD) as well as retrievals of aerosol absorption.

During SEAC^{4}RS (June 2012-June 2013), the DC-8 and ER-2 each flew more than 150 science flight hours; the Lear Jet flew over 50 hours. In the first part of the campaign, the aircraft were based out of the AFRC in Palmdale, CA and flew out of Ellington Field near Houston, TX for the remainder. Although the SEAC^{4}RS flights were concentrated more heavily in the southeastern US and the Gulf of Mexico, there were several flights over the western US to observe targets of interest; in particular, flights targeted smoke from fires in California and Oregon. Of particular interest was the flight on August 6, 2013, when instruments from both aircraft were able to observe and measure smoke properties above stratocumulus clouds. AirMSPI and RSP research teams used these datasets to develop and evaluate aerosol and cloud properties. For example, AirMSPI aerosol retrieval results for AOD, single scattering albedo, size distribution for a few cases are consistent with those derived from AERONET (Xu et al, 2017). Unfortunately, the AirMSPI in-flight calibrator did not work as well as in the PODEX field campaign, an issue that has been resolved for subsequent missions (van Harten et al, 2018). Initial RSP retrievals of cirrus cloud particle size, optical thickness, and asymmetry parameter compare favorably with those derived from coincident eMAS retrievals. During the same experiment, the PACS group flew the RPI portable imaging polarimeter (analogous to PACS) and the PI-Neph (Dolgos and Martins, 2014, Espinosa et al, 2017) for data validation on board the NASA DC-8 aircraft. Both instruments are being used for the development of ACE aerosol and cloud retrievals as well as potential validation for the ER-2 polarimeters.

Evaluation of aerosol algorithms and aerosol properties retrieved from ACE instruments will rely significantly on AERONET retrievals of column-averaged aerosol properties. Currently, the AERONET retrievals require a set of a minimum aerosol optical depth (at 440nm) of 0.4 and a solar zenith angle greater than 50° to obtain highest quality (L2.0) data products. SEAC^{4}RS measurements provided an

opportunity to test the representativeness of the AERONET absorption retrievals for a limited number of these high AOD cases as well as many other cases at lower AOD levels. SEAC⁴RS data can be used to compare different techniques for measuring and retrieving aerosol absorption.

ObseRvations of Aerosols above CLouds and their intEractionS (ORACLES)

The ORACLES field campaign was devoted to the observation of poorly understood aerosols above clouds in the South East Atlantic Ocean, where such phenomenon are dominant in the austral spring. The observation of aerosols above clouds, and corresponding radiative forcing and cloud indirect effects, has been difficult for most spaceborne sensors (Yu et al., 2013, Knobelspiesse et al., 2015), although new algorithms have been developed that determine the Aerosol Optical Depth with assumptions about aerosol microphysical properties (Jethva et al., 2013, 2014, Meyer et al., 2015, Sayer et al., 2016). ORACLES had the following scientific objectives (quoted from the ORACLES overview at https://espo.nasa.gov/ORACLES/content/ORACLES_Two-page_ORACLES_Flyer):

1. Determine the impact of African BB (Biomass Burning) aerosol on cloud properties and the radiation balance over the South Atlantic.

2. Acquire a process-level understanding of aerosol-radiation interactions and resulting cloud adjustments, and aerosol-cloud interactions, that can be applied globally.

3. Substantiate future measurements by gathering testbed datasets that can be used to verify and refine current and future observation methods and simulation techniques.

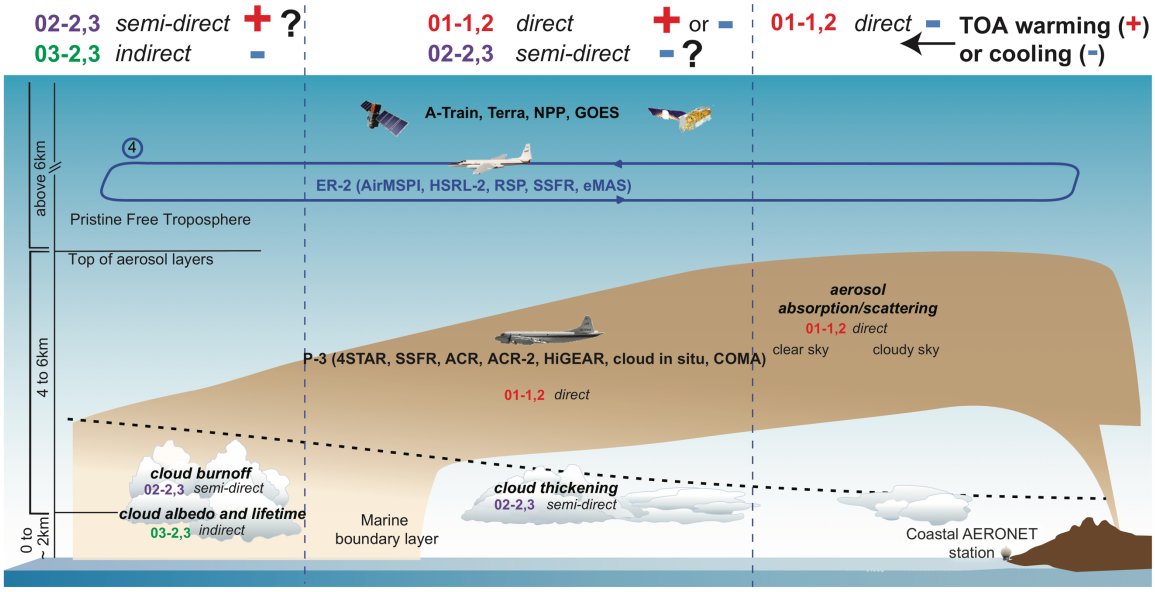

Figure 5.4 Schematic of ORACLES mission plan

ORACLES consisted of three deployments to the South East Atlantic Ocean. In 2016, the ER-2 and the P-3 were based in Walvis Bay, Namibia. The ER-2 carried a payload of remote sensing instruments, including the AirMSPI and RSP polarimeters, and the HSRL-2 lidar. The P-3 was primarily intended for in-situ aerosol and cloud sampling, although it also carried a second copy of the RSP and a cloud and precipitation radar. Deployments in 2017 and 2018 were made with the P-3 only, and were based on the island of São Tomé, São Tomé and Príncipe. In these years, the P-3 had both a remote sensing and an in-situ sampling role, and for the former the HSRL-2 was moved to the P-3 (along with the RSP and radars that were also deployed in 2016).

Several other field campaigns were conducted in this region at roughly the same time. The UK CLARIFY (Clouds and Aerosol Radiative Impacts and Forcing: Year 2017), headed by the UK Met Office, deployed the FAAM BAe-146 aircraft from Ascension Island in 2017, with which the ORACLES P-3 performed coordinated flights. The DOE funded LASIC (Layered Atlantic Smoke Interactions with Clouds) campaign deployed the ARM Mobile Facility to Ascension island for multiple years. The French AEROCLO-sA (Aerosol Radiation and Clouds in southern Africa) campaign enhanced ground sites in Namibia and South Africa and deployed the F20 aircraft to Walvis Bay, Namibia in 2017. More details on these campaigns can be found in Zuidema et al. (2016).

While data processing and analysis are still underway, several papers have already been published with ORACLES results. Xu et al., (2018) presented an optimal estimation retrieval algorithm that determined cloud optical depth, droplet size distribution and top height along with aerosol optical depth and microphysical properties from AirMSPI observations. Segal-Rozenhaimer et al. (2018) created a neural network algorithm to determine cloud optical properties from RSP observations. It can be considered a complement to other RSP cloud retrieval algorithms, and it meant to be a stepping stone to neural network based simultaneous retrievals of aerosol and cloud optical properties from that instrument. Burton et al., (2018) presented an analysis of HSRL2 ORACLES observations as well. At least twenty other publications are in progress, both from ORACLES funded team members and external collaborators.

Additional Field Missions

Both AirMSPI and RSP were deployed on the ER-2 as piggyback instruments on flights that were conducted over California as part of the HyspIRI airborne campaign (https://hyspiri.jpl.nasa.gov/airborne, Lee et al, (2015)). The primary instruments flown in these flights were the Airborne Visible/Infrared Imaging Spectrometer (AVIRIS) and the MODIS/ASTER Airborne Simulator (MASTER). RSP was deployed on the ER-2 for eleven flights between October 2013 and August 2014, and AirMSPI was deployed for seven of the flights during April and May 2014. They were not deployed simultaneously. Among other achievements, some of these observations were used to improve atmospheric correction techniques, by which aerosol impacts

on the remote sensing of land and ocean optical properties are removed (Kudela et al., (2015), Palacios et al., (2015), Thompson et al., (2015)).

RSP and the HSRL-1 were also deployed on a NASA Langley King Air aircraft during July-August 2014 for the Ship-Aircraft Bio-Optical Research (SABOR) experiment (Hostetler et al. 2014; Sinclair et al. 2014; Powell et al. 2014). Twenty-five research flights were conducted over the western Atlantic Ocean coincident with in-water bio-optical measurements made from the R/V Endeavor in 2014. Among other instruments, the R/V Endeavor deployed an above water polarimeter, the HyperSAS-POL (Ottaviani et al., 2018), of unique value in comparison to the airborne RSP. These data have been used to improve algorithms for lidar and polarimeter retrievals of ocean properties and atmospheric corrections for ocean color retrievals. Simultaneous retrieval of aerosol and ocean properties was tested with data from this campaign for new retrieval algorithms described in Gao et al, (2018) and Stamnes et al., (2018).

The North Atlantic Aerosols and Marine Ecosystems Study (NAAMES) field campaign was carried out in multiple deployments between 2015 and 2018. The primary NAAMES focus is ocean plankton ecology (Behrenfeld et al., 2017), however, one of the baseline science objectives is relevant for ACE: *"Resolve how remote marine aerosols and boundary layer clouds are influenced by plankton ecosystems in the North Atlantic"* For this effort, NAAMES deployed the R/V Atlantis from its base at Woods Hole to the North Atlantic for transects along the 40°W longitude line, and the NASA C-130 aircraft from St. John's in Newfoundland, Canada. Remote sensing instruments on the C-130 included the HSRL-1 lidar (optimized for in water ocean profiling), the GeoCAPE airborne simulator (GCAS), the Spectrometer for Sky-Scanning Sun-Tracking Atmospheric Research (4STAR) and the RSP. While cloud free conditions, ideal for passive remote sensing, are infrequent in the North Atlantic, this campaign gathered valuable lidar data, was used for GCAS atmospheric correction algorithm development (Zhang et al., 2018), provided data for polarimetric cloud retrieval validation (Alexandrov et al., 2018). Some of the cloud free scenes were used in previously mentioned in Gao et al, (2018) and Stamnes et al., (2018). Furthermore fundamental ocean/aerosol/cloud

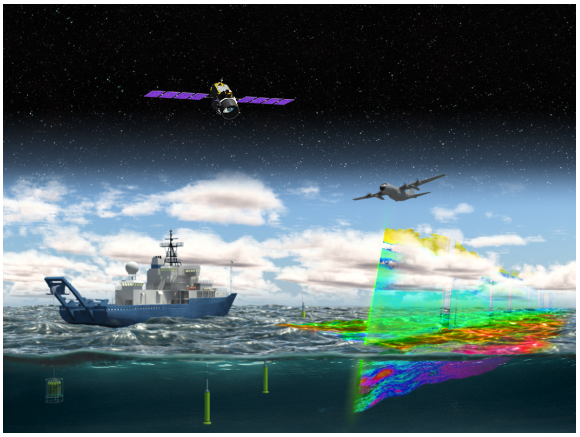

Figure 5.5 NAAMES mission graphic

relationships were explored with both remote sensing and in situ sampled data (Quinn et al., 2017, Sanchez et al., 2018).

In addition to the abovementioned campaigns, the airborne HSRL-2 acquired data while flying on the NASA LaRC King Air during four atmospheric field missions conducted since 2012. The first was during the DOE Two-Column Aerosol Project (TCAP) in July 2012 over the Atlantic Ocean east of Cape Cod (Müller et al. 2014). The following three deployments were in support of the NASA DISCOVER-AQ campaigns held in 1) the California central valley in January-February, 2012, (Ferrare et al. 2013, Hostetler et al. 2013) Houston in September 2013, and 3) Denver in July-August 2014 (Scarino et al. 2013, 2014). Approximately 260 science hours of data were acquired by the HSRL-2 during a total of 77 science flights during these four missions.

Beyond supporting the science of these particular missions, HSRL-2 data acquired during these missions are being used to help develop and assess the advanced lidar retrieval algorithms designed to meet the ACE aerosol requirements discussed in Section 2. Operational code has been developed to implement these retrievals. The code has been used to produce ACE-like L2 products including layer-resolved aerosol optical (scattering, extinction) and microphysical (size, concentration) properties in "curtains" below the aircraft. In addition, DISCOVER-AQ overflew the DRAGON AERONET network of Sun-sky photometers that had been specifically deployed during the campaign. These in situ aerosol measurements and AERONET retrievals have proven valuable for assessing the results of the multi-wavelength lidar aerosol retrieval algorithms and for comparing different techniques for measuring and retrieving aerosol properties (Scarino et al. 2013). These comparisons are ongoing as are efforts to improve the accuracy and speed of the retrievals.

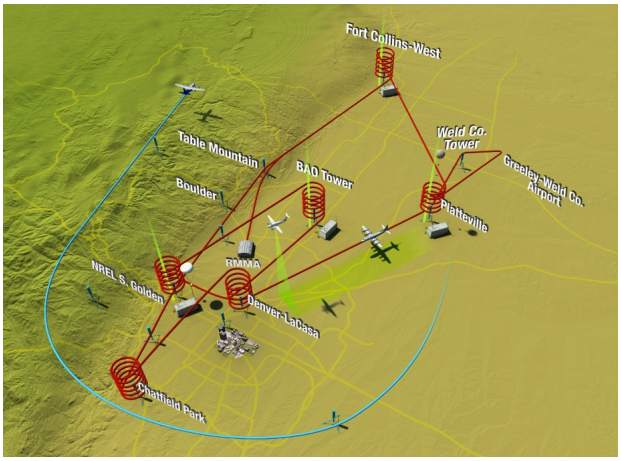

Figure 5.7 Map of the 2014 DISCOVER-AQ campaign near Denver, Colorado.

5.2 Cloud Related Campaigns

Over the past decade, NASA has invested heavily in generating suborbital data sets that are suitable for addressing many of the goals of ACE clouds. A critical aspect of this work is the coordinated collection of remote sensing datasets (which mimic or can be used to mimic measurements that will be used by ACE) and in situ measurements of a variety of cloud microphysical properties needed to assess retrieval approaches and measurement needs. Relevant data sets were collected in

the 2007 NASA TC^4 campaign where both remote sensing from the ER-2 and DC-8 are available in addition to extensive in situ data by the DC-8 that was collected in close coordination with the ER-2. However, the radar suite on the ER-2 did not identically mimic what is planned for ACE although dual frequency Doppler radar data (W and X bands) were collected along with passive microwave (AMPR) and visible and IR radiance data (MODIS Airborne Simulator). Several flights also included sub millimeter wavelength measurements from the COSSIR instrument. Another data set that can be useful to ACE clouds was collected during the SEAC^{4}RS campaign in 2013. In SEAC^{4}RS, the NASA DC-8 carried the APR-2 radar that collected scanning Doppler data in the Ku and Ka bands. The Stratton Park Engineering Corporation Lear Jet provided in situ validation. The primary target in SEAC^{4}RS was convection both over continental locations and over the Gulf of Mexico.

More recently, the ACE program directly supported two cloud campaigns the "Integrated Precipitation and Hydrology Experiment" (IPHEX) and the "OLYMPic mountain EXperiment" (OLYMPEX). Both of these experiments were undertaken in coordination with the GPM Ground Validation team to the mutual benefit of both programs.

The ACE portion of these two campaigns is also known by the acronyms RADEX-2014/RADEX-2015 (for RAdar Definition Experiment) - though we will use the names IPHEX and OLYMPEX throughout this document rather than RADEX. As the title RADEX suggests, and what sets IPHEX and OLYMPEX apart from other field experiments, was a focus on (and recognition of the need for) more ACE-like packages to test measurement synergies – and in particular the need for multi-frequency radar datasets with collocated in situ data.

Integrated Precipitation and Hydrology EXperiment (IPHEX)

During IPHEX, the ER-2 was instrumented with three Doppler radars built by Gerry Heymsfield's group at NASA Goddard and collected data in the W, Ka, Ku, and X bands. In addition, the ER-2 carried the AMPR and the CoSMIR microwave radiometers. The payload is shown below in Figure 5.8 as an example of data collected during IPHEX. The University of North Dakota (UND) Cessna Citation collected coordinated in situ data. ACE funding augmented the instrumentation and

total number of Citation flight hours.

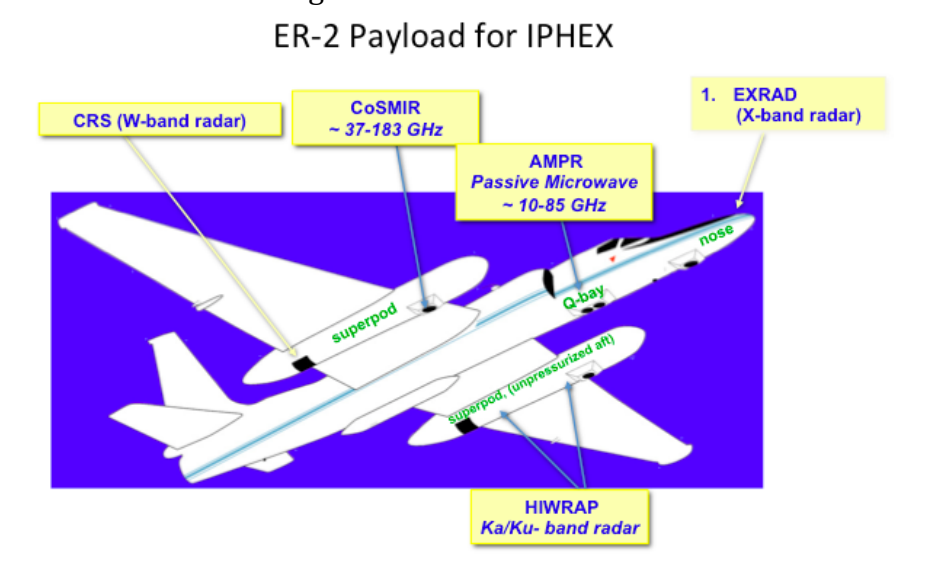

Figure 5.8 ER-2 Payload for IPHEX

ACE clouds had two specific targets for IPHEX: first warm rain in shallow convection and second clouds producing stratiform precipitation that was initiated as snow above the freezing level. Several IPHEX flights collected data in shallow warm cumulus in addition to extensive mixed phase clouds and convection both offshore and over the mountains of North Carolina. Table 5.2 provides a more detailed breakdown of the flight targets.

Table 5.2. Case studies of note for ACE-related science goals generated during IPHEX. Many of these flight days were funded by GPM GV indicating the fruitful collaboration between ACE and GPM GV.

Date (2014)	Notes
May 12: Offshore Convection	Developing convergence line resulted in deepening convection along the Gulf Stream. ER-2 sampled convection in various stages of the lifecycle while the Citation collected data in situ nearby.
May 16: Offshore Frontal Precipitation	Deep frontal clouds and stratiform rain with embedded convection were systematically sampled by the ER-2 while the Citation collected in situ data along sections of the ER-2 track.
May 18: Baroclinic system over the Appalachians	Clouds and precipitation formed by a weak synoptic system in the early morning hours were sampled over the Appalachians by the ER-2 and Citation.
May 19: GPM overpass and warm rain offshore	ER-2 and Citation collected data in a weakening precipitation area offshore. The GPM overpass was closely coordinated by the ER-2 over deeper clouds. Following the overpass, shallower clouds producing warm rain were sampled by both aircraft.

May 28: Warm rain offshore	This flight provided excellent coordinated data in shallow convection and warm rain offshore. ER-2 and Citation were closely coordinated. Likely the best case for warm rain during the campaign.
June 6: Congestus over ground-based	Congestus over Maggie Valley was sampled by ground-based remote sensors in the ACHIEVE instrument suite while the Citation collected data in situ.

OLYMPic mountain EXperiment (OLYMPEX)

While IPHEX produced a multi-frequency radar & microwave radiometer dataset, it did not include any lidar, VIS-IR imager or polarimeter measurements. Between IPHEX and OLYMPEx, additional modifications where made to facilitate a larger ER-2 payload to enable a more ACE-like package, as shown below in Figure 5.9. During OLYMPEX both the CRS (W-band) and HIWRAP (Ka/Ku band) were placed in the same superpod making space to include the MODIS airborne simulator (MAS), a VIS-IR imager. A backscatter lidar (CPL) replaced CoSMIR (which flew on the DC-8), and in addition, two ER-2 noses where used. One nose carrying EXRAD (X-band radar) and one carrying AirMISP-2, a scanning imaging polarimeter. Of the ten ER-2 flights during OLYMPEX, five included AirMISPI and focused on collecting data in or near the solar principal plane offshore and five (more focused on heavy precipitation) included EXRAD.

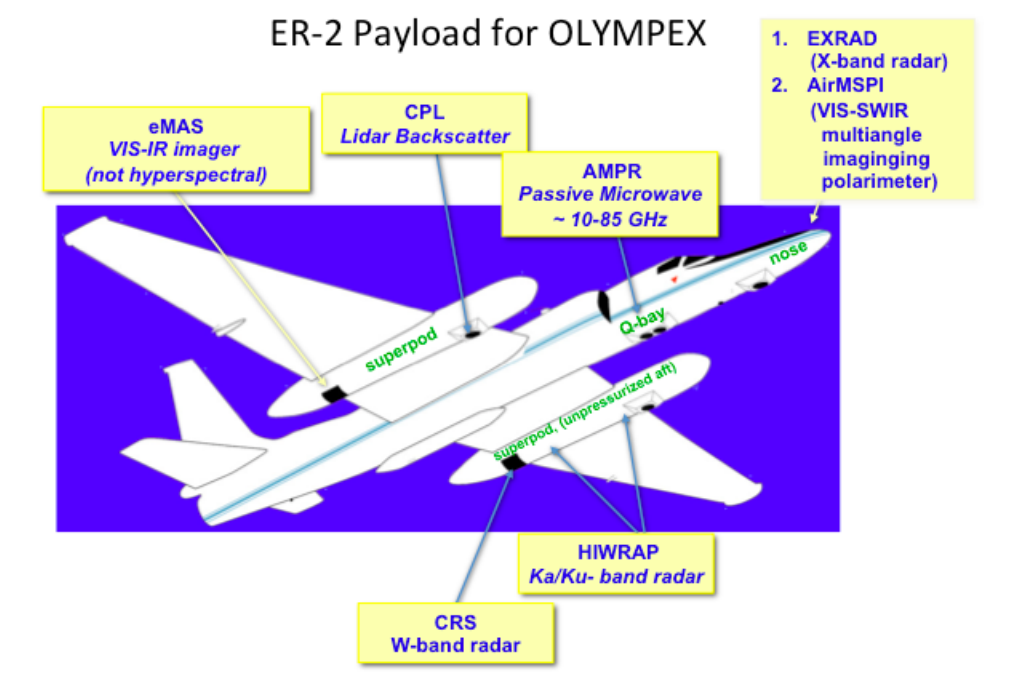

Figure 5.9 ER-2 Payload for OLYMPEX

In addition to the ER-2, the DC-8 and UND citation also participated in OLYMPEX. The DC-8 carried CoSMIR, APR3 (scanning W, Ku, and Ka band radars), and dropsondes, and was frequently flown in tight coordination with the ER-2. The UND

citation was configured to measure in situ cloud microphysics (including 2D-S, 2D-C, CPI, and two HVPS oriented horizontally and vertically) and on several occasions made two forays, stopping to refuel in between.

OLYMPEX took place during November/December of 2015, as part of a campaign to examine liquid and mixed phase clouds over and offshore of the Olympic Peninsula in Washington State [Houze et al. 2017]. The Peninsula was extensively instrumented for the experiment, as shown in Figure 5.10. This includes ground based Doppler radars at several frequency and several sites (various squares) and other ground sites with a variety of precipitation gauges, disdrometers and other instrument for characterizing the surface precipitation (white x's).

Specific ACE-cloud goals in OLYMPEX were to: 1) collect an ACE-like data set for maritime convection in cold air sector behind fronts, 2) examine the warm rain process in stratiform clouds ahead of fronts, and 3) collect mixed and ice-phase cloud and precipitation data in frontal bands. Each of these situations represent significant and specific challenges for algorithm development where cloud processes in turbulent vertical motions generate precipitation in the cloud that is eventually realized at the surface as either rain or snow. Demonstrating the degree to which these processes can be diagnosed with actual data is fundamental to the goals of ACE clouds.

During the experiment, the ER-2 typically (though not exclusively) flew either long racetracks up or down the Quinault Valley passing over the high terrain and extending well offshore, or smaller racetracks flown offshore and aligned with the solar principal plane. These racetracks are conceptually illustrated in Figure 5.10 as with dashed orange lines. Figure 5.11 shows an example of radar reflectivity measurements during one transect down the Quinault Valley and extending offshore during an atmospheric river event (that is, warm-sector precipitation from a particularly moist cyclonic system). The melting-layer can be seen dipping downward (lowering in altitude) near the high topography due in large measure to increasing precipitation as one approaches the western slopes of the Olympic mountains. All three radar frequencies show interesting structures resulting from changes in ice crystal habits that were often observed to be associated with layers of supercooled liquid water.

Postfrontal conditions were also a focus of ER-2 flights. In particular, postfrontal low clouds were observed (with supporting in situ cloud microphysics) on several flights including 11/14, 12/04, and 12/13. All three of these flights contain scenes which can be used to test polarimetric and other retrievals for low clouds, and such work is currently underway (Figure 5.12).

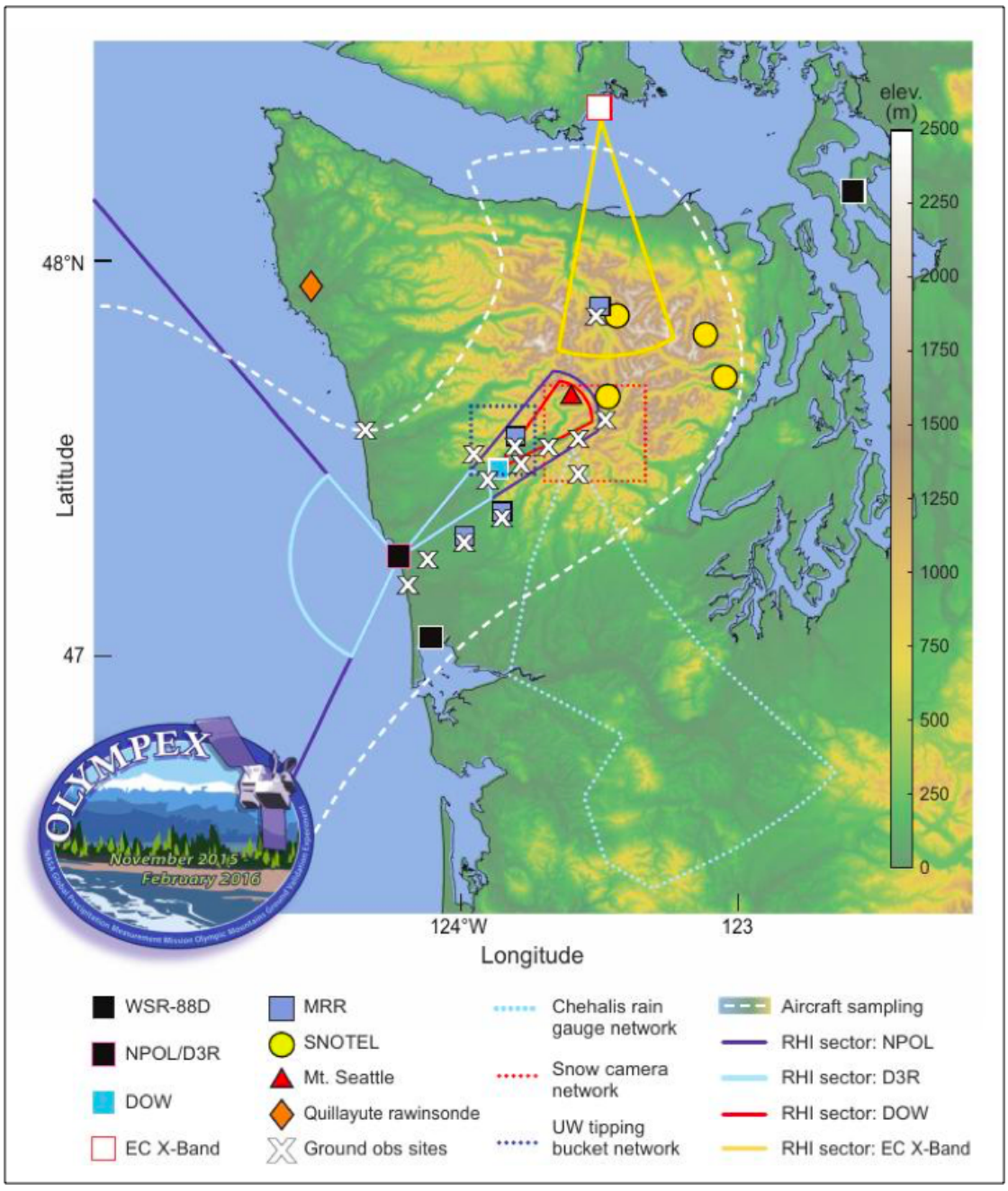

Figure 5.10 Map of OLYMPEX Ground Network. Dashed orange line shows "racetrack" patterns often used by ER-2. Flights often featured a long transect either up or down the Quinault Valley passing over the high terrain and extending offshore where NPOL radar was making sector scans, or with generally smaller racetracks flown offshore and aligned with the solar principal plane.

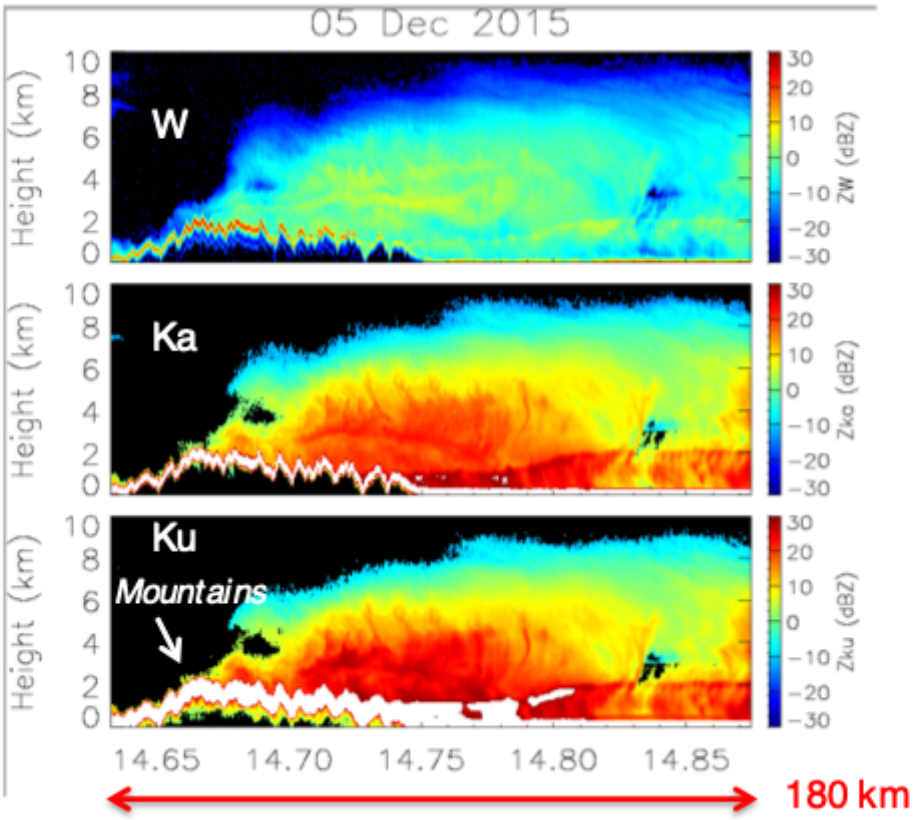

Figure 5.11 Example of ER-2 CRS & HIWRAP radar reflectivity data along Quinault Valley

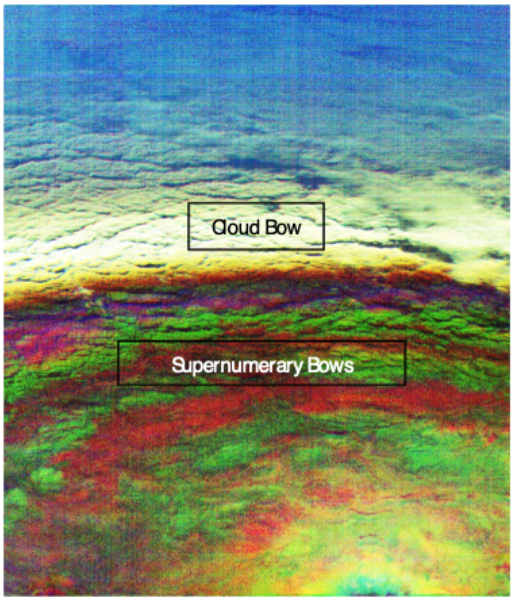

Figure 5.12 Example of Supernumerary and Cloud Bows for stratocumulus observed on 11/24 from AirMSPI (Degree of Linear Polarization; DOLP)

Summary and Discussion of Cloud Related Campaigns

In summary, the ACE supported IPHEX & OLYMPEX experiments have gathered multifrequency radar datasets with coordinated collection of in situ measurements of a wide variety of cloud microphysical properties. These rich observational datasets are being used by ACE investigators (see section 4.2) to study ACE-cloud measurement needs and retrieval approaches – though we note that much still needs to be done in this regard (see section ??). A very short recap of the IPHEX and OLYMPEX targets is given below, with more detailed list of flight conditions given in Tables 5.2 and 5.3.

As valuable as these datasets are, it is worth noting that a full ACE-equivalent dataset, meaning the full (not baseline) measurement package = multi-frequency Doppler radar (at least W+Ka bands) + high spectral resolution lidar (HSRL) + high resolution VIS-IR imagery (with polarization or separate polarimeter) + microwave and submillimeter wavelength radiometers does not exist. OLYMPEX comes close, but still lacked HSRL and some shorter wavelength (sub millimeter) radiometer measurements – both of which are expected to be valuable in constraining the properties of ice particles (including ice crystal habit) near cloud top, and more generally, for optically thin ice clouds.

Likewise, while IPHEX and OLYMPEX cases cover many cloud types, a greater number and breadth of cases remains highly desirable. In particular, the "full" measurement suite targeting a variety of cirrus types and the tops of thick high-altitude ice clouds (convective and otherwise) AND includes a focus in situ cloud observations near the tops of high-ice clouds should be considered. While OLYMPEX certainly includes deep frontal clouds, the in situ microphysics contains little data regarding properties near cloud top (in addition to lacking HSRL and sub-millimeter emissions).

Short summary of IPHEX and OLYMPEX cases:

- IPHEX
    - Off-shore warm rain in shallow convection (2 cases)
    - Off-shore deeper convection (2 cases) with stratiform precipitation that was initiated as snow above the freezing level (1 case).
    - Congestus and/or weak frontal convection over land (2 cases).
- OLYMPEX
    - Warm conveyor and/or fronts (ice phase processes) (4 cases)
    - Post frontal conditions (4 flights)
    - Only a few cases (1?) with embedded frontal convection

Table 5.3. Detailed summary of OLYMPEX ER-2 flights. See also: http://olympex.atmos.washington.edu/missions/Marchand_Mace_LEcuyer_RADEX_Flight_Summary.pdf

Flight	Target / Highlight	Instruments / Other Notes
11/18	A cirrus shield from an advancing warm frontal overrunning system was approaching from the Southwest while post frontal shallow showers continued in the cold air behind the previous frontal system. DC8 and ER2 conducted multiple long coordinated race tracks that had their eastern ends near the NPOL radar site. The first race track was oriented east-west and a second race track was set up more southwest-northeast. The Citation conducted stepped sampling in the advancing ice cloud.	Due to disk switch issue, lost about 1 hour of data from HIWRAP and CRS. Other Instruments nominal. Noted +30db from showers under high overcast on NPOL. Stratiform rain at far end of racetrack by end of flight.
11/23	ER2 and DC8 conducted a coordinated flight in an advancing frontal band offshore of the Olympic Peninsula. SW-NE oriented race tracks that were entirely offshore were conducted initially followed by a NW-SE oriented racetrack that had NPOL on SE end. Citation conducted two flights. Early flight was conducted under the NE end of the early race tracks. Second flight was near the SE end of the later racetrack. Frontal Rainbands advanced and clouds thickened during the flight. The early racetracks were oriented along the flow while the later race track was oriented perpendicular to the flow.	All instruments nominal except some data loss by Hiwrap and CRS near the end and during a brief period when during the flight. 2nd Citation flight took place after the DC8 and ER2 departed to RTB.
11/24	An Inland cold front with strong northerly post frontal flow over the Olympex region. All three aircraft targeted orographically enhanced snow along the northern slopes of the Olympics form ~15 to 17 UTC. Coordinated ER2 and citation sampling of offshore transition from cloud free to extensive stratocumulus cloud cover from ~ 19:30 to 22 UTC.	GMAO model runs indicated a continental aerosol plume being advected offshore, consistent with CPL backscatter and Citation observations of high cloud droplet number concentrations. ER-2: flew near principal plane during off shore legs, AirMSPI was in the nose. Some loss (20-30 minutes) Hiwrap (Ku and Ka) early in the flight.

12/1	An occluded front with stratiform precipitation, and significant orographic enhancement. ER-2 and DC-8 flew coordinated racetracks over Quinault valley (radar sites) 22 to 24 UTC with coincident citation profiles. Strong rain shadow to the NE of the Olympics.	Variety of ice crystal habits (irregulars, plates, plate aggregates needles), melting layer near 7 kft (was sloping). EXRAD in nose but went/stayed down after 23:30 UTC. HIWRAP up after 22:06 UTC.
12/3	Strong Frontal/Pre-Frontal Precipitation over the Olympex. Coordinated data from all three aircraft with a GPM overpass of the high Olympics at 15:22 UTC. The GPM under-flight was followed by sampling along the Quinault Valley using a racetrack similar to that used during the Dec. 1 flight until ~ 16:45 UTC.	Citation observed a variety of (large aggregates, needles, slide plates on aggregates, capped columns, stellar plates and signficant quantites of supercooled liquid near the time over the GPM overpass. EXRAD in nose. AMPR 19 GHz channel failed (others OK).
12/4	Post-frontal conditions with shallow convection along the coast after about 10 UTC. All three aircraft sampled a shallow precipitating convective line that was propagating eastward at 13 UTC just off the coast near the NPOL radar site. A small, developing low-level offshore cumulus was observed by ER-2 and UND Citation between 17:45 and 19:10 UTC.	Near 13 UTC: Citation observed large amounts of cloud liquid water (at -2 C) and irregular aggregates at colder temperature through the convective line. ~ 17:30 to 19:30 UTC: The ER-2 flew a variety of legs in the solar principal plane. Polarimetric (AirMSPI) data appear to be of very good quality for retrievals.

12/5	Warm sector precipitation with orographic enhancement near coast and heavy snow over the Olympic mountains All three aircraft sampled heavy snow along the Quinault Valley west of the mountains crossing into the rain shadow to the east. Coordination with Citation in situ was good along the valley. The elongated southwest to northeast racetracks of the ER-2 include ~30 nm of sampling light rain over the ocean. The ER-2 flew two long/level N-S loops in decaying light rain behind the front all the way north to Vancouver Island that may provide a good target for sensitivity testing.	1450 UTC: Citation sampled cloud along valley at multiple altitudes reporting large aggregates at (-8 C) but no super-cooled LWC; capped columns at -20 C; and small ice crystals extending up to 30 kft 1525 UTC: ER-2 crossed bands of embedded convection offshore
12/8	Offshore precipitation associated with 'atmospheric river' event ER-2 flew independent flight consisting of three 200 nm racetracks offshore including a Suomi NPP underflight (though west of the nadir ground track). EXRAD, HIWRAP, and CRS operated in test mode during the first racetrack but collected science data in light to moderate liquid precipitation along the other two. Flight hours were split between RADEX and Gerry Heymsfield's radar test flight.	The North-South racetrack from 21-22 UTC provides an interesting transect across the northern half of the moisture plume. AMPR characterized the transition from moderate stratiform precipitation with embedded convection to non-precipitating liquid clouds. More than 6" of rain reported at OLYMPEX ground sites over this 24 hour period
12/10	Tail-end of occluded front followed by post-frontal shallow convection. ER-2 and DC-8 flew beautifully coordinated racetracks, along Quinault continuing well offshore between 17 and 19 UTC.. After 19 UTC, the ER-2 began a sequence of off shore legs in the solar principal plane to sample classic post-frontal shallow convection. Some cirrus was present but also some cirrus free cloud suitable for polarimetric "rainbow" retrievals is also visible.	No ER-2 + Citation: Citation and DC-8 were on station earlier than ER-2. Citation left at 16:40 UTC, with the intent of refueling and returning, but encountered a maintenance issue and was unable to return. AirMSPI in nose. Worked well. CPL backscatter images suggest noteworthy levels of boundary layer aerosols, perhaps due to very high surface winds.

12/12	Occluding warm front and trailing showers. The DC-8 dropped 8 dropsondes along a racetrack across front prior to ER-2 takeoff. Citation collected microphysics at 2, 5, 8, 11, 14, 17, and 20 kft along one leg of this track. ER-2 flew independent NNE-SSW racetracks near the shore aligned with the coast (due to ER-2 delayed takeoff). ER-2 observed overrunning precipitation while northbound and trailing isolated warm showers on the southbound leg.	Citation observed significant supercooled liquid up to -15 C and a wide variety of crystals from large aggregates to columns. CRS data collection failed (other frequencies operated nominally). eMAS IR channels were also suboptimal.
12/13	A surface low centered over/near Vancouver Island brought cold, moist NW flow and significant post-frontal precipitation to the Washington coast. 17 to 19 UTC: All three aircraft sampled shallow convection with ample upper level ice cloud on/near the coast. 19:31 UTC: Terra underflight by ER-2. 20 to 20:30 UTC: ER2 and Citation sampled low-level clouds and shallow convection off shore. Some lingering cirrus complicates analysis.	ER-2: CRS failed near start of flight, and despite several tries could not be operated. HIWRAP was operated without CRS after ~17 UTC. AirMPSI in the nose, flew in principal plane after 20 UTC. 2DC went out during on the part of mission for about 20 minutes, but otherwise was fine.

5.3 Ocean Related Field Campaigns

For ocean ecosystem science objectives, an important attribute of the ACE mission design is its combination of an advanced ocean radiometer, subsurface- and vertically-resolving lidar, and advanced polarimeter. Each of these instruments provides unique, as well as complementary information on ocean properties. However, field campaigns demonstrating the utility of this instrument suite have been virtually non-existent. To address this issue, two major ocean field campaigns have recently been conducted involving aircraft, ship, and satellite measurements and including lidar, polarimeter, and ocean radiometer measurements. The two studies were referred to as the 2012 Azores Campaign and the 2014 SABOR campaign. While ACE pre-formulation funding contributed to these field efforts, additional major support was provided by NASA's Ocean Biology and Biogeochemistry Program, the CALIPSO mission, the United Kingdom's Atlantic Meridional Transect (AMT) program, and individual PI grants. The outcome of these campaigns has been highly relevant to both ACE and PACE missions. Data analysis from both campaigns is still on-going, but early results have been highly encouraging.

2012 Azores Campaign

The primary objective during the 2012 Azores campaign, was to collect simultaneous ship, aircraft, and satellite ocean optical measurements of particulate scattering coefficients. The study involved collaborators from Oregon State University, Langley Research Center (LaRC), and Plymouth Marine Lab and enjoyed some support by the CALIPSO and ACE projects for supplemental flight hours. Satellite data included lidar measurements from CALIOP and ocean color measurements from MODIS Aqua. Aircraft instruments included the NASA GISS Research Scanning Polarimeter (RSP) and the LaRC High Spectral Resolution Lidar (HSRL). Ship data focused on in-line, continuous flow-through measurements of surface layer particulate scattering and absorption coefficients.

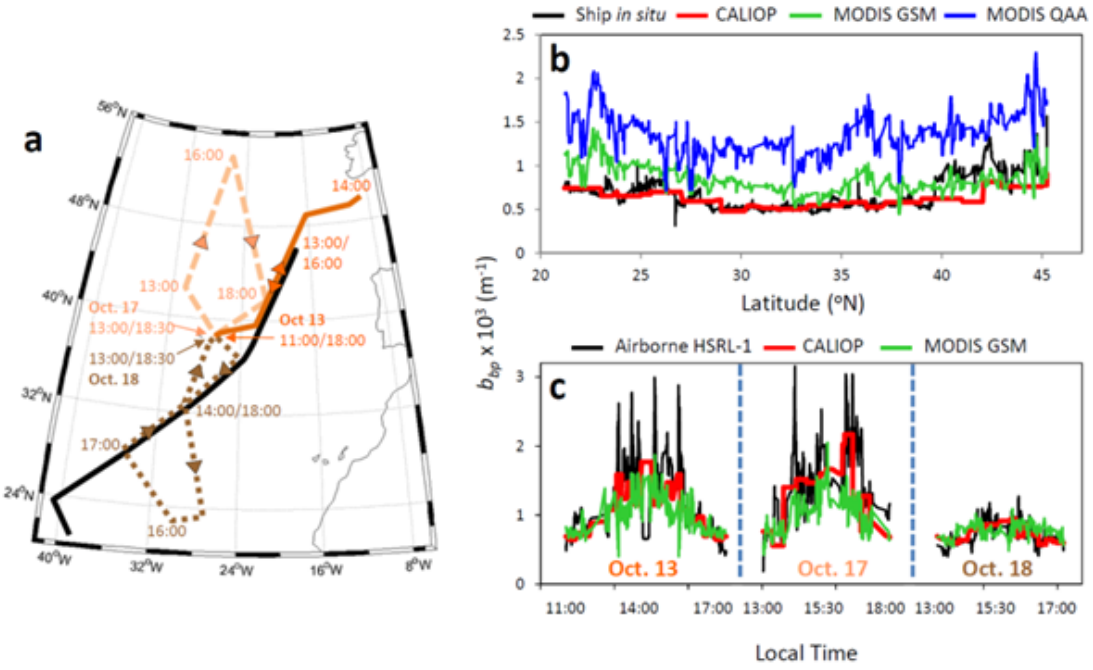

Figure 5.13 Ocean particulate backscattering coefficients (bbp) during the 2012 Azores campaign. (a) black line indicates ship track, solid orange, dashed peach, and dotted brown lines indicate aircraft tracks. (b) bbp values for (black) in situ ship data, (red) CALIOP retrievals, MODIS (green) GSM and (blue) QAA products. (c) bbp values for the airborne campaigns (see panel a). From Behrenfeld et al. (2013)

Figure 5.13 panel a shows the ship track and aircraft flight tracks during the campaign. Aircraft flights were optimized to overfly ship in situ measurements, as well as data collected by CALIOP. Figure 5.13 panel b shows match-up data for ocean particulate backscatter coefficients (b_{bp}) measured in situ (black line), by CALIOP (red line), and as retrieved from MODIS using current ocean color inversion algorithms (green line = Garver-Siegel-Maritorena (GSM) algorithm; blue line = quasi-analytical algorithm (QAA). Fig 5.3c shows match-up results for b_{bp} from the

airborne HSRL, CALIOP, and MODIS data using the GSM algorithm and corresponding to the 3 flight tracks shown in Fig 5.3a.

The 2012 Azores campaign was a highly successful study. The demonstrated correspondence between in situ, aircraft, and CALIOP lidar retrievals provided a key proof-of-concept for the ACE instrument configuration regarding ocean ecosystem retrievals. It was also the first demonstration of effective ocean scattering retrievals from CALIOP and yielded the first space lidar algorithm for assessing phytoplankton carbon and total particulate organic carbon (see Section 4 above). Initial results from the polarimeter measurements are also encouraging, although final data analysis is still on-going. Another outcome of the campaign was that it highlighted some of the technical challenges associated with subsurface particle scattering measurements with a lidar, leading to subsequent revisions in the HSRL instrument design in preparation for the subsequent 2014 SABOR campaign.

The 2012 AMT ship transect was also used to conduct daily radiometric and supporting measurements across 10,000km of the Atlantic Ocean in an ACE funded effort to assemble field matchup data for satellite FLH products. Similar data were collected during the 2014 SABOR campaign. Analysis of FLH matchup data is on-going.

2014 SABOR Campaign

The Ship-Aircraft Bio-Optical Research (SABOR) campaign, was, observationally, a greatly expanded experiment compared to the 2012 Azores study. SABOR was only recently conducted between 17 July to 7 August, 2014, so only preliminary results are currently available. SABOR measurements were focused on the strong ecological gradients persistent over the US northeast continental shelf region (Figure 5.14). The campaign brought together several PI-lead science projects focused on the biogeochemistry of plankton, radiative transfer, and in situ and remotely sensed ocean optics. The ship measurement contingency included (1) seven flow-through instruments collecting optical data from which are derived a dozen inherent optical properties of seawater, (2) eight instruments for ocean profiling optical measurements for assessing inherent optical properties through the water column, and (3) a wide diversity of discrete surface and subsurface sample collections for assessing biogeochemical properties, including particulate and phytoplankton carbon and plankton species composition. Similar to the 2012 Azores study, the airborne instrument complement during SABOR included and upgraded LaRC HSRL and the GISS RSP. Flights were conducted out of Massachusetts, Bermuda, and Virginia. Some additional flight hours for the campaign were made possible with

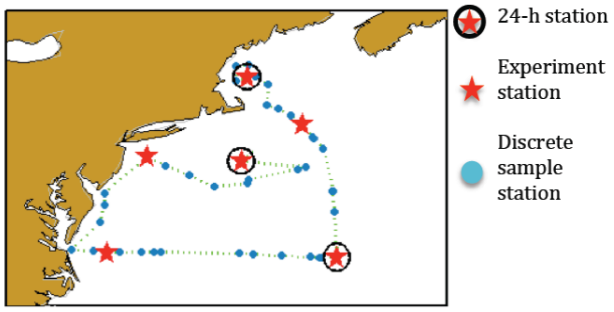

Figure 5.14 hip track and sampling stations during SABOR.

additional support from CALIPSO and ACE projects. Supporting satellite data were provided by CALIOP, MODIS Aqua, and NPP VIIRS.

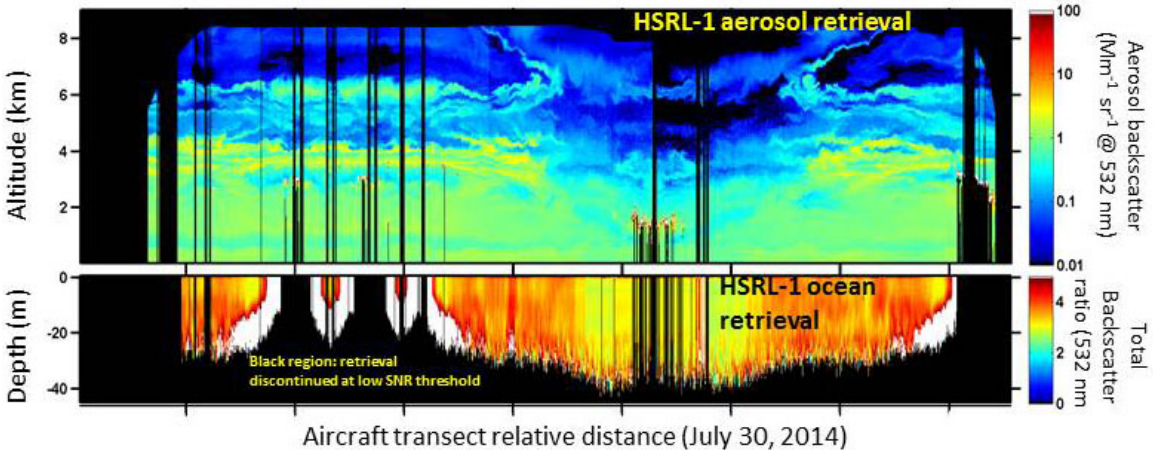

Figure 5.15 Preliminary HSRL results from the SABOR campaign. Top panel = vertical distributions of aerosol backscatter. Bottom panel = subsurface ocean total backscatter ratio. Data from a single aircraft transect conducted on July 30, 2014.

With respect to ACE ocean ecosystem science objectives (as well as atmospheric science objectives), data collected during the 2014 SABOR campaign will be highly beneficial for the development of advanced satellite retrieval algorithms. The upgraded HSRL used during SABOR will allow assessment of design improvements for the ACE lidar (Figure 5.51). In water and aircraft polarimetric measurements during SABOR is highly relevant to the ACE objective of using a space-based polarimeter to address atmospheric and ocean related science. Furthermore, the extensive ship-based optical and biogeochemical measurements collected during SABOR will provide critical insights on algorithm development for retrieving key geophysical properties from ACE remote sensing data. These measurements included the assemblage and testing of an instrument package for measuring water column Inherent Optical Properties (IOPs) (Figure 5.16), which are properties fundamental to ACE Ocean Ecosystem objectives. The package employed state-of-the-art sensor technology, including custom MASCOT and Sequoia LISST sensors which, in combination, measured the full angular volume scattering function for light scattering in water. The instruments also measured the dissolved phase and attenuation in an open path (not pumped) configuration. Preliminary analyses indicate that resultant data are if the highest quality possible.

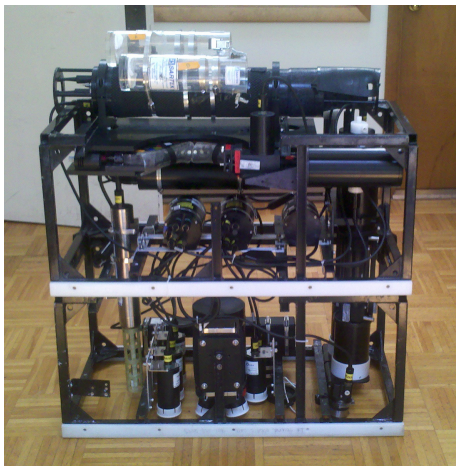

Figure 5.16: Inherent optical property instrument package deployed during SABOR.

NAAMES Campaign

The NAAMES project was funded as an Earth Venture Suborbital 2 mission, but provided extensive data relevant to the ACE mission. NAAMES observations include diverse optical, chemical, and ecological ship-based measurements, airborne remote sensing with an advanced HSRL, the RSP, a hyperspectral ocean color sensor (GCAS), and downward radiance sensor (4STAR). NAAMES encompassed four field deployments targeting specific events in the annual plankton cycle in the subarctic Atlantic. NAAMES science objectives focused on understanding drivers of the annual phytoplankton bloom and links between ocean ecosystems, aerosols, and clouds. Ship deployments were largely based out of Wood Hole, MA., while the airborne campaign deployed from Saint Johns, Newfoundland. As the final NAAMES campaign was completed only shortly before preparation of the current ACE final report, most data analyses remain on-going.

Potential locations for future field studies of marine organic aerosols

Ocean surface waters contain large concentrations of small particulates including phytoplankton, algae, bacteria, viruses, fragments of larger organisms and organic detritus. Organic matter in the oceans contributes to one of the largest active reservoirs of organic carbon on Earth. A growing body of evidence shows that this seawater-derived organic matter can be transferred in the atmosphere where it can also undergo photochemical and bacterial degradation (aging) leading to physicochemical modification of organic compounds. Important effect of seawater-derived organic matter on atmospheric solar radiation transfer and cloud processes has been well documented. Yet, due to the complex mixture of oceanic and continental precursors, very few studies have attempted to characterize aging of marine organics. Through implementation of marine organic aerosol tracers in global chemistry-transport model we are able to identify the regions with large contributions of freshly-emitted or aged aerosol, potential locations for future field studies focused on improved characterization of marine organic aerosols (see Figure 5.17). Additional details were published in Gantt et al. (2014).

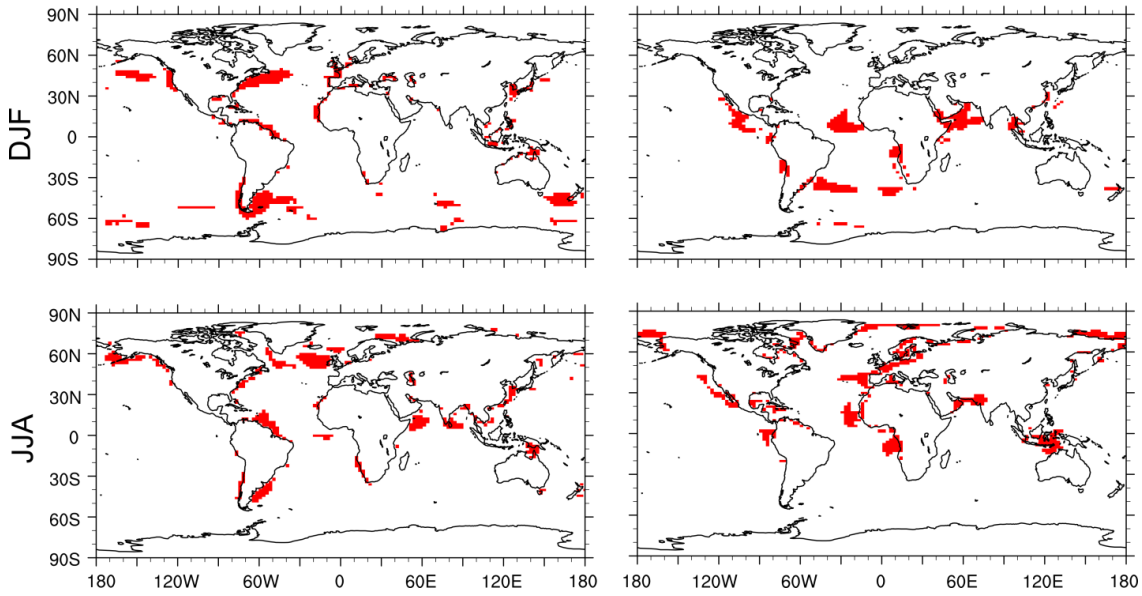

Figure 5.17 Regions (in red) with GEOS-Chem predicted seasonal submicron marine organic aerosol concentrations > 200 ng m^{-3} for low aged (left column) and highly aged (right column) regimes.

6 Funding History: FY16-FY18 Update

The ACE science funding history from FY11 to FY15 is detailed in the unredacted version of the ACE 2011-2015 Progress Report and Future Outlook of September 2016. Below we present a brief update of the ACE funding history for the period FY16-FY18.

6.1 Support for Field Campaigns

ACE successfully completed 2 additional airborne campaigns:

- Radar Definition Experiment (RADEX-15) during November-December 2015, in collaboration with the GPM Ground Validation OLYMPEX campaign.
- Aerosol Characterization from Polarimeter and Lidar (ACEPOL) during October-November 2017

6.2 ACE Funding by Institutions

Table 6.6 summarizes the ACE funding received in FY16-FY18 per NASA center, with Grants being issued by GSFC.

Redacted

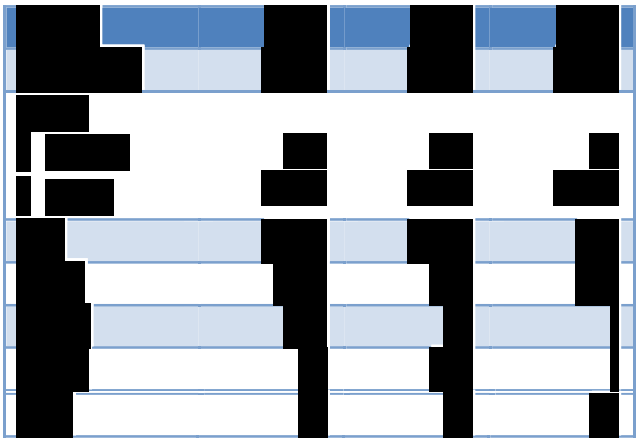

2 Redacted

6.3 ACE Grants

During the FY16-FY18 period, two new grants were awarded and three grants were renewed as shown in Table 6.2.

Table 6.2 New and renewed ACE Grants for the FY16-18 period.

Federal Award Id Grant Number	PI, Institution	Title	Summary
[redacted]	[redacted]	Redacted	[redacted]
[redacted]	[redacted]	[redacted]	[redacted]
[redacted]	[redacted]	[redacted]	[redacted]
[redacted]	[redacted]	[redacted]	[redacted]
[redacted]	[redacted]	[redacted]	[redacted]

6.4 Justification for No-cost Extension of Grants

No-costs extension were given to the following grants:

Table 6.23 Summary of ACE Grant extensions.

Federal Award Id	PI, Institution	Title	Justification
[redacted]	[redacted]	Redacted	[redacted]
[redacted]	[redacted]	[redacted]	[redacted]

7 ACE and the 2017 Decadal Survey

The science and technology advancements produced by the ACE study, together with the expertise gained by the scientists and engineers involved in the ACE study, provides to a large degree the basis for upcoming work addressing the 2017 Decadal Survey's recommendations as specified below.

The Decadal Survey for Earth science and applications from space (referred to as 'Decadal Survey') provides long term guidance for NASA Earth Science Division. Members of US Earth Science community define NASA's Earth Science priorities for the coming 10 years, recommend observations, and funds needed to address the science questions. The title of the 2017 report (PDF: http://nap.edu/24938 DOI:10.17226/24938) is "Thriving on Our Changing Planet: A Decadal Strategy for Earth Observation from Space". In order to perform ambitious science, despite constraints, it calls in a strategic framework to:

- Embrace innovative methodologies for integrated science/applications;
- Commit to sustained science and applications;
- Amplify the cross-benefit of science and applications; and
- Leverage external resources and partnerships (incl. international).

The observable approach of the Decadal Survey is as follows:

- Program of Record to be completed
- Designated Observables (Observing System)
    - Most important science / Large missions
    - Instruments are competed or contributed (incl. international)
    - Science team and calibration/validation program are competed
    - Cost cap: $300 to $800 M (full mission costs)
- Earth Explorer
    - Very important science / Medium missions
    - Cost cap: <$350 M (full mission costs)
- Incubation to mature technology
- Earth Venture Continuity (addition to Suborbital, Instrument, and Mission strand)
    - To demonstrate sustained observations at lower costs
    - Cost cap: <$150 M
    -

More information on the 2017 Decadal Survey and NASA's response to it can be found here: https://science.nasa.gov/earth-science/decadal-surveys

Observable	Science/Applications Summary	Candidate Measurement Approach	ESAS maximum cost
Aerosols	**Aerosol properties, aerosol vertical profiles, and cloud properties** to understand their effects on climate and air quality	Backscatter lidar and multichannel/multi-angle/polarization imaging radiometer flown together on the same platform	CATE Cap $800M
Clouds, Convection, And Precipitation	**Coupled cloud-precipitation state and dynamics** for monitoring global hydrological cycle and understanding contributing processes including cloud feedback	Radar(s), with multi-frequency passive microwave and sub-mm radiometer	CATE Cap $800M
Mass Change	**Large-scale Earth dynamics** measured by the changing mass distribution within and between the Earth's atmosphere, oceans, ground water, and ice sheets	Spacecraft ranging measurement of gravity anomaly	Est Cap $300M
Surface Biology and Geology	**Earth surface geology and biology,** ground/water temperature, snow reflectivity, active geologic processes, vegetation traits and algal biomass	Hyperspectral imagery in the visible and shortwave infrared, multi- or hyperspectral imagery in the thermal IR	CATE Cap $650M
Surface Deformation and Change	**Earth surface dynamics** from earthquakes and landslides to ice sheets and permafrost	Interferometric Synthetic Aperture Radar (InSAR) with ionospheric correction	Est Cap $500M

Table 8.1. Designated Observables Summary from the 2017 Decadal Survey.

7.1 Aerosols Observable

During the ACE meeting in May 2018, the ACE aerosol STM was reviewed in light of the 2017 Decadal Survey recommendation for a Designated Aerosol Mission. Many of the Decadal Survey aerosol-related science objectives were very similar to the ACE aerosol-related objectives discussed in section 2.1. The objectives associated with the Decadal Survey Climate Variability and Change panel in particular were very similar to the ACE aerosol objectives. For example, the Decadal Survey recommendation to reduce the IPCC AR5 total aerosol radiative forcing uncertainty by a factor of two is similar to the ACE DARF/DARE goals. The Decadal Survey recommendation to improve estimates of the emissions of natural and anthropogenic aerosols and their precursors is very similar to the ACE sources, processes, transport, and sinks (SPTS) goals. The Decadal Survey recommendation to quantify the effect that aerosol has on cloud formation, cloud height, and cloud properties, including semi-direct effects, is very similar to the ACE goals associated with aerosol-cloud interactions. The Decadal Survey aerosol objectives include an increased emphasis on air quality related objectives; in particular on observing PM concentration and speciation. Consequently, moving forward, the aerosol STM should expand to include the air quality related questions/objectives.

In light of these Decadal Survey recommendations, the ACE aerosol community developed the following set of recommendations:

Science Objectives and Science Traceability Matrix

- Establish a process for prioritizing Decadal Survey science objectives, corresponding measurement requirements, and instrument capabilities that

capitalize on ACE progress and advances and fit within the Decadal Survey cost cap

- Develop threshold and baseline aerosol mission, which includes prioritized aerosol science objectives
- Science question Q4 in the ACE STM should be moved to the aerosol-cloud interactions subsection (i.e. cloud response to the aerosol radiative heating should be part of aerosol-cloud interactions).
- The science associated with the Aerosols-Ocean STM should move forward as much as possible.

Observing System

- Observing System design studies should include representatives of multidisciplinary stakeholder communities, including applications, that have expertise and knowledge of satellite measurements and capabilities (e.g. air quality, oceans, etc.)
- Observing System designs should perform orbit and measurement trade studies that address lidar and polarimeter overlap and how this affects instrument design, capabilities, technical resources and costs.
- Different coverages and implementations (single platform, multiplatform) should be considered, in the context of the existing Program of Record, when addressing the science questions
- The importance of data latency and availability should be considered as they relate to the science questions and objectives
- Observing System designs need to account for science requirements, instrument capabilities, and costs
- Complementary suborbital/ground measurements to address science questions and objectives unattainable from space should be considered. These include systematic and/or targeted airborne measurements, ground networks, etc.
- Identify LEO and GEO satellites and aerosol transport models that will be operational in the future and map their capabilities and contributions to Decadal Survey objectives
- The role of models to fill in observational gaps must be considered

Algorithm Development

- Algorithm development needs to account for different combinations of lidar and polarimeter capabilities to address the science objectives

- Algorithms should examine the measurements that will be used to constrain and evaluate models

7.2 Aerosol-Ocean Ecosystems Synergisms

The ACE Aerosol-Ocean science objectives are highly synergistic to ACE Aerosol, Cloud, and Ocean Ecosystems Elements and address mutually interacting processes – *atmosphere to ocean interactions, marine biology to atmosphere interactions, aeolian fertilization of the oceans, emission of primary marine aerosol, and release to the atmosphere of highly reactive trace gases by the marine ecosystem* – all of which have key effects on the marine boundary layer cloud condensation nuclei budget and microphysical properties of maritime clouds. The detailed mechanisms for aerosol-ocean interaction processes and their radiative feedbacks in the Earth climate system are best understood through the combination of in situ data, satellite remote sensing, and models. Due to its importance for improved climate change assessments and highly interdisciplinary nature, the aerosol-ocean interaction remains an area of increasing interest to the scientific community (e.g., Carslaw et al., 2013; McCoy et al., 2015; DeMott et al., 2016; Pope et al., 2017; Dani & Loreto, 2017; Meskhidze et al., 2017; Hostetler et al., 2018). Several topics of interest are summarized below:

Clouds in remote high-latitude oceans (i.e., in the Arctic, the Southern Ocean, and the Antarctic marginal seas) play a significant role in regulating climate. Yet many existing data sources have weaknesses that restrict their usability, particularly at high latitudes.

Ocean-derived primary aerosol and precursor gases leading to aerosol production are believed to be a significant source of Cloud Condensation Nuclei (CCN) and Ice Nucleating Particles (INP) in the remote marine boundary layers and quantifying their impact will be necessary for resolving relative contributions of natural and anthropogenic aerosol radiative effects on climate

Current analyses establish correlations between ocean ecosystem state and cloud properties. However, quantitative knowledge of aerosol-ocean interaction is required for establishing process linkages and development of physically-based parameterizations for models. These process linkages must be built into coupled Earth System Models (ESMs) to predict the impact of ocean ecosystem change on clouds and radiation as the ecosystem responds to warming oceans.

This is truly interdisciplinary science topic that requires expertise in atmospheric chemistry, organic geochemistry, photochemistry, optics, chemical oceanography, dust/aerosol geochemistry, and various aspects of atmospheric, ocean, and Earth system studies

7.3 Other Cross-cutting aspects

The designated observables, as suggested by the 2017 Decadal Survey, on Aerosols and on Cloud, Convection, Precipitation (A-CCP) provide substantial opportunities

for synergies with other designated observables and many other aspects of NASA's Earth Science Division portfolio.

In particular, the Surface Biology and Geology (SBG) designated observable could strongly benefit from precise aerosol information (e.g. spectral AOD and aerosol type) to reduce uncertainties in the atmospheric correction process. In return, A-CCP may benefit from additional spectral information content for radiative transfer calculations to be used with polarimeter data. In return, data from SBG, for example, might be helpful to better constrain the chemical composition of atmospheric constituents and the spectral surface albedo. Another example of synergies to the Mass Change (MC) designated observable is given through the connection of precipitation (water and snow) with groundwater storage and ice sheet mass changes. And similarly, the Surface Deformation and Change (SDC) designated observable can be linked to A-CCP by volcanic plume characterizations (3D shape and composition) through multiangle and lidar aerosol observations. Those are just a few examples. Those and more areas of synergies will be looked at during the A-CCP study leading up to the A-CCP Mission Concept Review in early 2022.

A-CCP may also provide benefits and crucial observations for science areas not covered by the designated observable. For example, it has been shown that a spaceborne atmospheric lidar can provide useful data for ocean ecosystems research (see above). Further synergies are likely found where optimized A-CCP observations can provide data for science addressed by the explorer and incubator programs, such as snow depth and ecosystem structure.

Realization of some of the synergies will depend on the observing system implementation and operation. The designated observable studies, which started in early FY19, are encouraged to identify and address those synergies and suggest implementable approaches. Some of those approached may include airborne, small satellites, or other non-traditional components, including the current program of record. Models will likely play a fundamental role in connecting different observables with different science and application objectives.

8 Programmatic Assessment and Recommendations

In this section we present the programmatic assessment and recommendations for improvement of the process of development of Decadal Survey Satellite Missions. The 2007 Decadal Survey recommended a series of satellite missions with supporting science questions and science traceability matrixes as well as recommendations for sensor payloads and mission architectures. Some of these preliminary mission concepts, ACE included, were assigned to science working groups to develop and refine the Decadal Survey recommendations so the recommended missions could be transitioned from pre-formulation to formulation.

Little guidance was provided as to what was required of the science working groups and when it was due. Into that vacuum, a false sense of urgency pervaded the science working groups, which lead to the perception that the sooner a complete plan was submitted, the sooner that mission would transition to formulation.

This false sense of urgency lead to a number of undesirable outcomes. First, many aspects of the proposed missions were addressed in a parallel stove-piped fashion. As a result, the refinement of the science questions and development of science traceability matrixes were more separate than they should have been from development of instrument concepts and mission architecture. For example, changes in the science traceability matrixes did not propagate as quickly and completely through the rest of the ACE study as would have been optimal; the process cost more than it should have. Second, worthwhile cross mission fertilization essentially did not take place. Further, neither the augmentation of existing satellite constellations nor the development of next generation satellite constellations was seriously considered. Third, the rush to becoming formulation ready limited working with the Earth Science Technology Office (ESTO) to develop new technologies. This is not to imply ESTO did not work with the Decadal Survey mission science working groups. Quite the opposite is true. However, the interactions were mostly with those who developed sensor concepts. Thus, the cross mission, inter-sensor perspective was largely missing.

A remedy for these issues is fairly straightforward. Headquarters should provide guidance as to a task description due date for output from the science working group. Financial guidance would also be helpful. The leadership of the science working groups should be encouraged to carry out the mission studies in a more serial manner. Science questions and science traceability matrixes should be developed first. As the science traceability matrixes become fairly mature, appropriate instrument concept studies should be transitioned from a lower level preliminary state to a larger focused effort. Headquarters should establish a study group whose task is to study cross mission fertilization and augmentation of existing satellite constellations or the development of new satellite constellations. Lastly, plans for mission architecture should be developed based on the recommendations of the science working group and recommendations from the Headquarters instituted cross mission/constellation study group.

References

Ackerman, A.S., M.P. Kirkpatrick, D.E. Stevens, and O.B. Toon, 2004: The impact of humidity above stratiform clouds on indirect aerosol climate forcing. *Nature*, 432, 1014-1017, doi:10.1038/nature03174.

Adams-Selin, R. D., van den Heever, S. C., & Johnson, R. H. (2013). Sensitivity of bow-echo simulation to microphysical parameterizations. *Weather and Forecasting*, *28*(5), 1188-1209.

Adams-Selin, R. D., van den Heever, S. C., & Johnson, R. H. (2013). Impact of graupel parameterization schemes on idealized bow echo simulations. *Monthly Weather Review*, *141*(4), 1241-1262. doi:10.1175/MWR-D-12-00064.1

Alexandrov, M.D., B. Cairns, C. Emde, A.S. Ackerman, and B. van Diedenhoven (2012a). Accuracy assessments of cloud droplet size retrievals from polarized reflectance measurements by the research scanning polarimeter. *Rem. Sens. Environ*. 125, 92–111.

Alexandrov, M.D., B. Cairns, and M.I. Mishchenko, (2012b). Rainbow Fourier transform. *J. Quant. Spectrosc. Radiat. Transfer*, 113, 2521-2535, doi:10.1016/j.jqsrt.2012.03.025.

Alexandrov, M.D., Cairns, B., van Diedenhoven, B., Wasilewski, A. P., & Ackerman, A. S. (2014). Characterization of Super-Cooled Liquid Water Clouds Using the Research Scanning Polarimeter Measurements. In *AGU Fall Meeting Abstracts* (Vol. 1, p. 3044).

Alexandrov, M.D., B. Cairns, A.P. Wasilewski, A.S. Ackerman, M.J. McGill, J.E. Yorks, J.E. Hlavka, S.E. Platnick, G.T. Arnold, B. van Diedenhoven, J. Chowdhary, M. Ottaviani, and K.D. Knobelspiesse, 2015: Liquid water cloud properties during the Polarimeter Definition Experiment (PODEX). Remote Sens. Environ., 169, 20-36, doi:10.1016/j.rse.2015.07.029.

Alexandrov, M.D., B. Cairns, B. van Diedenhoven, A.S. Ackerman, A.P. Wasilewski, M.J. McGill, J.E. Yorks, D.L. Hlavka, S.E. Platnick, and G.T. Arnold, 2016: Polarized view of supercooled liquid water clouds. Remote Sens. Environ., 181, 96-110, doi:10.1016/j.rse.2016.04.002.

Alexandrov, M.D., B. Cairns, K. Sinclair, A.P. Wasilewski, L. Ziemba, E. Crosbie, R. Moore, J. Hair, A.J. Scarino, Y. Hu, S. Stamnes, M.A. Shook, and G. Chen, 2018: Retrievals of cloud droplet size from the research scanning polarimeter data: Validation using in situ measurements. Remote Sens. Environ., 210, 76-95, doi:10.1016/j.rse.2018.03.005.

Altman, D. G., Bland, J. M. , “Measurement in medicine: the analysis of method comparison studies,” The Statistician 32, 307–317 (1983).

Andreae, M. O. (2007). Aerosols Before Pollution. *Science*, 315(5808), 50–51. doi:10.1126/science.1136529

Beauchamp, R.M., Tanelli, S., Peral, E., Chandrasekar, V., "Pulse Compression Waveform and Filter Optimization for Spaceborne Cloud and Precipitation Radar," in IEEE Transactions on Geoscience and Remote Sensing. Sensing, vol. 55, no. 2, pp. 915-931. doi: 10.1109/TGRS.2016.2616898, 2017

Behrenfeld, M.J., Randerson, J., McClain, C., Feldman, G., Los, S., Tucker, C., Falkowski, P.G., Field, C., Frouin, R., Esaias, W., Kolber, D., Pollack, N. Biospheric primary production during an ENSO transition. Science 291: 2594-2597, 2001

Behrenfeld, M.J., O'Malley, R., Siegel, D.A., McClain, C, Sarmiento, J., Feldman, G., Milligan, A., Falkowski, P., Letelier, R., Boss, E. Climate-driven trends in contemporary ocean productivity. Nature 444, 752-755, 2006

Behrenfeld, M. J., & Milligan, A. J. (2013). Photophysiological expressions of iron stress in phytoplankton. Annual review of marine science, 5, 217-246.

Behrenfeld, M. J., Hu, Y., Hostetler, C. A., Dall'Olmo, G., Rodier, S. D., Hair, J. W., & Trepte, C. R. (2013). Space-based lidar measurements of global ocean carbon stocks. Geophysical Research Letters, 40(16), 4355-4360.

Behrenfeld, M.J., Hu, Y. O'Malley, R.T, Boss, E.S., Hostetler, C.A., Siegel, D.A., Sarmiento, J., Schulien, J., Hair, J.W., Lu, X., Rodier, S., Scarino, A-J. Annual boom-bust cycles of polar phytoplankton biomass revealed by space-based lidar. Nature Geoscience doi: 10.1038/NGEO2861, 2016.

Berry, E. and G. G. Mace, 2014: Cloud properties and radiative effects derived from A-Train satellite data in Southeast Asia. Journal of Geophysical Research, 119, 9492-9508.

Bony, S., & Dufresne, J. L. (2005). Marine boundary layer clouds at the heart of tropical cloud feedback uncertainties in climate models. *Geophysical Research Letters*, *32*(20).

Bony, S., Stevens, B., Frierson, D. M., Jakob, C., Kageyama, M., Pincus, R., Shepherd, T.G., Sherwood, S.C., Siebesma, A.P., Sobel, A.H., Watanabe, M., & Webb, M. J. (2015). Clouds, circulation and climate sensitivity. *Nature Geoscience*, *8*(4), 261-268.

Bland, J. M., D. Altman, D., "Statistical methods for assessing agreement between two methods of clinical measurement," The Lancet 327, 307–310 (1986).

Bréon, F. M., and Goloub, P. (1998). Cloud droplet effective radius from spaceborne polarization measurements. *Geophysical research letters*, *25*(11), 1879-1882.

Bréon, F. M., and Doutriaux-Boucher (2005). A comparison of cloud droplet radii measured from space. IEEE Transactions on Geoscience and Remote Sensing, 43(8).

Bréon, F. M., and Henriot, N. (2006). Spaceborne observations of ocean glint reflectance and modeling of wave slope distributions. *Journal of Geophysical Research: Oceans (1978–2012)*, *111*(C6).

Burton, S. P., R. A. Ferrare, C. A. Hostetler, J. W. Hair, R. R. Rogers, M. D. Obland, C. F. Butler, A. L. Cook, D. B. Harper, and K. D. Froyd. "Aerosol classification using airborne High Spectral Resolution Lidar measurements–methodology and examples." *Atmospheric Measurement Techniques* 5, no. 1 (2012): 73-98.

Burton, S. P., Ferrare, R. A., Vaughan, M. A., Omar, A. H., Rogers, R. R., Hostetler, C. A., and Hair, J. W.: Aerosol classification from airborne HSRL and comparisons with the CALIPSO vertical feature mask, Atmos. Meas. Tech., 6, 1397-1412, doi:10.5194/amt-6-1397-2013, 2013.

Burton, S.P., Vaughan, M.A., Ferrare, R.A. and Hostetler, C.A., 2014. Separating mixtures of aerosol types in airborne High Spectral Resolution Lidar data. *Atmospheric Measurement Techniques*, *7*(2), p.419.

Burton, S.P., Chemyakin, E., Liu, X., Knobelspiesse, K., Stamnes, S., Sawamura, P., Moore, R.H., Hostetler, C.A. and Ferrare, R.A., 2016. Information content and sensitivity of the 3β+ 2α lidar measurement system for aerosol microphysical retrievals. *Atmospheric Measurement Techniques*, *9*(11), pp.5555-5574.

Burton, S.P., C.A. Hostetler, A.L. Cook, J.W. Hair, S.T. Seaman, S. Scola, D.B. Harper, J.A. Smith, M.A. Fenn, R.A. Ferrare, P.E. Saide, E.V. Chemyakin, and D. Müller (2018), "Calibration of a high spectral resolution lidar using a Michelson interferometer, with data examples from ORACLES", *Applied optics, 57(21), pp.6061-6075.*

Cairns, B., E.E. Russell, and L.D. Travis. The Research Scanning Polarimeter: Calibration and ground-based measurements. Proc. SPIE, vol. 3754, 186, 1999.

Cairns, B., F. Waquet, K. Knobelspiesse, J. Chowdhary, and J.-L. Deuzé, 2009a: Polarimetric remote sensing of aerosols over land surfaces. In *Satellite Aerosol Remote Sensing over Land*. A.A. Kokhanovsky, and G. De Leeuw, Eds., Springer-Praxis Books in Environmental Sciences. Springer, 295-325, doi:10.1007/978-3-540-69397-0_10.

Cairns, B., A. Lacis, B. Carlson, K. Knobelspiesse and M. Alexandrov, 2009b: Inversion of Multi-angle Radiation Measurements. pp. 118-127, *Proceedings of the International Conference on Mathematics, Computational Methods & Reactor Physics 2009* (M&C 2009), Saratoga Springs, New York.

Cairns, B., K. D. Knobelspiesse and M. Alexandrov, 2010: Passive determination of cloud physical thickness and droplet number concentration, *Proceedings of 13th Conference on Atmospheric Radiation of the American Meteorological Society*, Portland Oregon.

Carslaw, K. S., Lee, L. A., Reddington, C. L., Pringle, K. J., Rap, A., Forster, P. M., et al. (2013). Large contribution of natural aerosols to uncertainty in indirect forcing. *Nature*, 503(7474), 67–71. doi:10.1038/nature12674

Cetinic, I., McClain, C.R., and Werdell, P.J. 2018. ACE ocean working group recommendations and instrument requirements for an advanced ocean

ecology mission. PACE Technical Report Series Volume 1. NASA/TM-2018-219027.

Chase, A. P., E. Boss, I. Cetinic and W. Slade, 2017. Estimation of Phytoplankton Accessory Pigments from Hyperspectral Reflectance Spectra: Toward a Global Algorithm. Journal of Geophysical Research: Oceans, 122. doi:10.1002/2017JC012859, 2017

Chase, R. J., Finlon, J. A., Borque, P., McFarquhar, G. M., Nesbitt, S. W., Tanelli, S., et al.: Evaluation of triple-frequency radar retrieval of snowfall properties using coincident airborne in situ observations during OLYMPEX. Geophysical Research Letters, 45, 5752–5760. doi:10.1029/2018GL077997, 2018

Chowdhary, J., B. Cairns, M.I. Mishchenko, P.V. Hobbs, G.F. Cota, J. Redemann, K. Rutledge, B.N. Holben, and E. Russell: Retrieval of aerosol scattering and absorption properties from photopolarimetric observations over the ocean during the CLAMS experiment. *J. Atmos. Sci.*, **62**, 1093-1117, doi:10.1175/JAS3389.1.

Chowdhary, J., B. Cairns, F. Waquet, K. Knobelspiesse, M. Ottaviani, J. Redemann, L. Travis, and M. Mishchenko, 2012: Sensitivity of multiangle, multispectral polarimetric remote sensing over open oceans to water-leaving radiance: Analyses of RSP data acquired during the MILAGRO campaign. Remote Sens. Environ., 118, 284-308, doi:10.1016/j.rse.2011.11.003.

Cox, C., & Munk, W. (1954). Measurement of the roughness of the sea surface from photographs of the sun's glitter. *JOSA*, *44*(11), 838-850.

Davis, A., A. Marshak, R. Cahalan, and W. Wiscombe, "The Landsat scale break in stratocumulus as a three-dimensional radiative transfer effect: Implications for cloud remote sensing." *J. Atmos. Sci.* 54, 241, 1997.

Dani, K. G. S., & Loreto, F. (2017). Trade-Off Between Dimethyl Sulfide and Isoprene Emissions from Marine Phytoplankton. *Trends in Plant Science*, *22*(5), 361–372. doi:10.1016/j.tplants.2017.01.006

Dawson, K. W., Meskhidze, N., Josset, D., & Gassó, S. (2015). Spaceborne observations of the lidar ratio of marine aerosols. *Atmospheric Chemistry and Physics*, *15*(6), 3241–3255. doi:10.5194/acp-15-3241-2015

Dawson, K.W., Meskhidze, N., Burton, S.P., Johnson, M.S., Kacenelenbogen, M.S., Hostetler, C.A. and Hu, Y., 2017. Creating Aerosol Types from CHemistry (CATCH): A new algorithm to extend the link between remote sensing and models. *Journal of Geophysical Research: Atmospheres*, *122*(22).

DeMott, P. J., Hill, T. C. J., McCluskey, C. S., Prather, K. A., Collins, D. B., Sullivan, R. C., et al. (2016). Sea spray aerosol as a unique source of ice nucleating particles. *Proceedings of the National Academy of Sciences*, *113*(21), 5797–5803. doi:10.1073/pnas.1514034112

Desmons, M., Ferlay, N., Parol, F., Mcharek, L., and Vanbauce, C.: Improved information about the vertical location and extent of monolayer clouds from

POLDER3 measurements in the oxygen A-band, *Atmos. Meas. Tech*., 6, 2221-2238, doi:10.5194/amt-6-2221-2013, 2013.

Di Noia, A., O.P. Hasekamp, L. Wu, B. van Diedenhoven, B. Cairns, and J.E. Yorks, 2017: Combined neural network/Phillips-Tikhonov approach to aerosol retrievals over land from the NASA Research Scanning Polarimeter. Atmos. Meas. Tech., 10, 4235-4252, doi:10.5194/amt-10-4235-2017.

Diedenhoven, B.V., Cairns, B., Fridlind, A.M., Ackerman, A.S. and Garrett, T.J., 2013. Remote sensing of ice crystal asymmetry parameter using multi-directional polarization measurements–Part 2: Application to the Research Scanning Polarimeter. *Atmospheric Chemistry and Physics*, *13*(6), pp.3185-3203.

Diner, D.J., J.V. Martonchik, R.A. Kahn, B. Pinty, N. Gobron, D.L. Nelson, and B.N. Holben, "Using angular and spectral shape similarity constraints to improve MISR aerosol and surface retrievals over land." *Rem. Sens. Environ*. 94, 155, 2005.

Diner, D. J., Davis, A., Hancock, B., Gutt, G., Chipman, R. A., and Cairns, B.: Dual photoelastic modulator-based polarimetric imaging concept for aerosol remote sensing, *Appl. Optics*, 46, 8428–8445, 2007.

Diner, D. J., Davis, A., Hancock, B., Geier, S., Rheingans, B., Jovanovic, V., Bull, M., Rider, D. M., Chipman, R. A., Mahler,A., and McClain, S. C.: First results from a dual photoelastic modulator-based polarimetric camera, *Appl. Optics*, 49, 2929–2946, 2010.

Diner, D. J., Xu, F., Martonchik, J. V., Rheingans, B. E., Geier, S., Jovanovic, V. M., Davis, A., Chipman, R. A., and McClain, S. C.: Exploration of a polarized surface bidirectional reflectance model using the Ground-based Multiangle SpectroPolarimetric Imager, *Atmosphere*, 3, 591–619, 2012.

Diner et al. 2013a -Diner, D. J., Xu, F., Garay, M. J., Martonchik, J. V., Rheingans, B. E., Geier, S., Davis, A., Hancock, B. R., Jovanovic, V. M., Bull, M. A., Capraro, K., Chipman, R. A., and McClain, S. C.: The Airborne Multiangle SpectroPolarimetric Imager (AirMSPI): a new tool for aerosol and cloud remote sensing, Atmos. Meas. Tech., 6, 2007-2025, doi:10.5194/amt-6-2007-2013, 2013.

Diner et al. 2013b - Diner, D. J., Garay, M. J., Kalashnikova, O. V., Rheingans, B. E., Geier, S., Bull, M. A., ... & Chipman, R. A. (2013, September). Airborne multiangle spectropolarimetric imager (AirMSPI) observations over California during NASA's polarimeter definition experiment (PODEX). In *SPIE Optical Engineering+ Applications* (pp. 88730B-88730B). International Society for Optics and Photonics.

Diner, D., M. Garay, C. Bruegge, F. Seidel, M. Bull, V. Jovanovic, I. Tkatcheva, B. Rheingans, G. van Harten, 2017. AirMSPI Data Quality Statement: PODEX campaign. Technical Report of the Jet Propulsion Laboratory, California Institute of Technology JPL D-97927. Available:

https://eosweb.larc.nasa.gov/project/airmspi/quality_summaries/AirMSPI-Data_Quality_PODEX_V005.pdf

Dolgos, G., & Martins, J. V. (2014). Polarized Imaging Nephelometer for in situ airborne measurements of aerosol light scattering. *Optics express*, *22*(18), 21972-21990.

Dubovik, O., Sinyuk, A., Lapyonok, T., Holben, B. N., Mishchenko, M., Yang, P., ... & Slutsker, I. (2006). Application of spheroid models to account for aerosol particle nonsphericity in remote sensing of desert dust. *Journal of Geophysical Research: Atmospheres (1984–2012)*, *111*(D11).

Dubovik, O., Herman, M., Holdak, A., Lapyonok, T., Tanré, D., Deuzé, J. L., ... & Lopatin, A. (2011). Statistically optimized inversion algorithm for enhanced retrieval of aerosol properties from spectral multi-angle polarimetric satellite observations. *Meas. Tech*, *4*(20), 975-1018.

Dubovik, O., Lapyonok, T., Litvinov, P., Herman, M., Fuertes, D., Ducos, F., et al. (2014). GRASP: a versatile algorithm for characterizing the atmosphere. *SPIE Newsroom*, 1–4. http://doi.org/10.1117/2.1201408.005558

Dubovik, O., Z. Li, M.I. Mishchenko, D. Tanré, Y. Karol, B. Bojkov, B. Cairns, D.J. Diner, W.R. Espinosa, P. Goloub, X. Gu, O. Hasekamp, J. Hong, W. Hou, K.D. Knobelspiesse, J. Landgraf, L. Li, P. Litvinov, Y. Liu, A. Lopatin, T. Marbach, H. Maring, V. Martins, Y. Meijer, G. Milinevsky, S. Mukai, F. Parol, Y. Qiao, L. Remer, J. Rietjens, I. Sano, P. Stammes, S. Stamnes, X. Sun, P. Tabary, L.D. Travis, F. Waquet, F. Xu, C. Yan, and D. Yin, 2019: Polarimetric remote sensing of atmospheric aerosols: instruments, methodologies, results, and perspectives. J. Quant. Spectrosc. Radiat. Transfer, 224, 474-511, doi:10.1016/j.jqsrt.2018.11.024.

Duce, R. A. (1986). The impact of atmospheric nitrogen, phosphorus, and iron species on marine biological productivity. In *The role of air-sea exchange in geochemical cycling* Buat-Ménard, P. (Ed.) (pp. 497-529). Springer Netherlands.

Emmanouil, P. et al. (2017), EARLINET Validation of CATS L2 Products, International Laser-Radar Conference (ILRC), Bucharest, Romania, 25-30 June 2017.

Espinosa, W. R., Remer, L. A., Dubovik, O., Ziemba, L., Beyersdorf, A., Orozco, D., Schuster, G., Lapyonok, T., Fuertes, D., and Martins, J. V.: Retrievals of aerosol optical and microphysical properties from Imaging Polar Nephelometer scattering measurements, Atmos. Meas. Tech., 10, 811-824, doi:10.5194/amt-10-811-2017, 2017.

Jethva, H., Torres, O., Remer, L.A. and Bhartia, P.K., 2013. A color ratio method for simultaneous retrieval of aerosol and cloud optical thickness of above-cloud absorbing aerosols from passive sensors: Application to MODIS measurements. IEEE Transactions on Geoscience and Remote Sensing, 51(7), pp.3862-3870.

Jethva, H., Torres, O., Waquet, F., Chand, D. and Hu, Y., 2014. How do A‐train sensors intercompare in the retrieval of above‐cloud aerosol optical depth? A case study‐based assessment. Geophysical Research Letters, 41(1), pp.186-192.

Ferlay, N., F. Thieuleux, C. Cornet, A. B. Davis, P. Dubuisson, F. Ducos, F. Parol, J. Riédi, and C. Vanbauce, 2010: Toward New Inferences about Cloud Structures from Multidirectional Measurements in the Oxygen A Band: Middle-of-Cloud Pressure and Cloud Geometrical Thickness from POLDER-3/PARASOL. *J. Appl. Meteor. Climatol.*, 49, 2492–2507. doi:10.1175/2010JAMC2550.1

Fernandez-Borda, R., E. Waluschka, S. Pellicori, J.V. Martins, L.Ramos-Izquierda, J.D. Cieslak, P. Thompson, 2009: Evaluation of the polarization properties of a Philips-type prism for the construction of imaging polarimeters. SPIE Polarization Science and Remote Sensing IV, Joseph A. Shaw; J. Scott Tyo, Editors, 746113, doi: 10.1117/12.829080

Ferrare, R. A., Burton, S. P., Scarino, A. J., Hostetler, C. A., Hair, J. W., Rogers, R. R., ... & Sawamura, P. (2013, December). Measurements of aerosol distributions and properties from Airborne High Spectral Resolution Lidar and DRAGON during the DISCOVER-AQ California Experiment. In *AGU Fall Meeting Abstracts* (Vol. 1, p. 02).

Field, C.B., Behrenfeld, M.J., Randerson, J.T., Falkowski, P.G. Primary production of the biosphere: Integrating terrestrial and oceanic components. Science 281: 237-240, 1998

Forster, P. M., Andrews, T., Good, P., Gregory, J. M., Jackson, L. S., & Zelinka, M. (2013). Evaluating adjusted forcing and model spread for historical and future scenarios in the CMIP5 generation of climate models. *Journal of Geophysical Research: Atmospheres*, *118*(3), 1139-1150.

Frouin, R., & Pelletier, B. (2014). Bayesian Methodology for Inverting Satellite Ocean-Color Data. Rem. Sens. Environ., in revision.

Gantt, B., M. S. Johnson, M. Crippa, A. S. H. Prévôt, and N. Meskhidze (2014), Implementing marine organic aerosols into the GEOS-Chem model, *Geosci. Model Dev. Discuss.*, 7, 5965-5992, doi:10.5194/gmdd-7-5965-2014

Ghan, S. J., Smith, S. J., Wang, M., Zhang, K., Pringle, K., Carslaw, K., et al. (2013). A simple model of global aerosol indirect effects. *Journal of Geophysical Research: Atmospheres*, *118*(12), 6688–6707. doi:10.1002/jgrd.50567

Goloub, P., M. Herman, H. Chepfer, J. Riedi, G. Brogniez, P. Couvert, and G. Se´ ze, 2000: Cloud thermodynamical phase classification from the POLDER spaceborne instrument. J. Geophys. Res., 105 (D11), 14 747–14 759.

Gordon, H. R., & Wang, M. (1994). Retrieval of water-leaving radiance and aerosol optical thickness over the oceans with SeaWiFS: a preliminary algorithm. *Applied optics*, *33*(3), 443-452.

Groß, S., Freudenthaler, V., Wirth, M. and Weinzierl, B., 2015. Towards an aerosol classification scheme for future EarthCARE lidar observations and implications for research needs. *Atmospheric Science Letters*, *16*(1), pp.77-82

Grosvenor, D.P., O. Souderval, P. Zuidema, A.S. Ackerman, M.D. Alexandrov, R. Bennartz, R. Boers, B. Cairns, J.C. Chiu, M. Christensen, H. Deneke, M. Diamond, G. Feingold, A. Fridlind, A. Hünerbein, C. Knist, P. Kollias, A. Marshak, D. McCoy, D. Merk, D. Painemal, J. Rausch, D. Rosenfeld, H. Russchenberg, P. Seifert, K. Sinclair, P. Stier, B. van Diedenhoven, M. Wendisch, F. Werner, R. Wood, Z. Zhang, and J. Quaas, 2018: Remote sensing of cloud droplet number concentration: Review of current and perspectives for new approaches. Rev. Geophys., 56, no. 2, 409-453, doi:10.1029/2017RG000593.

Hair, J. W., Hostetler, C. A., Cook, A. L., Harper, D. B., Ferrare, R. A., Mack, T. L., ... & Hovis, F. E. (2008). Airborne high spectral resolution lidar for profiling aerosol optical properties. *Applied Optics*, *47*(36), 6734-6752.

Hair, J., Hostetler, C., Hu, Y., Behrenfeld, M., Butler, C., Harper, D., Hare, R., Berkoff, T., Cook, A., Collins, J. and Stockley, N., 2016. Combined atmospheric and ocean profiling from an airborne high spectral resolution lidar. In *EPJ Web of Conferences* (Vol. 119, p. 22001). EDP Sciences.

Hansen, J.E., and L.D. Travis. Light scattering in planetary atmospheres, Space Sci. Rev., 16, 527-610, 1974.

Hasekamp, O. P., Litvinov, P., & Butz, A. (2011). Aerosol properties over the ocean from PARASOL multiangle photopolarimetric measurements. *Journal of Geophysical Research: Atmospheres (1984–2012)*, *116*(D14).

Heath, N. K., H. E. Fuelberg, S. Tanelli,F. J. Turk, R. P. Lawson, S. Woods, and S. Freeman: WRF nested large-eddy simulations of deep convection during SEAC^{4}RS, J. Geophys. Res. Atmos., 122, 3953–3974, doi:10.1002/2016JD025465, 2017

Heymsfield, A., Bansemer, A., Wood, N.B., Liu, G., Tanelli, S., Sy, O.O., Poellot, M., Liu, C. (2017): Toward Improving Ice Water Content and Snow Rate Retrievals from Radars Part II: Results From Three Wavelength Radar /Collocated In Situ Measurements and CloudSat/GPM/TRMM Radar Data. *J. Appl. Meteor. Climatol., early online release,* doi:10.1175/JAMC-D-17-0164.1

Hooker, S. B., Bernhard, G., Morrow, J. H., Booth, C. R., Comer, T., Lind, R. N., and Quang, V.: Optical Sensors for Planetary Radiant Energy (OSPREy): Calibration and Validation of Current and Next-Generation NASA Missions, NASA Tech. Memo. 2012–215872, NASA Goddard Space Flight Center, 117 pp., Greenbelt, Maryland, 2012.

Hooker, S.B., J.H. Morrow, and A. Matsuoka, 2013. Apparent optical properties of the Canadian Beaufort Sea, part II: The 1% and 1cm perspective in deriving and validating AOP data products. Biogeosciences, 10, 4,511–4,527

Hooker, S.B., 2014: Mobilization Protocols for Hybrid Sensors for Environmental AOP Sampling (HySEAS) Observations. NASA Tech. Pub. 2014-217518, NASA Goddard Space Flight Center, Greenbelt, Maryland, 105pp.

Hoose, C., Kristjánsson, J. E., Iversen, T., Kirkevåg, A., Seland, ø., & Gettelman, A. (2009). Constraining cloud droplet number concentration in GCMs suppresses the aerosol indirect effect. *Geophysical Research Letters*, *36*(12). doi:10.1029/2009GL038568

Hostetler, C. A., Burton, S. P., Ferrare, R. A., Rogers, R. R., Mueller, D., Chemyakin, E., ... & Anderson, B. E. (2013, December). Multi-wavelength airborne High Spectral Resolution Lidar observations of aerosol above clouds in California during DISCOVER-AQ. In *AGU Fall Meeting Abstracts* (Vol. 1, p. 0009).

Hostetler, C. A., Hair, J. W., Hu, Y., Behrenfeld, M. J., Cetinic, I., Butler, C. F., ... & Woodell, G. A. (2014, December). Airborne lidar for ocean-atmosphere studies and assessment of future satellite mission concepts. In *AGU Fall Meeting Abstracts* (Vol. 1, p. 06).

Hostetler, C. A., Behrenfeld, M. J., Hu, Y., Hair, J. W., & Schulien, J. A. (2018). Spaceborne Lidar in the Study of Marine Systems. *Annual Review of Marine Science*, *10*(1), 121–147.

Houze, R.A., L.A. McMurdie, W.A. Petersen, M.R. Schwaller, W. Baccus, J.D. Lundquist, C.F. Mass, B. Nijssen, S.A. Rutledge, D.R. Hudak, S. Tanelli, G.G. Mace, M.R. Poellot, D.P. Lettenmaier, J.P. Zagrodnik, A.K. Rowe, J.C. DeHart, L.E. Madaus, H.C. Barnes, and V. Chandrasekar: The Olympic Mountains Experiment (OLYMPEX). Bull. Amer. Meteor. Soc., 98, 2167–2188, doi:10.1175/BAMS-D-16-0182.1, 2017

Hughes, E. J., J. E. Yorks, N. A. Krotkov, A. M. da Silva, *and* M. McGill *(*2016*),* Using CATS Near-Realtime Lidar Observations to Monitor and Constrain Volcanic Sulfur Dioxide (SO_2) Forecasts, Geophys. Res. Lett., 43, *doi:*10.1002/2016GL070119*.*

Igel, A. L., van den Heever, S. C., Naud, C. M., Saleeby, S. M., & Posselt, D. J. (2013). Sensitivity of warm-frontal processes to cloud-nucleating aerosol concentrations. *Journal of the Atmospheric Sciences*, *70*(6), 1768-1783.

IPCC. (2013). *Climate Change 2013: The Physical Science Basis: Summary for Policymakers*. Cambridge, UK.

Jacob, D. J., Crawford, J. H., Maring, H., Clarke, A. D., Dibb, J. E., Emmons, L. K., Ferrare, R. A., Hostetler, C. A., Russell, P. B., Singh, H. B., Thompson, A. M., Shaw, G. E., McCauley, E., Pederson, J. R., and Fisher, J. A.: The Arctic Research of the Composition of the Troposphere from Aircraft and Satellites (ARCTAS) mission: design, execution, and first results, Atmos. Chem. Phys., 10, 5191-5212, doi:10.5194/acp-10-5191-2010, 2010.

Jickells, T. D., An, Z. S., Andersen, K. K., Baker, A. R., Bergametti, G., Brooks, N., Cao, J.J., Boyd, P.W., Duce, R.A., Hunter, K.A., Kawahata, H., Kubilay, N., laRoche, J., Liss,

P.S., Mahowalk, N., Prospero, J.M., Ridgwell, A.J., Tegen, I., & Torres, R. (2005). Global iron connections between desert dust, ocean biogeochemistry, and climate. *Science*, *308*(5718), 67-71.

Jovanovic, V. M., Smyth, M. M., Zong, J., Ando, R., & Bothwell, G. W. (1998). MISR photogrammetric data reduction for geophysical retrievals. *Geoscience and Remote Sensing, IEEE Transactions on*, *36*(4), 1290-1301.

Jovanovic, V. M., Bull, M., Smyth, M. M., & Zong, J. (2002). MISR in-flight camera geometric model calibration and georectification performance. *Geoscience and Remote Sensing, IEEE Transactions on*, *40*(7), 1512-1519.

Jovanovic, V. M., M. Bull, D. J. Diner, S. Geier, and B. Rheingans, Automated data production for a novel Airborne Multiangle SpectroPolarimetric Imager (AirMSPI), Int. Arch. Photogramm. Remote Sens. Spatial Inf. Sci., XXXIX-B1, 33-38, 2012.

Kahn, R.A., T. Berkoff, C. Brock, G. Chen, R. Ferrare, S. Ghan, T. Hansico, D. Hegg, J.V. Martins, C.S. McNaughton, D.M. Murphy, J.A. Ogren, J.E. Penner, P. Pilewskie, J. Seinfeld, and D. Worsnop, (2017). *SAM-CAAM*: A Concept for Acquiring Systematic Aircraft Measurements to Characterize Aerosol Air Masses. *Bull. Am. Meteoro. Soc.* 2215-2228, doi: 10.1175/BAMS-D-16-0003.1**.**

Kalashnikova, O. V., M. J. Garay, K. H. Bates, C. M. Kenseth, W. Kong, C. D. Cappa, A. I. Lyapustin, H. H. Jonsson, F. C. Seidel, F. Xu, D. J. Diner, and J. H. Seinfeld, Photopolarimetric sensitivity to black carbon content of wildfire smoke: Results from the 2016 ImPACT-PM field campaign, J. Geophys. Res. Atmos. 123, 5376-5396, 2018

Kaufman, Y. J., Tanré, D., & Boucher, O. (2002). A satellite view of aerosols in the climate system. *Nature*, *419*(6903), 215-223.

Klein, S.A.,Y. Zhang,M.D. Zelinka,R. Pincus, J. Boyle, and P. J.Gleckler, 2013: Are climate model simulations of clouds improving? An evaluation using the ISCCP simulator, J. Geophys. Res. Atmos., 118, 1329–1342, doi:10.1002/jgrd.50141.

Kiehl, J. T. (2007). Twentieth century climate model response and climate sensitivity. *Geophysical Research Letters*, *34*(22).

Kiliyanpilakkil, V. P., & Meskhidze, N. (2011). Deriving the effect of wind speed on clean marine aerosol optical properties using the A-Train satellites. *Atmospheric Chemistry and Physics*, *11*(22), 11401–11413. doi:10.5194/acp-11-11401-2011

Knobelspiesse, K., Cairns, B., Redemann, J., Bergstrom, R. W., & Stohl, A. (2011a). Simultaneous retrieval of aerosol and cloud properties during the MILAGRO field campaign. *Atmospheric Chemistry and Physics*, *11*(13), 6245-6263.

Knobelspiesse, K., Cairns, B., Ottaviani, M., Ferrare, R., Hair, J., Hostetler, C., Obland, M., Rogers, R., Redemann, J., Shinozuka, Y., Clarke, A., Freitag, S., Howell, S., Kapustin, V., and McNaughton, C.: Combined retrievals of boreal forest fire

aerosol properties with a polarimeter and lidar, Atmos. Chem. Phys., 11, 7045-7067, doi:10.5194/acp-11-7045-2011, 2011.

Knobelspiesse, K., Diedenhoven, B. V., Marshak, A., Dunagan, S., Holben, B., & Slutsker, I. (2014). Cloud thermodynamic phase detection with polarimetrically sensitive passive sky radiometers. *Atmospheric Measurement Techniques Discussions*, *7*(12), 11991-12036.

Knobelspiesse, K., Cairns, B., Jethva, H., Kacenelenbogen, M., Segal-Rosenheimer, M. and Torres, O., 2015. Remote sensing of above cloud aerosols. In Light Scattering Reviews 9 (pp. 167-210). Springer, Berlin, Heidelberg.

Knobelspiesse, K. Q. Tan, C. Bruegge, B. Cairns, J. Chowdhary, B. van Diedenhoven, D. Diner, R. Ferrare, G. van Harten, V. Jovanovic, M. Ottaviani, J. Redemann, F. Seidel, and K. Sinclair, "Intercomparison of airborne multi-angle polarimeter observations from the Polarimeter Definition Experiment," Appl. Opt. 58, 650-669 (2019) doi:10.1364/AO.58.000650

Knutti, R., D. Masson, and A. Gettelman, 2013: Climate model genealogy: generation CMIP5 and how we got there. Geophys. Res. Lett*.,* 40, 1194-1199, doi:10.1002/grl.50256.

Koren, I., G. Dagan, and O. Altaratz, 2014: From aerosol-limited to invigoration of warm convective clouds. Science, 344, 1145-1149, doi: 10.1126/science1252595.

Kudela, R.M., Palacios, S.L., Austerberry, D.C., Accorsi, E.K., Guild, L.S. and Torres-Perez, J., 2015. Application of hyperspectral remote sensing to cyanobacterial blooms in inland waters. Remote Sensing of Environment, 167, pp.196-205.

Krüger, O. and H. Graßl (2011), Southern Ocean phytoplankton increases cloud albedo and reduces precipitation, *Geophys. Res. Lett.,* 38, L08809, doi:10.1029/2011GL047116.

Larson, V. E., Schanen, D. P., Wang, M., Ovchinnikov, M., & Ghan, S. (2012). PDF parameterization of boundary layer clouds in models with horizontal grid spacings from 2 to 16 km. *Monthly Weather Review*, *140*(1), 285-306.

Lee, C.M., Cable, M.L., Hook, S.J., Green, R.O., Ustin, S.L., Mandl, D.J. and Middleton, E.M., 2015. An introduction to the NASA Hyperspectral InfraRed Imager (HyspIRI) mission and preparatory activities. Remote Sensing of Environment, 167, pp.6-19.

Lee, Z. P., Y. Huot (2014), On the non-closure of particle backscattering coefficient in oligotrophic oceans, Opt. Exp., 22, 29223-29233.

Lee, Z.P., Shang, S., Hu, C., Lewis, M., Arnone, R., Li, Y., & Lubac, B. (2010). Time series of bio-optical properties in a subtropical gyre: Implications for the evaluation of interannual trends of biogeochemical properties. Journal of Geophysical Research Oceans, 115, C09012.

Lee, Z., Hu, C., Shang, S., Du, K., Lewis, M., Arnone, R., & Brewin, R. (2013). Penetration of UV-visible solar radiation in the global oceans: Insights from ocean color remote sensing. Journal of Geophysical Research Oceans, 118, 4241-4255, doi:10.1002/jgrc.20308

Liang, L., & Di Girolamo, L. (2013). A global analysis on the view-angle dependence of plane-parallel oceanic liquid water cloud optical thickness using data synergy from MISR and MODIS. *Journal of Geophysical Research: Atmospheres*, *118*(5), 2389-2403. doi: 10.1029/2012JD018201.

Litvinov, P., Hasekamp, O., Dubovik, O., & Cairns, B. (2012). Model for land surface reflectance treatment: Physical derivation, application for bare soil and evaluation on airborne and satellite measurements. *Journal of Quantitative Spectroscopy and Radiative Transfer*, *113*(16), 2023-2039.

Liu, D., C. Hostetler, I. Miller, A. Cook, and J. Hair, (2012). "System analysis of a tilted field-widened Michelson interferometer for high spectral resolution lidar," Opt. Express 20, 1406-1420.

Liu, X., Stamnes, S., Ferrare, R.A., Hostetler, C.A., Burton, A.S., Chemyakin, E., Sawamura, P. and Mueller, D., 2017, December. A Combined Retrieval of Aerosol Microphysical Properties using active HSRL and Passive Polarimeter Multi-sensor Data. In *AGU Fall Meeting Abstracts*.

Mace, G. G., Zhang, Q., Vaughan, M., Marchand, R., Stephens, G., Trepte, C., & Winker, D. (2009). A description of hydrometeor layer occurrence statistics derived from the first year of merged Cloudsat and CALIPSO data. *Journal of Geophysical Research: Atmospheres (1984–2012)*, *114*(D8).

Mace, G. G. and Zhang, 2014: The Cloudsat Radar-Lidar Geometrical Profile Algorithm (RL-GeoProf): Updates, Improvements, and Selected Results. Journal of Geophysical Research, DOI: 10.1002/2013JD021374.

Mace, G. G., S. Avey, S. Cooper, M. Lebsock, S. Tanelli, and G. Dobrowalski, 2015: Retrieving co-occurring cloud and precipitation properties of warm marine boundary layer clouds with A-Train data. Provisionally accepted to Journal of Geophysical Research.

Mace, G., M. Behrenfeld, C. Hostetler, D. Winker, Arlindo da Silva, Gail Skofronick-Jaskson, C. Trepte, R. Ferrare, D. Vane, S. Tanelli, E. Im, M. Lebsock, L'Ecuyer, and G. Heymsfield, 2016: A Next Generation Earth Science Satellite Constellation Opportunity to Advance Aerosol, Cloud, Precipitation and Ocean Ecosystem Science. White paper submitted to the Second RFI by the 2017 Decadal Survey Panel. Available on-line from: https://acemission.gsfc.nasa.gov/whitepapers.html

Mahler, A. B., & Chipman, R. A. (2011). Polarization state generator: a polarimeter calibration standard.

Maritorena S., D.A. Siegel & A. Peterson. 2002. Optimization of a Semi-Analytical Ocean Color Model for Global Scale Applications. Applied Optics. 41(15): 2705-2714.

Maritorena S., O. Hembise Fanton d'Andon, A. Mangin, D.A. Siegel. 2010. Merged Satellite Ocean Color Data Products Using a Bio-Optical Model: Characteristics, Benefits and Issues. Remote Sensing of Environment, 114, 8: 1791-1804 (doi: 10.1016/j.rse.2010.04.002).

Martin, W., B. Cairns, and G. Bal, 2014: Adjoint methods for adjusting three-dimensional atmosphere and surface properties to fit multi-angle/multi-pixel polarimetric measurements. *J. Quant. Spectrosc. Radiat. Transfer*, **144**, 68-85, doi:10.1016/j.jqsrt.2014.03.030.

Martins, J. V.; R. Fernandez-Borda; B. McBride; L. A. Remer ; H. M. J. Barbosa; The HARP Hyper Angular Imaging Polarimeter and the Need for Small Satellite Payloads with High Science Payoff for Earth Science Remote Sensing. IEEE International Geoscience and Remote Sensing Symposium, 2018; Page(s):6304 – 6307. DOI: 10.1109/IGARSS.2018.8518823

McClain, C. R., Christian, J. R., Signorini, S. R., Lewis, M. R., Asanuma, I., Turk, D., & Dupouy-Douchement, C. (2002). Satellite ocean-color observations of the tropical Pacific Ocean. *Deep Sea Research Part II: Topical Studies in Oceanography*, *49*(13), 2533-2560.

McClain et al. 2012 The Ocean Radiometer for Carbon Assessment (ORCA): Development history within an advanced ocean mission concept, science objectives, design rationale, and sensor prototype description. NASA T/M-2012-215894, NASA Goddard Space Flight Center, Greenbelt, Maryland, pp. 55.

McCoy, D. T., Burrows, S. M., Wood, R., Grosvenor, D. P., Elliott, S. M., Ma, P.-L., et al. (2015). Natural aerosols explain seasonal and spatial patterns of Southern Ocean cloud albedo. *Science Advances*, *1*(6), e1500157–e1500157. doi:10.1126/sciadv.1500157

McGill, M.J., J. E. Yorks, V. S. Scott, A. W. Kupchock, P. A. Selmer (2015), The Cloud-Aerosol Transport System (CATS): a technology demonstration on the International Space Station, Proc. SPIE 9612, Lidar Remote Sensing for Environmental Monitoring XV, 96120A, doi:10.1117/12.2190841.

McGill, M.J., R.J. Swap, J. E. Yorks, and P. A. Selmer (2018), Observation and quantification of westerly outflow from southern Africa using spaceborne lidar, Geophys. Res. Let., in review.

McKinna, L.I.W., P.J. Werdell, and C.W. Proctor, "Implementation of an analytical Raman scattering correction for satellite ocean color processing," Optics Express 24, doi:10.1364/OE.24.0A1123 (2016).

Mahler A.-B., and R. A. Chipman, Polarization state generator: a polarimeter calibration standard, Appl. Opt. 50, 1726-1734, 2011.

Meister, G., C. R. McClain, Z. Ahmad, S. W. Bailey, R. A. Barnes, S. Brown, R. E. Eplee, B. Franz, A. Holmes, W. B. Monosmith, F. S. Patt, R. P. Stumpf, K. R. Turpie, and P. J. Werdell (2011) *Requirements for an advanced ocean radiometer*. *NASA T/M-2011-215883,* NASA Goddard Space Flight Center, Greenbelt, Maryland, pp. 40.

Meskhidze, N., Chameides, W. L., & Nenes, A. (2005). Dust and pollution: a recipe for enhanced ocean fertilization? *Journal of Geophysical Research: Atmospheres (1984–2012)*, *110*(D3).

Meskhidze, N., & Nenes, A. (2006). Phytoplankton and cloudiness in the Southern Ocean. *Science*, *314*(5804), 1419-1423.

Meskhidze, N., Petters, M. D., Tsigaridis, K., Bates, T., O'Dowd, C., Reid, J., et al. (2013). Production mechanisms, number concentration, size distribution, chemical composition, and optical properties of sea spray aerosols: Production and properties of sea spray aerosol. *Atmospheric Science Letters*, *14*(4), 207–213. doi:10.1002/asl2.441

Meskhidze, N., Hurley, D., Royalty, T. M., & Johnson, M. S. (2017). Potential effect of atmospheric dissolved organic carbon on the iron solubility in seawater. *Marine Chemistry*, *194*, 124–132. doi:10.1016/j.marchem.2017.05.011

Meyer, K., Platnick, S. and Zhang, Z., 2015. Simultaneously inferring above‐cloud absorbing aerosol optical thickness and underlying liquid phase cloud optical and microphysical properties using MODIS. Journal of Geophysical Research: Atmospheres, 120(11), pp.5524-5547.

Morrow, J., S. Hooker, C. Booth, G. Bernhard, R. Lind, J. Brown. (2010). Advances in measuring the apparent optical properties (AOPs) of optically complex waters, NASA Report NASA/TM-2010-215856. NASA, Goddard Space Flight Center, Greenbelt, MD.

Müller, D., et al. (2001) Comprehensive particle characterization from three-wavelength Raman-lidar observations: case study. *Applied Optics* **40**, 4863-4869.

Müller, D., et al. (2002) European pollution outbreaks during ACE 2: Microphysical particle properties and single-scattering albedo inferred from multiwavelength lidar observations. *Journal of Geophysical Research-Atmospheres* **107**, - DOI: Artn 4248,Doi 10.1029/2001jd001110.

Müller, D., Hostetler, C. A., Ferrare, R. A., Burton, S. P., Chemyakin, E., Kolgotin, A., ... & Schmid, B. (2014). Airborne Multiwavelength High Spectral Resolution Lidar (HSRL-2) observations during TCAP 2012: vertical profiles of optical and microphysical properties of a smoke/urban haze plume over the northeastern coast of the US. *Atmospheric Measurement Techniques*.

Nakajima, T., & King, M. D. (1990). Determination of the optical thickness and effective particle radius of clouds from reflected solar radiation

measurements. Part I: Theory. *Journal of the atmospheric sciences*, *47*(15), 1878-1893.

Noel, V., H. Chepfer, M. Chiriaco, and J.E. Yorks (2018), The diurnal cycle of cloud profiles over land and ocean between 51° S and 51° N, seen by the CATS spaceborne lidar from the International Space Station, Atmos. Chem. Phys., 18, 9457-9473, doi:10.5194/acp-18-9457-2018.

NRC. (2007). Earth Science and Applications from Space: National Imperatives for the Next Decade and Beyond, The National Academies Press, Washington, D.C., retrieved at: http://www.nap.edu/catalog/11820.html

NSF. (2014). EarthCube End User Workshop Executive Summaries. retrieved from: http://earthcube.org/sites/default/files/doc-repository/CombinedSummaries_12Dec2014.pdf

O'Malley, R.T., Behrenfeld, M.J., Westberry, T.K., Milligan, A.J., Shang, S., Yan, J. (2014), Geostationary satellite observations of dynamic phytoplankton photophysiology, Geophysical Research Letters, doi:10.10002/2014GL060246

Ottaviani, M., B. Cairns, R.R. Rogers, and R. Ferrare, 2012: Iterative atmospheric correction scheme and the polarization color of alpine snow. *J. Quant. Spectrosc. Radiat. Transfer*, **113**, 789-804, doi:10.1016/j.jqsrt.2012.03.014.

Ottaviani, M., van Diedenhoven, B., and Cairns, B.: Photopolarimetric retrievals of snow properties, The Cryosphere, 9, 1933-1942, doi:10.5194/tc-9-1933-2015, 2015.

Palacios, S.L., Kudela, R.M., Guild, L.S., Negrey, K.H., Torres-Perez, J. and Broughton, J., 2015. Remote sensing of phytoplankton functional types in the coastal ocean from the HyspIRI Preparatory Flight Campaign. Remote Sensing of Environment, 167, pp.269-280.

Papagiannopoulos, N., Mona, L., Amodeo, A., D'Amico, G., Gumà Claramunt, P., Pappalardo, G., Alados-Arboledas, L., Guerrero-Rascado, J. L., Amiridis, V., Kokkalis, P., Apituley, A., Baars, H., Schwarz, A., Wandinger, U., Binietoglou, I., Nicolae, D., Bortoli, D., Comerón, A., Rodríguez-Gómez, A., Sicard, M., Papayannis, A., and Wiegner, M.: An automatic observation-based aerosol typing method for EARLINET, Atmos. Chem. Phys., 18, 15879-15901, 10.5194/acp-18-15879-2018, 2018.

Piironen, P., & Eloranta, E. W. (1994). Demonstration of a high-spectral-resolution lidar based on an iodine absorption filter. *Optics letters*, *19*(3), 234-236.

Pingree, P. J., Looking up: The MCubed/COVE mission, 2014 Spring Cubesat Developers' Workshop, 2014.

Platnick, S. (2000). Vertical photon transport in cloud remote sensing problems. *Journal of Geophysical Research*, *105*(22), 919-22.

Pope, A., Wagner, P., Johnson, R., Shutler, J. D., Baeseman, J., & Newman, L. (2017). Community review of Southern Ocean satellite data needs. *Antarctic Science*, *29*(02), 97–138. doi:10.1017/S0954102016000390

Posselt, D. J., Stephens, G. L., & Miller, M. (2008). CloudSat: Adding a new dimension to a classical view of extratropical cyclones. *Bulletin of the American Meteorological Society*, *89*(5), 599-609.

Posselt, D. J., & Vukicevic, T. (2010). Robust characterization of model physics uncertainty for simulations of deep moist convection. *Monthly Weather Review*, *138*(5), 1513-1535.

Posselt, D. J., & Mace, G. G. (2014). MCMC-Based Assessment of the Error Characteristics of a Surface-Based Combined Radar–Passive Microwave Cloud Property Retrieval. *Journal of Applied Meteorology and Climatology*, *53*(8), 2034-2057.

Povel H., H. Aebersold, and J. O. Stenflo, Charge-coupled device image sensor as a demodulator in a 2-D polarimeter with a piezoelastic modulator, Appl. Opt. 29, 1186–1190, 1990.

Powell, K. A., Vaughan, M., Burton, S. P., Hair, J. W., Hostetler, C. A., & Kowch, R. S. (2014, December). An assessment of a software simulation tool for lidar atmosphere and ocean measurements. In *AGU Fall Meeting Abstracts* (Vol. 1, p. 1177).

Rajapakshe, C., Z. Zhang, J. E. Yorks, H. Yu, Q. Tan, K. Meyer, S. Platnick (2017), Seasonally Transported Aerosol Layers over Southeast Atlantic are Closer to Underlying Clouds than Previously Reported*,* Geophys. Res. Lett.*,* 44*, doi:10.1002/2017GL073559.*

Ramanathan, V. (2001). Aerosols, Climate, and the Hydrological Cycle. *Science*, *294*(5549), 2119–2124. doi:10.1126/science.1064034

Remer, L., et al. Polarimetry in the PACE mission. Science team concensus document. White paper submitted to NASA HQ, July 23, 2015

Rosenfeld, D., S. Sherwood, R. Wood, and L. Donner, 2014: Climate effects of aersol-cloud interactions, *Science*, 343, 379-380.

Saleeby, S. M., & van den Heever, S. C. (2013). Developments in the CSU-RAMS aerosol model: Emissions, nucleation, regeneration, deposition, and radiation. *Journal of Applied Meteorology and Climatology*, *52*(12), 2601-2622.

Satoh, M. T. Matsuno, H. Tomita, H. Miura, T. Nasuno, and S. Iga, 2008: Non-hydrostatic icosahedral atmospheric model (NICAM) for global cloud resolving simulations. *Journal of Computational Physics*, 227, 2486-3514.

Sawamura, P., Müller, D., Hoff, R. M., Hostetler, C. A., Ferrare, R. A., Hair, J. W., ... & Holben, B. N. (2014). Aerosol optical and microphysical retrievals from a

hybrid multiwavelength lidar data set–DISCOVER-AQ 2011. *Atmospheric Measurement Techniques*, *7*(9), 3095-3112.

Sawamura, P., Moore, R.H., Burton, S.P., Chemyakin, E., Müller, D., Kolgotin, A., Ferrare, R.A., Hostetler, C.A., Ziemba, L.D., Beyersdorf, A.J. and Anderson, B.E., 2017. HSRL-2 aerosol optical measurements and microphysical retrievals vs. airborne in situ measurements during DISCOVER-AQ 2013: an intercomparison study. *Atmospheric Chemistry and Physics*, *17*(11), pp.7229-7243.

Sayer, A.M., Hsu, N.C., Bettenhausen, C., Lee, J., Redemann, J., Schmid, B. and Shinozuka, Y., 2016. Extending "Deep Blue" aerosol retrieval coverage to cases of absorbing aerosols above clouds: Sensitivity analysis and first case studies. Journal of Geophysical Research: Atmospheres, 121(9), pp.4830-4854.

Segal-Rozenhaimer, M., Miller, D.J., Knobelspiesse, K., Redemann, J., Cairns, B. and Alexandrov, M.D., 2018. Development of neural network retrievals of liquid cloud properties from multi-angle polarimetric observations. Journal of Quantitative Spectroscopy and Radiative Transfer, 220, pp.39-51.

Scarino, A. J., Ferrare, R. A., Burton, S. P., Hostetler, C. A., Hair, J. W., Rogers, R. R., ... & Hodges, G. (2013, December). Aerosol Optical Thickness comparisons between NASA LaRC Airborne HSRL and AERONET during the DISCOVER-AQ field campaigns. In *AGU Fall Meeting Abstracts* (Vol. 1, p. 0071).

Scarino, A. J., Ferrare, R. A., Burton, S. P., Hostetler, C. A., Hair, J. W., Rogers, R. R., ... & Randles, C. A. (2014, December). Assessing Aerosol Mixed Layer Heights from the NASA Larc Airborne High Spectral Resolution Lidar (HSRL) during the Discover-AQ Field Campaigns. In *AGU Fall Meeting Abstracts* (Vol. 1, p. 3040).

Schulien, J.A., Behrenfeld, M.J., Hair, J.W., Hostetler, C.A. and Twardowski, M.S., 2017. Vertically-resolved phytoplankton carbon and net primary production from a high spectral resolution lidar. *Optics Express*, *25*(12), pp.13577-13587.

Seaman, S.T., Cook, A.L., Scola, S.J., Hostetler, C.A., Miller, I. and Welch, W., 2015, September. Performance characterization of a pressure-tuned wide-angle Michelson interferometric spectral filter for high spectral resolution lidar. In *Lidar Remote Sensing for Environmental Monitoring XV*(Vol. 9612, p. 96120H). International Society for Optics and Photonics.

Silsbe, G.M., Behrenfeld, M.J., Halsey, K.H., Milligan, A.J., Westberry, T.K. The CAFE Model: An Accurate Absorption-Based Net Phytoplankton Production Model for the Global Ocean. Global Biogeochem. Cycl. 30, 1756–1777, 2016.

Sinclair, K., Cairns, B., Hair, J. W., Hu, Y., & Hostetler, C. A. (2014, December). Polarimetric Retrievals of Cloud Droplet Number Concentrations. In *AGU Fall Meeting Abstracts* (Vol. 1, p. 3042).

Sinclair, K., B. van Diedenhoven, B. Cairns, M. Alexandrov, R. Moore, E. Crosbie and L. Ziemba, 2019: Polarimetric Retrievals of Cloud Droplet Number Concentrations, submitted to Remote Sensing of the Environment.

Soden, B. J., & Held, I. M. (2006). An assessment of climate feedbacks in coupled ocean-atmosphere models. *Journal of Climate*, *19*(14), 3354-3360.

Soden, B. J., & Vecchi, G. A. (2011). The vertical distribution of cloud feedback in coupled ocean-atmosphere models. *Geophysical Research Letters*, *38*(12) L12704, doi:10.1029/2011GL047632.

Stamnes, Snorre, et al. "Simultaneous aerosol/ocean products retrieved during the 2014 SABOR campaign using the NASA Research Scanning Polarimeter (RSP)." AGU Fall Meeting Abstracts. 2017

Stamnes, S., C. Hostetler, R. Ferrare, S. Burton, X. Liu, J. Hair, Y. Hu, A. Wasilewski, W. Martin, B. van Diedenhoven, J. Chowdhary, I. Cetinic, L. Berg, K. Stamnes, and B. Cairns, 2018: Simultaneous polarimeter retrievals of microphysical aerosol and ocean color parameters from the "MAPP" algorithm with comparison to high spectral resolution lidar aerosol and ocean products. Appl. Opt., 57, no. 10, 2394-2413, doi:10.1364/AO.57.002394.

Stephens, G. L., 2005: Cloud feedbacks in the climate system: A critical review. J. Cli. 18, 237-273.

Stevens, B., and S. Bony, 2013: What are climate models missing?. Science, 340, 1053, DOI: 10.1126/science.12375543

Stevens, B., & Feingold, G. (2009). Untangling aerosol effects on clouds and precipitation in a buffered system. *Nature*, *461*(7264), 607-613.

Stramski, D., R. A. Reynolds, S. Kaczmarek, J. Uitz and G. Zheng. 2015. Correction of pathlength amplification in the filter-pad technique for measurements of particulate absorption coefficient in the visible spectral region. Applied Optics, 54, 6763-6782. doi: 10.1364/AO.54.006763

Su, W., Charlock, T. P., & Rutledge, K. (2002). Observations of reflectance distribution around sunglint from a coastal ocean platform. *Applied optics*, *41*(35), 7369-7383.

Tamminen, J. (2004). Validation of nonlinear inverse algorithms with Markov chain Monte Carlo method. *Journal of Geophysical Research: Atmospheres (1984–2012)*, *109*(D19).

Tanelli, S., Tao, W. K., Matsui, T., Hostetler, C. A., Hair, J. W., Butler, C., ... & Turk, F. J. (2012, November). Integrated instrument simulator suites for Earth Science. In *SPIE Asia-Pacific Remote Sensing* (pp. 85290D-85290D). International Society for Optics and Photonics.

Tarantola 2005; Tarantola, A. (2005). *Inverse problem theory and methods for model parameter estimation*. siam.

Thompson, D.R., Gao, B.C., Green, R.O., Roberts, D.A., Dennison, P.E. and Lundeen, S.R., 2015. Atmospheric correction for global mapping spectroscopy: ATREM advances for the HyspIRI preparatory campaign. Remote Sensing of Environment, 167, pp.64-77.

Tinbergen. J. Astronomical Polarimetry. Cambridge University Press, 1996. 158 pp. ISBN 0 521 47531 7

Toon, O. B., et al. (2016), Planning, implementation, and scientific goals of the Studies of Emissions and Atmospheric Composition, Clouds and Climate Coupling by Regional Surveys (SEAC4RS) field mission, J. Geophys. Res. Atmos., 121,4967–5009, doi:10.1002/2015JD024297

Tsay S.C., N. C. Hsu, K.-M. Lau, C. Li, P. M. Gabriel, Q. Ji, B. N. Holben, E. J. Welton, X. A., Nguyen, S. Janjai, N.-H. Lin, J. S. Reid, J. Boonjawat, S. G. Howell, B. Huebert, J. S. Fu, R. A. Hansell, A. M. Sayer, R. Gautam, S.-H. Wang, C. S. Goodloe, L. R. Miko, P. K. Shu, A. M. Loftus, J. Huang, J. Y. Kim, M.-J. Jeong, and P. Pantina, (2013), "From BASE-ASIA towards 7-SEAS: A Satellite-Surface Perspective of Boreal Spring Biomass-Burning Aerosols and Clouds in Southeast Asia," *Atmos. Environ.,* **78**, 20-34, doi: 10.1016/j.atmosenv.2012.12.013.

van den Heever, S. C., Stephens, G. L., & Wood, N. B. (2011). Aerosol indirect effects on tropical convection characteristics under conditions of radiative-convective equilibrium. *Journal of the Atmospheric Sciences*, *68*(4), 699-718.

Van Diedenhoven, B., A.M. Fridlind, A.S. Ackerman, and B. Cairns, 2012a: Evaluation of hydrometeor phase and ice properties in cloud-resolving model simulations of tropical deep convection using radiance and polarization measurements. J. Atmos. Sci., 69, 3290-3314, doi:10.1175/JAS-D-11-0314.1.

Van Diedenhoven, B., B. Cairns, I.V. Geogdzhayev, A.M. Fridlind, A.S. Ackerman, P. Yang, and B.A. Baum, 2012b: Remote sensing of ice crystal asymmetry parameter using multi-directional polarization measurements. Part I: Methodology and evaluation with simulated measurements. Atmos. Meas. Tech., 5, 2361-2374, doi:10.5194/amt-5-2361-2012.

Van Diedenhoven, B., B. Cairns, A.M. Fridlind, A.S. Ackerman, and T.J. Garrett, 2013: Remote sensing of ice crystal asymmetry parameter using multi-directional polarization measurements — Part 2: Application to the Research Scanning Polarimeter. Atmos. Chem. Phys., 13, 3185-3203, doi:10.5194/acp-13-3185-2013.

Van Diedenhoven, B., A.S. Ackerman, A.M. Fridlind, and B. Cairns, 2016b: On averaging aspect ratios and distortion parameters over ice crystal population ensembles for estimating effective scattering properties. J. Atmos. Sci., 73, no. 2, 775-787, doi:10.1175/JAS-D-15-0150.1.

Van Diedenhoven, B., A.M. Fridlind, B. Cairns, A.S. Ackerman, and J. Yorks, 2016a: Vertical variation of ice particle size in convective cloud tops. Geophys. Res. Lett., 43, no. 9, 4586-4593, doi:10.1002/2016GL068548.

Van Diedenhoven, B., 2018: Remote sensing of crystal shapes in ice clouds. In Springer Series in Light Scattering, Volume 2: Light Scattering, Radiative Transfer and Remote Sensing. A. Kokhanovsky, Ed. Springer International, pp. 197-250, doi:10.1007/978-3-319-70808-9_5.

Van Harten, G., D. J. Diner, B. J. S. Daugherty, B. E. Rheingans, M. A. Bull, F. C. Seidel, R. A. Chipman, B. Cairns, A. P. Wasilewski, and K. D. Knobelspiesse, Calibration and validation of Airborne Multiangle SpectroPolarimetric Imager (AirMSPI) polarization measurements, Appl. Opt. 57, 4499-4513, 2018.

Veselovskii, I., Kolgotin, A., Griaznov, V., Müller, D., Wandinger, U., & Whiteman, D. N. (2002). Inversion with regularization for the retrieval of tropospheric aerosol parameters from multiwavelength lidar sounding. *Applied optics*, *41*(18), 3685-3699.

Wandinger, U., Müller, D., Böckmann, C., Althausen, D., Matthias, V., Bösenberg, J., ... & Ansmann, A. (2002). Optical and microphysical characterization of biomass-burning and industrial-pollution aerosols from-multiwavelength lidar and aircraft measurements. *Journal of Geophysical Research: Atmospheres (1984–2012)*, *107*(D21), LAC-7.

Waquet, F., Riedi, J., Labonnote, L. C., Goloub, P., Cairns, B., Deuzé, J. L., & Tanré, D. (2009). Aerosol remote sensing over clouds using A-Train observations. *Journal of the Atmospheric Sciences*, *66*(8), 2468-2480.

Waquet, F., Cornet, C., Deuzé, J. L., Dubovik, O., Ducos, F., Goloub, P., ... & Vanbauce, C. (2013). Retrieval of aerosol microphysical and optical properties above liquid clouds from POLDER/PARASOL polarization measurements. *Atmospheric Measurement Techniques*, *6*(4), 991-1016.

Werdell, P. J., Franz, B. A., Bailey, S. W., Feldman, G. C., Boss, E., Brando, V. E., ... & Mangin, A. (2013a). Generalized ocean color inversion model for retrieving marine inherent optical properties. *Applied optics*, 52(10), 2019-2037.

Werdell, P. J., Roesler, C. S., & Goes, J. I. (2014). Discrimination of phytoplankton functional groups using an ocean reflectance inversion model. *Applied optics*, 53(22), 4833-4849.

Westberry, T. K., Behrenfeld, M. J., Milligan, A. J., & Doney, S. C. (2013). Retrospective satellite ocean color analysis of purposeful and natural ocean iron fertilization. *Deep Sea Research Part I: Oceanographic Research Papers*, 73, 1-16.

Westberry, T. K., E. Boss, and Z. Lee, 2013. Influence of Raman scattering on ocean color inversion models. *Applied Optics*, 52, No. 22, 5552-5561.

Westberry, T.K., Behrenfeld, M.J. Oceanic net primary production. In: Biophysical Applications of Satellite Remote Sensing (ed. J.M. Hanes). Chapter 8. Springer Remote Sensing/Photogrammetry, DOI: 10.1007/978-3-642-25047-7_8. pp. 205-230, 2014.

Wind, G., S. Platnick, M.D. King, P.A. Hubanks, M.J. Pavolonis, A.K. Heidinger, P.Yang, B. Baum, 2010: Multilayer Cloud Detection with the MODIS Near-Infrared Water Vapor Absorption Band. *J. App. Met. Clim.* **49**, 2315-2333.

Winker, D.M., Vaughan, M.A., Omar, A., Hu, Y., Powell, K.A., Liu, Z., Hunt, W.H. and Young, S.A., 2009. Overview of the CALIPSO mission and CALIOP data processing algorithms. *Journal of Atmospheric and Oceanic Technology*, *26*(11), pp.2310-2323.

Wu, L., O. Hasekamp, B. van Diedenhoven, and B. Cairns, 2015: Aerosol retrieval from multiangle, multispectral photopolarimetric measurements: Importance of spectral range and angular resolution. Atmos. Meas. Tech., 8, 2625-2638, doi:10.5194/amt-8-2625-2015.

Wu, L., O. Hasekamp, B. van Diedenhoven, B. Cairns, J.E. Yorks, and J. Chowdhary, 2016: Passive remote sensing of aerosol layer height using near-UV multi-angle polarization measurements. Geophys. Res. Lett., 43, no. 16, 8783-8790, doi:10.1002/2016GL069848.

Xu, F., Davis, A. B., Sanghavi, S. V., Martonchik, J. V., & Diner, D. J. (2012). Linearization of Markov chain formalism for vector radiative transfer in a plane-parallel atmosphere/surface system. *Applied Optics*, *51*(16), 3491-3507.

Xu, F., O. Dubovik, P.-W. Zhai, D. J. Diner, O. V. Kalashnikova, F. C. Seidel, P. Litvinov, A. Bovchaliuk, M. J. Garay, G. van Harten, and A. B. Davis, Joint retrieval of aerosol and water-leaving radiance from multi-spectral, multi-angular and polarimetric measurements over ocean, Atmos. Meas. Tech. 9, 2877-2907, 2016.

Xu, F., G. van Harten, D. J. Diner, O. V. Kalashnikova, F. C. Seidel, C. J. Bruegge, and O. Dubovik, Coupled retrieval of aerosol properties and land surface reflection using the Airborne Multiangle SpectroPolarimetric Imager, J. Geophys. Res. Atmos., 122, 7004-7026, 2017.

Xu, F., G. van Harten, D. J. Diner., A. B. Davis, F. Seidel, B. Rheingans, M. Tosca, M. Alexandrov, B. Cairns, R. Ferrare, S. Burton, M. Fenn, C. Hostetler, R. Wood, and J. Redemann, Coupled retrieval of cloud and aerosol above cloud properties using AirMSPI, J. Geophys. Res. Atmos., 123, 3175-3204, 2018.

Xue, H., Feingold, G., & Stevens, B. (2008). Aerosol effects on clouds, precipitation, and the organization of shallow cumulus convection. *Journal of the Atmospheric Sciences*, *65*(2), 392-406.

Yorks, J. E., M. McGill, V. S. Scott, A. Kupchock, S. Wake, D. Hlavka, W. Hart, P. Selmer (2014), The Airborne Cloud-Aerosol Transport System: Overview and Description of the Instrument and Retrieval Algorithms, *J. Atmos. Oceanic Technol*., 31, 2482–2497, doi:10.1175/JTECH-D-14-00044.1.

Yorks, J. E., M. J. McGill, S.P. Palm, D. L. Hlavka, P.A. Selmer, E. Nowottnick, M. A. Vaughan, S. Rodier, and W. D. Hart (2016), An Overview of the CATS Level 1 Data Products and Processing Algorithms, *Geophys. Res. Let.*, 43, *doi:*10.1002/2016GL068006*.*

Yu, H. and Zhang, Z., 2013. New Directions: Emerging satellite observations of above-cloud aerosols and direct radiative forcing. Atmospheric environment, 72, pp.36-40.

Zaveri, R.A., W.J. Shaw, D.J. Cziczo, B. Schmid, R.A. Ferrare, M.L. Alexander, M. Alexandrov, R.J. Alvarez, W.P. Arnott, D.B. Atkinson, S. Baidar, R.M. Banta, J.C. Barnard, J. Beranek, L.K. Berg, F. Brechtel, W.A. Brewer, J.F. Cahill, B. Cairns, C.D. Cappa, D. Chand, S. China, J.M. Comstock, M.K. Dubey, R.C. Easter, M.H. Erickson, J.D. Fast, C. Floerchinger, B.A. Flowers, E. Fortner, J.S. Gaffney, M.K. Gilles, K. Gorkowski, W.I. Gustafson, M. Gyawali, J. Hair, R.M. Hardesty, J.W. Harworth, S. Herndon, N. Hiranuma, C. Hostetler, J.M. Hubbe, J.T. Jayne, H. Jeong, B.T. Jobson, E.I. Kassianov, L.I. Kleinman, C. Kluzek, B. Knighton, K.R. Kolesar, C. Kuang, A. Kubátová, A.O. Langford, A. Laskin, N. Laulainen, R.D. Marchbanks, C. Mazzoleni, F. Mei, R.C. Moffet, D. Nelson, M.D. Obland, H. Oetjen, T.B. Onasch, I. Ortega, M. Ottaviani, M. Pekour, K.A. Prather, J.G. Radney, R.R. Rogers, S.P. Sandberg, A. Sedlacek, C.J. Senff, G. Senum, A. Setyan, J.E. Shilling, M. Shrivastava, C. Song, S.R. Springston, R. Subramanian, K. Suski, J. Tomlinson, R. Volkamer, H.W. Wallace, J. Wang, A.M. Weickmann, D.R. Worsnop, X.-Y. Yu, A. Zelenyuk, and Q. Zhang, 2012: Overview of the 2010 Carbonaceous Aerosols and Radiative Effects Study (CARES). *Atmos. Chem. Phys.*, **12**, 7647-7687, doi:10.5194/acp-12-7647-2012.

Zelinka, M. D., & Hartmann, D. L. (2012). Climate feedbacks and their implications for poleward energy flux changes in a warming climate. *Journal of Climate*, *25*(2), 608-624.

Zelinka, M. D., Klein, S. A., & Hartmann, D. L. (2012). Computing and partitioning cloud feedbacks using cloud property histograms. Part I: Cloud radiative kernels. *Journal of Climate*, *25*(11), 3715-3735.

Zelinka, M. D., Klein, S. A., & Hartmann, D. L. (2012). Computing and partitioning cloud feedbacks using cloud property histograms. Part II: Attribution to changes in cloud amount, altitude, and optical depth. *Journal of Climate*, *25*(11), 3736-3754.

Zelinka, M. D., Klein, S. A., Taylor, K. E., Andrews, T., Webb, M. J., Gregory, J. M., & Forster, P. M. (2013). Contributions of different cloud types to feedbacks and rapid adjustments in CMIP5*. *Journal of Climate*, *26*(14), 5007-5027.

Zhai, P., Y. Hu, C. R. Trepte, and P. L. Lucker, (2009): A vector radiative transfer model for coupled atmosphere and ocean systems based on successive order of scattering method, *Opt. Express* 17, 2057-2079.

Zhai, P., Y. Hu, C.R. Trepte, P. L. Lucker, D. B. Josset, (2010a): Decoupling error for the atmospheric correction in ocean color remote sensing algorithms, *J Quant Spectrosc Radiat Transf*, 111, 1958-1963.

Zhai P., Y. Hu, J. Chowdhary, C. R. Trepte, P. L. Lucker, D. B. Josset, "A vector radiative transfer model for coupled atmosphere and ocean systems with a rough interface," *J Quant Spectrosc Radiat Transf*, 111, 1025-1040 (2010b).

Zhai, P., Y. Hu, C. Hostetler, B. Cairns, R. Ferrare, K. Knobelspiess, D. Josset, C. Trepte, P. Lucker, J. Chowdhary, (2013): Uncertainty and interpretation of aerosol

remote sensing due to vertical inhomogeneity, *J Quant Spectrosc Radiat Transf*, 114, 91-100.

Zibordi, G., B. Holben, I. Slutsker, D. Giles, D. D'Alimonte, F. Mélin, J.F. Berthon, D. Vandemark, H. Feng, G. Schuster, B.E. Fabbri, S. Kaitala, and J. Seppälä (2009): AERONET-OC: A Network for the Validation of Ocean Color Primary Products. *J. Atmos. Oceanic Technol.*, *26*, 1634–1651, DOI: 10.1175/2009JTECHO654.1

Zubko, E., Muinonen, K., Shkuratov, Y., Videen, G., & Nousiainen, T. (2007). Scattering of light by roughened Gaussian random particles. *Journal of Quantitative Spectroscopy and Radiative Transfer*, *106*(1), 604-615.

Zuidema, P., Redemann, J., Haywood, J., Wood, R., Piketh, S., Hipondoka, M., & Formenti, P. (2016). Smoke and clouds above the southeast Atlantic: Upcoming field campaigns probe absorbing aerosol's impact on climate. *Bulletin of the American Meteorological Society*, *97*(7), 1131-1135.

List of Acronyms

ACATS – Airborne Cloud Aerosol Transport System

A-CCP - Aerosols and Cloud, Convection, Precipitation Designated Observable

aCDOM – absorption by Colored/CHROMOPHORIC Dissolved Organic Matter

ACE – Aerosol Cloud Ecosystems mission

ACERAD – Atmospheric Profiling Radar for ACE

ACHIEVE - Aerosol, Cloud, Humidity, Interactions Exploring and Validating Enterprise

ACI – Aerosol-Cloud Interactions

ACR - Airborne Cloud Radar/CloudSat Validation Radar

ACT - Advanced Component Technologies Program

AERONET – Aerosol Robotic Network

AESLA – Active Electronically Scanning Linear Arrays

AFRC – NASA's Armstrong Flight Research Center (formerly Dryden Research Flight Center)

AirMISR – Airborne Multi-angle Imaging SpectroRadiometer

AirMSPI - Airborne Multiangle SpectroPolarimetric Imager

AITT - Airborne Instrument Technology Transition

AMPR – Advanced Microwave Precipitation Radiometer

AMS - Autonomous Modular Sensor

AMSR-E - Advanced Microwave Scanning Radio

AMT – Atlantic Meridional Transect program of the United Kingdo

AOD – Aerosol Optical Depth

APR-2 - Airborne Second Generation Precipitation Radar

APS – Aerosol Polarimetry Sensor

ASIC – Application Specific Integrated Circuit

ASTER - Advanced Spaceborne Thermal Emission and Reflection Radiometer

A-Train – The "Afternoon Constellation" including the OCO-2, GCOM-W1, Aqua, CALIPSO, CloudSat, PARASOL, and Aura satellites.

AVIRIS - Airborne Visible/Infrared Imaging Spectrometer

$\boldsymbol{b_{bp}}$ - ocean particulate backscatter coefficients

BRF – Bidirectional Reflectance Factors

CALIPSO - The Cloud-Aerosol Lidar and Infrared Pathfinder Satellite Observation (C

CALIOP - Cloud-Aerosol Lidar with Orthogonal Polarization

CAMP²Ex – Cloud-Aerosol-Monsoon Philippines Experiment

CARES - Carbonaceous Aerosols and Radiative Effects Study

CATS – Cloud Aerosol Transport System

CCN – Cloud Condensation Nuclei

CDOM – Colored Dissolved Organic Matter

[Chl-a] - chlorophyll-a concentration

CloudSat – the NASA satellite-based cloud experiment mission

CO_2 – Carbon Dioxide

C-OPS - Compact-Optical Profiling System

COSSIR - Compact Scanning Sub-millimeter-wave Imaging Radiometer

CoSMIR - Conical Scanning Millimeter-wave Imaging Radiometer

COTS – Commercial Orbital Transportation Services

COVE-2 - CubeSat On-board processing Validation Experiment-2

CPL – Cloud Physics Lidar

CPR – Cloud Profiling Radar

CRM – Common Research Model

C-PrOPS - Compact-Propulsion Option for Profiling Systems

CRS – Cloud Radar System (at 94GHz)

CubeSat - a type of miniaturized satellite for space research that is made up of multiples of 10×10×11.35 cm cubic units

DAOF - Dryden Aircraft Operations Facility

DARF – Direct Aerosol Radiative Forcing

DISCOVER-AQ - Deriving Information on Surface Conditions from COlumn and VERtically. Resolved Observations Relevant to Air Quality

DOLP – Degree of Linear Polarization

DRAGON - Distributed Regional Aerosol Gridded Observation Network

DS – Decadal Survey

EC - EarthCARE - Earth Clouds, Aerosols and Radiation Explorer

eMAS – enhanced MODIS Airborne Simulator

EMC – ElectroMagnetic Compatability

EMI – ElectroMagnetic Interference

ER-2 – NASA/Civilian version of the Air Force's U2-S reconnaisance platform

ERF – Effective Radiative Forcing

ESPO – NASA's Earth Science Project Office

ESTO – NASA's Earth Science Technology Office

EV-I – Earth Venture Instrument

EV-M – Earth Venture Mission

EV-S – Earth Venture Suborbital with EV-S1 being the first round of EV-S funding the EV-S2 being the recently competed and awarded (FY-15) second opportunity of EV-S funding.

EXRAD – ER-2 X-Band Radar

FLH – Satellite Chlorophyll Fluorescence

FPGA – Field Programmable Gate Array

GCM – General Circulation Model

GH – NASA Global Hawk Unmanned Airborne Platform

GIOP – Generalized Inherent Optical Properties

GIOP-DC – GIOP default configuration

GISS – NASA Goddard Institute for Space Studies

GOCECP – Global Ocean Carbon Ecosystems and Coastal Processes mission

GOCI – Geostationary Ocean Color Imager

GEOS-5 – Goddard Earth Observing System Model Version 5

GPM – Global Precipitation Measurement

GPM-GV – Global Precipitation Measurement Ground Validation program

GPU – Graphical Processing Unit

GRASP - Generalized Retrieval of Aerosol and Surface Properties

GroundMSPI – portable, ground-based Multiangle SpectroPolarimetric Imager

GSFC - NASA Goddard Space Flight Center

GSM - Garver-Siegel-Maritorena Algorithm

HARP – HyperAngular Rainbow Polarimeter

HIWRAP – High-Altitude Imaging Wind and Rain Airborne Profiler

HSRL – High Spectral Resolution Lidar

HSRL-1 – First generation

HSRL-2 – Second generation

HyspIRI - Hyperspectral Infrared Imager

ICDH - Instrument Command Data Handling

IDL – Instrument Design Laboratory

IFOV – instantaneous field of view

IIP – ESTO Instrument Incubator Program

IMDL – Integrated Mission Design Laboratory

IOP – Inherent Optical Properties

IPCC – Intergovernmental Panel on Climate Change

IPHEx – Integrated Precipitation & Hydrology Experiment

IRAD – Internal Research and Development

ISS – International Space Station

ITCZ – Inter-Tropical Convergence Zone

JPL – NASA's Jet Propulsion Laboratory

Ka-Band – segment of the microwave region of the electromagnetic spectrum 26.5-40 GHz

Ku-Band - segment of the microwave region of the electromagnetic spectrum 12-18 GHz

LaRC – NASA Langley Research Center

LDCM – Landsat Data Continuity Mission

LED – Light Emitting Diode

LEO – Low Earth Orbit

LES – Large Eddy Simulations

LISST - Submersible Suspended Sediment Sensor/laser particle size analyzer

MAS – MODIS Airborne Simulator

MASTER - MODIS/ASTER Airborne Simulator

MCAD – Markov Chain Adding-Doubling

MCMC – Markov Chain Monte Carlo

MISR – Multi-angle Imaging SpectroRadiometer

ML – Mixed Layer

MODIS – Moderate-Resolution Imaging Spectroradiometer

MPC – Mission Peculiar Cost

mrad - milliradian

MSPI - Multiangle SpectroPolarimetric Imager

NAS – National Academy of Science

NEXRAD - Next-Generation Radar

NIR – Near Infrared portion of electromagnetic spectrum with wavelengths of 0.8-2.5μ

NPEO – NASA Plan for Earth Observations

NPP VIIRS – National Polar-orbiting Partnership Visible Infrared Imaging Radiometer Suite

NRC – National Research Council

OBB – NASA's Ocean Biology and Biochemistry Program

OCEaNS – Ocean Carbon Ecosystem and Near-Shore mission

OE – Optimal Estimation

OLYMPEX - Olympic Mountains Ground Validation Experiment supported by the GPM ground validation (GV) program

OMI – Ozone Monitoring Instrument

ORCA – Ocean Radiometer for Carbon Assessment

OSPREy - Optical Sensors for Planetary Radiance Energy

OSSE – Observational System Simulation Experiment

O_2 A-Band – oxygen absorption band in the electromagnetic spectrum near 0.76μ

PACE – Plankton, Aerosol, Cloud and Ocean ECOSystem mission; formerly Pre – Aerosol Cloud Ecosystem mission

PACS – Passive Aerosol and Cloud Suite multi angle imaging polarimeter

PDF – Probability Distribution Function

PEMs - photoelastic modulators

PhyLM – Physiology Lidar Multispectral Mission

PI-Neph - Polarized Imaging Nephelometer

PODEX – Polarimeter Definition Experiment

POLDER - POLarization and Directionality of the Earth's Reflectances

PSD – Particle Size Distribution

PSG – Polarization State Generator

PWG – Polarimeter Working Group

QAA – Quasi Analytical Algorithm

QRS – Quick Response System

QWPs – Quarter-waveplates

RADEX – Radar Definition Experiment

RFT – Rainbow Fourier Transform

ROIC - ReadOut Integrated Circuit

RPI – Rensselaer Polytechnic Institute

RSP – Research Scanning Polarimeter

RT – Radiation Transfer

SAA – Semi-Analytical Algorithm

SABOR - Ship-Aircraft Bio-Optical Research Field Campaign

SBIR – Small Business Innovation Research program

SCA – Sensor Chip Assembly

SCIPP – Super Composite Image Processing Pipeline

SCPR – Singly Curved Parabolic Reflector

SDT – Science Definition Team

SEAC⁴RS - Studies of Emissions and Atmospheric Composition, Clouds and Climate Coupling by Regional Surveys

SEL – Single Event Latchup

SEWG – Systems Engineering Working Group

SIDECAR - System for Image Digitization, Enhancement, Control And Retrieval

SNR – Signal to Noise Ratio

SODA - Synergized Optical Depth of Aerosols

SOS – Successive Order of Scattering

SPTS – Sources, Processes, Transports and Sinks

SSH – Seas Surface Height

SST – Sea Surface Temperature

STM – Science Traceability Matrix

STTR – Small Business Technology Transfer program

SWIR – Short-Wavelength Infrared portion of electromagnetic spectrum with wavelengths of 1.4-3μ

Tb – Brightness Temperature

TCAP – Two Column Aerosol Project funded by the DOE

TC⁴ – NASA's Tropical Composition, Cloud and Climate Coupling mission

TIRS – Thermal Infrared Sensor

TOA – Top of Atmosphere

TRL – Technical Readiness Level

X-Band - segment of the microwave region of the electromagnetic spectrum 8.0-12.0 GHz

UND – University of North Dakota

UV – Ultra-violet

UV DIAL – Ultra-Violet Differential Absorption Lidar

U10 – Ocean Surface Windspeed

VIS – Visible portion of the electromagnetic spectrum with wavelengths of 0.4-0.7 μ

VNIR – Visible and Near Infrared portion of electromagnetic spectrum with wavelengths of 0.4-1.4μ

W-Band - segment of the microwave region of the electromagnetic spectrum 75 – 110 GHz

WiSCR - Wide-Swath Shared Aperture Cloud Radar

3CPR – Three Band Cloud and Precipitation Radar

3β + 2α + 2δ – Backscatter in 3 Channels (1064, 532 and 355nm), Extinction in 2 Channels (532 and 355nm) and Depolarization in 2 Channels (532 and 355nm)

4STAR - Spectrometers for Sky-Scanning, Sun-Tracking Atmospheric Research